REPORT NO.
UCB/EERC-81/15
SEPTEMBER 1981

EARTHQUAKE ENGINEERING RESEARCH CENTER

THREE DIMENSIONAL DYNAMIC RESPONSE ANALYSIS OF EARTH DAMS

by

LELIO H. MEJIA
H. BOLTON SEED

A report on research sponsored by
the National Science Foundation

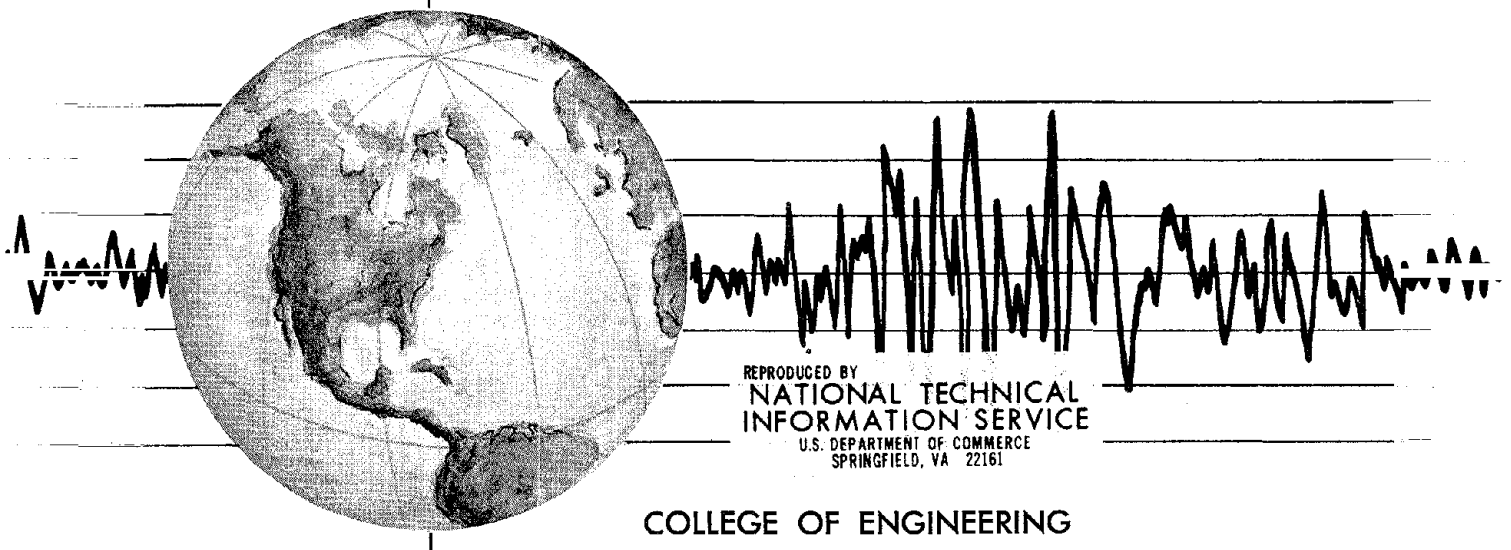

COLLEGE OF ENGINEERING

UNIVERSITY OF CALIFORNIA · Berkeley, California

For sale by the National Technical Information Service, U.S. Department of Commerce, Springfield, Virginia 22161.

See back of report for up to date listing of EERC reports.

DISCLAIMER

Any opinions, findings, and conclusions or recommendations expressed in this publication are those of the author and do not necessarily reflect the views of the National Science Foundation or the Earthquake Engineering Research Center, University of California, Berkeley.

EARTHQUAKE ENGINEERING RESEARCH CENTER

THREE DIMENSIONAL DYNAMIC RESPONSE ANALYSIS OF EARTH DAMS

by

Lelio H. Mejia

H. Bolton Seed

Report No. UCB/EERC-81/15

September 1981

A report on research sponsored by
the National Science Foundation

College of Engineering

University of California

Berkeley, California

50272-101

REPORT DOCUMENTATION PAGE	1. REPORT NO. NSF/CEE-81045	2.	3. Recipient's Accession No. PB82 137274

4. Title and Subtitle
Three Dimensional Dynamic Response Analysis of Earth Dams

5. Report Date
September 1981

6. 350001

7. Author(s)
Lelio H. Mejia and H. Bolton Seed

8. Performing Organization Rept. No.
UCB/EERC-81/15

9. Performing Organization Name and Address
Earthquake Engineering Research Center
University of California, Berkeley
47th Street & Hoffman Blvd.
Richmond, Calif. 94804

10. Project/Task/Work Unit No.

11. Contract(C) or Grant(G) No.
(C)
(G) PFR-7918267

12. Sponsoring Organization Name and Address
National Science Foundation
1800 G. Street, N.W.
Washington, D.C. 20550

13. Type of Report & Period Covered

14.

15. Supplementary Notes

16. Abstract (Limit: 200 words)

Many large dams exist for which the assumption of plane strain conditions during dynamic loading constitutes only an approximation of their true behavior. In these cases, a full three-dimensional dynamic response analysis appears to be warranted. The purpose of the present work has been to develop numerical techniques for the three-dimensional dynamic analysis of earth and rockfill dams and to compare the results obtained from such analyses with those determined by two-dimensional plane strain analyses.

17. Document Analysis a. Descriptors

b. Identifiers/Open-Ended Terms

c. COSATI Field/Group

18. Availability Statement:	19. Security Class (This Report)	21. No. of Pages
Release Unlimited		270
	20. Security Class (This Page)	22. Price

(See ANSI-Z39.18) *See Instructions on Reverse*

OPTIONAL FORM 272 (4-77)
(Formerly NTIS-35)
Department of Commerce

ACKNOWLEDGMENT

The study described in this report was conducted under the sponsorship of the National Science Foundation through Grant No. PFR-7918267. The support of the National Science Foundation is gratefully acknowledged.

ABSTRACT

Many large dams exist for which the assumption of plane strain conditions during dynamic loading constitutes only an approximation of their true behavior. In these cases, a full three-dimensional dynamic response analysis appears to be warranted. The purpose of the present work has been to develop numerical techniques for the three-dimensional dynamic analysis of earth and rockfill dams and to compare the results obtained from such analyses with those determined by two-dimensional plane strain analyses.

TABLE OF CONTENTS

LIST OF FIGURES

LIST OF TABLES

CHAPTER 1

INTRODUCTION

1.1 Seismic Stability of Earth Dams

Over the past two decades significant progress has been made in the development of analytical procedures for evaluating the response and stability of earth dams subjected to seismic loads. Methods of analysis have evolved from the use of a seismic coefficient in a pseudo-static stability analysis to much more involved procedures such as that proposed by Seed et al. (1969, 1973) and which involves the following steps:

1. Selection of the earthquake motions that are likely to affect the dam.

2. Determination of the state of stresses existing throughout the dam and the foundation before the earthquake.

3. Computation of the dynamic stresses induced in the embankment and foundation by the selected earthquake motions.

4. Determination in the laboratory of the response to the induced dynamic stresses of representative samples of the embankment and foundation materials.

5. Assessment of overall stability of the embankment dam and of the deformations likely to develop.

Specific details on the procedures to conduct each of these steps

can be found elsewhere (Seed et al., 1973) and only the computation of dynamic stresses will be discussed in greater depth in the paragraphs to follow.

Among the techniques available to compute the dynamic response induced in a dam by the earthquake motions are the vertical shear beam analysis (Mononobe et al., 1936; Ambraseys 1960) and the finite element method (Clough and Chopra, 1966; Idriss and Seed, 1967; Seed et al., 1969, 1973).

Assumptions inherent to the formulation of the shear beam analysis permit only the computation of an average response of the embankment and therefore limit its applicability to cases where a high degree of accuracy is not required. The finite element method on the other hand, is perhaps the most flexible tool currently available to perform dynamic response analysis of earth dams.

Limitations of computer speed and storage capacity have restricted until recently the use of the finite element method to two-dimensional problems. Although many earth dams fall within this category there are also many cases in which the assumption of plane strain behavior gives only approximate results and therefore a full three-dimensional analysis is warranted.

1.2 Previous Work in Three-dimensional Analysis

Numerical procedures for the static and dynamic three-dimensional analysis of linear elastic structures have been available for the past several years (Wilson, 1971; Wilson et al., 1972; Bathe el al., 1973).

Lefebre et al. (1973) reported comparisons between three-dimensional and two-dimensional static finite element analyses of dams in triangular canyons. The results of this study showed that for ratios of crest length to height of dam, L/H, as low as 6 (see Fig. 1-1(b)), a plane strain analysis of the maximum section of the dam predicts stresses with a degree of accuracy suitable in engineering practice.

Using the shear wedge method of analysis Hatanaka (1955) and Ambraseys (1960) studied the dynamic response of dams in rectangular canyons. It was found that for ratios of crest length to dam height, L/H, greater than 4 (Fig. 1-1(a)), the difference in the fundamental frequency of vibration between the two-dimensional and the three-dimensional representations of the dam was less than 10%.

Makdisi (1976) performed dynamic finite element analyses of dams in triangular canyons subjected to harmonic and earthquake motions. For a 100 foot high dam with a constant shear wave velocity of 500 fps the analyses show that even for crest length to height ratios, L/H, as high as 6 (Fig. 1-1(b)) there are significant differences in the crest amplification functions computed from 3-D and 2-D models of the dam. Differences as large as 200% were found in the computed stresses and accelerations when a dam with L/H equal to 3 was analyzed for earthquake motions.

Two-dimensional and three-dimensional finite element dynamic analyses of the Llyn Brianne Dam (United Kingdom) have been reported by Severn et al. (1979). The results of these analyses were compared with prototype dynamic load test measurements of the natural frequencies of vibration of the dam. Dynamic analyses for which static shear moduli

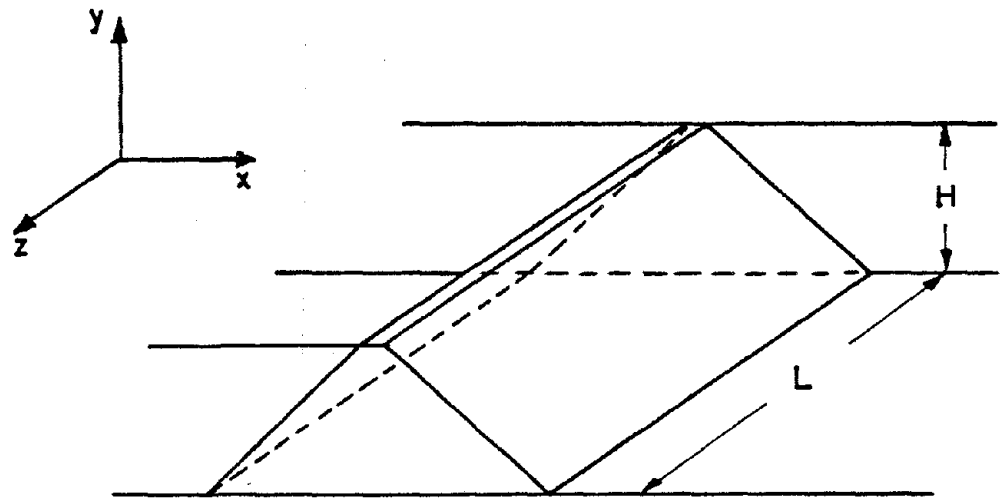

(a) Dam in rectangular canyon

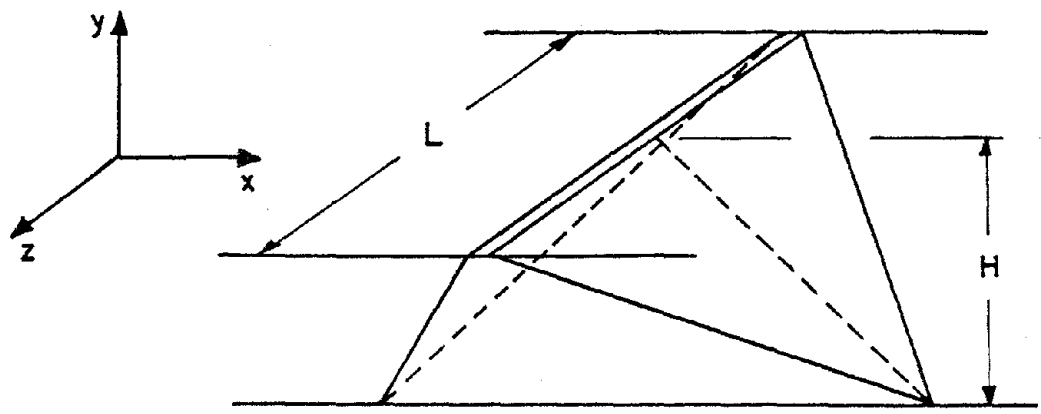

(b) Dam in triangular canyon

Fig. 1-1 Geometrical Models of Dams in Rectangular and Triangular Canyons.

were used gave very low natural frequency values. However, the fundamental natural frequency of vibration computed from a two-dimensional analysis using shear moduli indicated by shear wave velocity measurements was in good agreement with the results of the prototype load tests. In a later report Severn et al. (1980) include the computed three-dimensional mode shapes of vibration of the dam but they note that due to the small number of elements (4) used in the cross-valley direction (z direction in Fig. 1-1), only an approximate definition of the true mode shapes is obtained.

Abdel-Ghaffar and Scott (1978) used the shear wedge method to analyze the recorded response of Santa Felicia Dam (California) to the 1971 San Fernando and the 1976 Southern California earthquakes. By back-calculation from the abutment and crest acceleration records and from shear wave velocity measurements the dynamic properties of the dam and foundation materials were estimated over a wide range of strain levels. As a supplement to this work, prototype load tests were performed which yielded the natural frequencies and mode shapes of vibration of the dam at low levels of strain (Abdel-Ghaffar and Scott, 1979).

1.3 Oroville Dam

An example of an earth dam for which the dynamic response to earthquake loading will be of three-dimensional nature is the Oroville Dam (Fig. 1-2). Located about 150 miles northeast of San Francisco in the western foothills of the Sierra Nevada where the mountain slope dips under the tertiary and quaternary deposits of the Great Valley, the Oroville Dam is the largest earthfill dam in the U.S.A. and an important

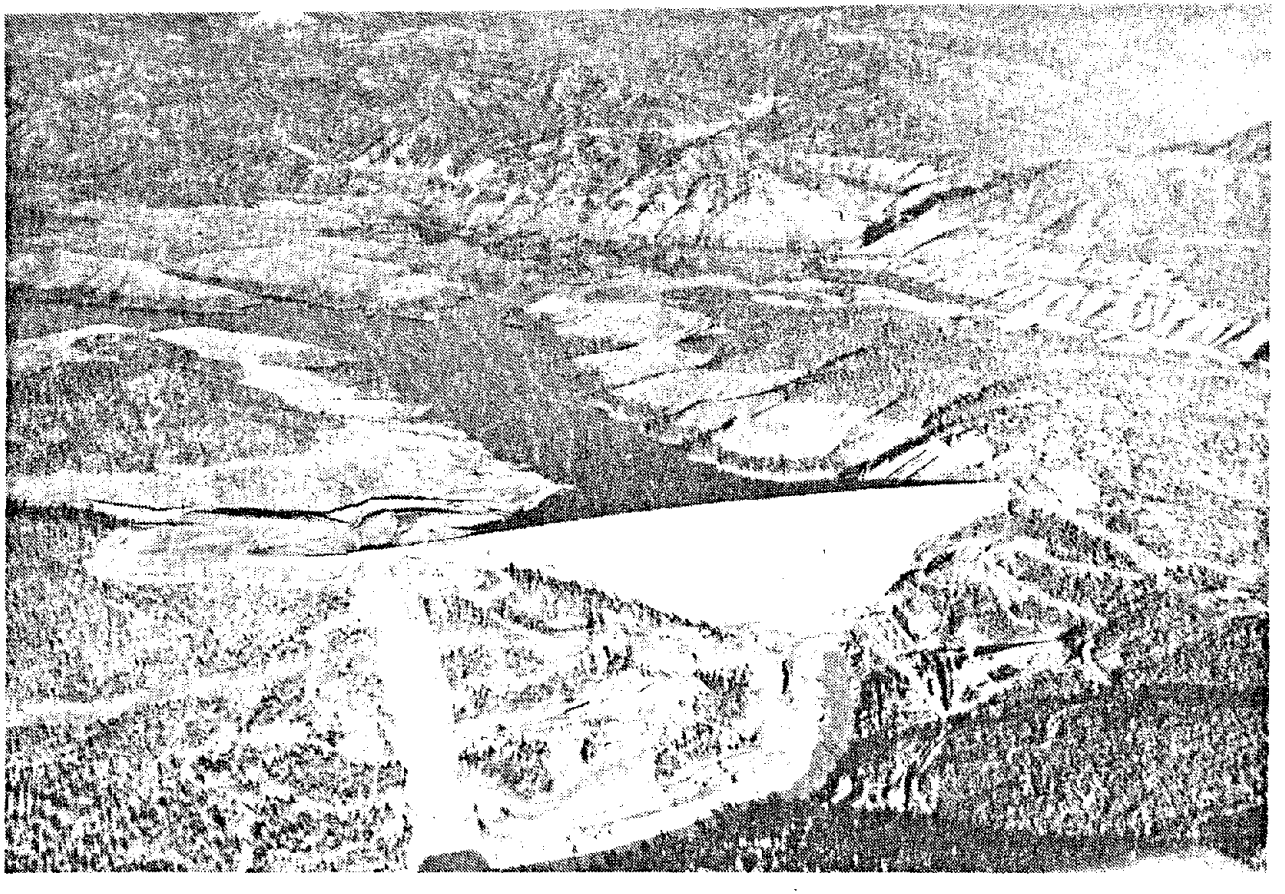

Fig. 1-2 View of Oroville Dam, Spillway and Reservoir

element of the State of California water supply system.

Designed and built for the State of California, Department of Water Resources, the dam is a zoned and rolled gravel-fill that rises 770 feet above the stream bed of the Feather River and has a crest length of 5600 feet. Its foundation and abutments are composed of a very competent rock classified as an amphibolite schist from the pre-jurassic period. The dam itself consists of three main zones and a 128 foot high concrete core block (Fig. 1-3). The latter provides adequate foundation support for the sloping clay core which consists of a well graded clayey sandy gravel. The transition zone materials are classified as well graded to poorly graded sandy gravels and the upstream and downstream shells were constructed with a mixture of cobbles, gravel and sand, also classified as well to poorly graded sandy gravels. Operation of the dam has been successful since the end of construction and its excellent performance has been well documented (DWR, 1979).

For several years the Lake Oroville area had been considered one of low seismicity for which older geological maps showed little fault activity, although, seismic stability was given due consideration in the design of the dam. The conventional pseudo-static method of analysis with a seismic coefficient of 0.1 g was used during the design stage to investigate the seismic stability of the dam, and model studies with simulated earthquake motions were used by Seed (1963) to show the ability of the embankment to withstand a major earthquake.

Occurrence of the August 1, 1975 Oroville earthquake and several aftershocks disclosed the existence of a previously unidentified fault in the vicinity of the dam. The presence of this fault and the seismic

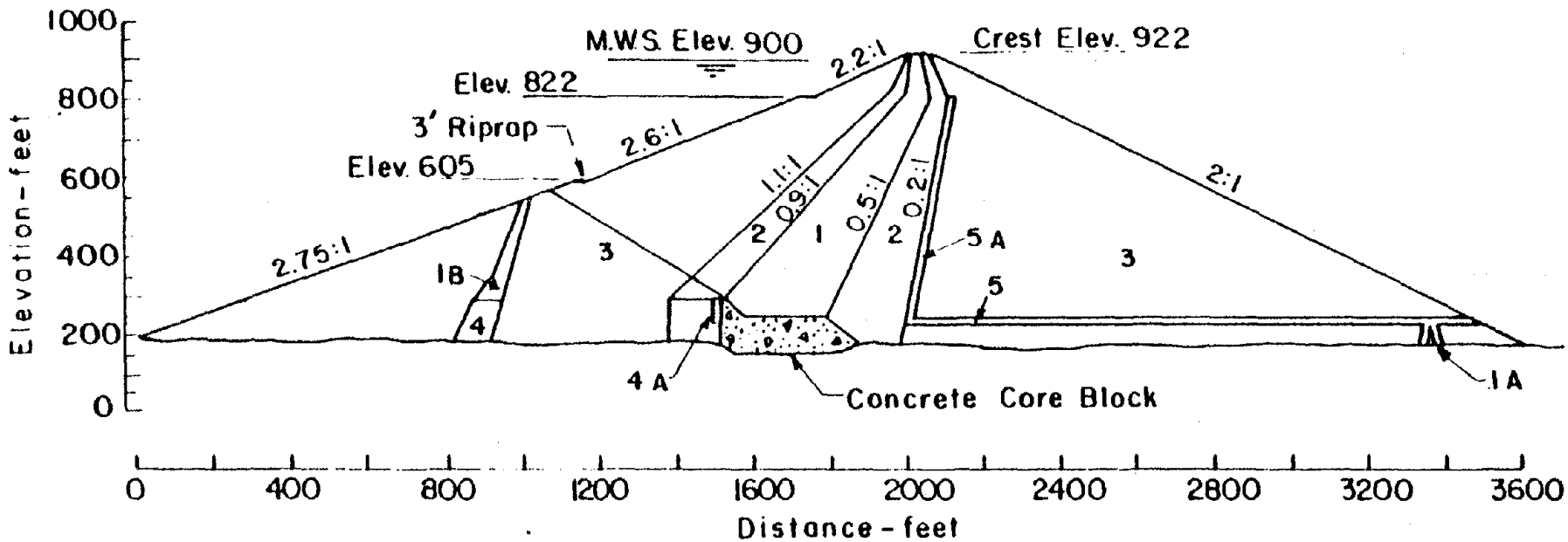

Zone	MATERIAL
1, 1A, 1B	Impervious Core
2	Transition
3	Pervious Shell
4, 4A	Impervious (Abutment Stripping)
5, 5A	Drain (Selected Shell)

Fig. 1-3 Oroville Dam Maximum Section.

activity registered during the Oroville earthquake series of 1975 raised the possibility of a 6.5 magnitude earthquake occurring at a hypocentral distance of less than 5 miles from the dam.

In view of the limitations of the pseudo-static method of stability analysis, the presence of a nearby fault, and the fact that the dam had been designed believing it was located in a low seismicity area, the Department of Water Resources decided to re-evaluate the seismic stability of Oroville Dam using the present state-of-the-art procedures (DWR, 1979; Banerjee et al., 1979). Two-dimensional finite element procedures were used to compute the dynamic stresses induced in the dam by the earthquake and an approximate method was used to account for the three-dimensional behavior of the dam.

The importance of Oroville Dam, the three-dimensional nature of its dynamic response, the fact that extensive data on material properties as well as records of the response of the dam to the August 1, 1975 Oroville earthquake exist, make the dam an excellent example on which to test the applicability of three-dimensional dynamic analysis procedures.

1.4 Objectives and Organization

The number of earth dams built in narrow canyons in seismically active areas is substantial and continues to increase with time. A limited amount of work has been done to date to study the dynamic response of dams where three-dimensional behavior is predominant. It seems desirable therefore, to develop numerical techniques for the three-dimensional dynamic analysis of earth dams and to study the response of dams where 3-D effects are of importance. This is the purpose of the

work presented in this report, the objectives of which can be summarized as follows:

1. Further development and implementation of existing finite element analysis techniques to perform three-dimensional dynamic analysis of earth dams.

2. Application of these techniques to the computation of the response of the Oroville Dam to the August 1, 1975 Oroville earthquake in order to back-calculate the dynamic material properties of the dam.

3. Study of the dynamic response characteristics of earth dams where three-dimensional effects are of concern in order to gain further understanding of their behavior.

4. Evaluation of the applicability of two-dimensional analysis to the computation of dynamic response of three-dimensional structures.

5. Study of the influence of element size in the cross-valley direction on the computed dynamic 3-D response of earth dams.

The work carried out to meet the above objectives is discussed in the following chapters.

Chapter 2 contains a brief description of the numerical procedures used during the course of this work. The components of three-dimensional finite element dynamic analysis procedures for earth dams as well as the modifications introduced into existing computer programs to perform such analysis are described.

The response of the Oroville Dam to the August 1, 1975 Oroville

earthquake is investigated using a 3-D model in Chapter 3. An assessment of the dynamic material properties of the dam is made by back-calculation from recorded field behavior during the Oroville earthquake.

Chapter 4 describes in terms of certain dynamic response parameters the results of three-dimensional dynamic analyses of the Oroville Dam and a fictitious dam with a ratio L/H equal to 2 (see Fig. 1-1(b)). Two earthquake records were used in these computations: The Oroville Reanalysis earthquake and the August 1, 1975 Oroville earthquake.

An evaluation of the applicability of 2-D analysis to compute the 3-D response of earth dams is made in Chapter 5. Comparisons in terms of computed accelerations and shear stresses between 2-D analysis of the maximum section and the quarter section and 3-D analysis of the entire structure are presented. The use of a modified stiffness in a two-dimensional analysis to simulate three-dimensional response is also studied.

Chapter 6 describes an investigation of the effects on the computed response of varying the number of elements in the cross-valley direction in the three-dimensional analysis of earth dams.

Finally, a summary of conclusions as well as recommendations for future research is presented in Chapter 7.

CHAPTER 2

METHODS OF ANALYSIS

2.1 Introduction

One of the first attempts to model analytically the dynamic response of earth dams was reported by Mononobe et al.(1936) who used the shear beam method of analysis to obtain analytical expressions for the natural frequencies and mode shapes of vibration of a dam. The same approach was later used by Ambraseys (1967) to find expressions for the seismic coefficient used in the pseudo-static method of analysis.

Introduction of the finite element method by Turner et al.(1956) led the way for the development of a tool with greater flexibility to handle nonhomogeneities, irregular model boundaries and complex material behavior. Chopra (1966) performed two-dimensional finite element analyses of earth dams and computed stress distributions, natural frequencies and mode shapes of vibration. Modal analysis was used to solve the equations of motion and a linear elastic material with viscous damping was used to model the soil behavior.

Idriss and Seed (1967) introduced the equivalent linear method to account for the strong nonlinear behavior of soils during earthquakes. Using step by step integration procedures (Wilson and Clough, 1962), and the equivalent linear method, Idriss et al.(1973) developed two-dimensional finite element procedures to evaluate the dynamic response of soil structures. Nonhomogeneous damping arising from the presence of different materials and different levels of induced strain was accounted

for by the use of Rayleigh damping. Although this form of damping tends to damp out the higher frequencies it does not affect the frequency range to which earth dams respond strongly.

Using a different type of approach, Lysmer et al.(1974, 1975), used the complex response method of analysis to permit variations in modulus and damping in different elements of a finite element model. The equations of motion were solved in the frequency domain. This numerical procedure was extended partially to three dimensions by Kagawa (1977) and later further extended by the author. It constitutes the subject of the present chapter which is composed of two sections.

The first section briefly describes the assumptions inherent in the analytical model, the equations of motion, the elements of the complex response method, and the elements of the equivalent linear method. Details of the finite element technique are not given since these can be found in standard textbooks on the subject (Zienkiewicz,1977).

A summary of the assumptions made by Kagawa (1977), an evaluation of these assumptions, and the modifications introduced by the author, are presented in the second section.

2.2 3-D Dynamic Finite Element Analysis.

The response of an earth dam to seismic loading is a complex phenomenon which is difficult to model analytically. The first approximation that has to be made is that of modelling a continuum system with a finite number of degrees of freedom. For open systems, such as earth dams, difficulties are encountered in the definition of the model

boundaries and in the characterization of the earthquake motions at these boundaries. Interaction between the dam and its abutments and between the dam and the reservoir is also difficult to assess. Although a substantial amount of work has been done on the characterization of material behavior, general and practical expressions for constitutive laws are also still lacking. In view of these difficulties, assumptions need to be made in order to simplify the problem.

Within the framework of the finite element techniques described in this chapter a typical earth dam will be modeled by an assemblage of elements as shown in Fig. 2-1. Eight node isoparametric brick elements with three degrees of freedom per node and linear displacement interpolation functions are used in the model.

It is assumed that the walls of the canyon are rigid and therefore all points on these boundaries move in phase and with the same displacement amplitudes. The validity of this assumption depends on several factors including: (1) the relative stiffness of the materials comprising the canyon walls and the dam, (2) the geometry of the canyon, (3) the size of the dam, and (4) the frequency range of interest in the analysis.

Trifunac (1973) studied the scattering of plane SH waves by a semi-cylindrical canyon and concluded that for wave-lengths shorter than 4 times the radius of the canyon significant differences in displacement amplitude and phase angle can be found between different points on the walls of the canyon. A similar study was performed by Bouchon (1973) who investigated the effects of topographic irregularities on surface motions. In the case of triangular canyons subjected to a train of

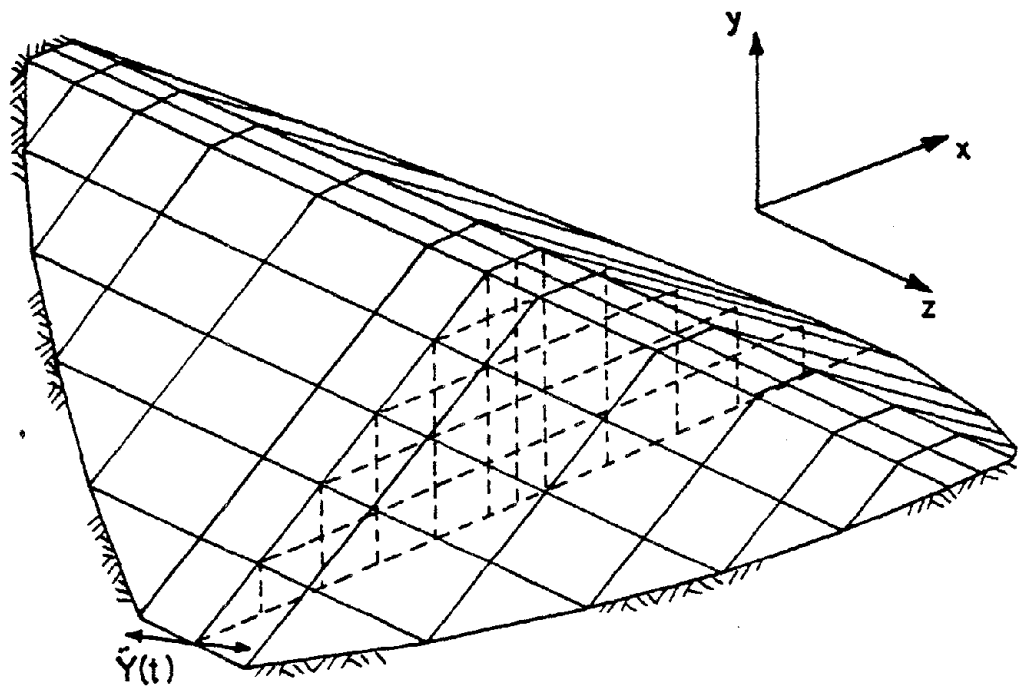

Fig. 2-1 Typical 3-D Finite Element Model of an Earth Dam.

incident P,SV and SH waves, differences in normalized maximum displacements at different points on the canyons slopes were found to be as large as 50%. These effects were also found to depend strongly on the geometry of the canyons.

Considering the present state of knowledge concerning earthquake ground motions and the computational difficulties involved in handling large numbers of degrees of freedom, the assumption of a rigid boundary seems to offer the most practical approach for the analysis of earth dams of moderate size, subjected to strong motions, and founded in competent rock canyons.

Considerations of dynamic equilibrium of the model shown in Fig. 2-1 lead to the following equations of motion:

$$[M]\{\ddot{U}\} + [K]\{U\} = -[M]\{r\}\ddot{y}(t) \qquad (2-1)$$

where:

$\{U\}$ = the nodal point displacements relative to the rigid boundary.

$\{\ddot{U}\}$ = the corresponding accelerations.

$[K]$ = the complex stiffness matrix.

$[M]$ = the mass matrix.

$\ddot{y}(t)$ = the input rigid boundary acceleration.

{r} = the load vector that gives the direction of the input motion.

The mass and stiffness matrices are assembled from the corresponding element matrices following standard finite element procedures and the direct stiffness method (Zienkiewicz, 1977). Viscous damping is introduced by the use of complex moduli in forming the element stiffness matrices

$$G^* = G(1 - 2B^2 + 2iB\sqrt{1 - B^2}) \qquad (2\text{-}2)$$

where:

G = the element shear modulus.

B = the element fraction of critical damping.

and thus the stiffness matrix for the system will have complex coefficients.

Equation (2-1) is solved using the complex response method which assumes that the system is linear and that the input motion is periodic and can therefore be written as:

$$\ddot{y}(t) = \mathrm{Re} \sum_{s=0}^{N/2} \ddot{Y}_s \exp(i\omega_s t) \qquad (2\text{-}3)$$

where:

N = the number of digitized points in the input motion.

$$\omega_s = \frac{2\pi s}{N\Delta t} \tag{2-4}$$

Δt = the time step of digitization.

$\ddot{Y}_s$ = the complex Fourier amplitudes given by:

$$\ddot{Y}_s = \frac{1}{N}\sum_{k=0}^{N-1} \ddot{y}_k \exp(-i\omega_s k\Delta t) \qquad \text{for } s=0,\ s=N/2 \tag{2-5a}$$

$$\ddot{Y}_s = \frac{2}{N}\sum_{k=0}^{N-1} \ddot{y}_k \exp(-i\omega_s k\Delta t) \qquad \text{for } 1 \leq s < N/2 \tag{2-5b}$$

The complex Fourier amplitudes, $\ddot{Y}_s$, can be computed efficiently using the Fast Fourier Transform algorithm devised by Cooley and Tukey (1965) which requires that N be a power of 2. This requirement is usually not a drawback since trailing zeroes must also be added to let damping in the system eliminate free vibrations that would otherwise interfere with adjacent cycles of the periodic motion.

Substitution of equation (2-3) into equation (2-1) leads to:

$$[M]\{\ddot{U}\} + [K]\{U\} = -[M]\{r\}\ \mathrm{Re}\sum_{s=0}^{N/2} \ddot{Y}_s \exp(i\omega_s t) \tag{2-6}$$

the steady state solution of which can also be expressed as a sum of harmonics:

$$\{U\} = \mathrm{Re} \sum_{s=0}^{N/2} \{U_s\}\exp(i\omega_s t). \tag{2-7}$$

The complex amplitudes $\{U_s\}$ can be obtained by substituting the above expression into equation (2-6) leading to:

$$([K] - \omega_s^2[M])\{U_s\} = -[M]\{r\}\ddot{Y}_s \tag{2-8}$$

which is a system of linear algebraic equations with complex coefficients and can be solved by Gauss elimination.

Solution of equation (2-8) for each frequency ω_s is impractical however, and therefore the following equation is solved instead:

$$([K] - \omega_s^2[M])\{A_s\} = -[M]\{r\}. \tag{2-9}$$

After selecting a cut-off frequency, the above expression is solved for a limited number of frequencies and a special interpolation technique is used to compute intermediate values of $\{A_s\}$. The displacement amplitudes can then be obtained from:

$$\{U_s\} = \{A_s\}\ddot{Y}_s. \tag{2-10}$$

Linear interpolation on the inverse of the amplification functions has been used in the past (Lysmer et al., 1974, 1975) as the technique to obtain intermediate values of $\{A_s\}$. In the case of three-dimensional systems where there is a closer spacing between natural frequencies than in two-dimensional systems this interpolation scheme has not proven to work reliably.

A more sophisticated technique developed by Tajirian (1981) makes use of the transfer function for a two-degree-of-freedom system to interpolate between the amplification function values $\{A_s\}$ and is used in the formulation described herein. The two-degree-of-freedom transfer function typically has two frequency peaks (see Fig. 2-2), and is completely defined by five points as can be concluded by examining its analytical expression:

$$A(\omega) = \frac{C_1\omega^4 + C_2\omega^2 + C_3}{\omega^4 + C_4\omega^2 + C_5} \qquad (2\text{-}11)$$

where:

ω = angular frequency.

$C_1, C_2, C_3, C_4, C_5,$ = complex constants.

The values of the amplification function $\{A_s\}$ at five particular frequencies spanning the range where interpolation is to be performed are necessary to determine the five constants that define the transfer function, which is then used to compute intermediate values of $\{A_s\}$. This interpolation scheme works very well even in the case of two close

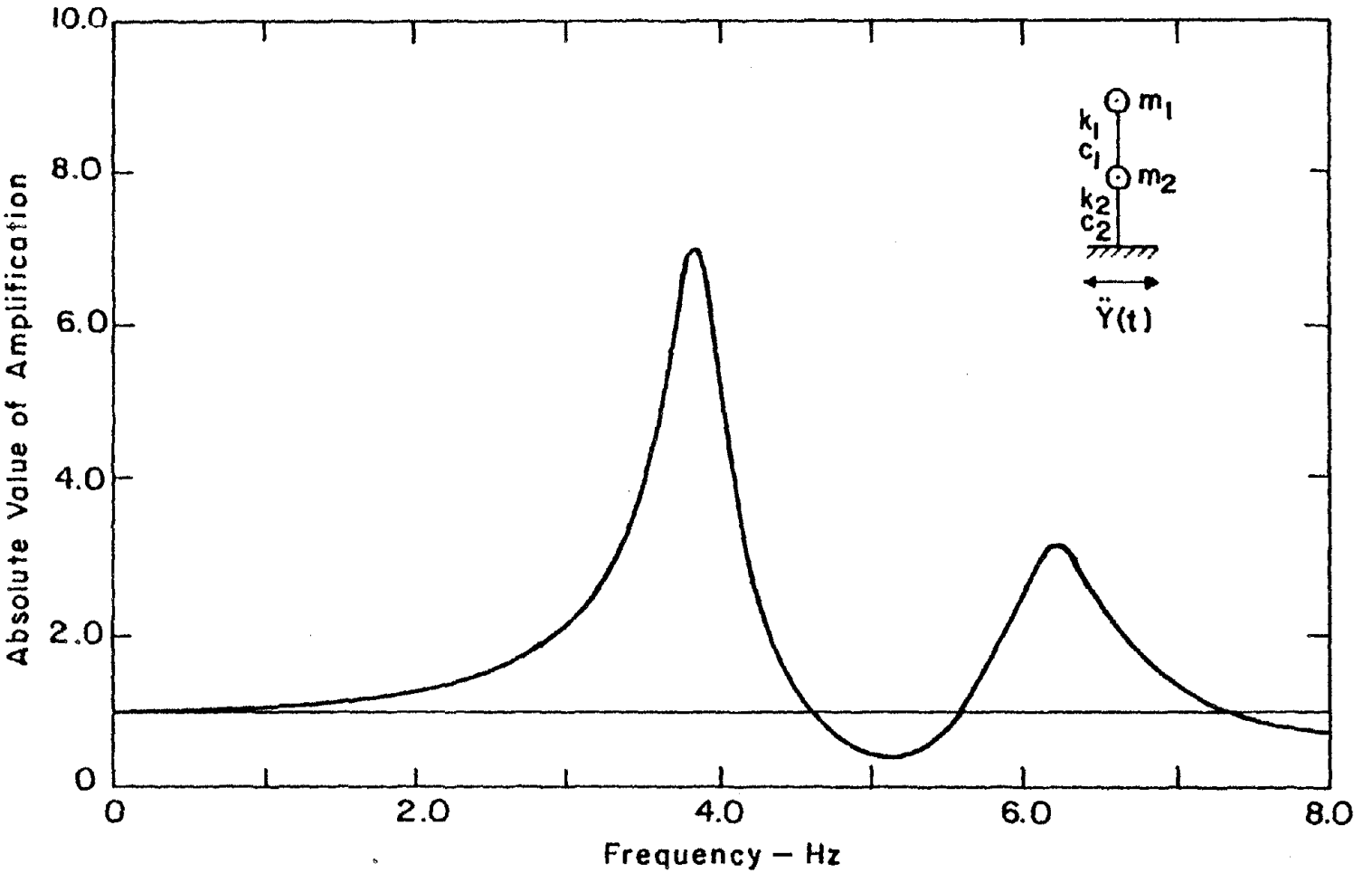

Fig. 2-2 Transfer Function Characteristic of a Two Degree of Freedom System.

frequency peaks and therefore is a more flexible tool than the inverse linear technique.

Computation of the nodal displacements {U} from equation (2-7) completely defines the response of the model. Other response parameters like velocities, accelerations and strains can be directly computed in the frequency domain from the displacement amplitudes $\{U_s\}$ and can then be transformed into the time domain.

Due to the extensive use of superposition, the procedures previously outlined are strictly valid only for linear systems. It is well known, however, that the response of soils to dynamic loading is highly non-linear in nature and must be accounted for in order to obtain meaningful results from the dynamic analysis of soil structures.

An approximate method that takes into account the non-linear behavior of soils has been presented by Idriss and Seed (1967). According to this method the non-linear response, in terms of relative displacements, of a soil structure can be approximated by a linear analysis for which the stiffness and damping are compatible with the induced strains at every point of the system.

The hysteretical stress-strain behavior of soils is schematically illustrated in Fig. 2-3 which also shows how to represent this behavior by an equivalent linear modulus and an equivalent fraction of damping. An extensive summary of data on strain compatible moduli and damping for clays and sands was presented by Seed and Idriss (1970) from which the curves in Fig. 2-4 were developed. Starting from selected initial moduli an damping values for each element in the model, these curves can

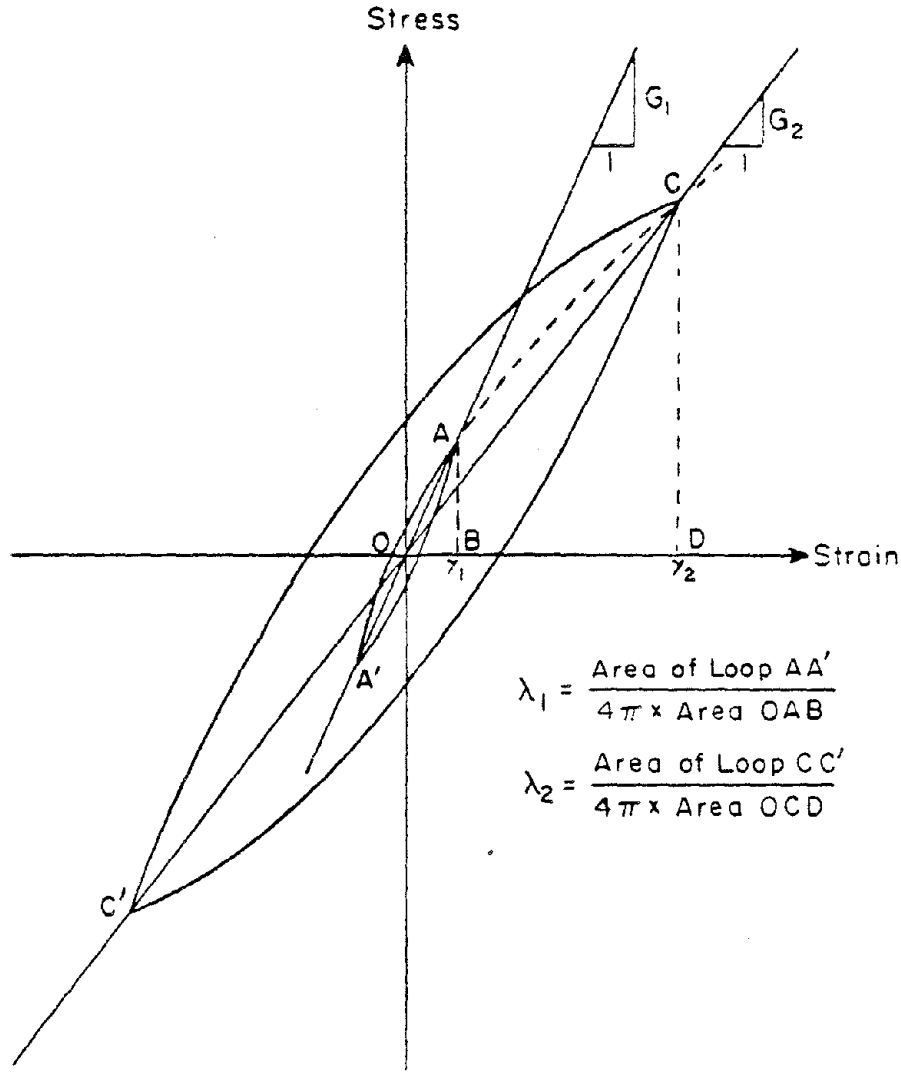

Fig. 2-3 Hysteretic Stress-strain Behavior at Different Strain Amplitudes.

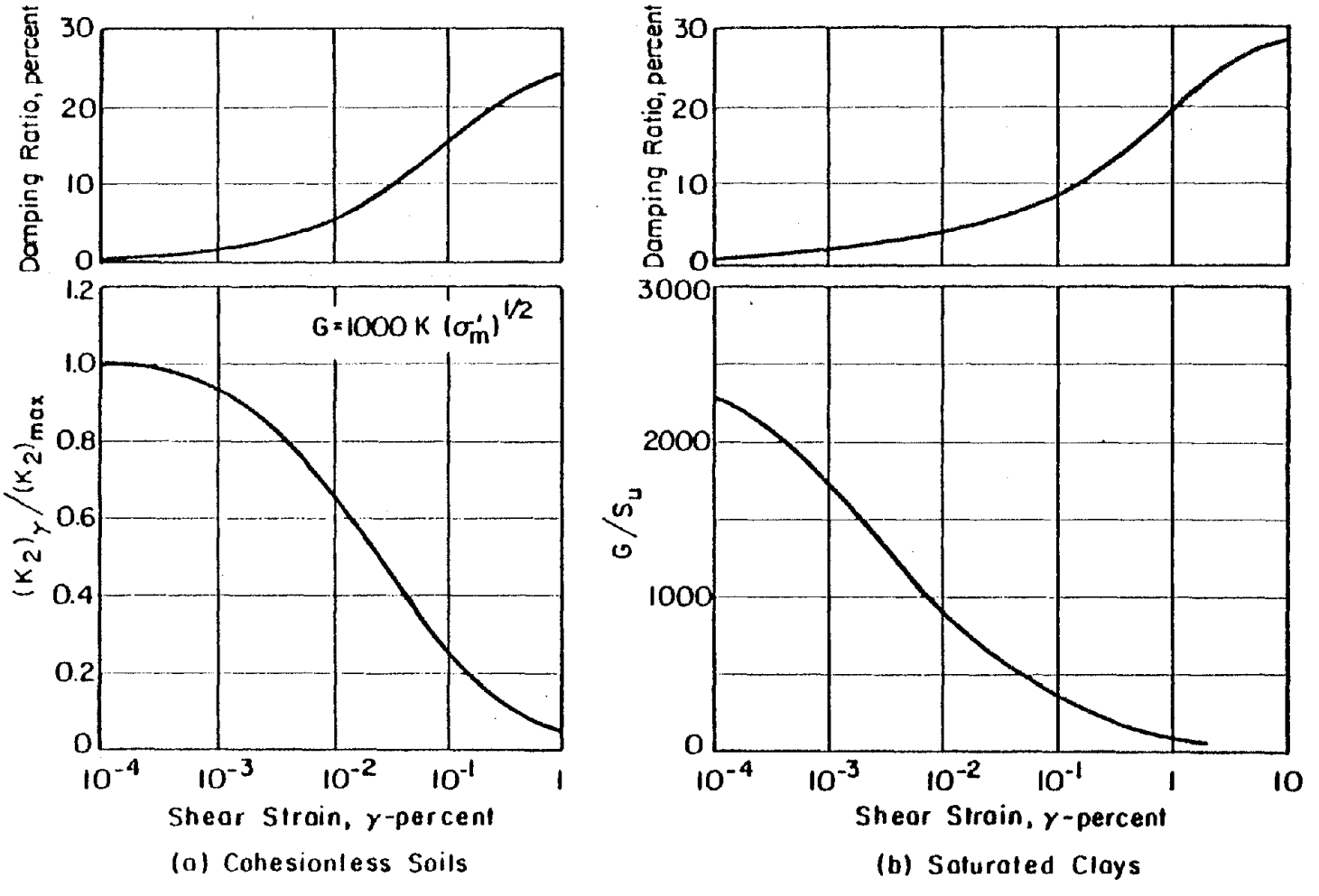

Fig. 2-4 Average Shear Moduli and Damping Characteristics of Soils.

be used iteratively to reach compatibility between the properties used in the analysis and the computed strains.

The three-dimensional strain state at a point can be described by a second order strain tensor with 6 independent terms which in a Cartesian coordinate system can be written as:

$$\underline{e} = \begin{pmatrix} e_{xx} & e_{xy} & e_{xz} \\ e_{yx} & e_{yy} & e_{yz} \\ e_{zx} & e_{zy} & e_{zz} \end{pmatrix} \qquad (2\text{-}12)$$

During the seismic response of a dam the strain state varies with time at each point and therefore the selection of a single value to represent both the directional and time variation of strain level is difficult.

Soils are materials with complex constitutive behavior which, strictly speaking, depends on all terms in expression (2-12). However, the state of present knowledge on constitutive laws for soils does not permit a complete characterization of material behavior. Seed and Idriss (1970) used the maximum shear strain as indicative of strain level. Griffin and Houston (1980) have presented data from coupled cyclic torsional and triaxial tests on sands and have related the secant shear modulus to octahedral strain.

In the procedures described herein the method proposed by Seed and Idriss (1970) will be adopted and therefore the strain level will be given by an effective shear strain defined as:

$$\gamma_{eff} = 0.65 \max_t |\gamma_{max}| . \qquad (2\text{-}13)$$

Time variation in the strain level is represented by the factor 0.65 which is purely empirical but is assumed to be indicative of an average time value of the maximum shear strain. The value of this factor is not critical, since the computed motions are not very sensitive to moderate variations in the estimate of the effective shear strain.

Two methods are available to compute the peak maximum shear strain that enters in equation (2-13). The first consists of obtaining the maximum and minimum principal strains in the time domain from a solution to the following equation for each time step and then computing the peak maximum shear strain.

$$\begin{vmatrix} e_{xx}-e & e_{xy} & e_{xz} \\ e_{yx} & e_{yy}-e & e_{yz} \\ e_{zx} & e_{zy} & e_{zz}-e \end{vmatrix} = 0 \qquad (2\text{-}14)$$

The second method makes use of the fact that the peak maximum shear strain can be estimated from the root-mean-square value of the maximum shear strain as follows:

$$\max_t |\gamma_{max}| \simeq c \cdot RMS(\gamma_{max}) \qquad (2\text{-}15)$$

where c is a constant approximately given by:

$$c = \max_t |y| / RMS(y). \qquad (2\text{-}16)$$

The root-mean-square values of y_{max} and y can be conveniently evaluated by making use of Parseval's identity which for an arbitrary function f(t) is given by:

$$RMS^2(f) = \frac{1}{2} \sum_{s=0}^{N/2} |F_s|^2 \qquad (2\text{-}17)$$

where F_s, s=0,1,2...N/2 are the complex Fourier amplitudes of the function f(t), that is:

$$f(t) = Re \sum_{s=0}^{N/2} F_s \exp(i\omega_s t). \qquad (2\text{-}18)$$

This method is substantially faster than the first one since equation (2-14) can be solved in terms of the strain amplitudes for each frequency and all computations are performed in the frequency domain without the need for numerous Fourier transforms.

2.3 Program Development

The analytical techniques described in the previous section are analogous to those used by Lysmer (1974,1975) in the development of two-dimensional finite element computer programs capable of analyzing dynamic soil-structure interaction problems as well as the dynamic response of soil structures. Kagawa (1977) modified the computer program LUSH (Lysmer, 1974) by replacing the plane strain 4-node isoparametric

quadrilateral element by an 8-node isoparametric brick element and thus gave it the capability of performing three-dimensional analyses of earth dams. In order to reduce computational costs an important restriction was imposed on the possible deformations of the dam by means of the following two assumptions:

1. The base motion was assumed to act within a plane parallel to the axis of the valley as shown by the x-y plane in Fig. 2-1.

2. No particle motion or deformation was allowed in the cross-valley direction of the dam. That is, all points in the dam were constrained to move in the x-y plane in Fig. 2-1, reducing in this way the number of degrees of freedom from three to two at each nodal point.

In order to evaluate the effects of these assumptions on the computed dynamic response of earth dams the results of an analysis with constrained degrees of freedom in the z direction (see Fig. 2-1) were compared with the results of an analysis with three degrees of freedom at each nodal point. A 100 foot high dam with 2:1 slopes, a constant shear wave velocity of 500 fps and located in a triangular canyon was selected for the above purpose. Crest length to height ratios, L/H, of 2, 3, and 6 were examined using the finite element model shown in Fig. 2-5. The structural analysis program SAPIV (Bathe et al., 1973) was used to obtain natural frequencies and mode shapes of vibration and to compute maximum displacements and stresses induced in the dam models by the first 15 sec. of the earthquake motions recorded at Taft during the 1952 Kern County earthquake.

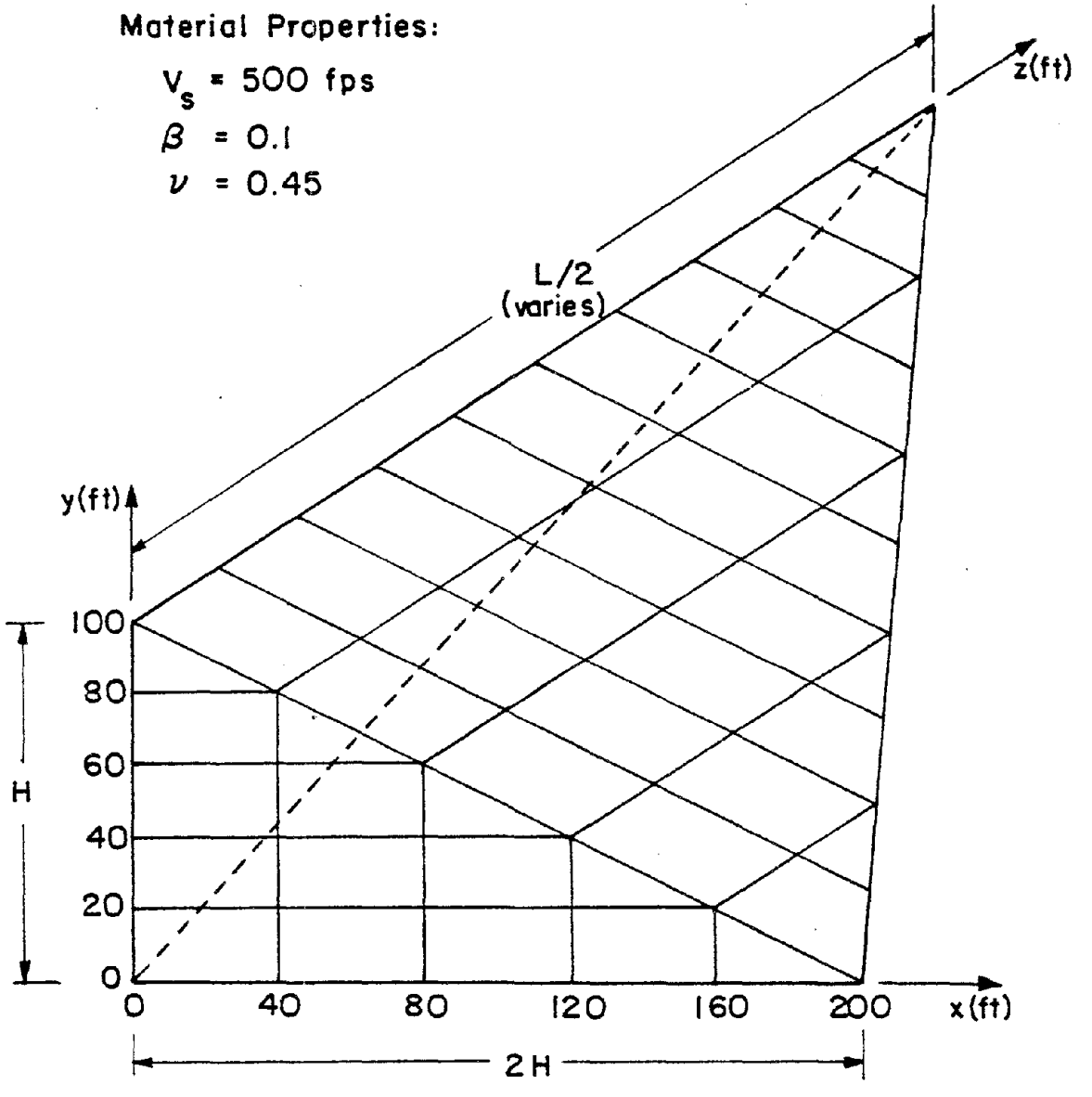

Fig. 2-5 Finite Element Model of Dam in Triangular Canyon.

Table 2-1 summarizes the computed natural frequencies for the first 10 modes of vibration of the models studied. The values computed for the free node case are compared with the values for the constrained node case (z deformations suppressed) for the three L/H ratios chosen. It is interesting to note the close spacing between natural frequencies and how this spacing decreases with increasing frequency number. From this observation it can be concluded that several modes of vibration will be accounted for in a frequency domain analysis with a cut-off frequency as low as 3 times the fundamental frequency of the dam. It can also be seen that a high order interpolation scheme is needed to interpolate on the amplification functions given the close spacing between natural frequencies.

The percent difference between computed natural frequencies for the free node and constrained node models is shown in table 2-2. It can be seen that constraining the z degrees of freedom (Fig. 2-5) increases the natural frequencies of the system by an average value of about 10 percent and that this difference shows an increasing trend with increasing L/H ratio. Differences in the computed peak displacements and peak horizontal shear stresses induced by the earthquake motions recorded at Taft are of the same order of magnitude and are somewhat higher than the differences in natural frequencies, as shown for the main section of the dam in Figs. 2-6 and 2-7. The results do not show any appreciable trend with varying L/H ratio and high differences, of the order of 50%, are occasionally found at scattered points in the dams.

The dynamic displacements and in general the dynamic response of a dam will be given by superposition of the individual contributions of

TABLE 2-1

NATURAL FREQUENCIES OF VIBRATION FOR DAM MODELS WITH FREE NODES AND CONSTRAINED NODES IN THE Z DIRECTION

	Natural Frequencies of Vibration in Hz.					
	L/H = 2		L/H = 3		L/H = 6	
Mode	Free Node	Constr. Node	Free Node	Constr. Node	Free Node	Constr. Node
1	3.03	3.14	2.60	2.71	2.18	2.28
2	4.66	4.72	4.19	4.31	3.02	3.27
3	5.16	5.26	4.30	4.51	3.34	3.87
4	5.43	5.95	4.51	5.01	3.75	4.00
5	5.85	6.10	5.00	5.61	3.82	4.44
6	6.23	6.95	5.32	5.89	4.18	4.53
7	6.44	7.09	5.58	6.06	4.26	4.59
8	6.98	7.40	5.69	6.57	4.34	4.70
9	7.08	7.76	5.89	6.84	4.55	4.97
10	7.10	7.92	6.08	6.99	4.59	4.99

TABLE 2-2

PERCENT DIFFERENCE BETWEEN COMPUTED NATURAL FREQUENCIES OF FREE NODE AND Z-CONSTRAINED NODE MODELS

Mode	L/H = 2	L/H = 3	L/H = 6
1	3.6	4.2	4.6
2	1.3	2.9	8.3
3	1.9	4.9	15.9
4	9.6	11.1	6.7
5	4.3	12.2	16.2
6	11.6	10.7	8.4
7	10.1	8.6	7.7
8	6.0	15.5	8.3
9	9.6	16.1	9.2
10	11.5	15.0	8.7

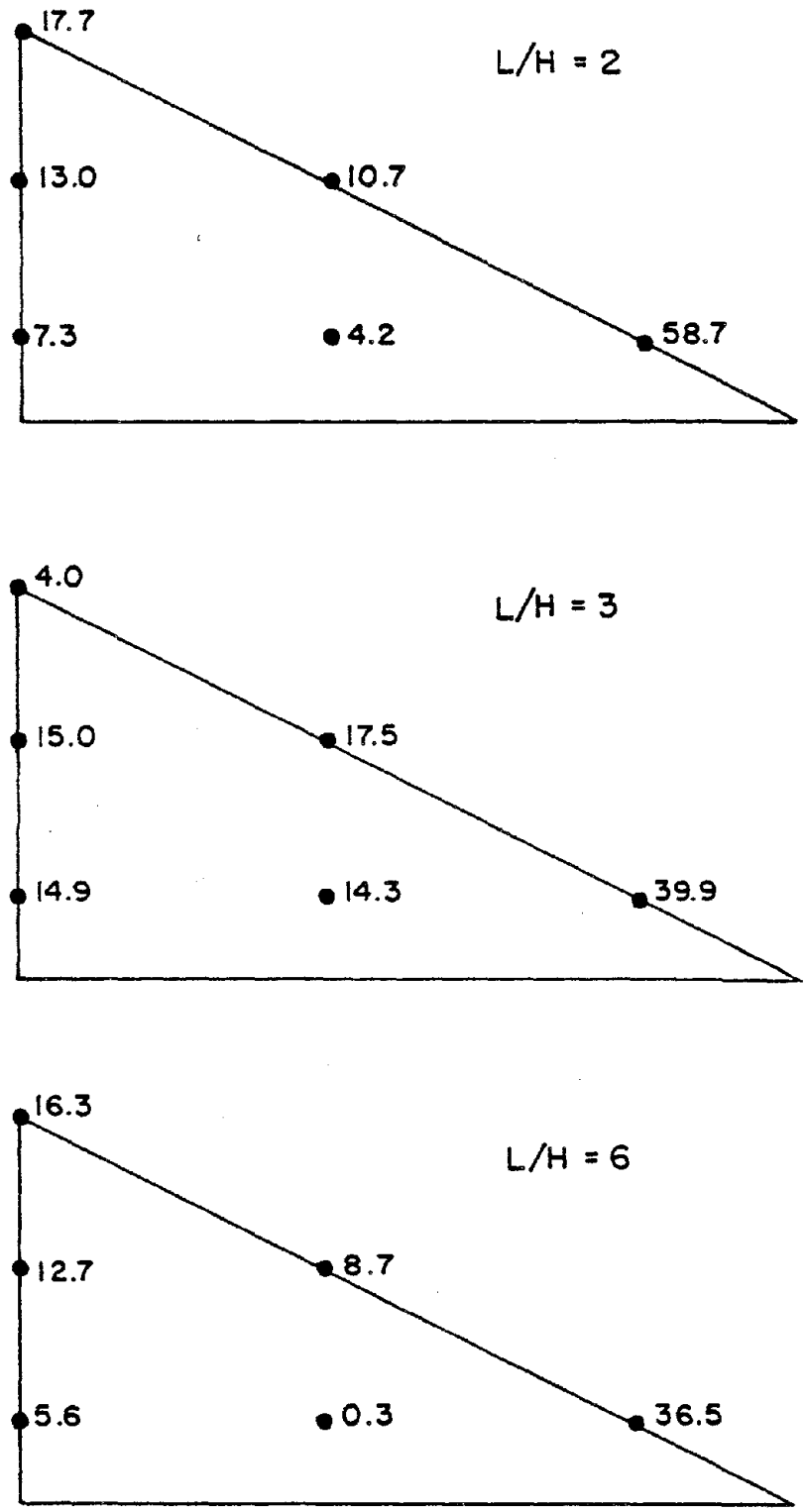

Fig. 2-6 Percent Differences Between Peak Horizontal Displacements of Free Node and Z-Constrained Node Models at Maximum Section.

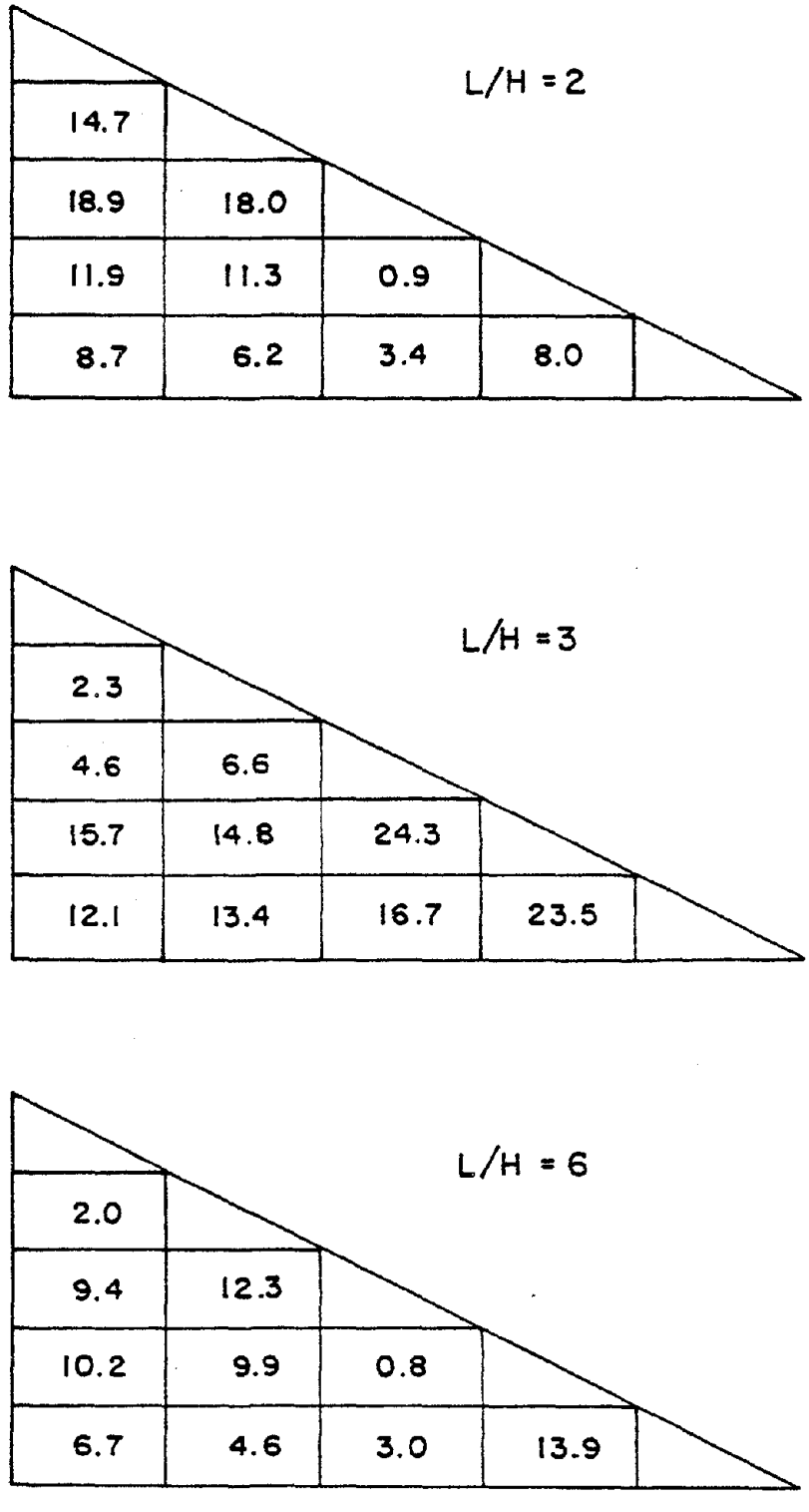

Fig. 2-7 Percent Differences Between Peak Horizontal Shear Stresses of Free Node and Z-Constrained Node Models at Maximum Section.

the natural mode shapes of vibration. The magnitude of the displacements in the z direction and their relative importance compared to displacements in other directions can therefore be assessed from an analysis of the natural mode shapes of vibration. For this reason and because the study of vibration modes will help to understand the 3-D dynamic behavior of earth dams, the mode shapes for the model with an L/H ratio of 3 have been computed.

The x,y and z displacements along the crest of the dam (see Fig. 2-5), along a line parallel to the z axis and with coordinates x=0 and y=60', and along a line parallel to the z axis and with coordinates x=80' and y=60', have been plotted for the first three modes of vibration. Figures 2-8, 2-9 and 2-10 show these displacements for the first, second and third modes respectively. All displacements have been normalized by the maximum displacement in the x direction for each mode. It can be seen that at the crest and along the line with coordinates x=0 and y=60' the displacements in the z direction are substantially smaller than those in the x direction (the y displacements are zero for these two lines) for the three modes studied. However, along the line with coordinates x=80' and y=60' the z displacements are comparable in magnitude to the x and y displacements especially in the second and third modes. This behavior is not surprising in view of the fact that the z displacements in the first few modes are due mostly to bending deformations of the dam.

The mid-section displacement patterns and the displacement patterns of a section located at a distance of 60 feet from the center of the dam, corresponding to the first, second and third modes of vibration are

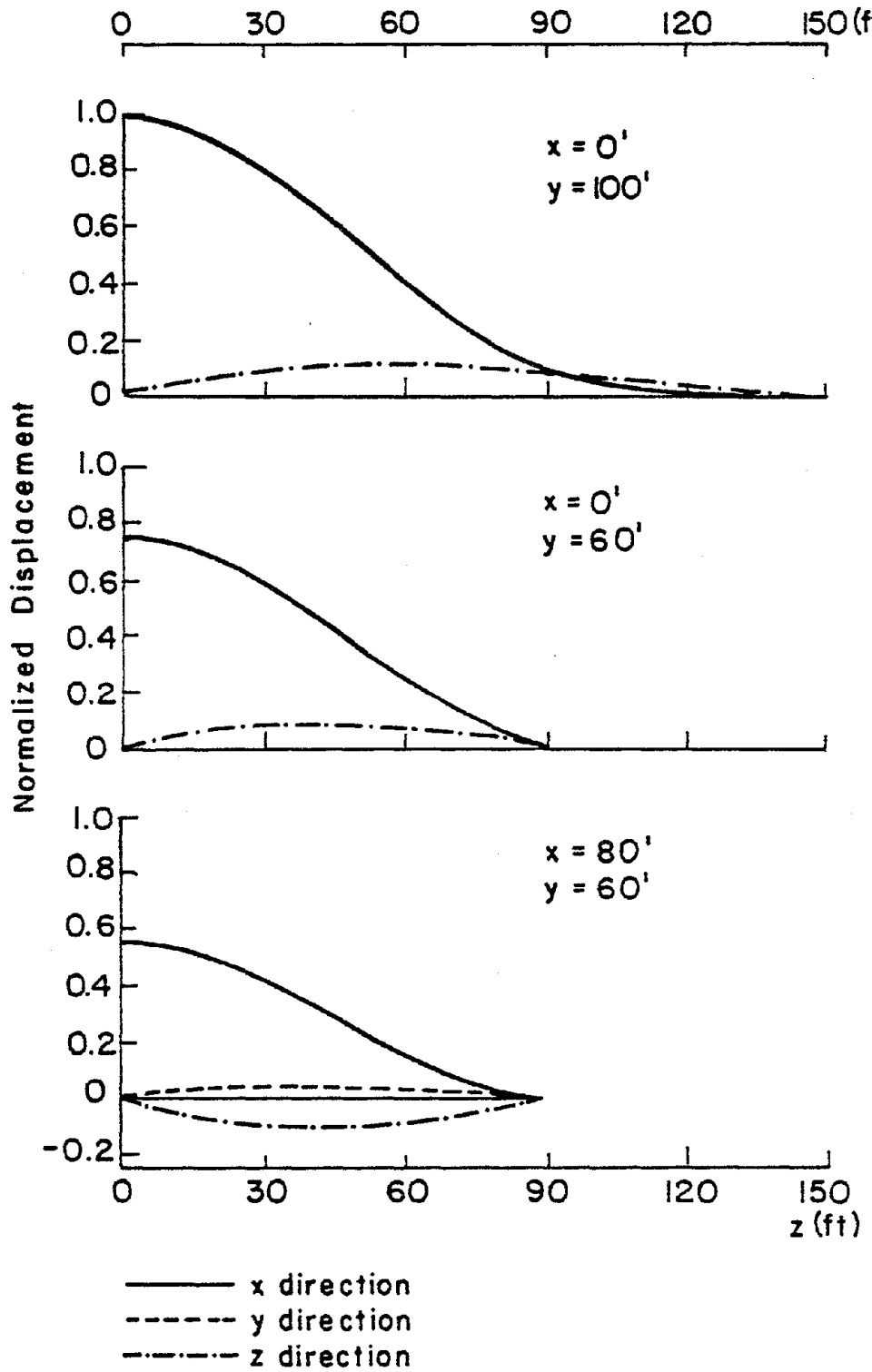

Fig. 2-8 Normalized Displacements Along Lines Parallel to the Z Axis for First Mode of Vibration of Dam with L/H = 3.

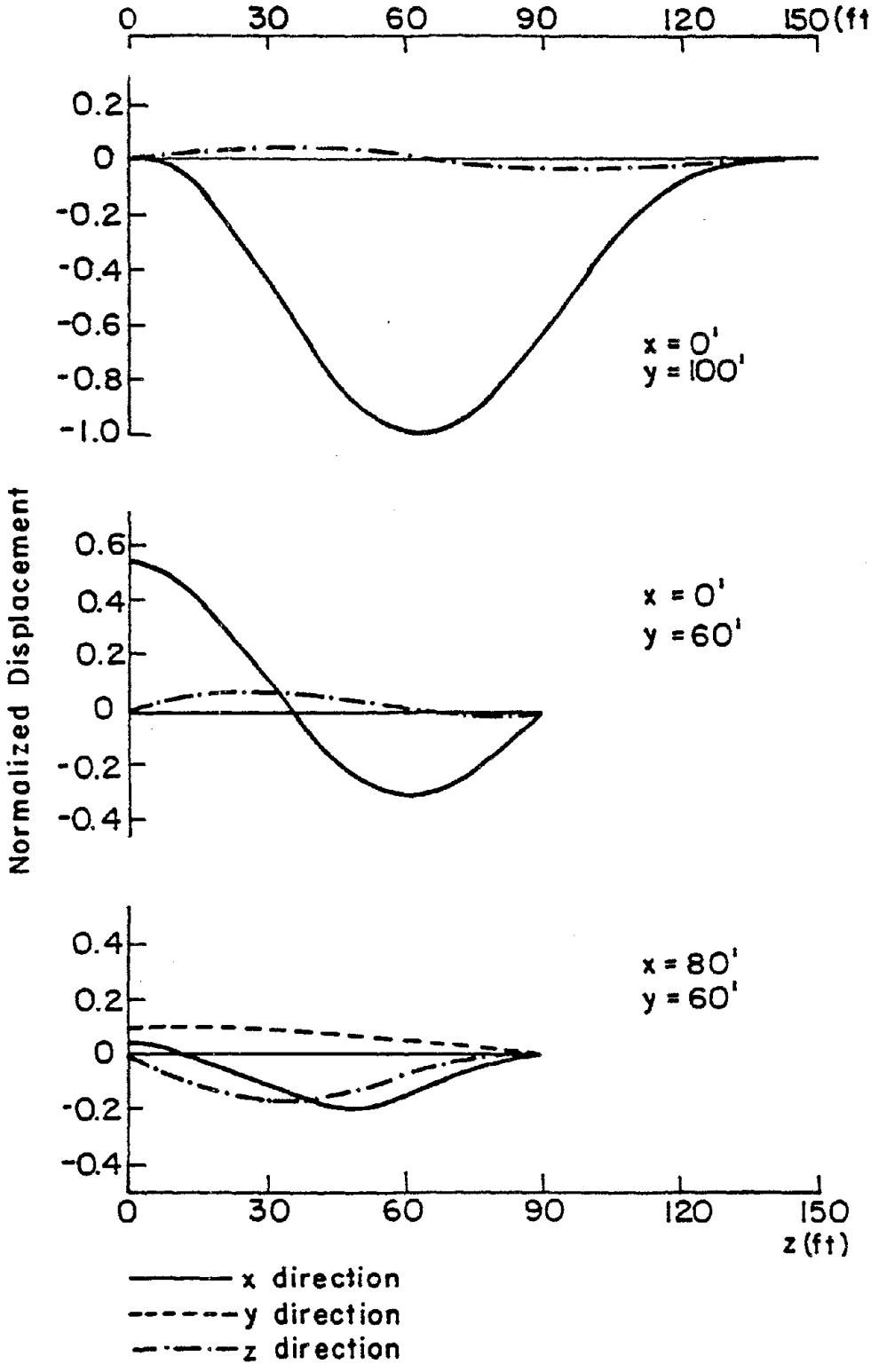

Fig. 2-9 Normalized Displacements Along Lines Parallel to the Z Axis for Second Mode of Vibration of Dam with L/H = 3.

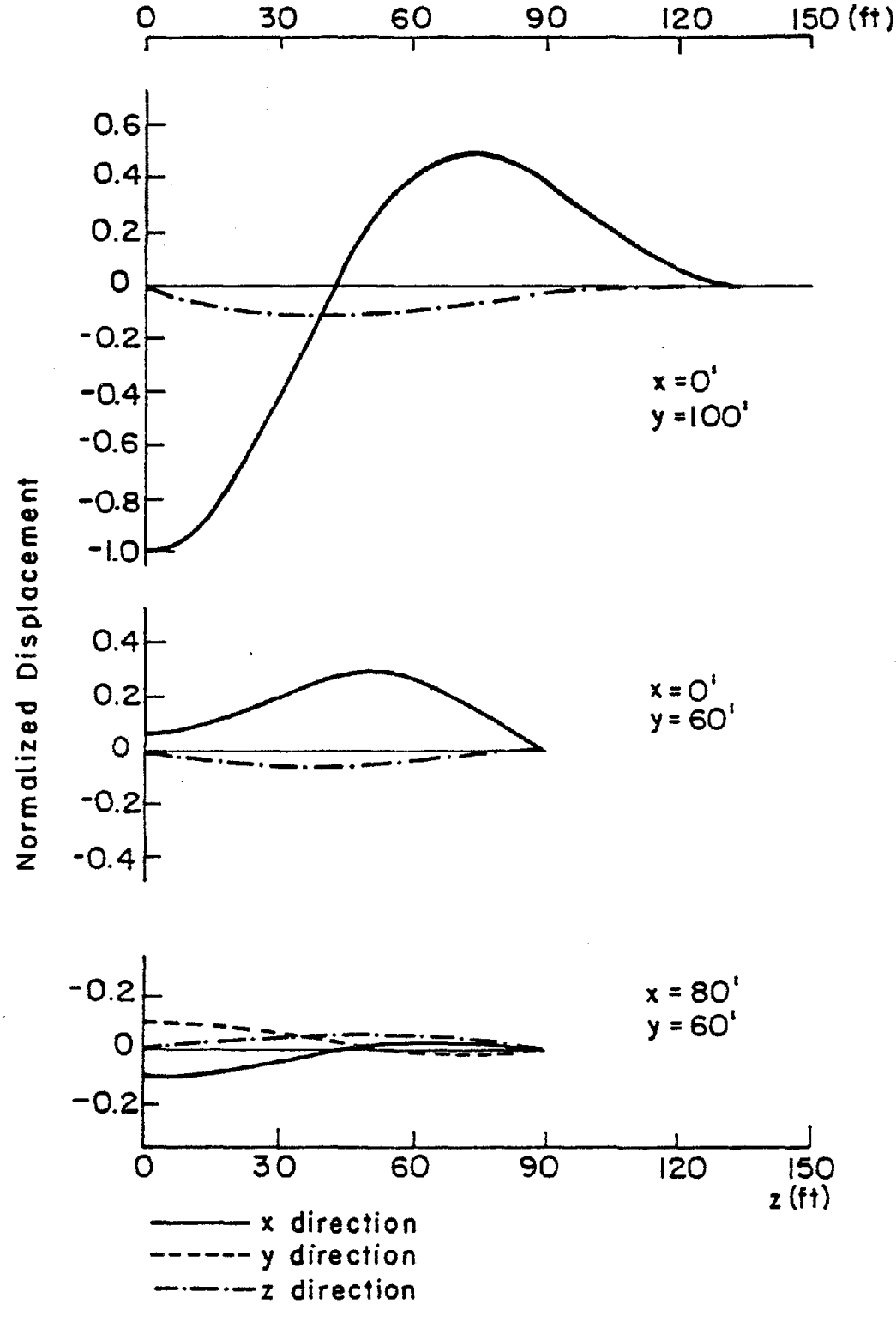

Fig. 2-10 Normalized Displacements Along Lines Parallel to the Z Axis for Third Mode of Vibration of Dam with L/H = 3.

shown in Figs. 2-11, 2-12 and 2-13 respectively.

From an analysis of the computed mode shapes the following observations can be made:

1. The displacements in the x, y and z directions are described by smooth curves on the z axis that generally show an increase in the number of points of inflection with increasing mode number.

2. The abutment ends of the dam (about 20% of the crest length) do not seem to show appreciable displacements in the lower modes of vibration.

3. The displacements in the z direction can be as large as the displacements in the x direction in the lower zones of the slopes of the dam but are generally smaller near the crest.

4. The mid-section displacement patterns resemble those for an infinitely long dam and therefore might be approximated by a plane strain analysis of the main section.

5. The variation of displacements in the z direction for the first few modes can be reasonably well fitted with a few (5 to 8) elements in the cross-valley direction.

On the basis of the preceding discussion and the results obtained from the comparison between computed stresses and displacements, with and without degrees of freedom in the z direction, it seems that the assumption of negligible z displacements might considerably affect the computed response of a dam. In order to account for these displacements, the computer program developed by Kagawa (1977) was modified by

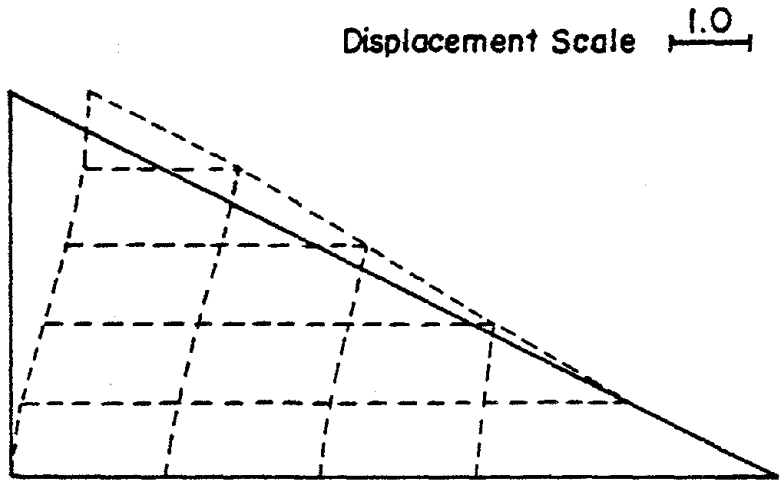

(a) Main section of dam

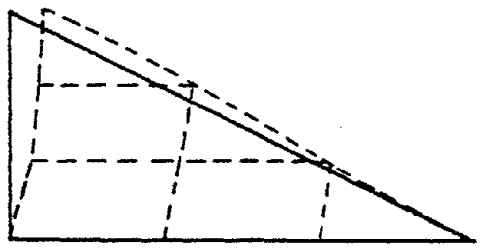

(b) Section at 60 feet from center of dam

Fig. 2-11 First Mode Normalized Displacement Pattern for Two Sections of Dam With L/H =3.

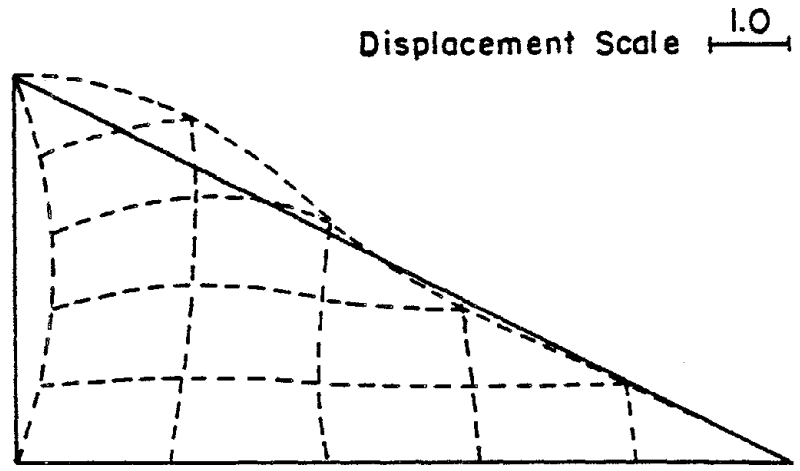

(a) Main section of dam

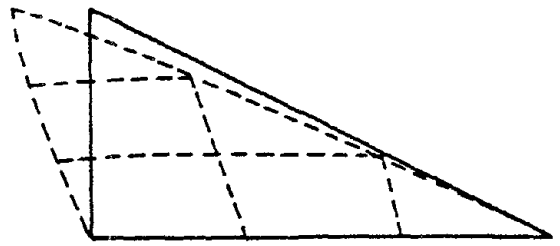

(b) Section at 60 feet from center of dam

Fig. 2-12 Second Mode Normalized Displacement Pattern for Two Sections of Dam With L/H = 3.

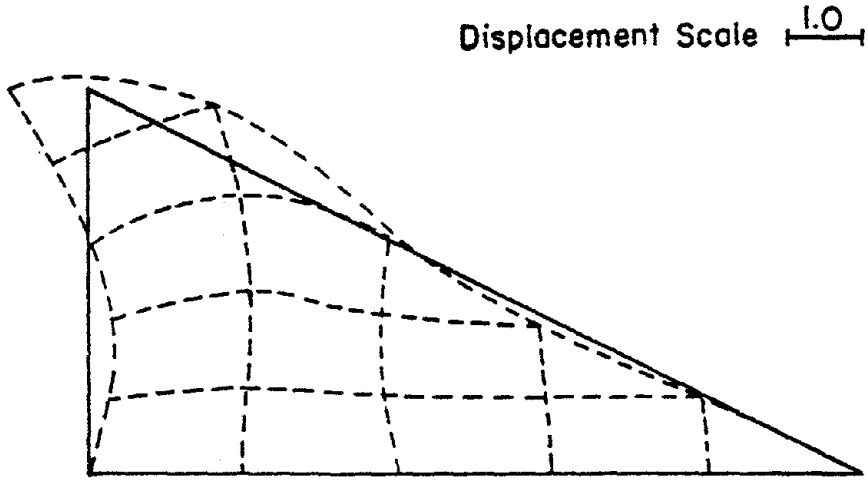

(a) Main section of dam

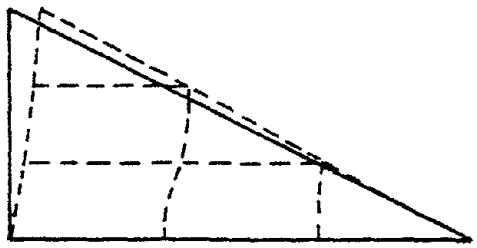

(b) Section at 60 feet from center of dam

Fig. 2-13 Third Mode Normalized Displacement Pattern for Two Sections of Dam with L/H = 3.

the authors and will be used in this updated form in the applications to be described in the following Chapters.

CHAPTER 3

RESPONSE ANALYSIS OF OROVILLE DAM FOR THE AUGUST 1, 1975 OROVILLE EARTHQUAKE

3.1 Introduction

The August 1, 1975 Oroville earthquake surprised the engineering profession due to the fact that it occurred in an area considered to be of low seismicity and disclosed the existence of a previously unidentified fault. The earthquake was assigned a magnitude of 5.7 on the Richter scale and its epicenter was located 5 miles south of the city of Oroville. From the trace at the surface and the coordinates of the hypocenter it was possible to define the fault plane which generated the earthquake and which appears to extend under the Oroville dam site. Available evidence suggests that this fault, known as the Cleveland Hill Fault, is capable of generating a magnitude 6.5 earthquake within the lifetime of the Oroville dam facilities. Although the embankment had an excellent performance during the 1975 Oroville earthquake series, the disastrous consequences of a failure pointed out the need for a re-evaluation of dynamic stability under the new seismic design conditions.

Construction of the dam took place between 1963 and 1967 and numerous geotechnical investigations were carried out during the design, construction and post-construction stages of the project. A substantial amount of data has been collected on the properties that characterize the static behavior of the shell materials and core materials (Marachi et al., 1969, Becker et al., 1972, DWR, 1969). Large scale triaxial and plane strain tests were used in order to test representative samples of

the shell material at the confining pressures expected to develop in the prototype. One of the significant results found during these investigations is that particle size does not have a strong influence on the static strength of cohesionless materials. Therefore, the static strength of coarse gravels and rockfill materials may be assessed in the laboratory from model gradation tests.

The dynamic properties of the dam shell materials have also been studied in recent years. Wong (1971) and Banerjee et al., (1979) determined liquefaction, dynamic stiffness and damping characteristics of model gradations of the Oroville gravels with the use of 12" diameter cyclic triaxial tests. However, as reported by Wong and indicated by other studies (Seed and Idriss, 1970), the shear moduli of cohesionless materials is strongly dependent on grain size. This means that in order to reliably assess the dynamic stiffness characteristics of the Oroville dam shell materials, large scale (36" diameter) dynamic tests would be necessary. Such tests are not feasible at the present time and would be extremely impractical.

Alternative approaches to determine the dynamic shear moduli necessary in a dynamic analysis of the embankment are the measurement of in-situ shear wave velocities and back-calculation from recorded field behavior. In fact, this last approach offers the most reliable procedure for determining dynamic properties that can subsequently be used in computing the response of the embankment dam to other earthquake motions. The procedure is basically one of trial and error in which different sets of dynamic properties are used in computing the response of the dam to earthquake motions for which the recorded response is

available. Those properties that yield the best match between computed and recorded response are representative of the in-situ dynamic properties of the dam materials.

The purpose of this chapter is to present the results obtained when using such a procedure to estimate the dynamic properties of Oroville Dam. A three-dimensional model was used to compute the dynamic response of the dam to the motions recorded during the August 1, 1975 Oroville earthquake for different sets of assumed dynamic properties. The computed response was then compared with the recorded response.

The following section presents a brief account of the performance of the dam during the 1975 Oroville earthquake. Previous studies to determine the dynamic properties of the shell materials, the results of static stress analyses of the dam and the results of the trial and error procedure to determine the dynamic properties of the dam are included in subsequent sections.

3.2 Performance of Oroville Dam During the August 1, 1975 Oroville Earthquake

Oroville dam is perhaps one of the most heavily instrumented dams in the U.S.A. The dynamic instrumentation of the dam at the time of the August 1, 1975 Oroville earthquake included 6 pore pressure cells, 4 strong motion accelerometers and 15 soil stress cells, as shown in Fig. 3-1. Additionally, the U.S.G.S. had installed accelerometers at the crest of the dam (at the same location as the DWR instrument), in the grout gallery and at the seismographic station, ORV, located at a distance of 1 mile from the dam. The instruments placed at the dam

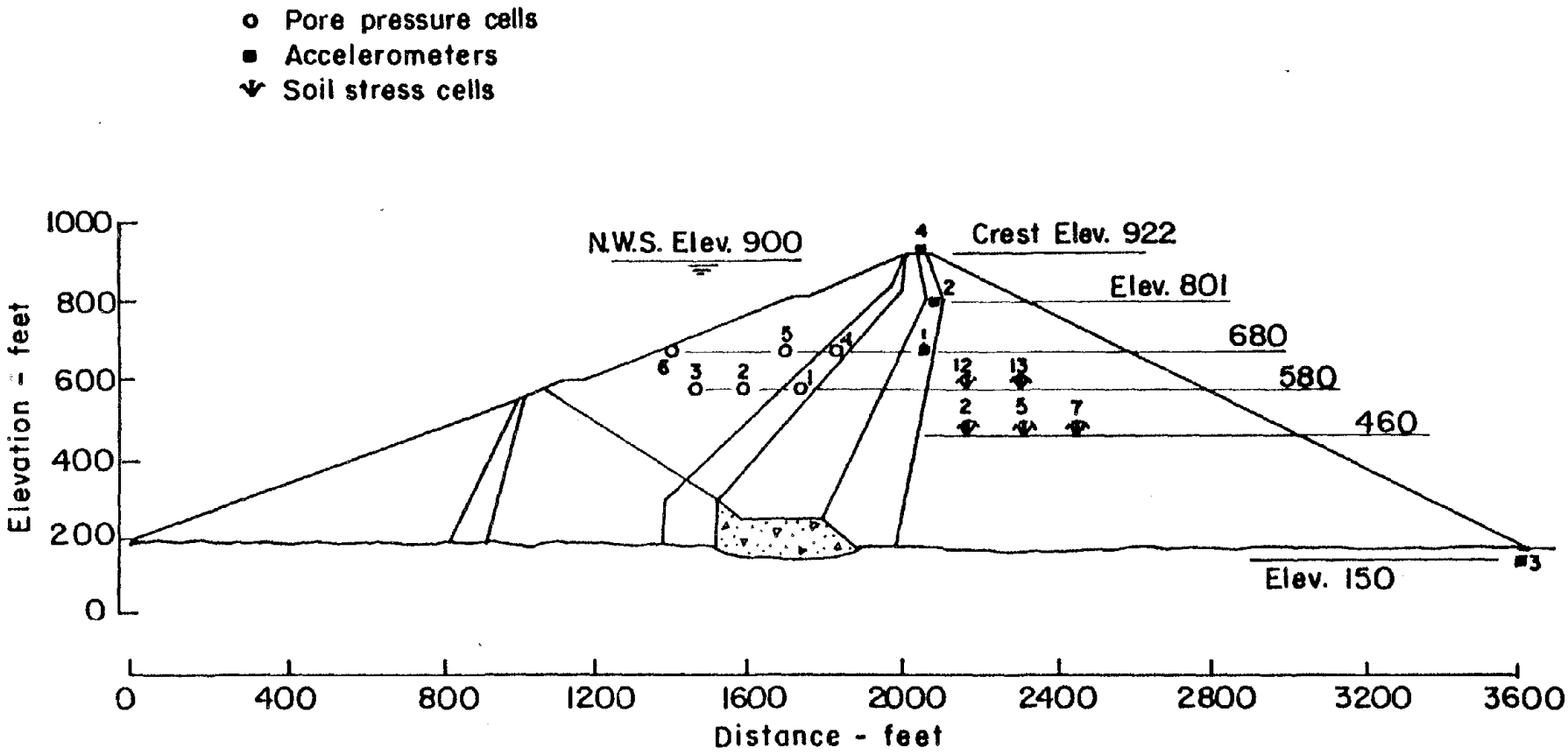

Fig. 3-1 Oroville Dam Dynamic Instrumentation.

measured accelerations along three orthogonal axes: vertical, upstream-downstream (N46°E), and cross-canyon. The seismographic station instrument was oriented with one of the horizontal axes at N37°E.

Performance of the dam was excellent throughout the Oroville earthquake series which started on June 28, 1975 and went on for several months with scattered aftershocks that registered magnitudes as high as 5.1. Several foreshocks with Richter magnitudes up to 4.7 preceded the main event of August 1, 1975.

The maximum settlement at the crest of the dam after the main shock was 0.03 ft. Horizontal displacements of the crest were in the upstream direction and lower than 0.05 ft. Shaking produced an increase in pore pressures in the core and in the upstream transition zone; the maximum increase was 54 ft. of water. This value decreased with time rather slowly indicating a low permeability of the transition materials and giving support to the assumption of undrained soil behavior during an earthquake. Seepage flow at the toe of the dam remained constant and increased slightly from 80 gpm to 91 gpm at the grout gallery (Stroppini, 1976).

All of the strong motion accelerometers were operable throughout the Oroville earthquake series except for the U.S.G.S instrument located at the grout gallery. Records were obtained for the strongest shocks, the most important of which were those on August 1, August 5 and September 27, 1975.

The September 27 event, which registered a 4.7 magnitude and for which the record at the toe of the dam had a predominant period of about

0.15 seconds, did not induce a strong response in the embankment. Unfortunately, gaps were present in the accelerograms recorded at the dam during the August 1 and August 5 shocks. The accelerographs in the dam had been triggered before the main shock of August 1 by a small foreshock; arrival of the strong shaking set off other devices like pore pressure cells and stress cells overloading the system and inducing a power failure. Fig. 3-2 shows the accelerograms in the upstream-downstream direction recorded during the August 1 main event at the crest and toe of the dam by the DWR and U.S.G.S. instruments. The length of the gaps present in the records was determined by re-enacting the power failure which was estimated to have lasted about 6 seconds.

The first 3 1/2 to 4 seconds of the U.S.G.S. crest record were lost due to instrument malfunction. Agreement between this record and the DWR record, where the traces of both are visible, is not surprising given the fact that they were obtained at the same location in the dam. The bottom record shown in Fig. 3-2 corresponds to that obtained at the U.S.G.S. seismograph station, ORV, located about 1 mile away from the dam on bedrock. Although there is a difference of 9° in orientation of the records and a difference of 970 ft. in elevation of the recording sites, the latter record shows some similarities with the available traces of the record at the toe of the dam. Both of these accelerograms suggest that the peak acceleration felt at the toe of the dam was on the order of 0.1 g. The peak acceleration recorded at the crest was 0.13 g, however, larger amplitudes might have occurred during the few seconds that are missing in the accelerograms.

The period of strong shaking lasted for about 3 seconds after which

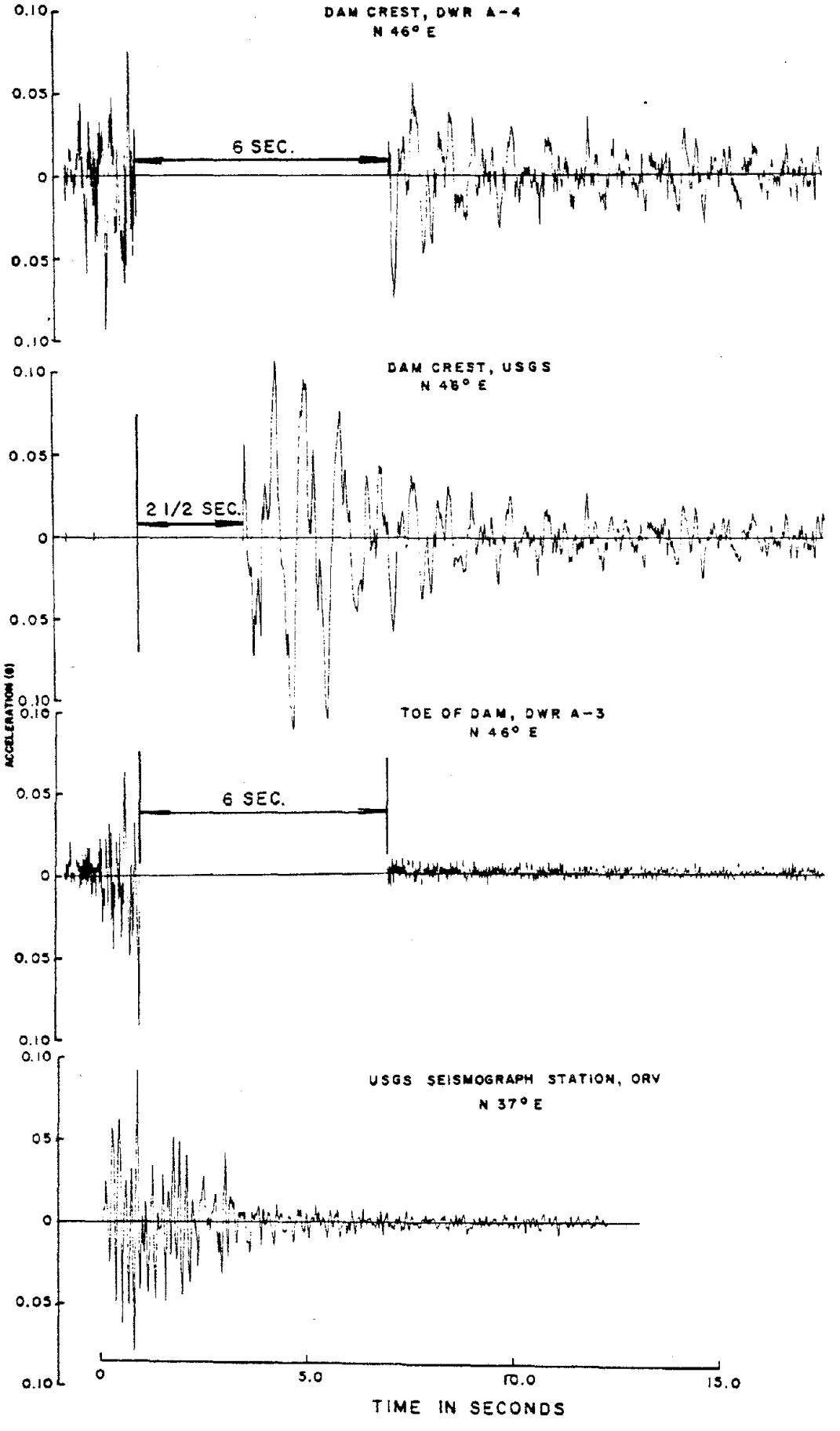

Fig. 3-2 August 1, 1975 Acceleration Records.

the dam continued to oscillate almost in free vibration for another 3 or 4 seconds. These free oscillations have a predominant period of about 0.8 seconds, which can be measured directly from the record, and at which the acceleration response spectra for these motions shows a pronounced peak (Fig. 3-3). Since free vibrations of a structure are strongly influenced by its fundamental period it can be concluded that the above value of 0.8 seconds corresponds closely to the fundamental period of Oroville dam for the level of shaking induced by the August 1, 1975 Oroville earthquake. This is an important finding since it can be used to estimate the dynamic properties of the dam materials as was done by the Department of Water Resources (DWR, 1979). A slightly different criterion which consists of selecting appropriate material properties to match the response spectra for the recorded crest motions can also be used to determine the stiffness characteristics of the dam. Both of the above mentioned criteria will be illustrated in subsequent sections.

3.3 Previous Experimental Studies

The exact constitutive behavior of soils under dynamic loading conditions is difficult to characterize analytically. In current practice, the strong non-linear behavior of these materials is taken into account by using equivalent linear elastic shear moduli and damping ratios compatible with the induced level of strain. The factors affecting the shear moduli and damping of different types of soils have been studied and summarized by Hardin and Drnevich (1970), and Seed and Idriss (1970).

The shear modulus of clays depends primarily on strain level and

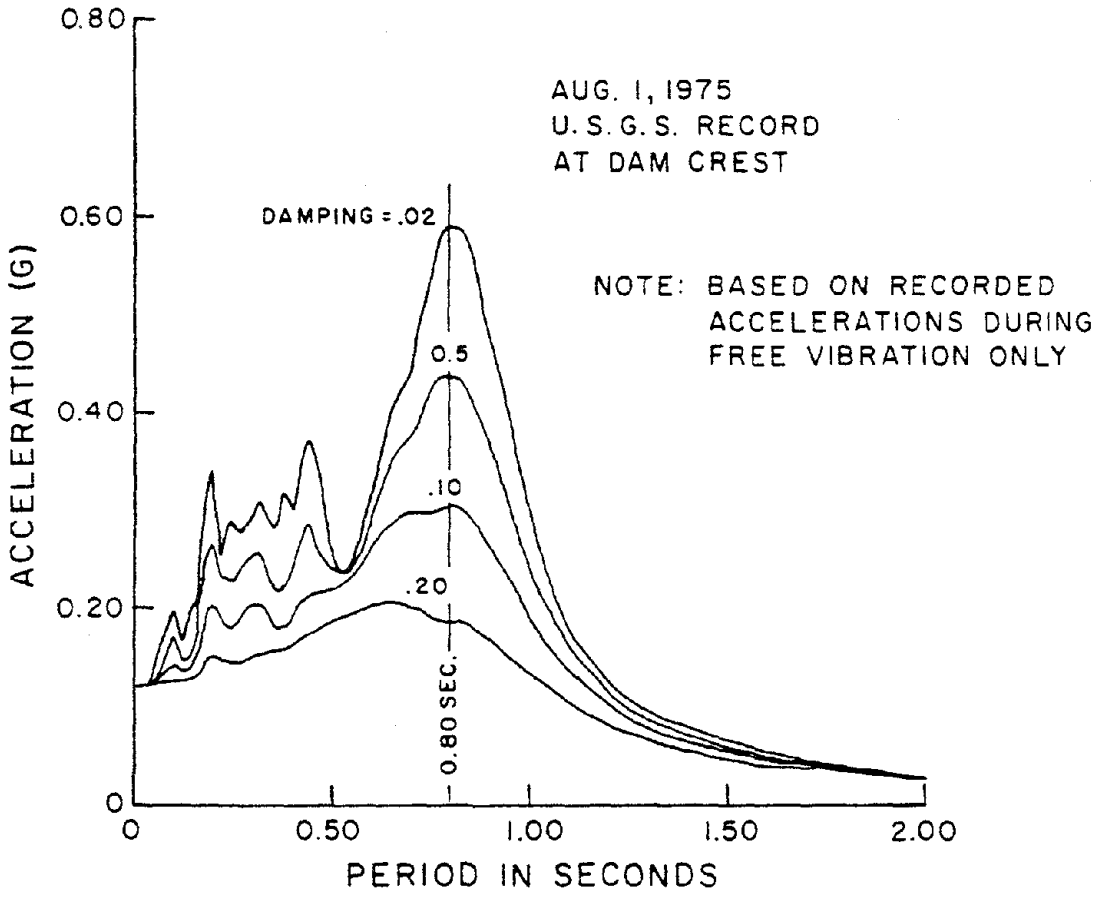

Fig. 3-3 Acceleration Response Spectra for Recorded Crest Motions.

the shear strength of the material in such a way that the ratio G/S_u can be expressed as a function of shear strain. The most significant factors affecting the shear moduli of sands are: shear strain, confining pressure and relative density (Seed and Idriss, 1970). The following expression for the modulus, which relates the above parameters is generally accepted:

$$G = 1000\, K_2(\sigma'_m)^{1/2} \qquad (3\text{-}1)$$

where:

G = shear modulus in psf

σ'_m = mean effective confining pressure in psf

K_2 = a function of strain level and relative density

Although little data has been presented on the shear moduli of gravels their dynamic behavior has been found to be analogous to that of sands. However, at comparable relative densities, confining pressures and levels of strain, gravels exhibit higher moduli than sands indicating a significant effect of grain size. Damping of cohesive and cohesionless soils, on the other hand, is only influenced strongly by strain level.

One of the first studies to determine the dynamic properties of the Oroville gravels was carried out by Wong (1971) who used model gradations of the material and 12" diameter cyclic triaxial tests. As reported by Wong, gradation and average grain size have an important effect on the shear moduli of gravels. At the same relative density,

confining pressure and level of strain, the shear modulus of these materials increased with increasing average grain size. However, the average variation of the ratio K_2/K_2max with strain level (the modulus reduction curve) was found to be the same as that for sands. As a consequence the shear moduli of the Oroville gravels will be completely defined by the value of K_2 at low strain levels, K_2max (see equation 3-1). Damping characteristics were found to be very similar to those of sands indicating that the effects of grain size on this factor can be neglected for practical purposes.

Given the fact that the average grain size for the Oroville gravels in-situ is about 6 times larger than the Oroville gravels tested by Wong it can be concluded, on the basis of the above discussion, that in-situ K_2 values for these materials will be higher than the values obtained in the mentioned tests. In-situ damping factors however, are likely to be close to average values presented for sands.

Data at high strain levels reported by Banerjee (1979) agrees well with the modulus-strain relationship computed by the DWR from field performance of Oroville dam. Although Banerjee used similar gradations, his values for shear moduli of the Oroville gravels are higher than those indicated by Wong's tests.

A summary of the above results is presented in Fig. 3-4 which describes the variation of the K_2 factor with strain for several soils. Included in this figure is the K_2-strain relationship back-calculated from field performance of the Oroville dam. The computations that led to this relationship will be described in the following section.

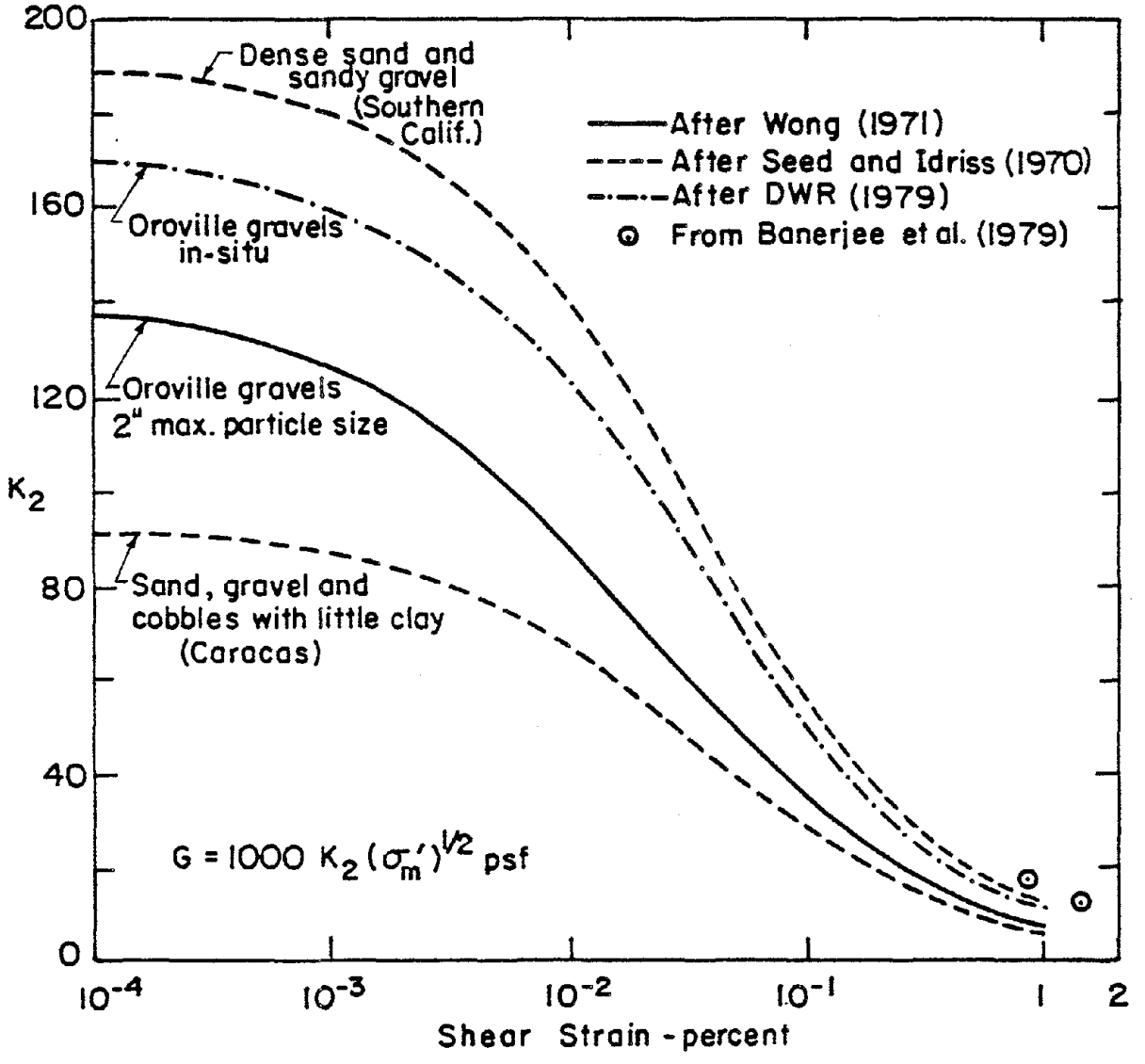

Fig. 3-4 Variation of K_2 with Strain for Gravelly Soils.

3.4 Determination of K_2max by the DWR

As mentioned before, back-calculation from recorded field behavior constitutes the best method for determining the in-situ dynamic stiffness characteristics of Oroville dam. Since the procedures followed by the DWR are similar to those used in the present investigation which uses a 3-D model, they are included in this section for comparison purposes.

In the case of Oroville Dam two distinct zones can be identified as far as dynamic behavior is concerned. The shells and transition zones of the dam have very similar dynamic properties and can therefore be treated as a single zone. The second zone contains the sloping core of the dam and the cofferdam core (see Fig. 1-3). In view of the fact that the core constitutes a small portion of the embankment and its dynamic stiffness is not very different from that of the shells, it can be concluded that the influence of this zone on the dynamic response of the dam will be small. For this reason, exact determination of the variation of the G/S_u ratio with strain and of the damping characteristics of these materials is not critical, and the average relationships for cohesive soils suggested by Seed and Idriss (1970) can be used.

As shown by the results presented by Wong (1971) the variation of the G/G_{max} ratio with strain, and the damping characteristics of the shells of Oroville Dam, can be described by the average relationships for sands presented by Seed and Idriss (1970). These relationships along with those used for the core are illustrated in Fig. 3-5.

The dynamic behavior of soil structures is dependent on the state

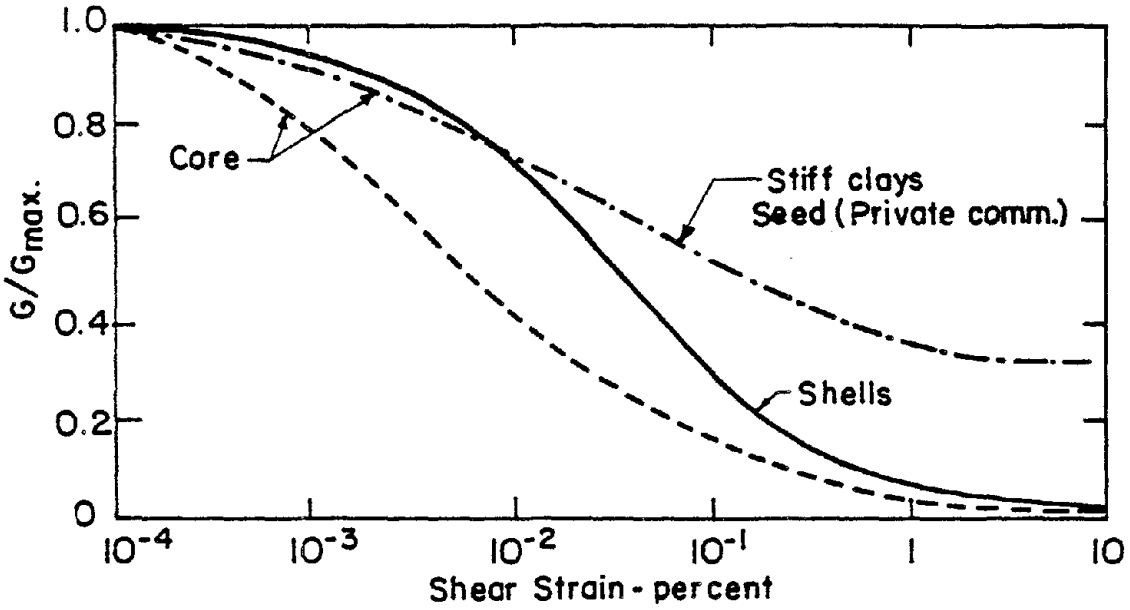

(a) Modulus reduction curves

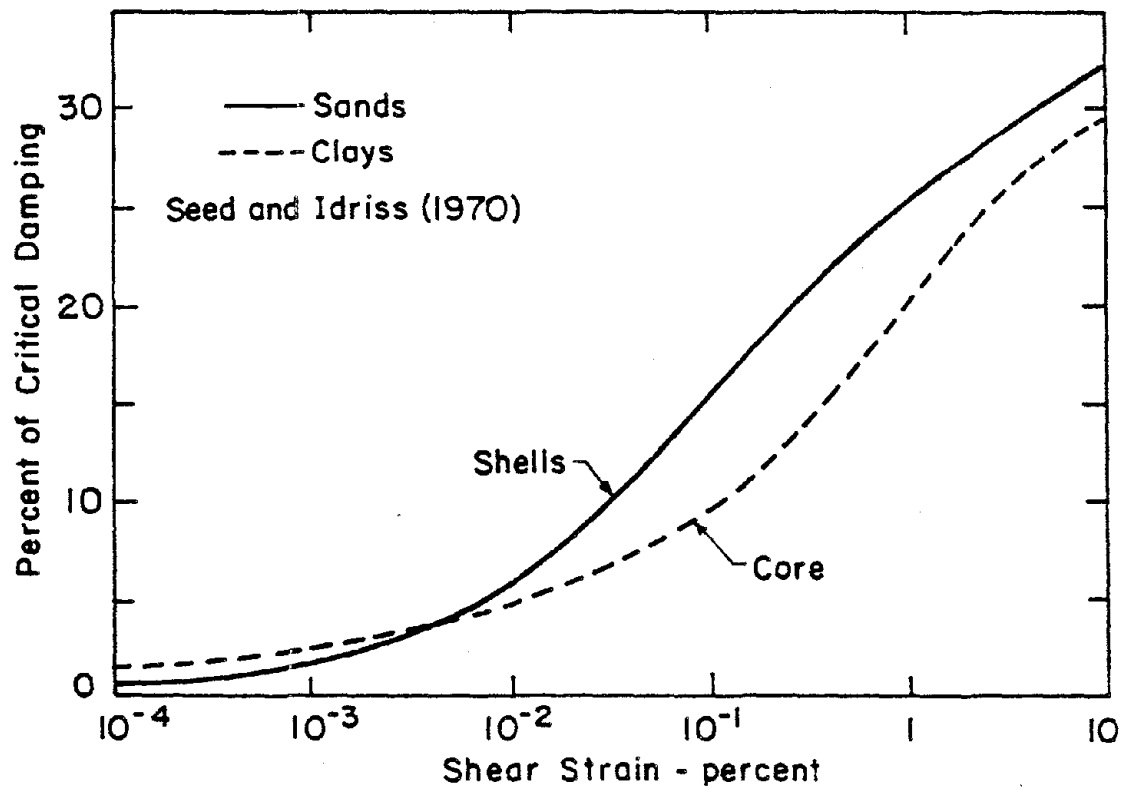

(b) Damping ratios

Fig. 3-5 Strain Compatible Dynamic Properties for Oroville Dam Soils.

of stress under static conditions as indicated by the σ'_m term in equation 3-1. In order to determine the static stress conditions in Oroville Dam the DWR performed suitable computations using plane strain finite element procedures. These results will be presented in the next section and will be used to determine the three-dimensional state of stresses in the dam.

Determination of the shell's K_2max value and the core's G_{max}/S_u ratio that yield the recorded natural period of the dam during the August 1, 1975 Oroville earthquake was done by a trial and error procedure. The computer program QUAD4 (Idriss et al., 1973) and the finite element mesh shown in Fig. 3-6 were used to compute the fundamental period of the dam for different values of K_2max and G_{max}/S_u. Fig. 3-7 shows the computed natural period as a function of K_2max for different G_{max}/S_u ratios. It can be seen that for a particular value of K_2max a change in the G_{max}/S_u ratio from 1100 to 4400 does not affect the computed period by more than 10% and therefore an average value of G_{max}/S_u=2200 can be assumed to be satisfactory for engineering purposes. It can also be seen from this figure that the value of K_2max that corresponds to a period of 0.8 seconds is approximately 350.

Oroville Dam is located in a triangular canyon and has a crest length of about 5100 feet and a maximum height of 733 feet. Since the crest length to height ratio, L/H, is on the order of 7, the dam will not exhibit plane strain behavior. Therefore, although a value of K_2max=350 will yield the correct natural period of the embankment with a plane strain analysis, it is not a true property of the Oroville gravels and must be corrected to account for the three-dimensional behavior of

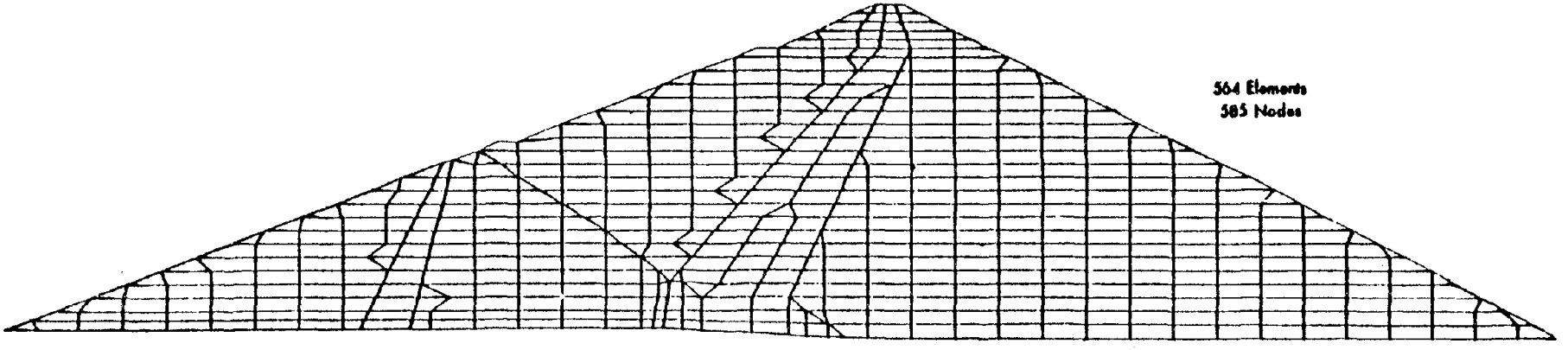

Fig. 3-6 Finite Element Mesh for the Maximum Section of Oroville Dam.

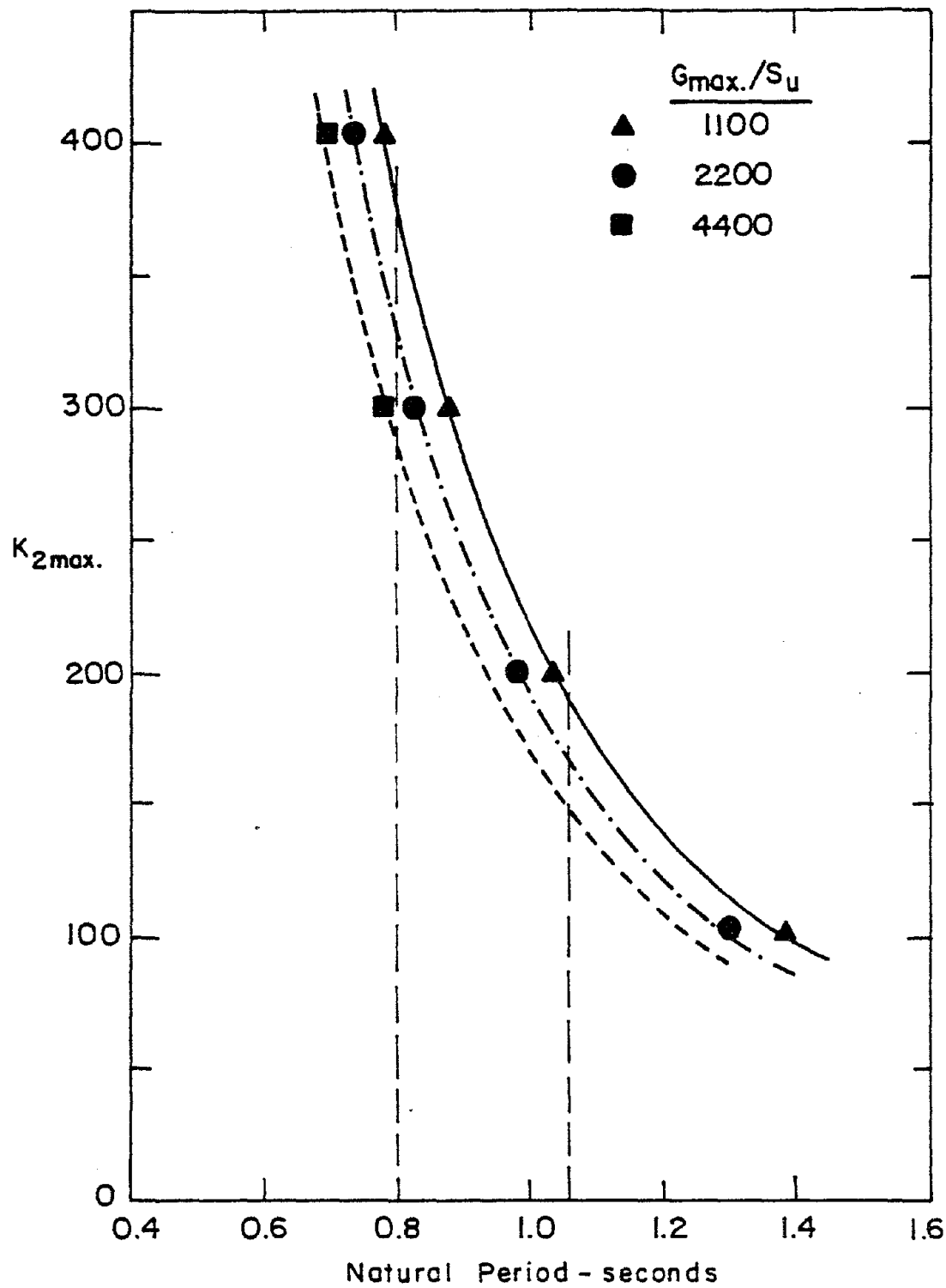

Fig. 3-7 K_{2max} Vs. Computed Natural Period of Embankment (After DWR, 1979).

the dam.

Recent studies by Makdisi (1976) have indicated that for a ratio L/H=7, the natural period of an embankment in a triangular canyon computed from a plane strain analysis is about 1.32 times higher than the period computed from a 3-D analysis (see Fig. 5-1). That is:

$$\frac{(T_n)_{ps}}{(T_n)_{3D}} \simeq 1.32 \qquad \text{for} \quad L/H=7$$

This means that if the natural period of Oroville Dam were to be computed with a plane strain analysis using the in-situ properties for the shell materials the computed period should be:

$$(T_n)_{ps} \simeq 1.32 \times 0.8 = 1.06 \text{ seconds}$$

From Fig. 3-7 it can be seen that with a plane strain analysis this value will be computed for a $K_2 max=170$ and therefore this number corresponds to the true properties of the shell materials.

Makdisi's studies involved a homogeneous, elastic dam, with 2:1 slopes and therefore their applicability in the case of Oroville Dam is uncertain. On this basis it seems desirable to perform the above computations using a three-dimensional finite element model.

3.5 Static Stress Analyses of Oroville Dam

Since the dynamic shear modulus of soil materials depends on the mean effective stress (see equation 3-1), the static state of stresses throughout Oroville Dam will be necessary in order to perform a three-dimensional dynamic analysis of the dam.

A number of studies have been carried out to determine the static stress conditions in Oroville Dam using plane strain finite element procedures. Kulhawy and Duncan (1970) performed static stress analyses using incremental techniques to simulate construction of the dam. Comparison of computed displacements and stresses with measured values indicated the ability of these procedures to predict field behavior. Nobari and Duncan (1972) computed the effects of reservoir filling on the embankment and presented results for the corresponding displacements and stress changes.

During the re-evaluation of the stability of the Oroville Dam, the Department of Water Resources (DWR, 1979), performed the static stress computations necessary for the dynamic analysis of the dam and for the assessment of the cyclic strength of the shell materials. The same finite element mesh as that used in the dynamic response analysis (Fig. 3-6), and the computer program ISBILD (Ozawa and Duncan, 1973), were used to compute the static stress conditions in the dam. This program uses the techniques developed by Kulhawy et al., (1969) to simulate the construction stages of the dam. The effects of water pressures and seepage forces due to reservoir filling were also taken into account. The same soil parameters used by Kulhawy and Duncan (1970), which were obtained from static strength tests on the dam materials, were adopted (Table 3-

1). As can be seen from this table the stress-strain parameters for the transition and shell materials are very similar and therefore these two zones were treated as a single zone in the analyses.

Figs. 3-8a and 3-8b show the computed contours of effective maximum principal stress and effective minimum principal stress respectively. These results agree fairly well both with Nobari and Duncan's results and with the values measured by stress cells in the dam. It can be seen that the stress contours are fairly parallel to the slopes of the dam and are evenly spaced throughout the main section of the dam except in the core and near the concrete core block. An observation of practical significance is that the minimum principal stresses are approximately equal to 40% of the maximum principal stresses at almost all points in the main section of the dam.

The above results have been obtained from plane strain analyses which are not strictly applicable to Oroville Dam since this is a three-dimensional structure in a triangular canyon with a crest length to height ratio, L/H, of about 7 (see Fig. 3-11).

Lefebvre et al., (1973) have presented comparisons between three-dimensional and two-dimensional static finite element analyses of earth dams in V-shaped canyons. The results from this study indicate that for dams with a ratio L/H=6 a plane strain analysis of the maximum section, gives values for the major and minor principal stresses that on the average (scatter of about 10%) are within 5% of the values computed from a 3-D analysis. For dams with a ratio L/H=2 the differences are 10% on the average, with a scatter of the order of 20%.

Table 3-1 Values of Stress-Strain Parameters for Pre-Earthquake Static Stress Analysis of Oroville Dam.

Parameter	Symbol	Values employed in analyses				
		Shell	Transition	Core	Soft Clay[a]	Concrete
Unit Weight (lb/ft^3)	γ	150	150	150	125	162
Cohesion ($tons/ft^2$)	c	0	0	1.32[b]	0.3	216[c]
Friction Angle (degrees)	ϕ	43.5	43.5	25.1[b]	13.0	0
Modulus Number	K	3780	3350	345	150	137,500
Modulus Exponent	n	0.19	0.19	0.76	1.0	0
Failure Ratio	R_f	0.76	0.76	0.88	0.90	1.0
Poisson's Ratio	G	0.43	0.43	0.30	0.49	0.15
Parameters	d	0.19	0.19	-0.05	0	0
	F	14.8	14.8	3.83	0	0

a. Zone of soft clay at upstream end of core block.

b. c and ϕ for $(\sigma_1 + \sigma_3) < 50$ $tons/ft^2$; $c = 10.2$ ton/ft^2. $\phi = 4$ degrees for $(\sigma_1 + \sigma_3) > 50$ $tons/ft^2$.

c. Tensile strength of concrete ≈ 14 $tons/ft^2$ (200 psi).

(After Kulhawy and Duncan, 1970)

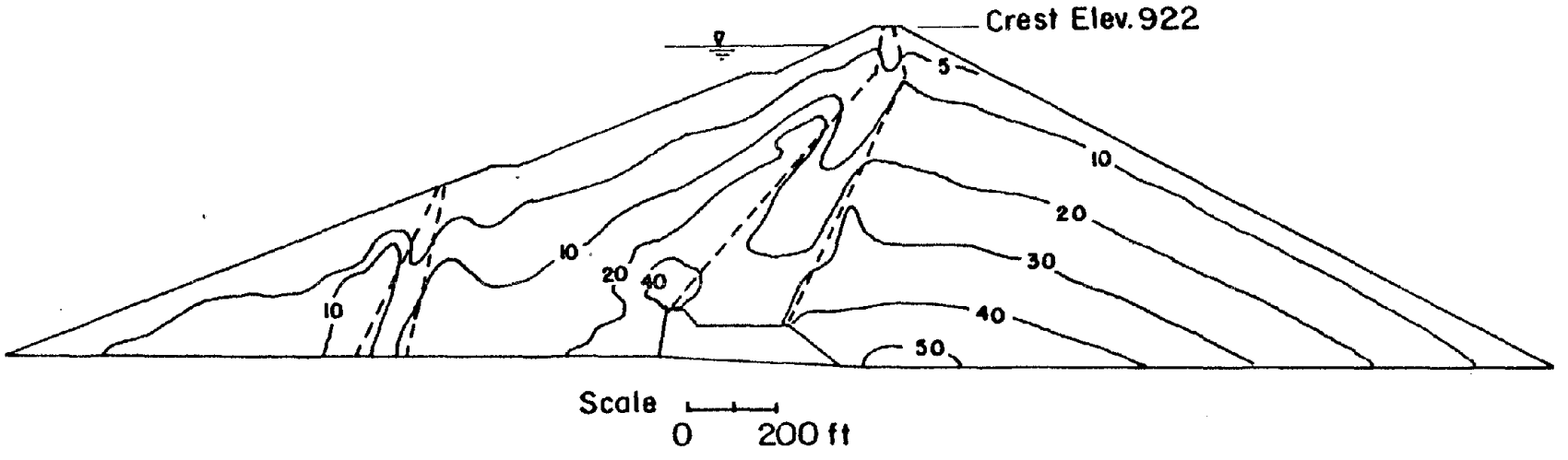

Fig. 3-8a Contours of Major Principal Stress (Tsf) in Oroville Dam (After DWR, 1979).

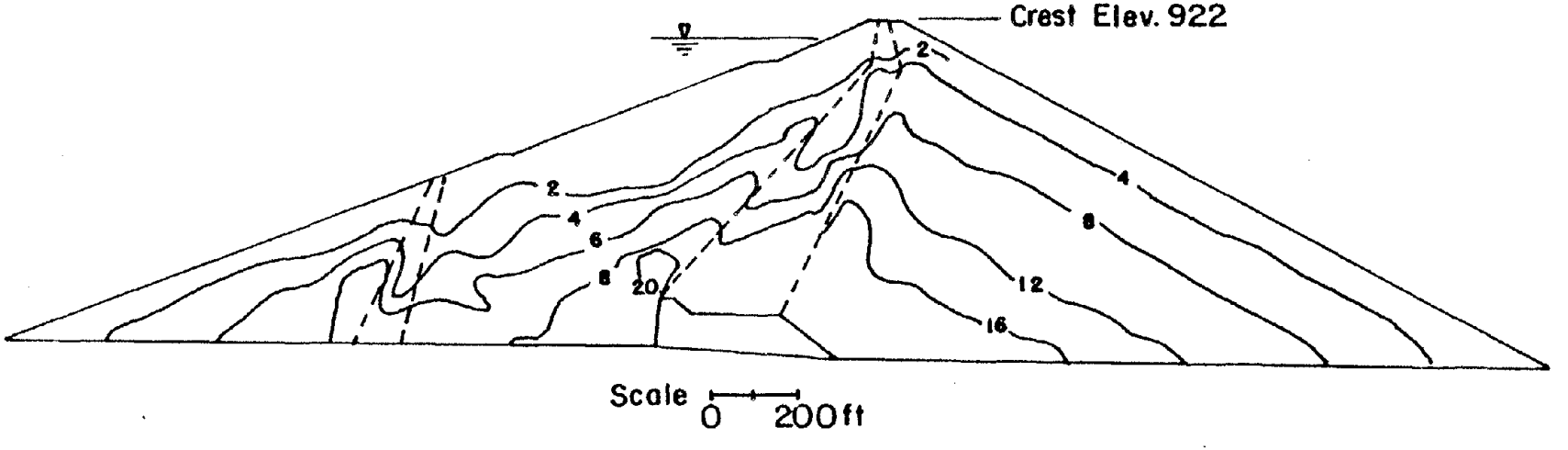

Fig. 3-8b Contours of Minor Principal Stress (Tsf) in Oroville Dam (After DWR, 1979).

The contours of major and minor principal stresses for the longitudinal sections of dams with crest length to height ratios, L/H, of 2, 6 and 12, computed from three-dimensional analyses, are shown in Figs. 3-9a and 3-9b. It can be seen that for dams with a ratio L/H=6 the principal stresses, at different sections in the dam, can be obtained with a reasonable degree of accuracy by horizontal projection of the values computed for the main section. Although larger errors may be incurred, this procedure will still give acceptable results for dams with L/H=2.

On the basis of the preceding discussion the following two conclusions can be made: a) the static stresses at the main section of Oroville Dam can be satisfactorily computed from a plane strain analysis of this section, and b) the static stresses at other sections in the dam can be obtained with a reasonable degree of accuracy by projecting horizontally the stresses computed at the main section.

3.6 Three-Dimensional Analysis of Oroville Dam for Different K_2max Values

In long dams subjected to motions in the upstream-downstream direction, where the restraining effects of the abutments on transverse deformations is small, plane strain conditions will exist. In the case of Oroville Dam, however, the abutments have a significant influence on the dynamic behavior of the embankment. To take this into account, the three-dimensional finite procedures described in Chapter 2 have been used in the back-calculation of the shell material K_2max factor from field behavior of the dam.

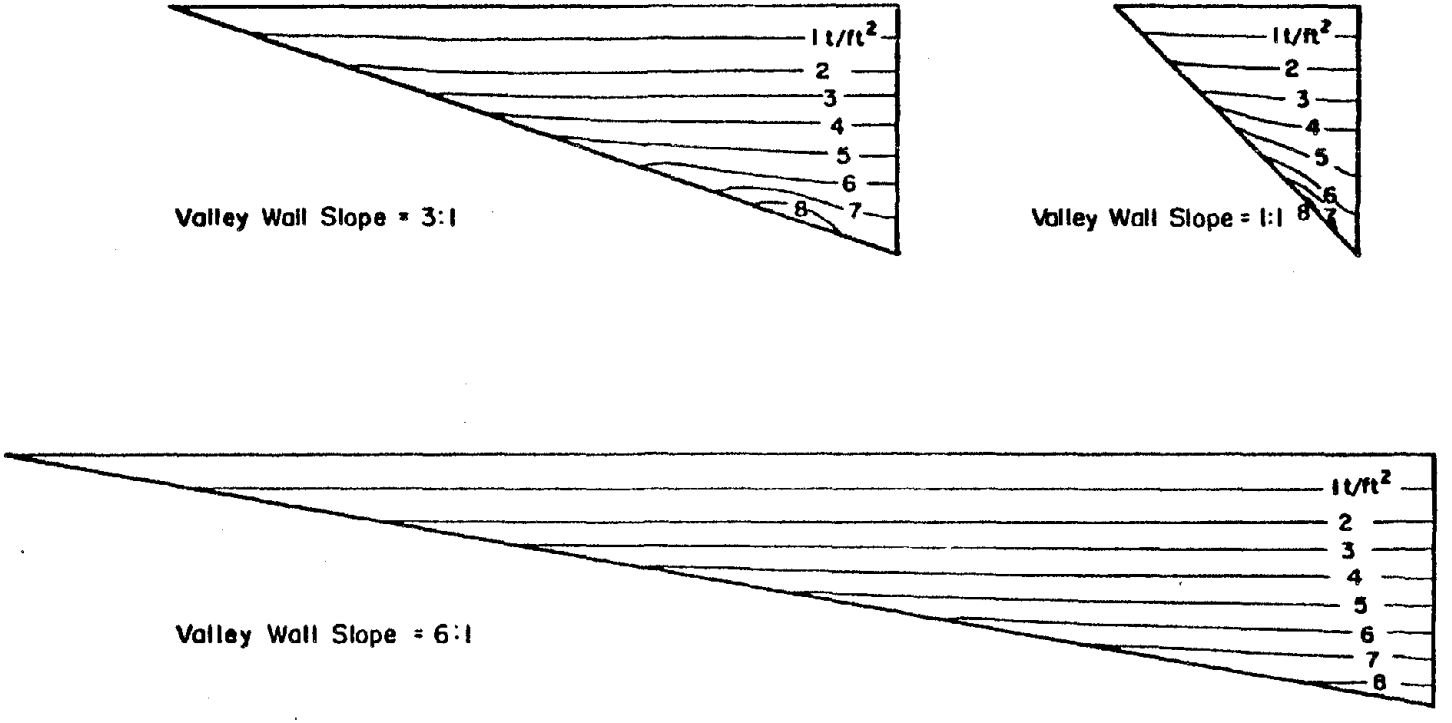

Fig. 3-9a Contours of Values of Major Principal Stress σ_1 in Longitudinal Section Calculated Using Three-Dimensional Analyses with Three Different Valley Wall Slopes (After Lefebre et al., 1973).

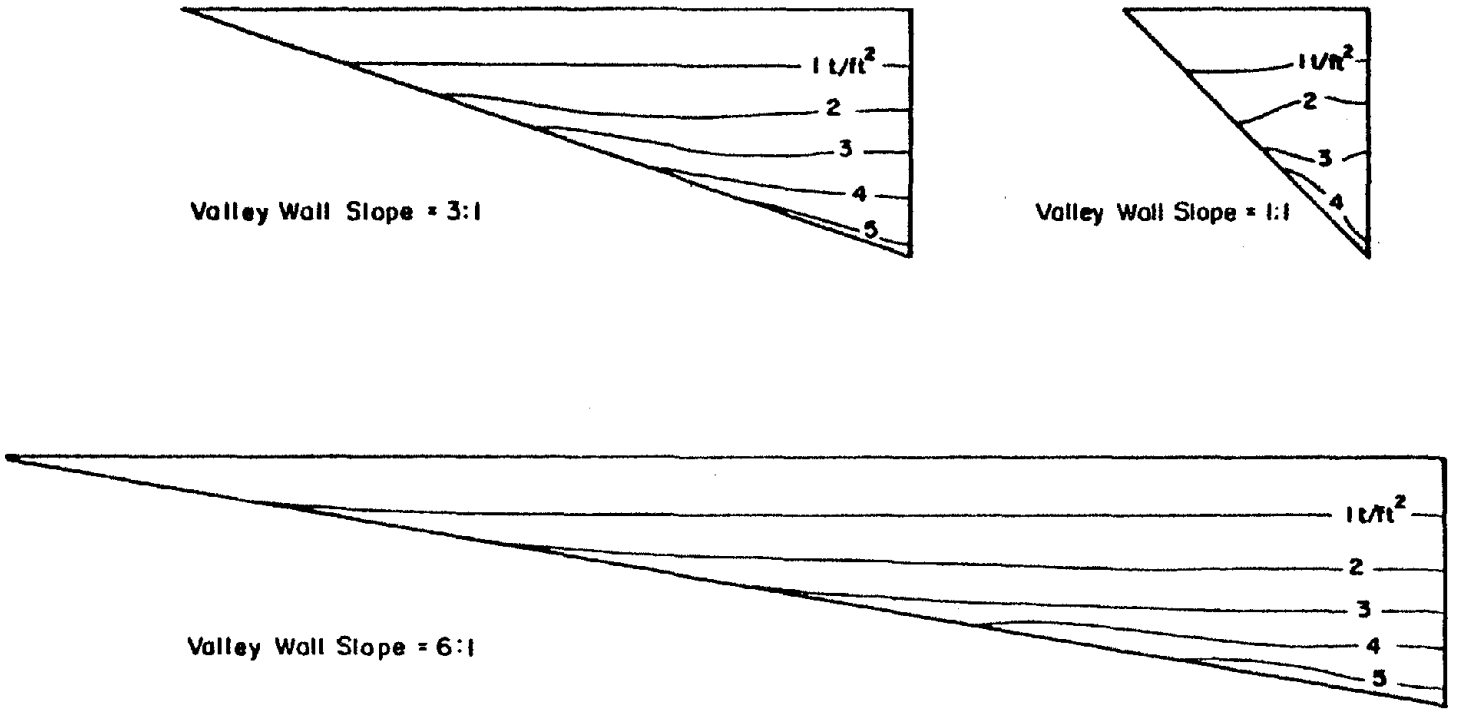

Fig. 3-9b Contours of Values of Minor Principal Stress σ_3 in Longitudinal Section Calculated Using Three-Dimensional Analyses with Three Different Valley Wall Slopes (After Lefebre et al., 1973).

As mentioned earlier, the accelerogram record in the upstream-downstream direction obtained by the U.S.G.S. instrument displayed the fundamental period of vibration of Oroville Dam for the level of shaking induced by the August 1, 1975 Oroville earthquake. A 3-D dynamic analysis of the embankment for the motions generated at the dam site by this earthquake, should predict reasonably well the recorded response, provided the in-situ K_2max value for the shell materials is used.

Relative coupling of transverse, vertical and longitudinal motions at the midpoint of the dam crest is likely to be small. Therefore, it can be assumed that the motions in the upstream-downstream direction at that point, were induced by the rock motions in the same direction. The accelerograms recorded at the toe of the dam were affected by a power failure and could not be used to analyze the response of the dam. Fortunately, records were obtained at the seismographic station, ORV, situated about 1 mile away from the dam site on bedrock. It is reasonable to assume that these motions are representative of the motions to which the dam was subjected. Fig. 3-10 shows the accelerogram record and the corresponding acceleration response spectra for the upstream-downstream motions used in the dynamic analysis of the dam. No correction was made for the fact that there is a difference of 9° between the orientation of the recording axis and the upstream-downstream direction of the canyon. As can be seen from the acceleration response spectra, the motions at the base of the dam had a high predominant frequency, on the order of 6.7 Hz.

Oroville Dam is situated in a V-shaped canyon with valley wall slopes of about 3.5:1. Fig. 3-11 shows in a continuous trace, a

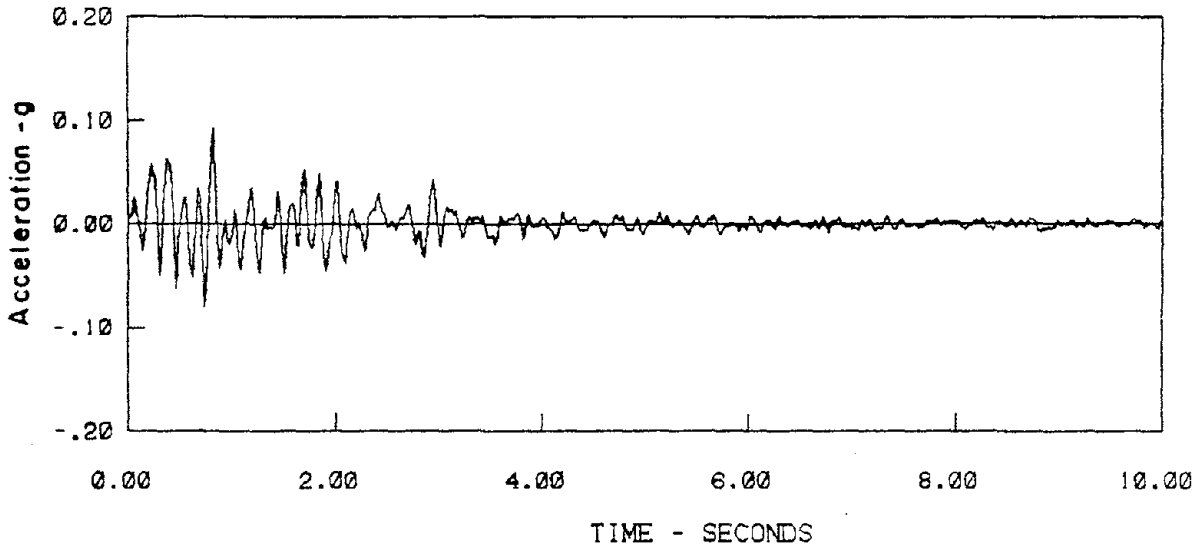

(a) Acceleration Time History

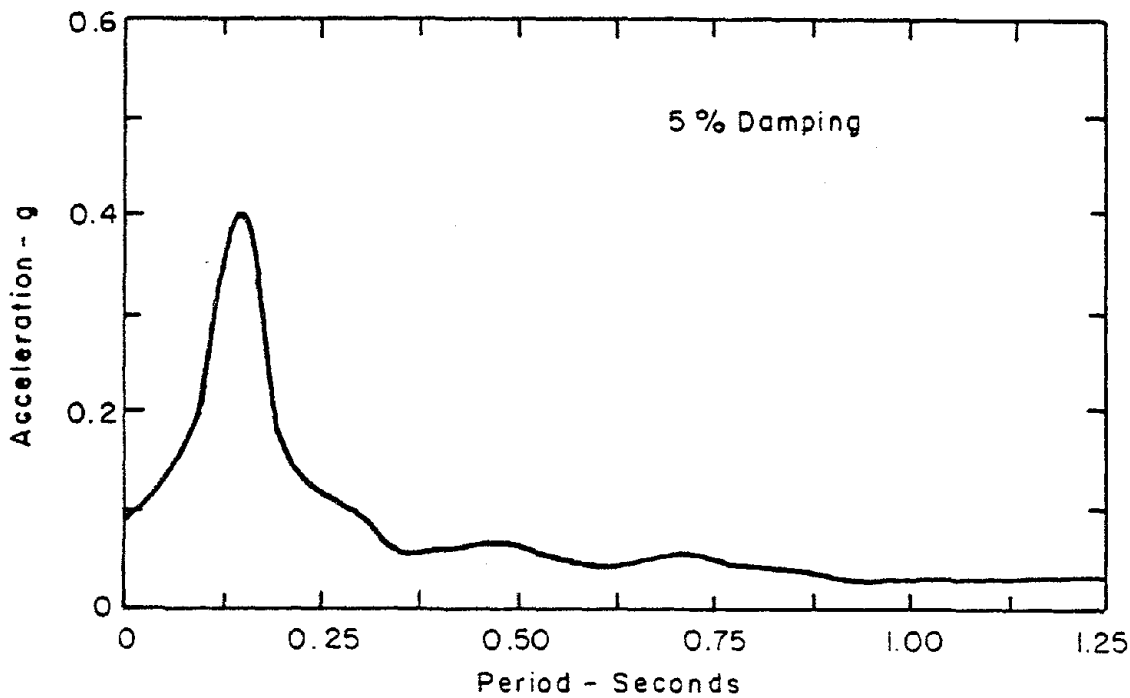

(b) Acceleration Response Spectra

Fig. 3-10 Acceleration Time History and Response Spectra for Input Motions.

vertical section along the dam axis and a plan view of the dam. As can be seen, the embankment is almost geometrically symmetrical with respect to its main section and therefore, for input motions in the upstream-downstream direction, it can be assumed to behave as a symmetric structure. This assumption will permit the use of a finer finite element mesh than otherwise possible, in this way helping to keep computational efforts within reasonable limits. The dotted lines in Fig. 3-11 illustrate the geometrical model adopted to represent the dam; plane boundaries have been assumed for simplicity. The corresponding 3-D finite element model is shown in Fig. 3-12. This model has 591 elements, 543 free nodal points and 8 sections in the cross-valley direction. Nodal points on the plane of symmetry, that is, the main section, will be constrained from moving in the z direction and no horizontal or vertical shear stresses will exist on this boundary. Given the fact that the dynamic behavior of the transition zone materials is very similar to that of the shell materials, these zones have been combined into a single zone in the model (DWR, 1979). Other zones modeled in these analyses are: the sloping core, the cofferdam core and the concrete core block.

The concrete core block has been assumed to behave elastically and the average Young's modulus, density and Poisson's ratio for concrete have been used as the dynamic properties of this zone. The results obtained by the DWR, 1979 indicate that exact determination of the dynamic properties for the central core and the cofferdam core is not critical and therefore the average ratio $G_{max}/S_u=2200$ for cohesive soils has been assumed. Shear strengths, S_u, necessary to compute the shear modulus were obtained by using the measured strength envelope for the

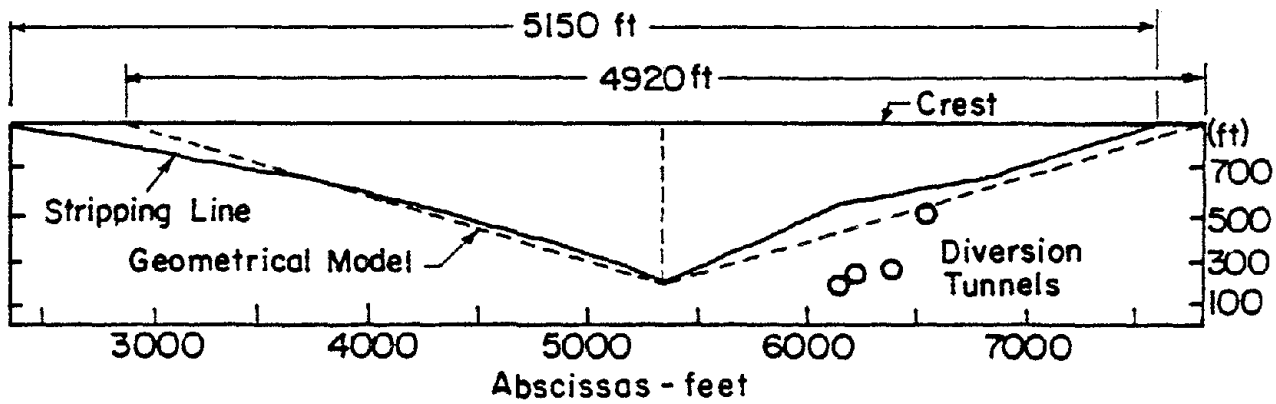

(a) Longitudinal section along main chord

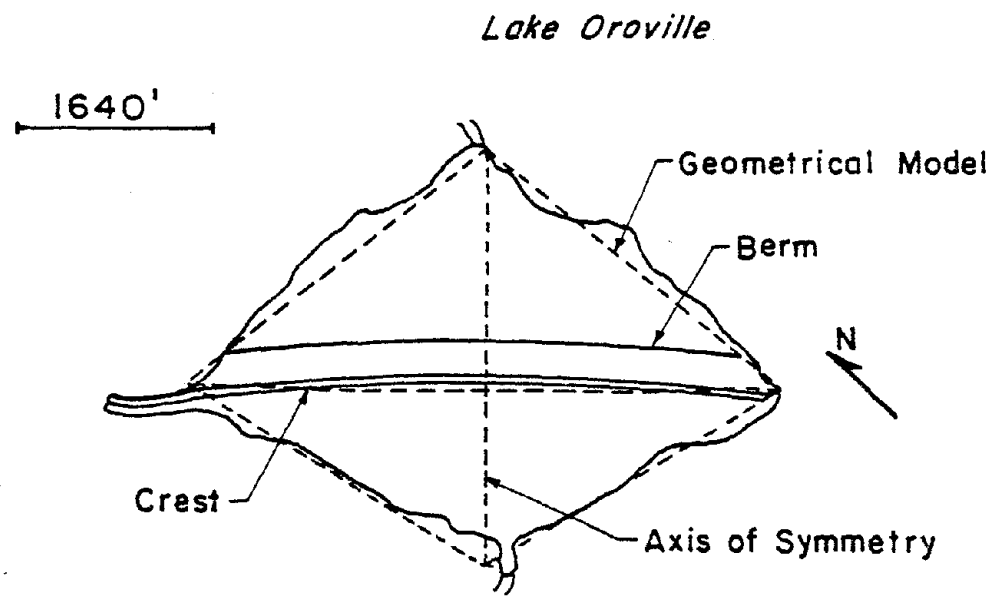

(b) Plan view

Fig. 3-11 Longitudinal Section and Plan View of Embankment and Geometrical Model.

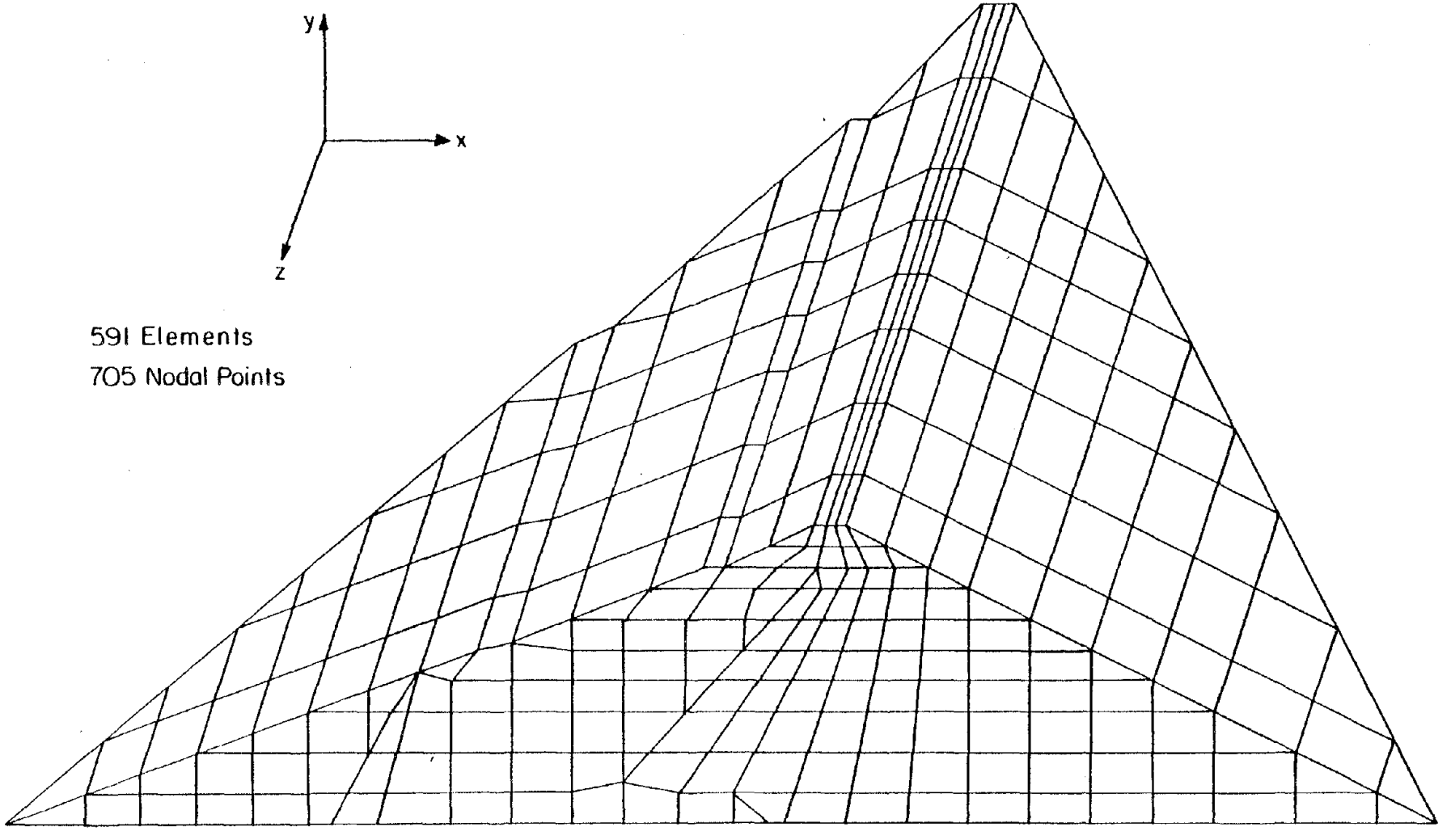

Fig. 3-12 Three Dimensional Finite Element Model of Oroville Dam.

core materials and the corresponding consolidation stresses. The modulus reduction and damping curves used for both the core and the shell materials are the same as those used by the DWR, 1979 and are shown in Fig. 3-5. On the basis of the results obtained by the DWR, a value of K_2max=170 for the shells of the dam was tried initially. In an attempt to shift the peak in the response spectra for the computed crest motions to higher periods (see Fig. 3-15), values for K_2max of 150 and 130 were also used in the analyses. Shear moduli for the shell materials were computed from equation (3-1). The mean effective stress that enters into this equation can be computed from:

$$\sigma'_m = \frac{\sigma'_1 + \sigma'_2 + \sigma'_3}{3} \qquad (3\text{-}2)$$

where σ'_1,σ'_2, and σ'_3 are the major, intermediate and minor effective principal stresses respectively.

On the basis of the results of the static stress analysis performed by the Department of Water Resources the minimum effective principal stress, σ'_3, was assumed to be equal to 40% of the maximum effective principal stress σ'_1. The intermediate effective principal stress, σ'_2, was assumed to be equal to 55% of σ'_1. According to these assumptions equation (3-2) reduces to:

$$\sigma'_m = 0.65\sigma'_1 \qquad (3\text{-}3)$$

The major effective principal stresses, σ'_1, for the main section of the dam were obtained from Fig. 3-8a. At other sections in the dam

the above stresses were obtained by projecting horizontally the corresponding stresses for the main section. A summary of the material properties used in the dynamic analyses presented in this section is given in the Table 3-2. These analyses were preformed by iterations until compatibility between shear moduli, damping and strain was achieved. A cut-off frequency of 8 Hz was used in the response computations.

The computed amplification functions at the midpoint of the crest of the dam for the selected shell K_2max values are shown in Fig. 3-13. These amplification functions give, for the spectrum of frequencies of harmonic excitation, the ratio between the amplitude of absolute acceleration at the crest midpoint and the amplitude of acceleration at the rigid boundaries of the model. The first peak in the crest amplification function occurs at the fundamental frequency of vibration of the dam. It can be concluded that for the level of strain induced by the Oroville earthquake the natural periods of vibration of the dam corresponding to K_2max values of 170, 150 and 130 are: 0.83, 0.93, 1.02 seconds respectively. In all cases a small response of the dam for frequencies greater than about 6 Hz and a close spacing between frequency peaks were observed.

The computed acceleration time histories at the crest of the dam are shown in Fig. 3-14. Also shown in this figure is the acceleration record obtained at the crest of the dam by the U.S.G.S. instrument, from which the first 3 to 4 seconds of motion were missing. The starting time for this record has been shown in the figure so that the best match with the computed time histories is obtained. It can be seen that the

TABLE 3-2

DYNAMIC PROPERTIES FOR 3-D ANALYSES OF OROVILLE DAM

Parameter	Shell	Core	Core Block
K_2max	170 150 130		G=200000 Ksf
G_{max}/S_u		2200	
Modulus reduction	Seed and Idriss	Seed and Idriss	Linear Elastic
Damping	Seed and Idriss	Seed and Idriss	B=4%
S_u		From strength env.	
Poisson's ratio	Upstream 0.4 Downstream 0.3	0.45	0.15
Density (pcf)	Upstream 153 Downstream 150	153	160

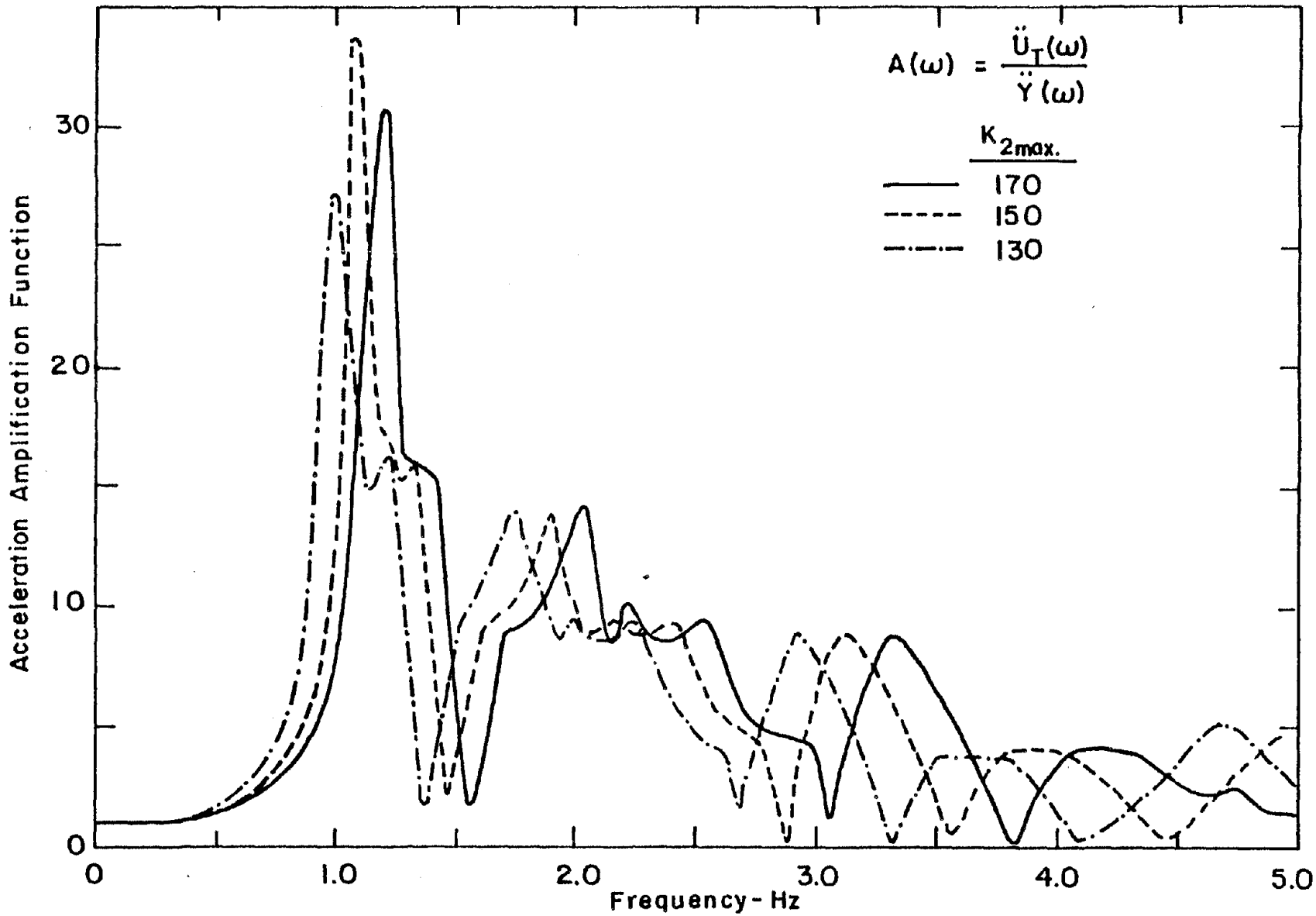

Fig. 3-13 Computed Amplification Functions for Crest Midpoint of Oroville Dam.

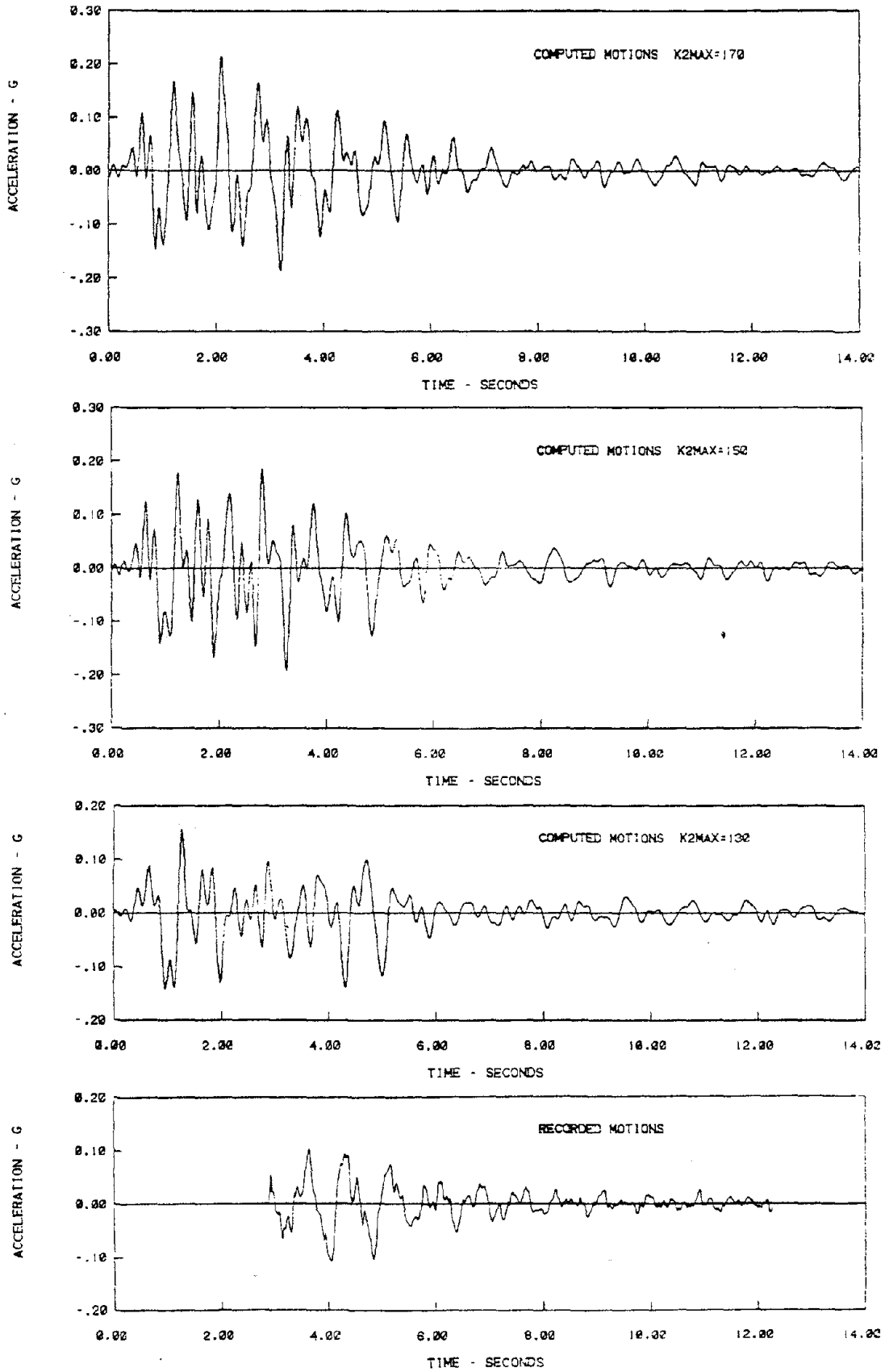

Fig. 3-14 Acceleration Time Histories for Crest Midpoint of Oroville Dam.

time history computed with a K_2max for the shell materials of 170 gives the best approximation to the recorded motions.

An easier comparison between computed and recorded response of the dam can be made in terms of the acceleration response spectra for the crest motions. The response spectra of the computed acceleration time histories have not been obtained for the entire length of these records. A comparison with the acceleration response spectrum for the recorded motions is only meaningful if the spectra for the computed time histories are obtained for accelerations starting at points in time, corresponding to the point where the recorded motions are assumed to start. Fig. 3-15 shows the acceleration response spectra for the computed time histories, obtained in accordance with the above reasoning, along with the spectrum for the recorded crest motions. It can be seen that although the differences between the spectra for the computed motions are not large, the best overall match to the spectrum for the recorded motions is provided by the response spectrum for the motions computed with a K_2max=170.

Considering that the natural period of the dam and the response at the crest, for the levels of strain induced by the Oroville earthquake, computed with a K_2max=170 offer the best match to the analogous recorded parameters, it can be concluded that the above value of K_2max is representative of the in-situ dynamic properties of the Oroville gravels. Given the number of approximations and assumptions made, the agreement between computed and recorded acceleration time histories and response spectra is considered reasonable. It is also noted that the results obtained in this section with the use of 3-D analyses agree very

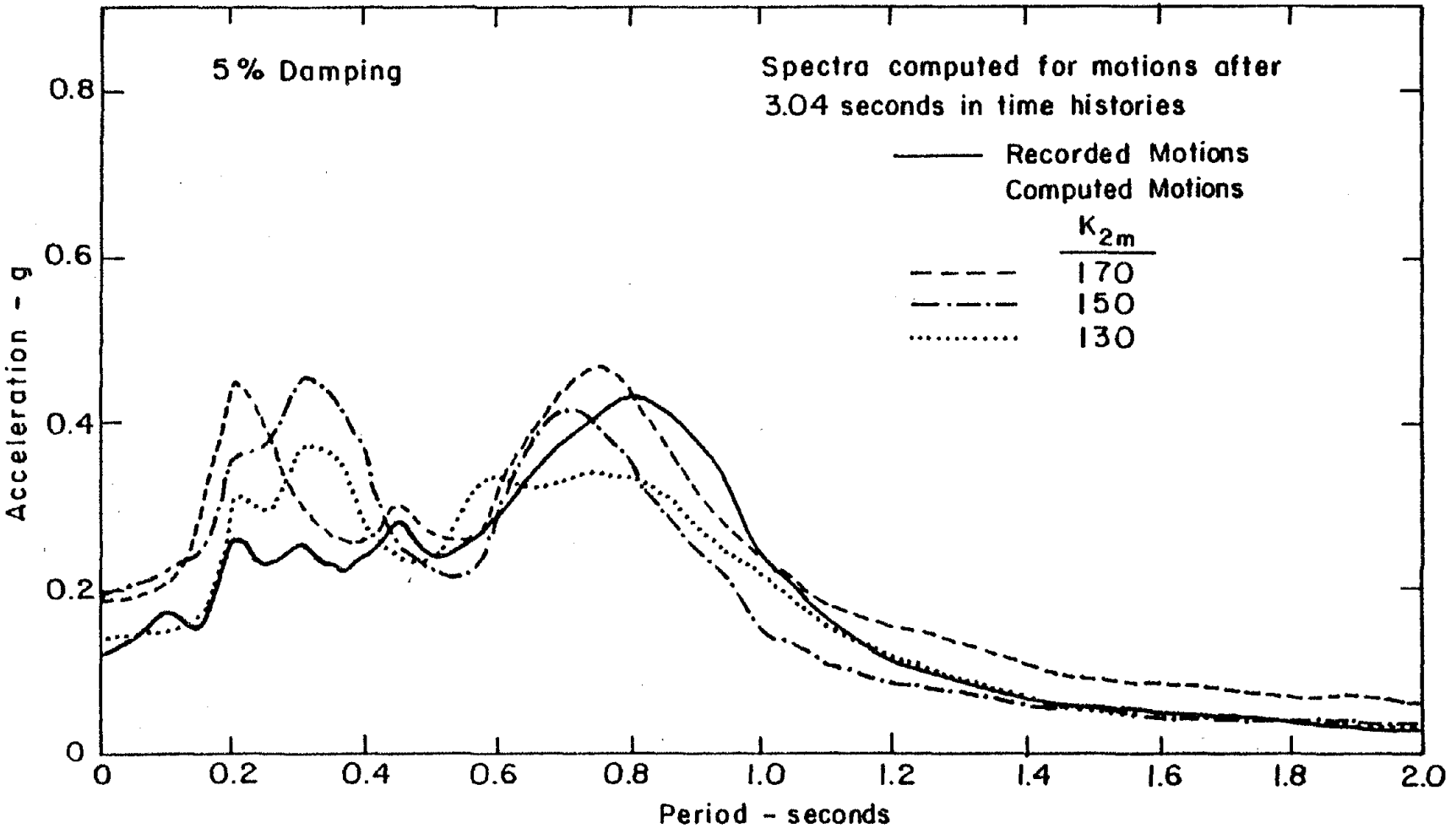

Fig. 3-15 Acceleration Response Spectra for Motions at Crest Midpoint of Oroville Dam, August 1, 1975 Event.

well with the results obtained by the Department of Water Resources.

There are many parameters of significance in the dynamic response of Oroville Dam to the August 1, 1975 Oroville earthquake. However, they are not presented in this section due to the fact that they cannot be compared against field performance. Additional results of the dynamic analysis of the dam for the Oroville earthquake are included in the next chapter of this report.

CHAPTER 4

THREE DIMENSIONAL DYNAMIC RESPONSE OF EARTH DAMS

4.1 Introduction

Assessment of the performance and stability of an earth dam during an earthquake often requires a dynamic response analysis of the structure. Several methods for assessing stability have been proposed and different parameters of dynamic response are required by the different methods. The selection of a critical sliding mass, and computation of a yield acceleration and a time history of average acceleration for this mass, are required in the method proposed by Newmark (1965) and successfully applied to cohesionless soil slopes by Goodman and Seed (1966). A simplified procedure based on this method has been presented by Makdisi and Seed (1977). This procedure can be used to determine approximately the permanent displacements of a sliding mass in a dam provided the yield acceleration for the sliding mass and the peak acceleration at the crest of the dam are known. The method proposed by Seed et al. (1973) involves the determination of the dynamic stresses induced in the dam by the earthquake motions and the determination, in the laboratory, of the behavior of representative samples of the dam materials when subjected to the computed stresses. The observed laboratory behavior can then be used in the assessment of the permanent deformations of the dam by using the procedures presented by Serff et al. (1976).

In conjunction with two-dimensional finite element dynamic analysis procedures the above methods are widely used in current engineering practice to determine the seismic stability of earth dams. Given the

lack of appropriate dynamic analysis procedures, three-dimensional structures have been analyzed using the same methods, and judgement has been used to estimate the effects of 3-D behavior. A very limited amount of work has been performed to study the dynamic response parameters necessary for the stability analysis of three-dimensional structures (Makdisi, 1976; Severn et al., 1980). In view of this fact it seems desirable to investigate the nature of such dynamic response parameters. In particular, it would be desirable to study the nature of acceleration and stress time histories at points of interest in a dam, the relative importance of the different components of the stress tensor and the distribution of peak accelerations and stresses within a dam.

The purpose of this chapter is to present results, in terms of the above parameters, from the analyses of two dams where three-dimensional dynamic behavior is of importance. A description of the dams and earthquakes along with the finite element models and other computational details used in the study is presented in the next section. The results of the analyses are included in subsequent sections and a summary of conclusions is presented in the last section.

4.2 Analyses Performed

The dynamic behavior of earth dams under earthquake loading is dependent on many factors which interact in a complex manner. Analytical procedures for the three-dimensional dynamic analysis of earth dams have been presented in Chapter 2. In accordance with the assumptions made and the model used in those procedures, the most important factors that will influence the dynamic response of an earth dam to seismic

loading are: (1)the geometry of the dam, (2)the dynamic properties of the materials comprising the dam and (3)the nature of the input motions.

Although main section geometries (slopes and zoning) might be somewhat standardized depending on the type of dam, canyon geometries vary widely in practice and are an important factor in determining the three-dimensional behavior of earth dams. In this regard, previous studies (Hatanaka, 1955; Ambraseys, 1960; Makdisi, 1976) have shown that the importance of 3-D effects in rectangular and triangular canyons depends on the crest length to height ratio, L/H (see Fig. 1-1).

In view of the importance of Oroville Dam and the fact that the static and dynamic properties of the dam materials are available, this structure has been selected as one of the dams for which the 3-D dynamic response under seismic loading is studied. Oroville Dam is situated in a triangular canyon and has a crest length to height ratio, L/H, of about 7 (see Fig. 3-11); it is therefore representative of dams with moderate valley wall slopes.

In order to study the effects of canyon geometry on the 3-D dynamic response of earth dams, a dam with a crest length to height ratio, L/H, of 2, has also been analyzed. This structure is representative of dams with steep valley wall slopes. Since there are very few large dams with these characteristics for which the data necessary for a dynamic analysis is available, and since the cross section of Oroville Dam is representative of cross sections for large earthfills in narrow canyons, the dam with valley wall slopes of 1:1 (L/H=2) has been assumed to have the same cross section and material properties as Oroville Dam. This choice of model has the added advantage of facilitating the comparison

of results obtained for the two dams.

Although two might seem a small number of cases to be studied, it is considered that the structures chosen span a range of geometries representative of many existing dams and possible dam sites, and that the results presented will give insight and help to understand the dynamic response of dams where 3-D effects are of concern.

As mentioned before, the finite element dynamic procedures presented in Chapter 2 were used in the analyses of the two structures chosen. It must be noted that the assumption of a rigid boundary deserves special consideration since it would appear that interaction with the abutments and wave propagation effects might be of importance given the size of the dams. Considering the excellent quality of the rocks composing the canyon walls the above assumption seems reasonable in the case of Oroville Dam. Assuming that the foundation rocks for the dam with steep canyon walls are comparable to those for Oroville Dam the afore-mentioned assumption would seem to be appropriate for strong motions during which the dam materials degrade significantly, and perhaps less so for low amplitude motions.

The static stress computations, material properties and finite element model for Oroville Dam have been presented in Chapter 3. The K_2max factor of 170 back-calculated from field behavior has been adopted as representative of the in-situ value for the shell materials.

In order to facilitate comparison of results and reduce manual effort the finite element model for the dam with valley wall slopes of 1:1 was chosen to be geometrically similar to that used for Oroville Dam

(Fig. 3-12). The z coordinates of all nodal points in the latter model were scaled down by a factor of 733/2460 so that a crest length to height ratio, L/H, of 2 was obtained. The material properties for this model were assumed to be the same as those used for Oroville Dam. The static stress distribution computed for the main section of Oroville Dam was assumed applicable and static stresses at the other sections of the model were computed using the same procedure as that adopted for Oroville Dam (Figs. 3-8 and 3-9). Using the same analysis parameters as those used for Oroville Dam has the advantage that the effects of canyon geometry on the three-dimensional behavior of dams are isolated.

The amplitude, frequency content and duration of input motions are important factors in determining the dynamic response of earth dams. In particular, these factors determine the amount of degrading in stiffness and the amount of damping in the dam materials as well as the predominant modes in the response of the structure.

Two earthquake motions of very different characteristics were used in the analyses in order to study the effects of the nature of the input motions on the dynamic response of the selected models. One of these earthquake motions is given by the strong motion record recommended by the Consulting Board convened by the DWR as the design accelerogram for the Oroville Dam facilities. This record is assumed to be representative of the motions which could be generated at the dam site by a magnitude 6.5 earthquake occurring very near the dam and from this point on will be referred to as the Reanalysis earthquake. As can be seen in Fig. 4-1 this accelerogram is composed of modified portions of the records obtained at Pacoima Dam during the 1971 San Fernando earthquake and at

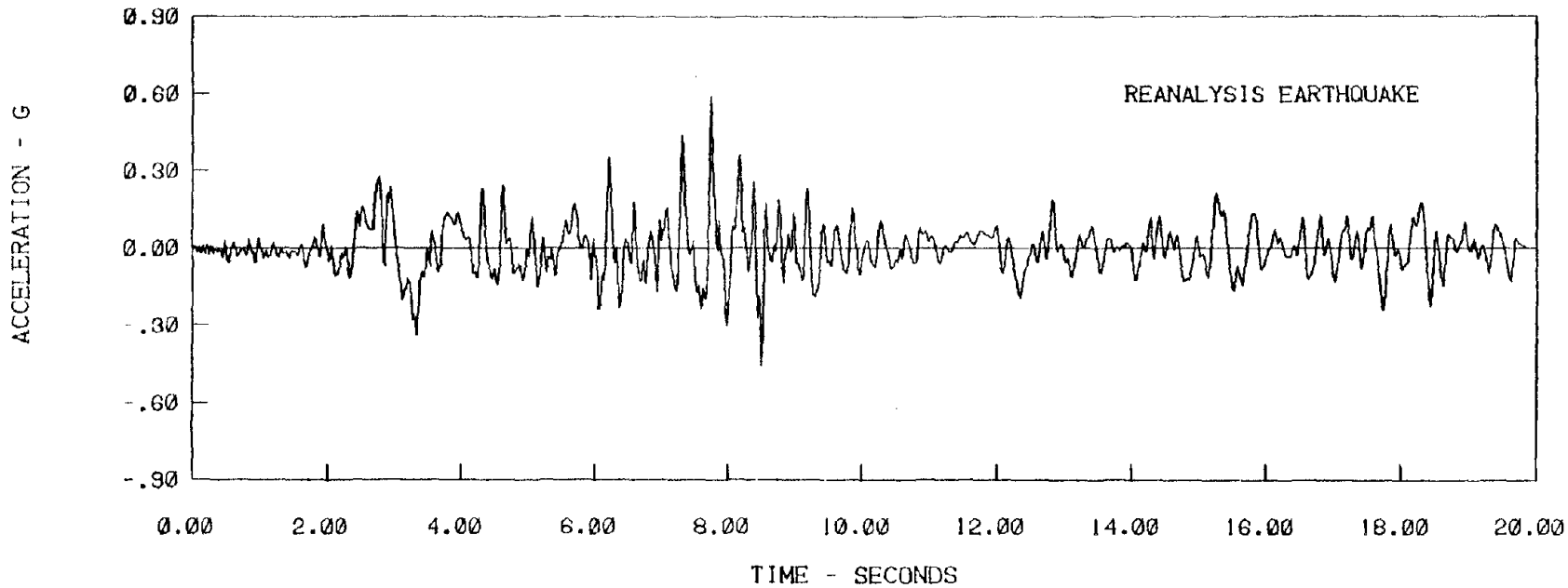

Fig. 4-1 Design Accelerogram for the Oroville Dam Facilities.

Taft during the 1952 Kern County earthquake. The record has a peak acceleration of 0.6 g and a predominant frequency of 2.5 Hz. The strong pulse at about 3.0 seconds has a predominant frequency of about 0.9 Hz and corresponds to the arrival of the shear wave phase. The total duration of the record is 20 seconds and the duration of strong shaking (a > 0.05 g) is on the order of 18 seconds. The acceleration response spectrum for this accelerogram is shown in Fig. 4-2.

The second accelerogram used in the analyses corresponds to the motions recorded at the seismographic station, ORV, during the August 1, 1975 Oroville earthquake. These motions are representative of a 5.7 magnitude earthquake occurring on the Cleveland Hill fault and have low amplitude (A_{max} = 0.09 g), a predominant frequency of 6.5 Hz and a duration of strong shaking of about 3 seconds. The acceleration time history and the corresponding acceleration response spectrum are shown in Fig. 3-10.

The input motions were assumed to act in the upstream-downstream direction of the dam. This is a common assumption since it constitutes the most severe condition of shaking. Vertical motions do not induce as large shear stresses as horizontal motions and therefore do not affect the stability of earth dams to the same degree as the horizontal motions. For the models considered in this study it is also safe to assume that longitudinal motions are less critical than motions in the direction of the canyon axis.

The results of the analyses of the two dam models selected, for the two earthquake motions previously described, are presented in the following sections. A cut-off frequency of 8 Hz was found adequate for the

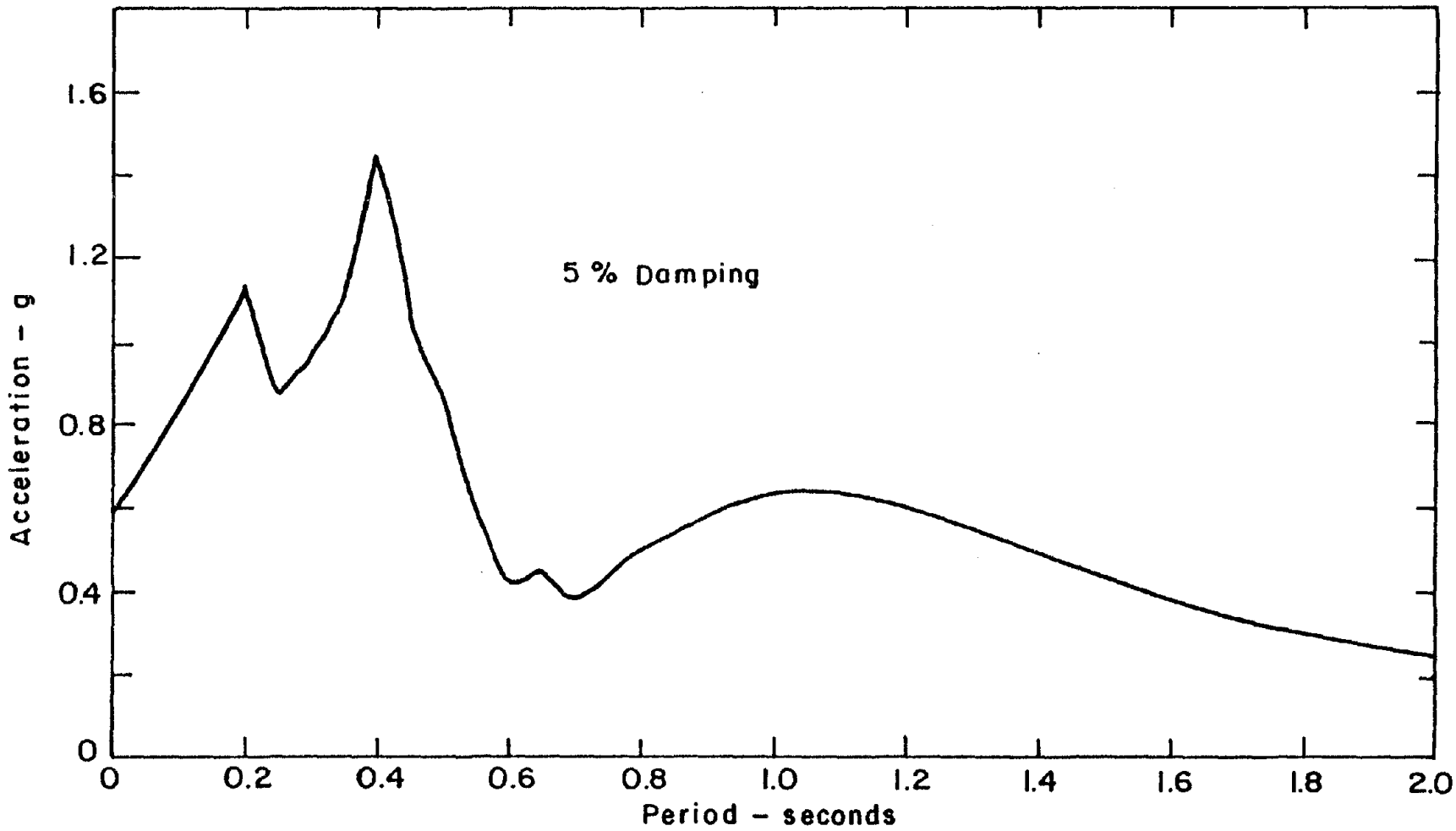

Fig. 4-2 Acceleration Response Spectrum for the Reanalysis Earthquake.

4 analyses performed.

4.3 Analysis of Oroville Dam for the Reanalysis Earthquake

The dynamic stability of earth dams is assessed in current engineering practice in terms of permanent displacements. Methods available, compute these displacements indirectly from the accelerations and stresses induced in the dam by the earthquake motions. For this reason the results of the dynamic analyses herein described will be presented in terms of these parameters.

The acceleration amplification function for the midpoint of the crest of Oroville Dam, for the level of strain induced by the Reanalysis earthquake is shown in Fig. 4-3. This function gives the ratio of amplitude of absolute acceleration at the crest midpoint to the amplitude of acceleration at the rigid boundaries for each frequency of harmonic excitation. It can be seen that the maximum amplification has a value of 8.9, that this peak occurs at a frequency of 0.71 Hz, and that there is very little response at the crest midpoint for frequencies higher than 2.5 Hz. From the peak frequency it can be concluded that the natural period of Oroville Dam for the level of strain induced by the Reanalysis earthquake is on the order of 1.41 seconds. The following reasons are responsible for the small response beyond 2.5 Hz: a) low shear moduli produced by degradation of the materials reduce natural frequencies of vibration, b) high damping produced by degradation of the materials (~ 15%) damps out the higher modes of vibration and c) even for low damping the response at the point considered is not large in the higher modes of vibration.

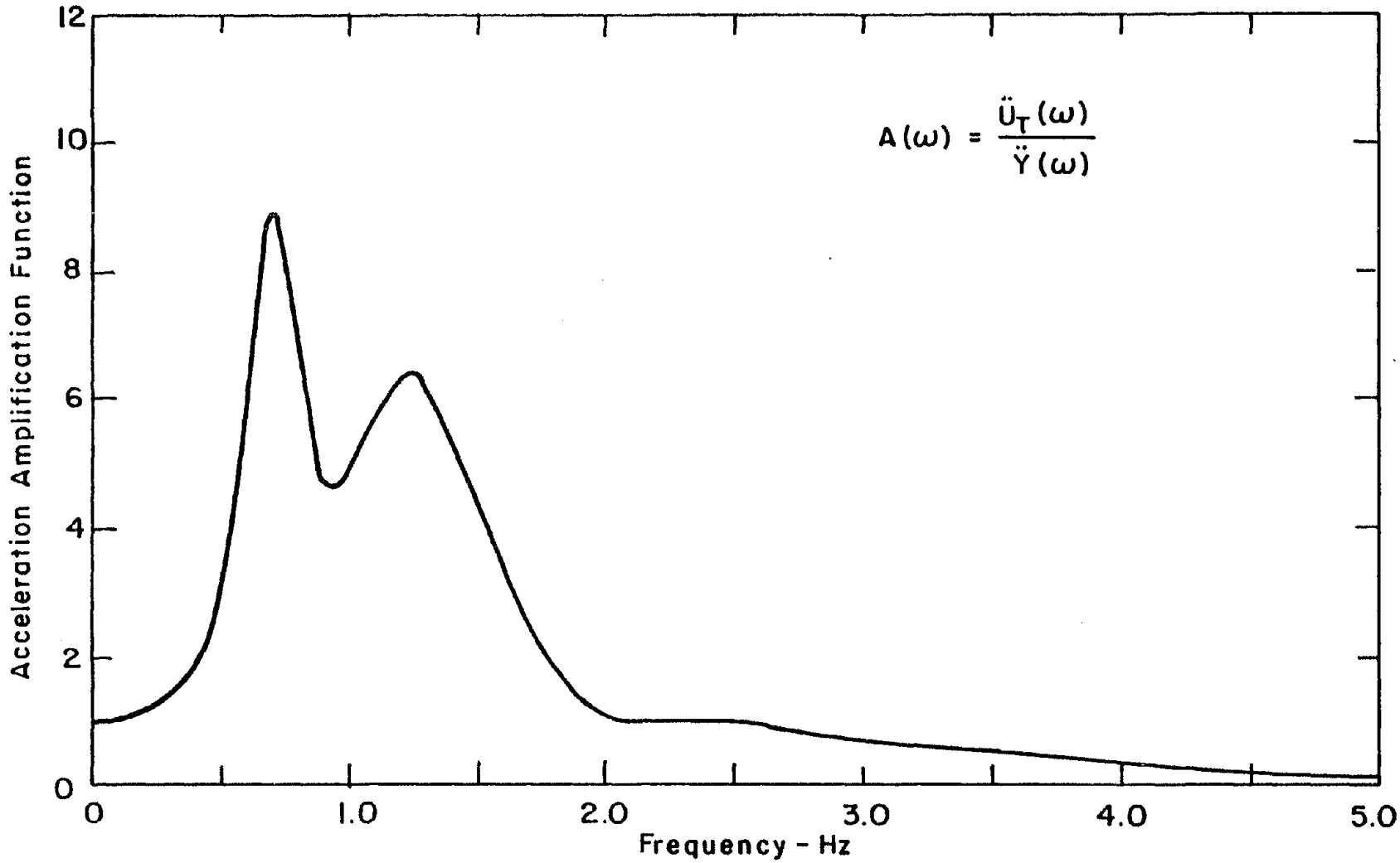

Fig. 4-3 Acceleration Amplification Function for Crest Midpoint of Oroville Dam.

Fig. 4-4 shows the finite element model used in the dynamic analyses and the nodal points for which acceleration time histories are presented. The time histories corresponding to the points along the contact between the core and the downstream shell of the dam are shown in Fig. 4-5. It is interesting to note the progressive amplification of the motions and the filtering of high frequency peaks with increasing elevation within the dam. The high frequency peak of 0.6 g present in the motions at the rigid boundary (Fig. 4-1) has disappeared at the level of nodal point 287 and the peak acceleration at this point is on the order of 0.33 g. The acceleration pulse present in the input motions at about 3.5 seconds is amplified at the crest midpoint about 3.3 times to give a peak acceleration at this location on the order of 1.0 g. This high amplification is not surprising in view of the fact that the period of this pulse is very close to the natural period of the dam. Stability of the crest under these high accelerations is of concern. It must be noted that due to the fact that the analytical model uses the equivalent linear method to take into account the non-linear behavior of soils, all computed displacements are elastic and the model cannot simulate permanent deformations arising from the true non-linear characteristics of the material.

The computed acceleration time histories for nodal points along the crest of the dam are shown in Fig. 4-6. It can be seen that high accelerations are obtained along the entire length of the crest. Except for points near the abutments where peak accelerations result from amplification of high frequency motions, peak accelerations along the crest come from the amplification of the strong pulse present in the input motions at 3.5 seconds.

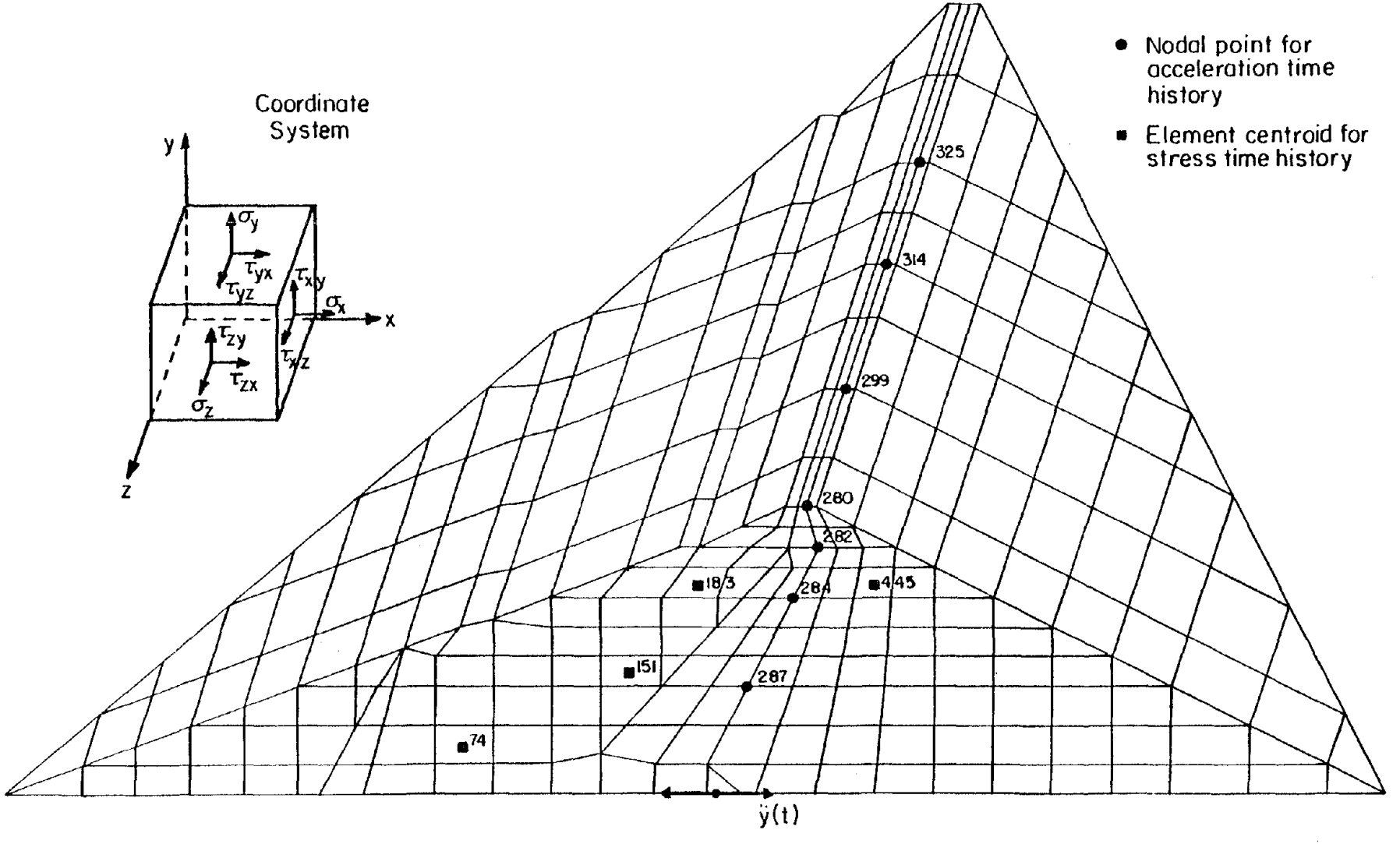

Fig. 4-4 Finite Element Model and Points for Time History Output.

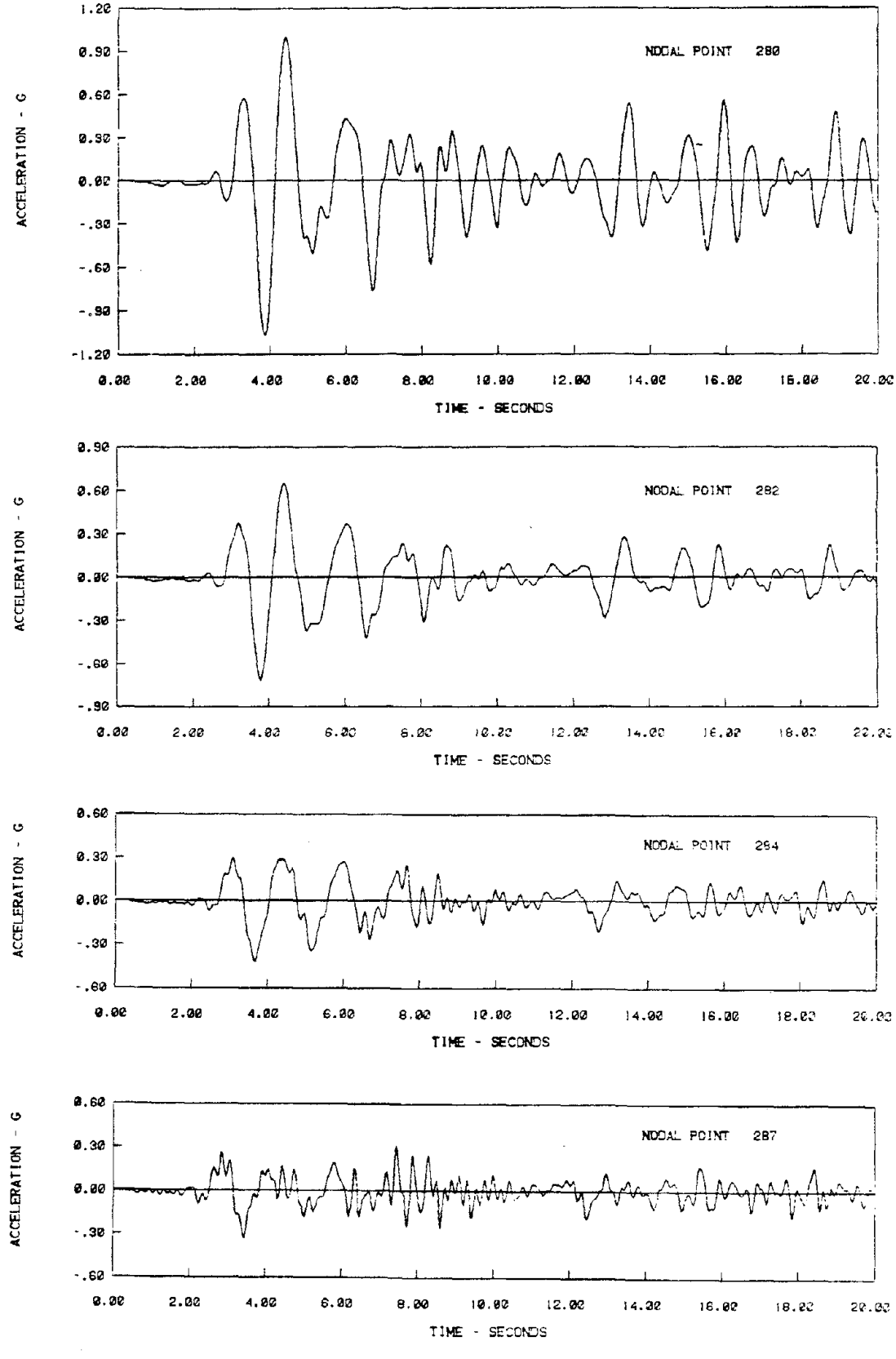

Fig. 4-5 Acceleration Time Histories for Points Along Core-shell Contact of Oroville Dam.

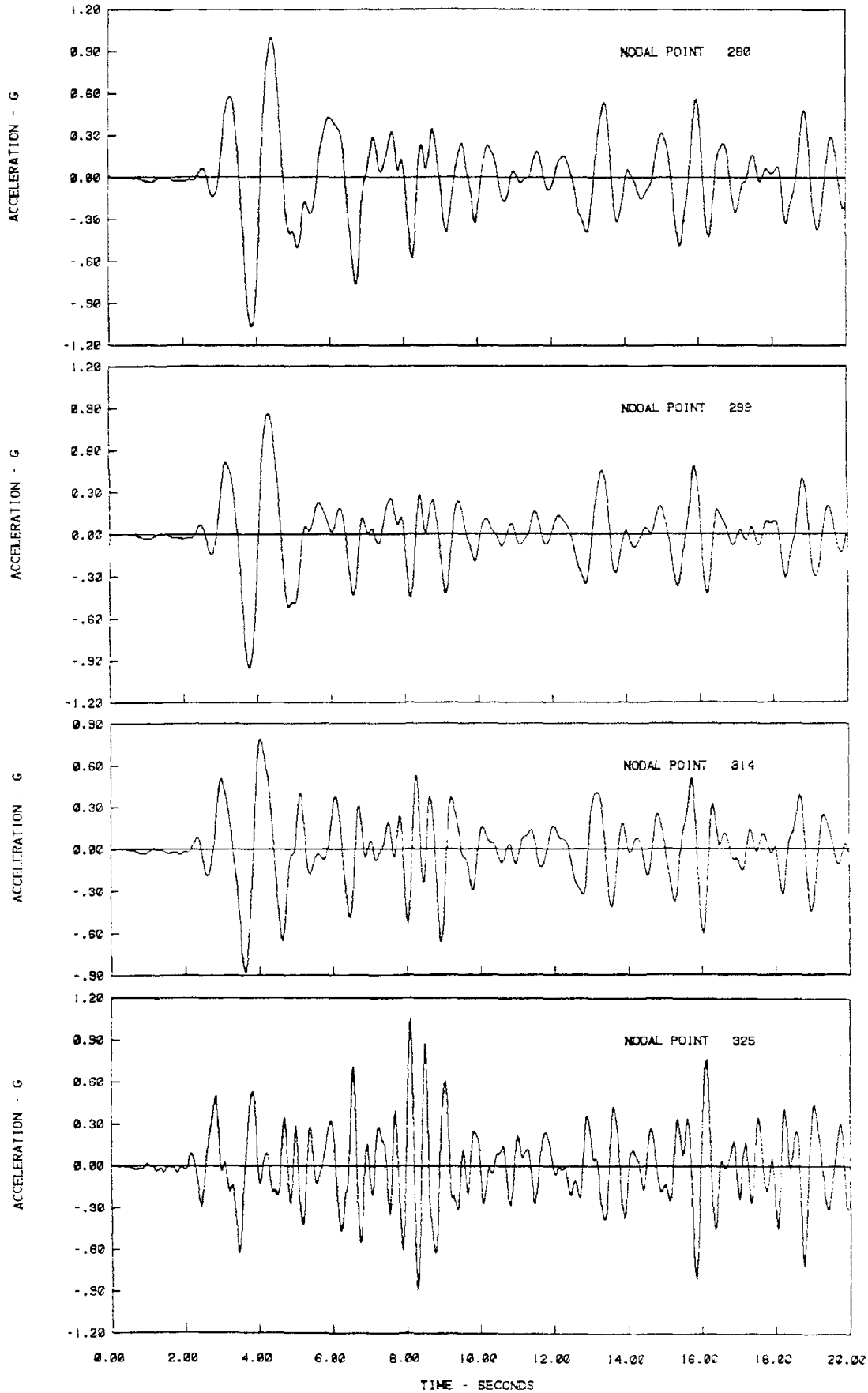

Fig. 4-6 Acceleration Time Histories for Points Along Crest of Oroville Dam.

A summary of peak accelerations for diverse points in the dam is shown in Fig. 4-7. The profile along the contact between the core and the downstream shell shows a decrease in peak acceleration from 0.6 g at the base to 0.33 g at midheight and then an increase to 1.05 g at the crest. Also shown is the variation of peak accelerations along the downstream slope and along two vertical lines in the downstream shell of the dam. Up to elevation 550 feet on the downstream slope peak accelerations are due to the amplification of high frequency amplitudes and beyond this point they are the result of the amplification of the 3.5 second pulse in the input motions. A similar discontinuity is observed in the profile of accelerations along the crest of the dam.

Although accelerations are of importance induced stresses in the dam are equally important if not more. This is especially true for dams built with materials susceptible to generation of pore pressures, strength loss and development of high strains under cyclic loading (Makdisi and Seed, 1977; Seed et. al, 1977).

Time histories of stress were computed for several elements in the dam. However, due to lack of space only those corresponding to the elements shown in Fig. 4-4 are presented here. Fig. 4-8 shows time histories of shear stress on horizontal planes in the x direction, τ_{yx} (same as τ_{xy}), for elements numbers 74, 183, 186, and 445. Element 186 does not appear in Fig. 4-4 since it is located near the quarter section of the dam at the same x and y coordinates as element 183. All stress time histories computed exhibited a common pattern. As can be seen in Fig. 4-8 the peak stress at all points examined occurs nearly at the same time (approximately 4.0 seconds) as a result of the strong pulse

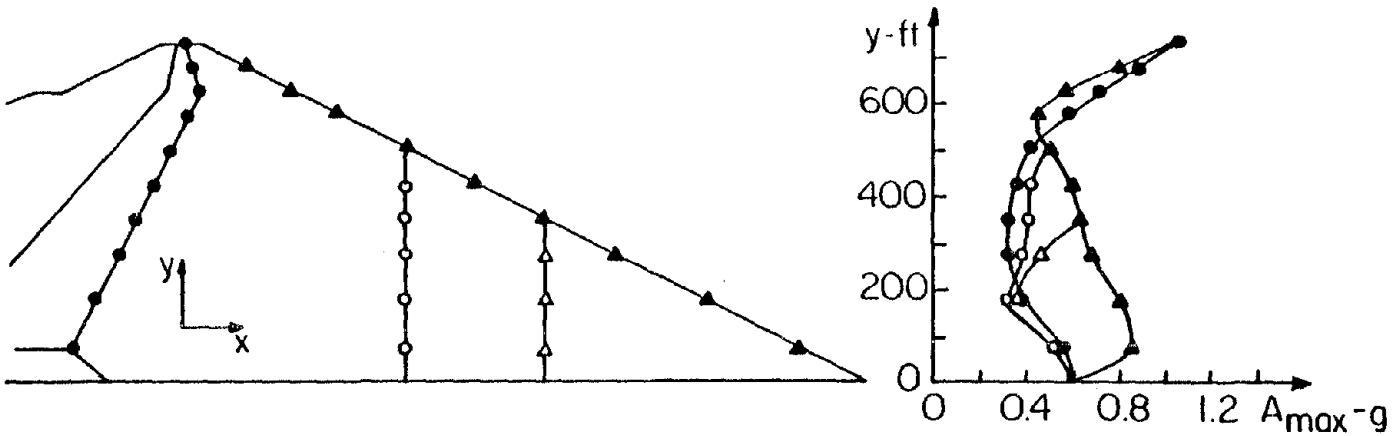

(a) Profiles along core-shell contact and along downstream slope

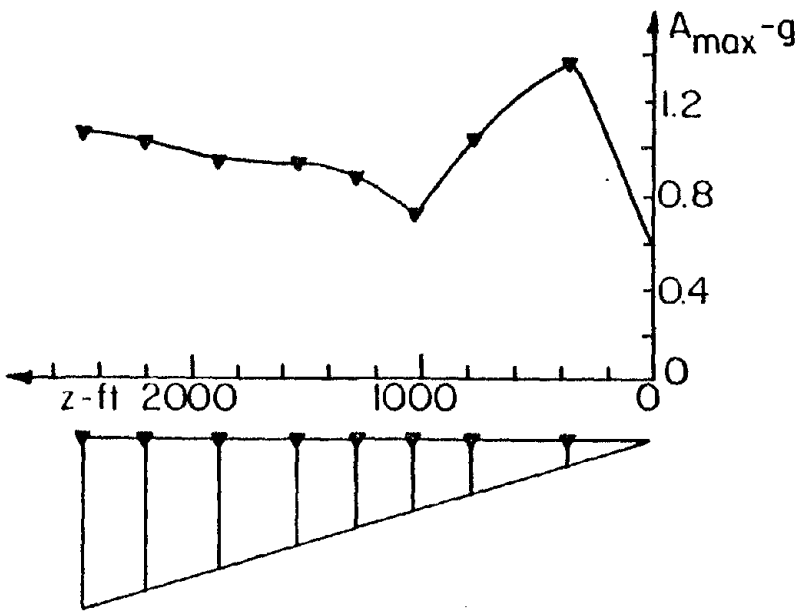

(b) Profile along crest

Fig. 4-7 Peak Horizontal Accelerations Computed from 3-D Analysis of Oroville Dam for the Reanalysis Earthquake.

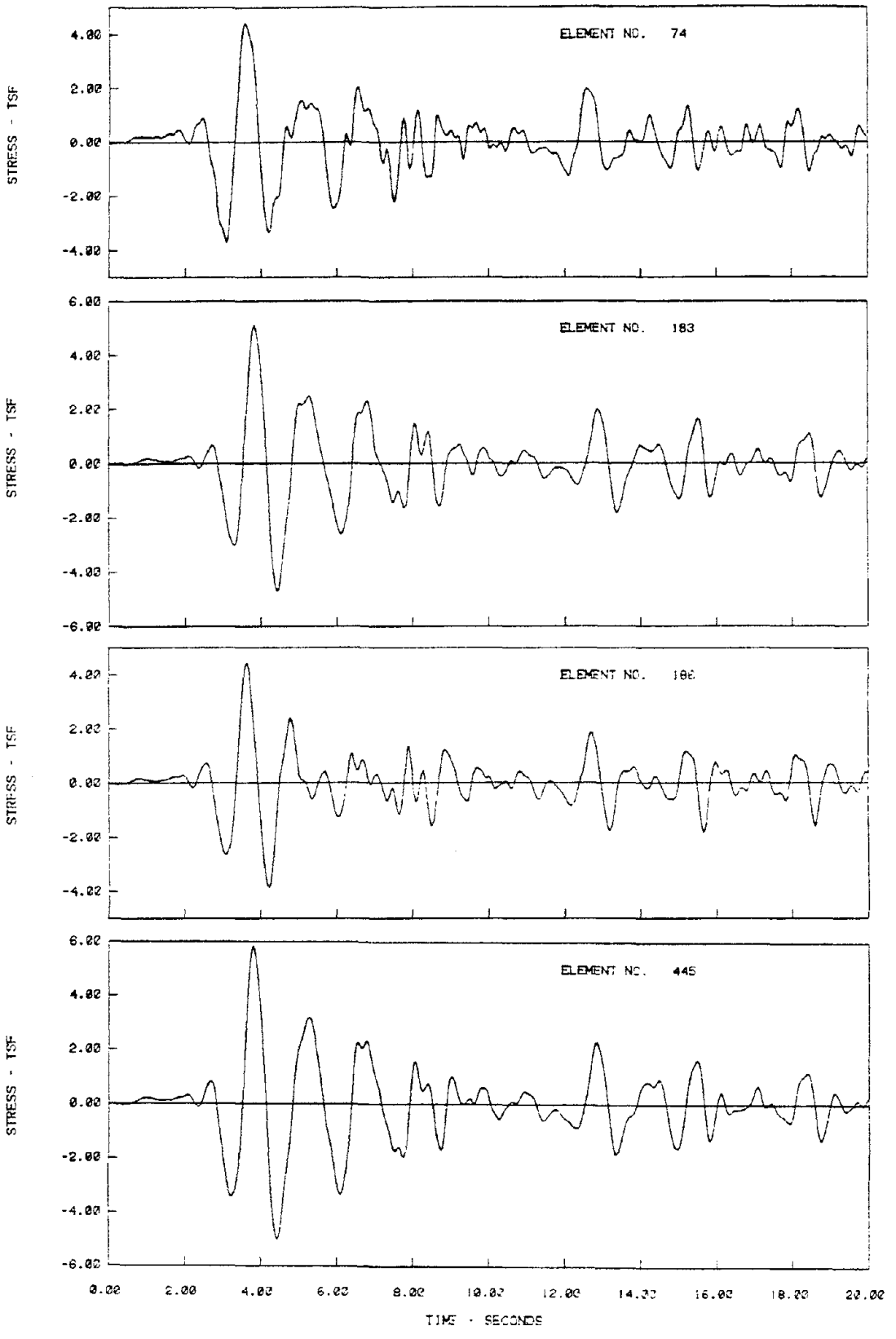

Fig. 4-8 Time Histories of Shear Stress τ_{xy} for Selected Points of Oroville Dam.

present at the beginning of strong shaking in the input motions. Due to the similarity in pattern the number of equivalent cycles (Seed et al., 1975) for all the computed stress time histories is approximately the same. The time histories for the components of the stress tensor at the centroid of element 151 are shown in Fig. 4-9. It can be seen that all components of stress except for the normal stress on the horizontal plane, σ_y, are considerably smaller than the shear stress on the horizontal plane τ_{xy} (same as τ_{yx}). It may be noted that although this observation might hold for points near the main section of the dam it is not necessarily true for points at other sections in the dam where significant horizontal shear stresses on the z plane, τ_{zx}, (see Figs. 4-4 and 4-12) might be present.

Assessment of the seismic stability of earth dams following the method first proposed by Seed, 1966 and further developed by Seed et al., 1969 and Seed et al., 1973 requires a comparison of the induced dynamic shear stresses with the cyclic strength of the material. It is customary to use the shear stress on horizontal planes in the x direction, τ_{yx}, in these comparisons, and to represent the time history of this stress component by an average value of about 65% of the peak stress and an equivalent number of cycles (Seed et al., 1975). Therefore, it is of interest to study the distribution of peak shear stresses, τ_{yx}, within the dam. For this reason the contours of equal shear stresses, τ_{yx}, have been computed and plotted for the sections of Oroville Dam shown in Fig. 4-10. As can be seen in this figure four sections evenly spaced along the longitudinal axis of the dam have been selected. The largest section, section A, is very close (within 130 ft) to the main section of the dam and section C is located near (within 70

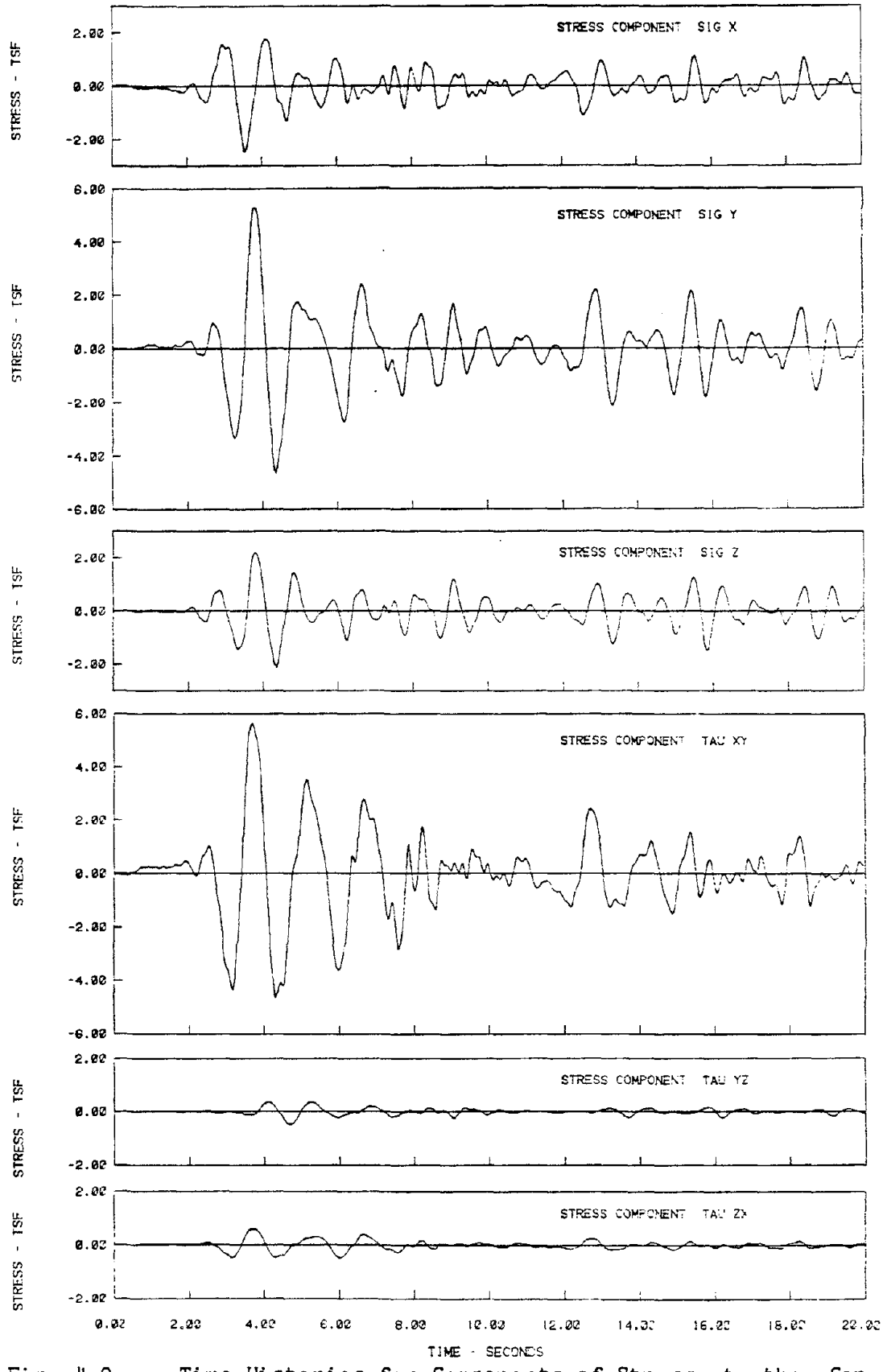

Fig. 4-9 Time Histories for Components of Stress at the Centroid of Element 151 of Oroville Dam.

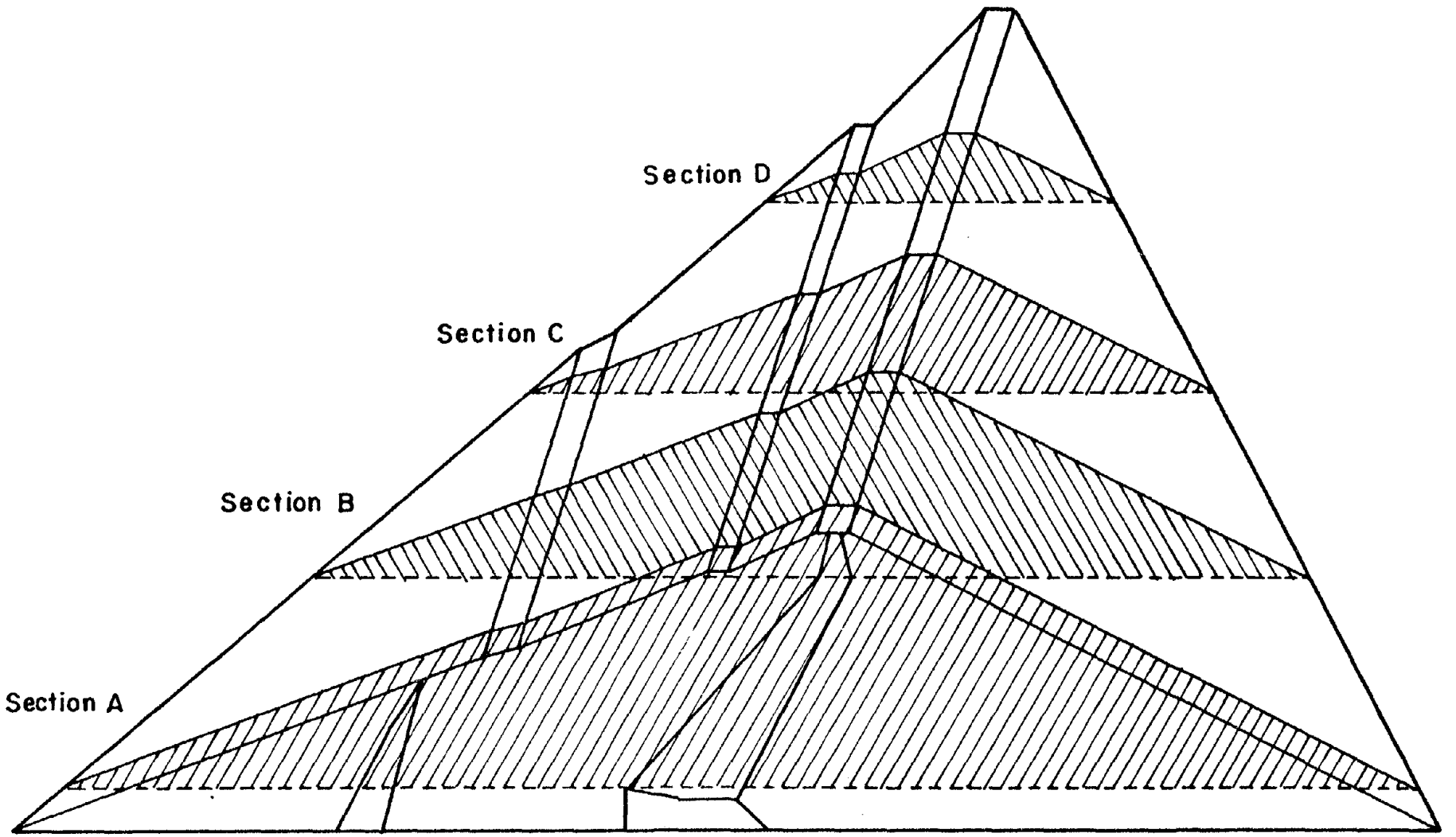

Fig. 4-10 Sections of Model Selected for Display of Stress Distributions.

ft) the quarter point of the crest.

The contours of equal peak shear stresses on horizontal planes, τ_{yx}, induced in Oroville Dam at the selected sections by the Reanalysis earthquake are shown in Fig. 4-11. In general it can be observed that the stress distributions at all sections show an increase in stress with increasing depth and a decrease in stress with increasing distance from the center of the dam. An exception to this observation occurs near the base of section A for which the maximum stresses occur in a small zone overlying the concrete core block. The stresses near the base of section A are smaller than in the overlying zones due to the three-dimensional effects caused by the vertex of the triangular canyon and due to the presence of the core block. The contours of stress bend downwards in the core given the fact that shear moduli for these materials are lower than those for the shell materials. A similar cause is in part responsible for the fact that the stresses in the downstream shell are higher than those in the upstream shell. A general decrease in shear stresses with increasing distance from the main section of the dam can also be noticed.

As mentioned before it is commonly assumed that the permanent deformations and general stability of earth dams are mainly dependent on the horizontal shear stresses, τ_{yx}. Given the fact that mean normal stresses do not induce significant strains in the material and that the τ_{yx} stresses are very close to the maximum shear stresses, the above assumption is adequate in the case of dams where plane strain conditions are predominant. This however, is not necessarily true for dams which exhibit considerable three-dimensional dynamic behavior and for which

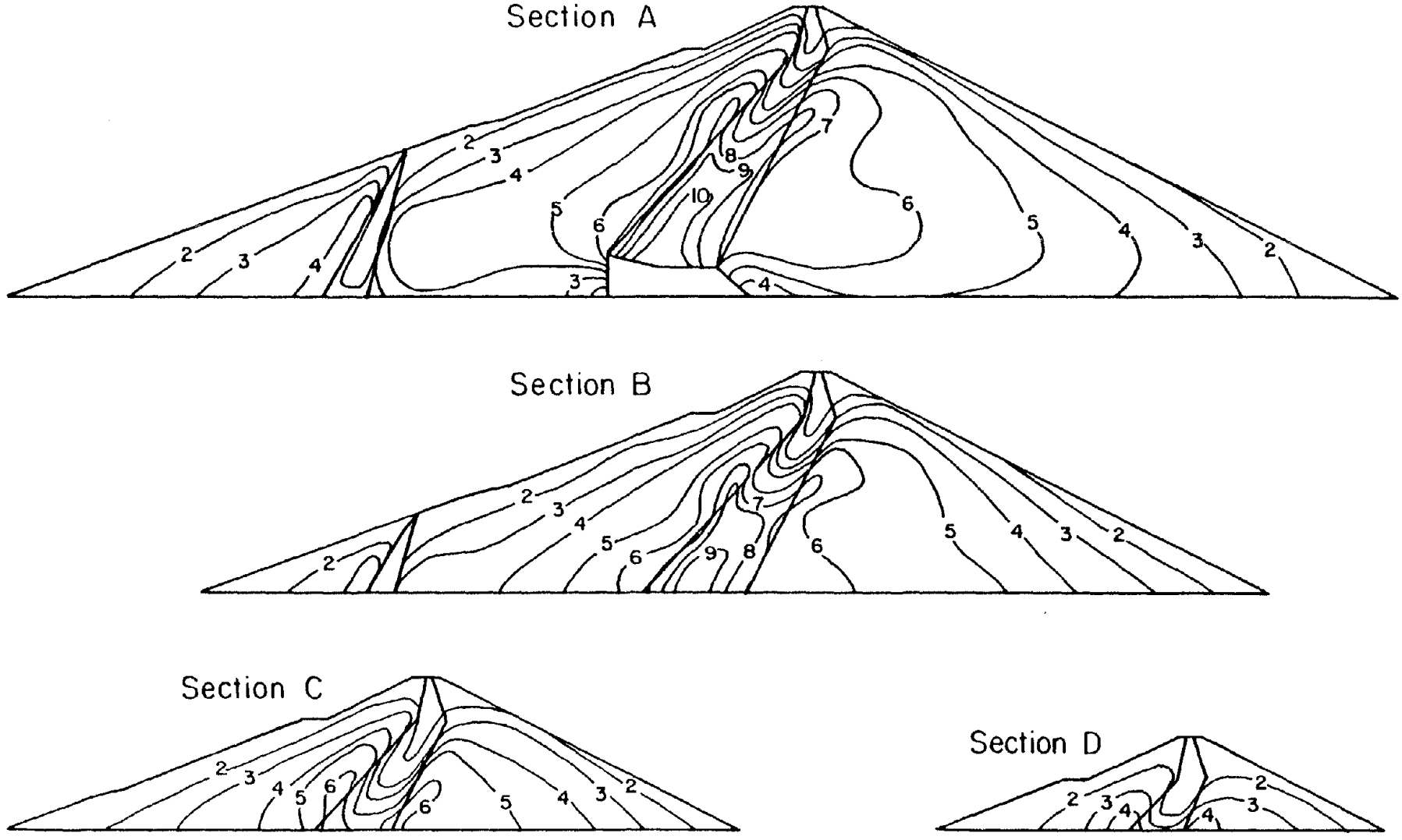

Fig. 4-11 Distribution of Peak Shear Stress τ_{xy} in Tsf Computed from 3-D Analysis of Oroville Dam for the Reanalysis Earthquake.

other components of the stress tensor might affect the deformational behavior of the materials. Therefore, it is desirable to investigate the relative importance of the different stress components, in particular the horizontal and vertical shear stresses on the z plane, τ_{zx} and τ_{zy} (see Fig 4-4).

Computation of the τ_{zy} stresses was performed at the centroid of all elements in the model and it was found that this component of stress exhibits very small values throughout the dam. This is not surprising in view of the fact that the input motions have been assumed to act in the upstream-downstream direction, that is, the x direction.

Fig. 4-12 shows the distribution of peak horizontal shear stresses on the z plane, τ_{zx} for the four sections shown in Fig. 4-10. In general it can be noticed that the magnitudes of these stresses are much lower than those of the τ_{yx} stresses and that they increase with depth. The stresses at section C are highest and they are lowest for section A (at comparable x and y coordinates). The fact that section A is near the main section of the dam which is a plane of symmetry is in part responsible for the low τ_{zx} stresses at the former.

A measure of the relative importance of the τ_{yx} stresses in regard to the development of strains and deformations of the dam materials can be obtained by computing the ratio of peak values, τ_{yx} / τ_{max}. Fig. 4-13 shows the contours of equal values of this ratio for the previously selected sections of the dam. It can be seen that this ratio is greater than 85% everywhere in the dam and is greater than 95% in large portions of the dam. On the basis of this observation it can be concluded that in the case of Oroville Dam subjected to the Reanalysis earthquake

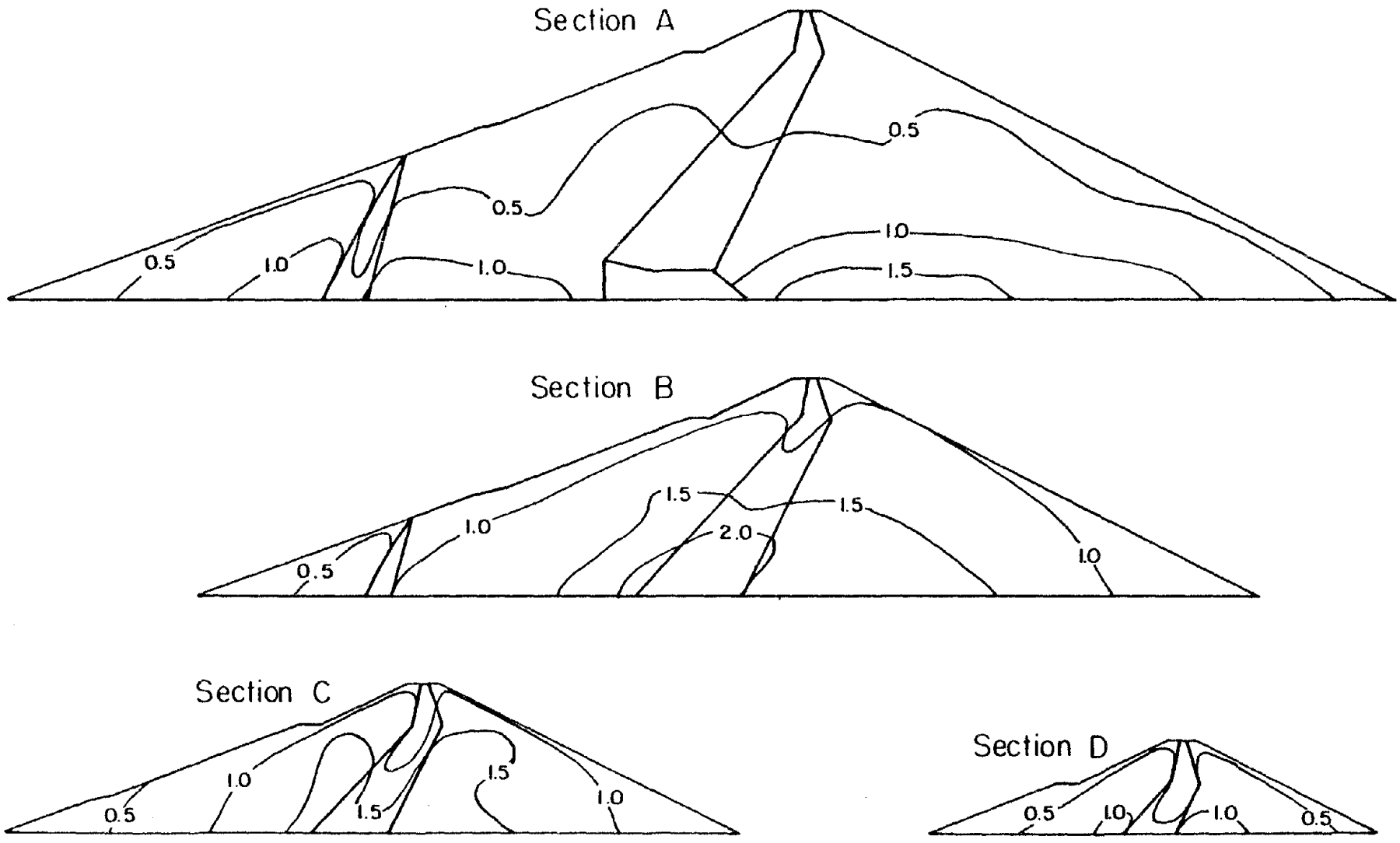

Fig. 4-12 Distribution of Peak Shear Stress τ_{xz} in Tsf Computed from 3-D Analysis of Oroville Dam for the Reanalysis Earthquake.

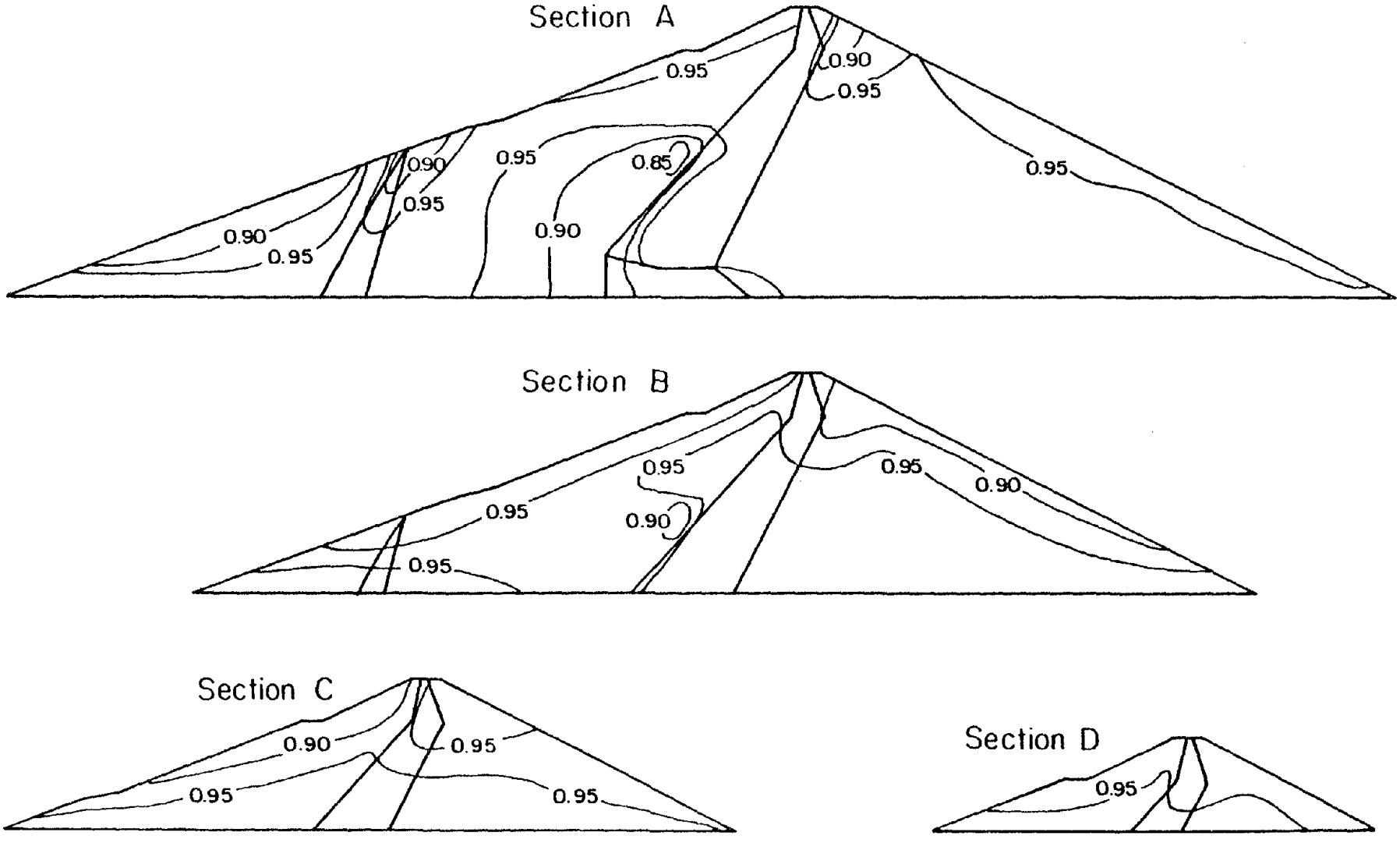

Fig. 4-13 Distribution of the Ratio τ_{xy}/τ_{max} Computed from 3-D Analysis of Oroville Dam for the Reanalysis Earthquake.

motions, in the upstream-downstream direction, the shear stresses on horizontal planes, τ_{xy}, are representative of the stress levels responsible for material deformations. Therefore, they are an adequate parameter to use in determining the stability and deformations of the dam.

4.4 Analysis of Oroville Dam for the Oroville Earthquake

Comparison of the results from the analysis of the Oroville Dam for the Oroville earthquake with those presented in the previous section will serve to illustrate several effects on the dynamic response of earth dams due to the nature of the input motions.

The amplification function at the midpoint of the crest of the dam for this analysis was shown in Fig. 3-13 (K_2max = 170). The computed natural period of the dam for the levels of strain induced by the Oroville earthquake was 0.83 seconds, a value that was found to to be very close to the observed natural period in the field. The large difference between this value and that computed in the previous section is due to the difference in strain levels induced by the two earthquakes. It can also be noticed that due to the much smaller level of damping present in this analysis a high amplification value (30.7) and several frequency peaks are observed in the crest amplification function.

The acceleration time history at the crest midpoint was presented in Fig. 3-14 (K_2max = 170). No particular section of the input motions record was amplified significantly. The acceleration time histories for points along the contact between the core and the downstream shell showed the same amplification and filtering effects with increasing height as those observed in the previous section. Similar observations

could be made for the motions along the crest of the dam.

The profiles of peak accelerations along the contact between the core and downstream shell, along the downstream slope of the dam and along the crest are shown in Fig. 4-14. The motions at the rigid boundary which have a peak acceleration of 0.09 g, are amplified to give a peak value of 0.23 g at the crest. It can be seen that the peak accelerations decrease gradually with depth with the lowest value corresponding to that of the input motions. The peak accelerations on the downstream slope vary erratically with a very high value of 0.39 g observed at elevation 75 ft. Peak values along the crest also vary erratically and, again, a high value of 0.37 g is observed. This variation in acceleration denotes a large influence of the higher modes of vibration of the dam, low damping, and small filtering of high frequency amplitudes.

The stress time histories at the same points studied in the previous section were computed. A similarity in pattern was observed and the number of equivalent cycles was approximately the same for the majority of elements in the dam. Fig. 4-15 shows the contours of shear stress on horizontal planes, τ_{xy}, for the sections shown in Fig. 4-10. It is noticed that the stress distribution is quite different from that obtained for the Reanalysis earthquake. Therefore, one cannot be obtained from the other by scaling by the average ratio between stresses in the two analyses. This ratio seems to be on the order of 6. As in the analysis of Oroville Dam for the Reanalysis earthquake, effects of the vertex of the canyon and of the concrete core block on the computed τ_{xy} stresses can be observed. The peak vertical and horizontal shear

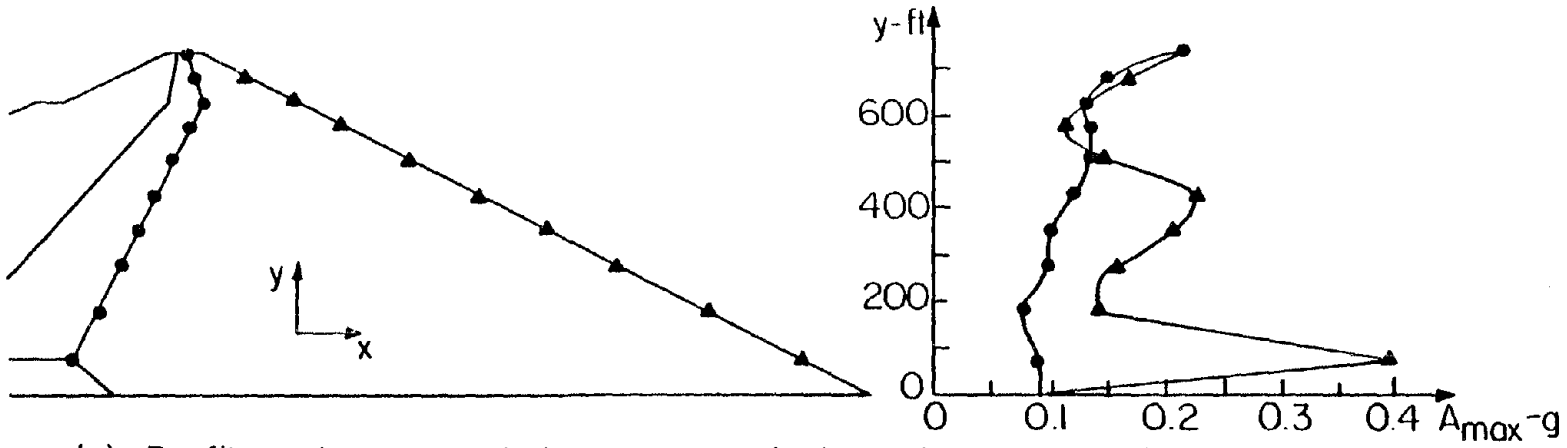

(a) Profiles along core-shell contact and along downstream slope

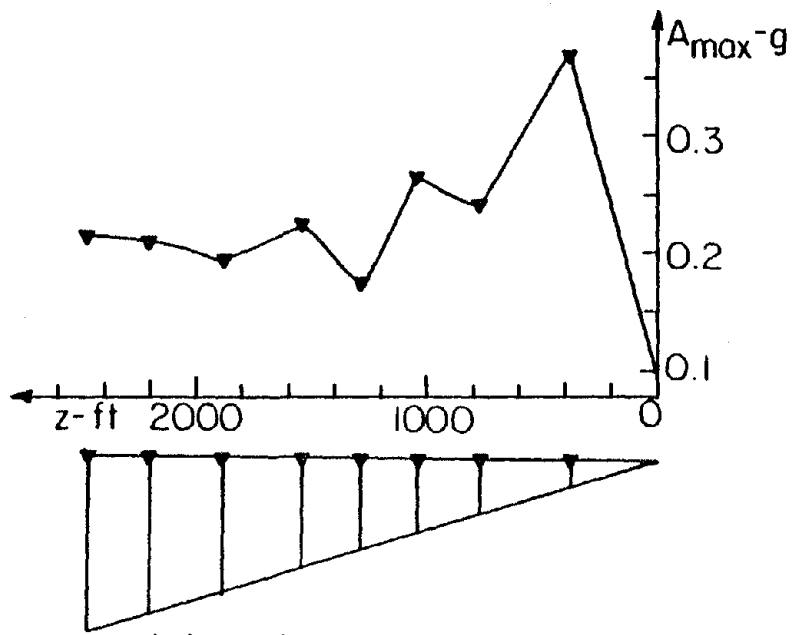

(b) Profile along crest

Fig. 4-14 Peak Horizontal Accelerations Computed from 3-D Analysis of Oroville Dam for the Oroville Earthquake.

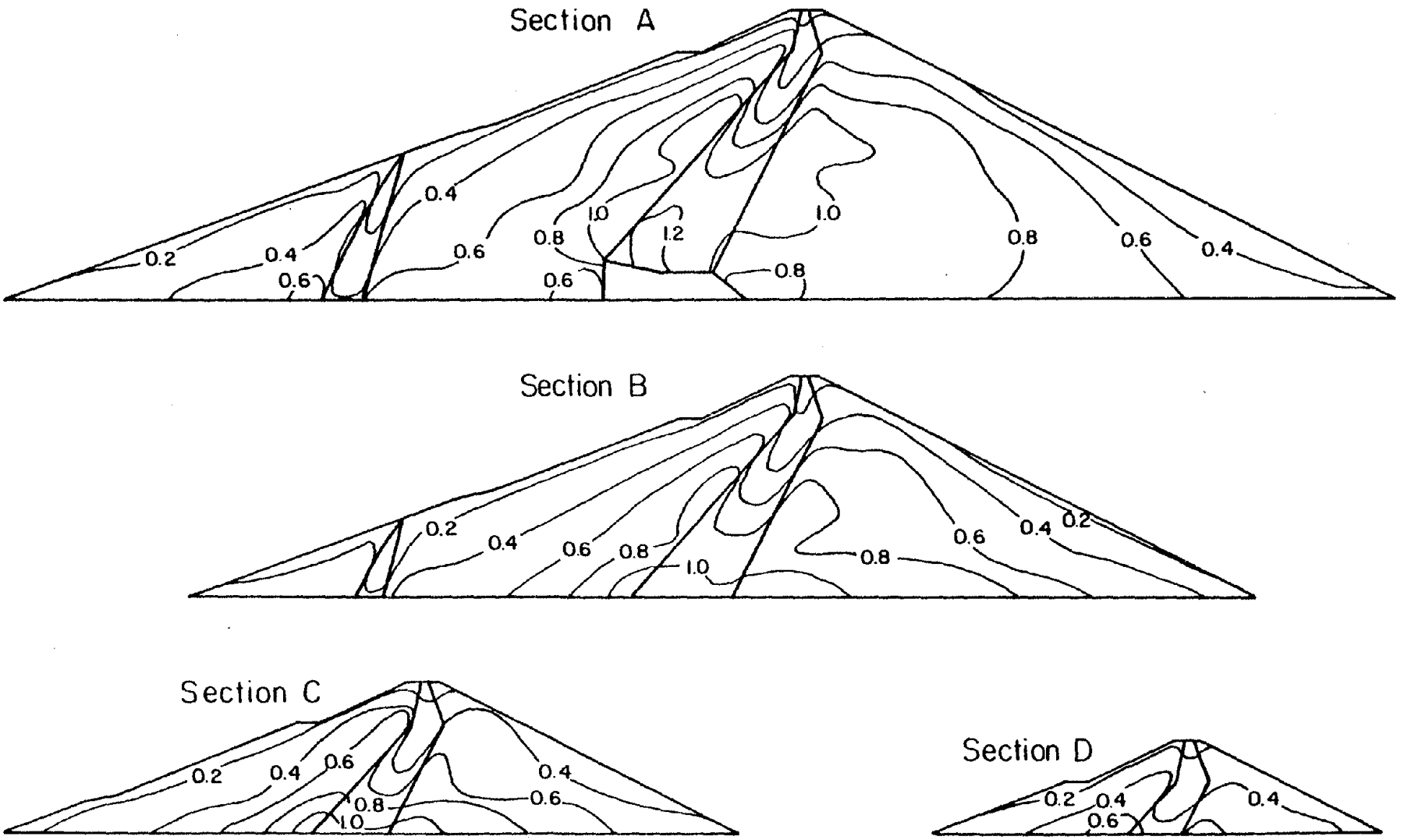

Fig. 4-15 Distribution of Peak Shear Stress τ_{xy} in Tsf Computed from 3-D Analysis of Oroville Dam for the Oroville Earthquake.

stresses on the z plane, τ_{zy} and τ_{zx}, were computed but given their small magnitudes, they were not plotted.

4.5 Analysis of Dam with Valley Wall Slopes of 1:1 for the Reanalysis Earthquake

Results from the analysis of the dam with canyon wall slopes of 1:1 for the Reanalysis earthquake are presented in this section. Comparison of these results with those obtained from the analysis of Oroville Dam for the same earthquake will illustrate the effects of canyon geometry.

The acceleration amplification function computed in this analysis for the midpoint of the crest of the dam is shown in Fig. 4-16. The fundamental natural frequency of vibration of the dam is on the order of 0.93 Hz which corresponds to a period of about 1.08 seconds. This period is 23% lower than the natural period of Oroville Dam for the same earthquake. The average level of strain induced in the dam was examined and it was found to be very similar to that induced in Oroville Dam by the same earthquake. Therefore, it can be concluded that the difference in natural periods for the two dams reflects the stiffening effect of the canyon geometry. The amplification function has a peak value of 10.2 which is 15% higher than the corresponding value for Oroville Dam. This slightly higher amplification coupled with the fact that it affects a broad band of frequencies in the vicinity of the predominant frequency of the strong pulse in the input motions, is responsible for the high accelerations obtained in this analysis. Fig. 4-17 shows the acceleration time histories for the nodal points along the contact between the core and the downstream shell shown in Fig. 4-4. Again, amplification

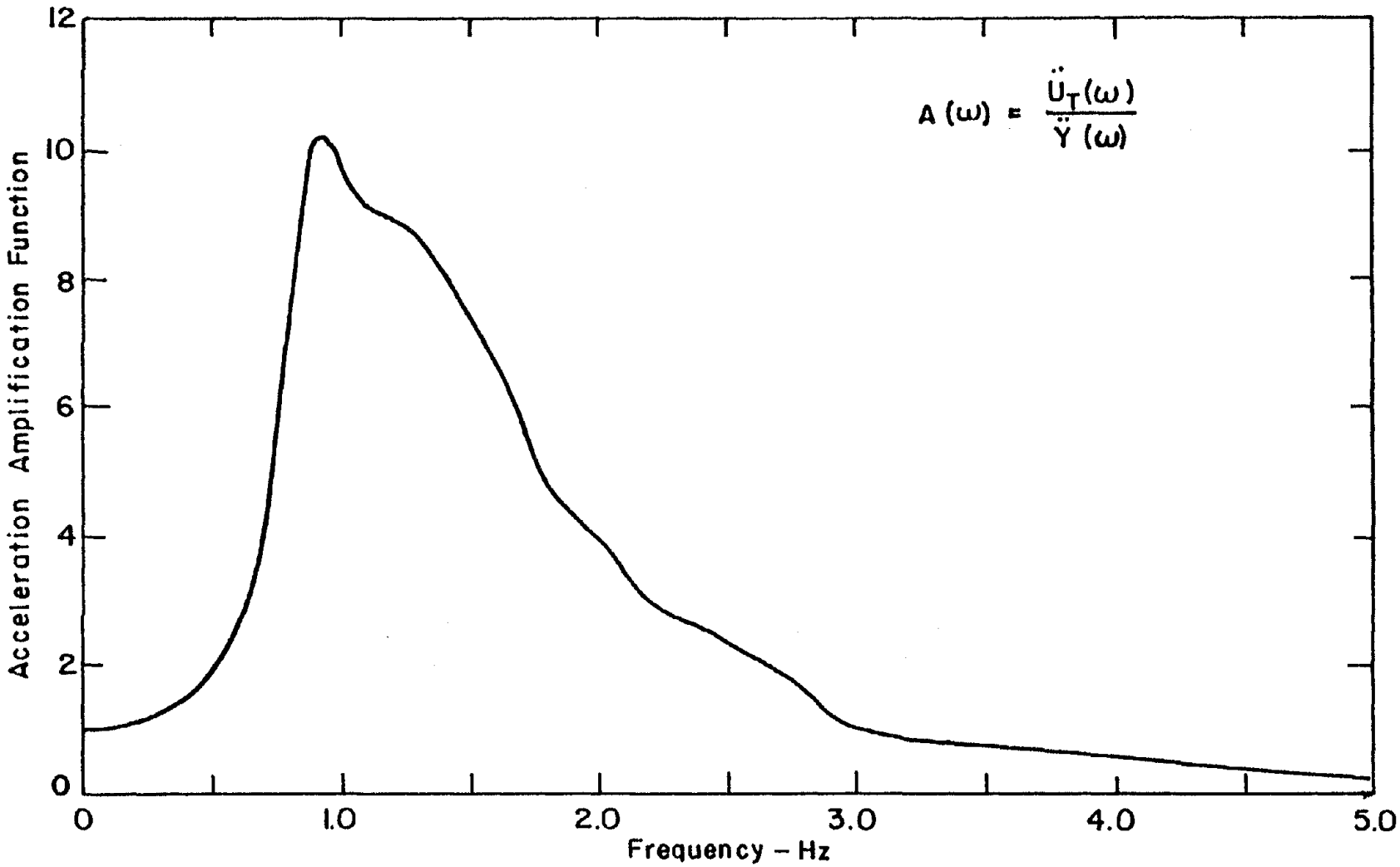

Fig. 4-16 Acceleration Amplification Function for Crest Midpoint of Dam with Valley Slopes of 1:1.

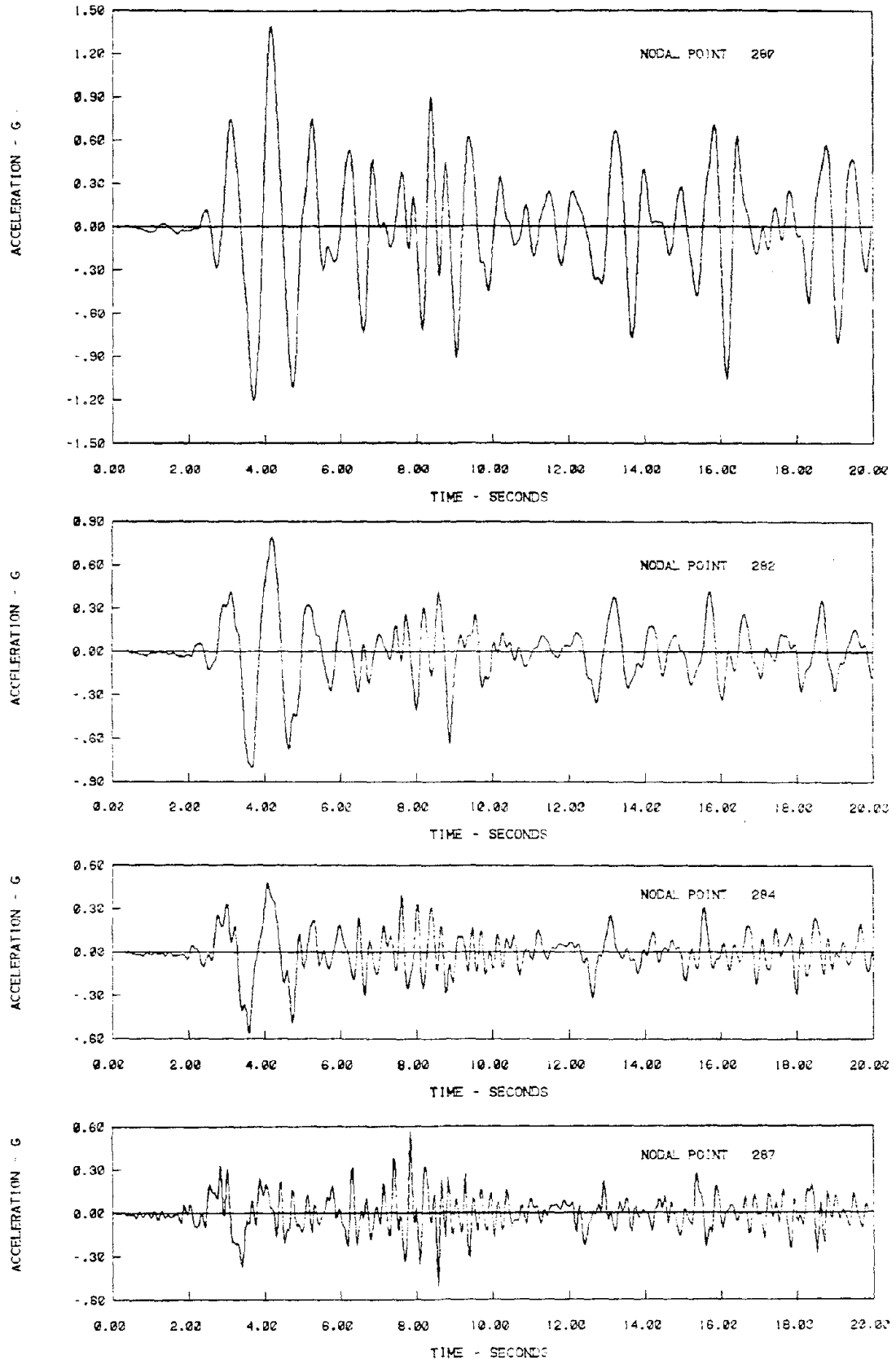

Fig. 4-17 Acceleration Time Histories for Points Along Core-Shell Contact of Dam with Valley Wall Slopes of 1:1.

of motions and filtering of high frequency amplitudes with increasing elevation can be observed. The time histories are quite similar in pattern to those computed for Oroville Dam at the same points. Considering the fact that for harmonic motions the amplitude of displacement is equal to the amplitude of acceleration divided by the square of the angular frequency, it can be concluded that the higher accelerations obtained in this analysis do not necessarily imply higher elastic displacements than in the case of Oroville Dam. An analogous statement can be made for permanent displacements. Nevertheless, stability of the crest of the dam under these high accelerations is of concern.

The variation of peak accelerations with depth, along the downstream slope and along the crest of the dam are shown in Fig. 4-18. It is interesting to note that a constant value of peak acceleration of about 0.6 g is observed up to elevation 500 feet and that there is a sharp increase to a value of 1.4 g in the last 230 feet indicating that most of the amplification effect takes place near the crest of the dam. Very high peak accelerations, on the order of 1.0 g, were computed all along the downstream slope. The variation of peak accelerations along the crest shows that the maximum occurs at the midsection of the dam and that there is a gradual decrease in peak accelerations towards the abutments.

Stress time histories were computed at several points in the dam and since they are quite similar to those computed for Oroville Dam they have not been included.

Peak stresses have been computed throughout the dam, and sections of the model, analogous in position to those selected for Oroville Dam

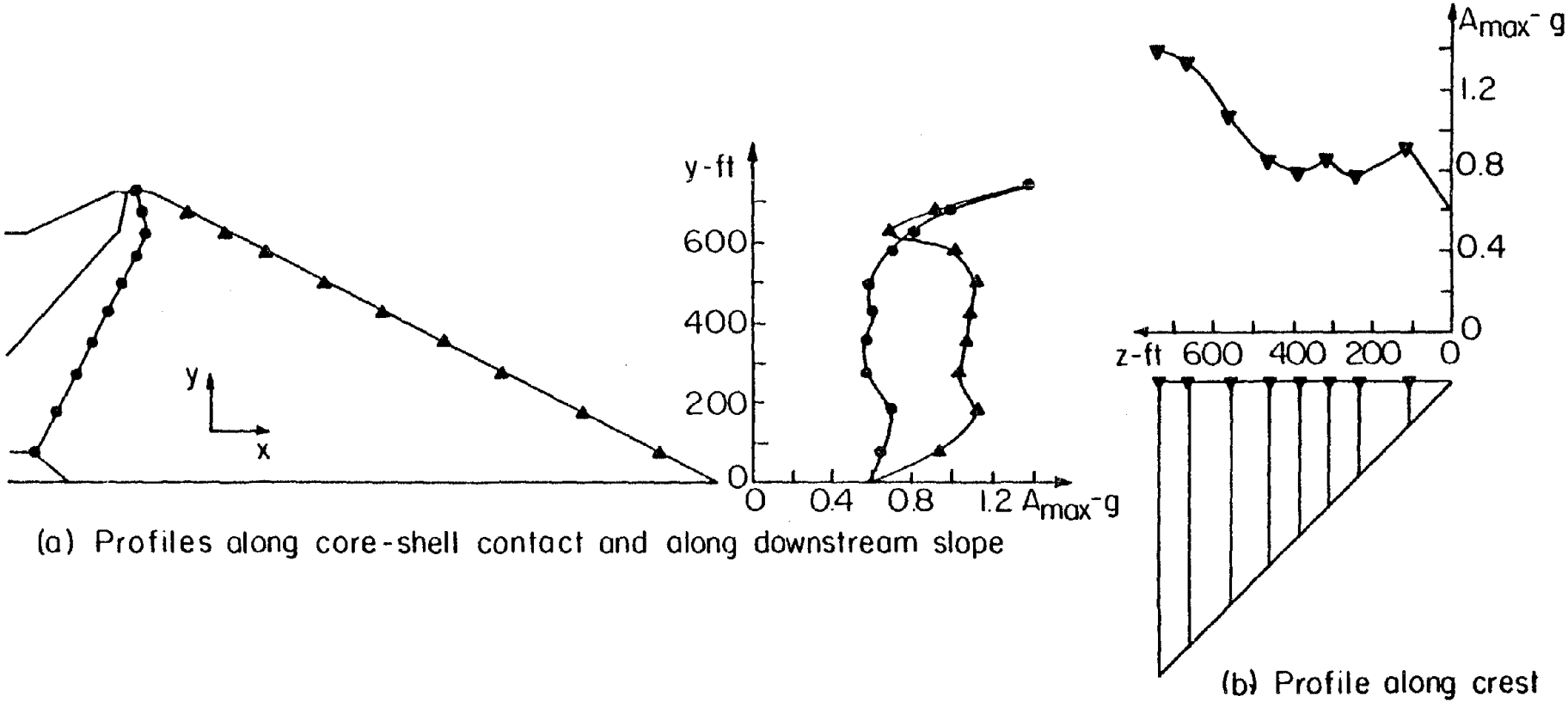

Fig. 4-18 Peak Horizontal Accelerations Computed from 3-D Analysis of Dam with Valley Wall Slopes of 1:1 for the Reanalysis Earthquake.

(Fig. 4-10), will be used for showing the stress distributions. Of interest are the contours of equal values of shear stress on horizontal planes, τ_{xy}, which are shown in Fig. 4-19. It can be seen that for section A the contours are closed, indicating that the highest stresses are not obtained at the base of the dam as is usually the case for plane strain conditions, but instead occur near the center of the dam at midheight. A similar observation can be made for section B. This distribution of stresses is a consequence of the geometry of the dam which is not suited for the development of high τ_{xy} stresses near the vertex of the canyon. A decrease in stresses with increasing distance from the main section is also observed. Comparison of these contours with those computed for Oroville Dam indicates that on the average, for analogous points in the two dams, lower τ_{xy} stresses are obtained in the dam with steep canyon walls.

As shown by Fig. 4-20 higher horizontal shear stresses on the z plane, τ_{zx}, than in Oroville Dam are obtained in this case. This fact is not surprising given the difference in geometries of the two canyons. For section A which is located at a short distance from the main section of the dam the τ_{zx} stresses are still significantly lower than the τ_{xy} stresses. However, at other sections of the dam they are of the same order of magnitude. An important conclusion arising from this fact is that τ_{xy} stresses are not a dominant component of the stress state throughout the dam and might not be an adequate parameter to use in computing the stability and permanent deformations of the dam.

In this respect it is of interest to examine the distribution of peak maximum shear stresses which is shown in Fig. 4-21. For section A

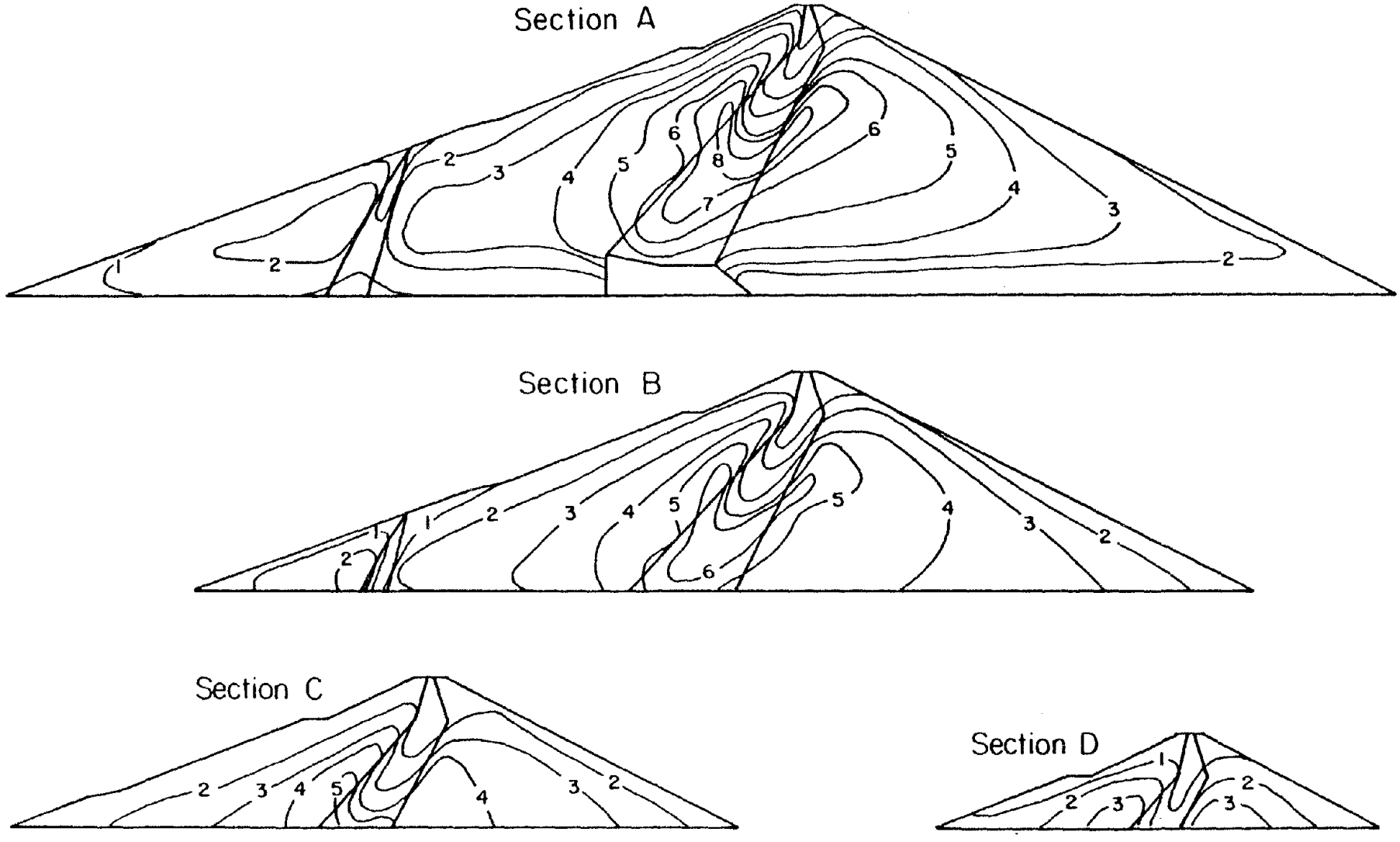

Fig. 4-19 Distribution of Peak Shear Stress τ_{xy} in Tsf Computed from 3-D Analysis of Dam with Valley Wall Slopes of 1:1 for the Reanalysis Earthquake.

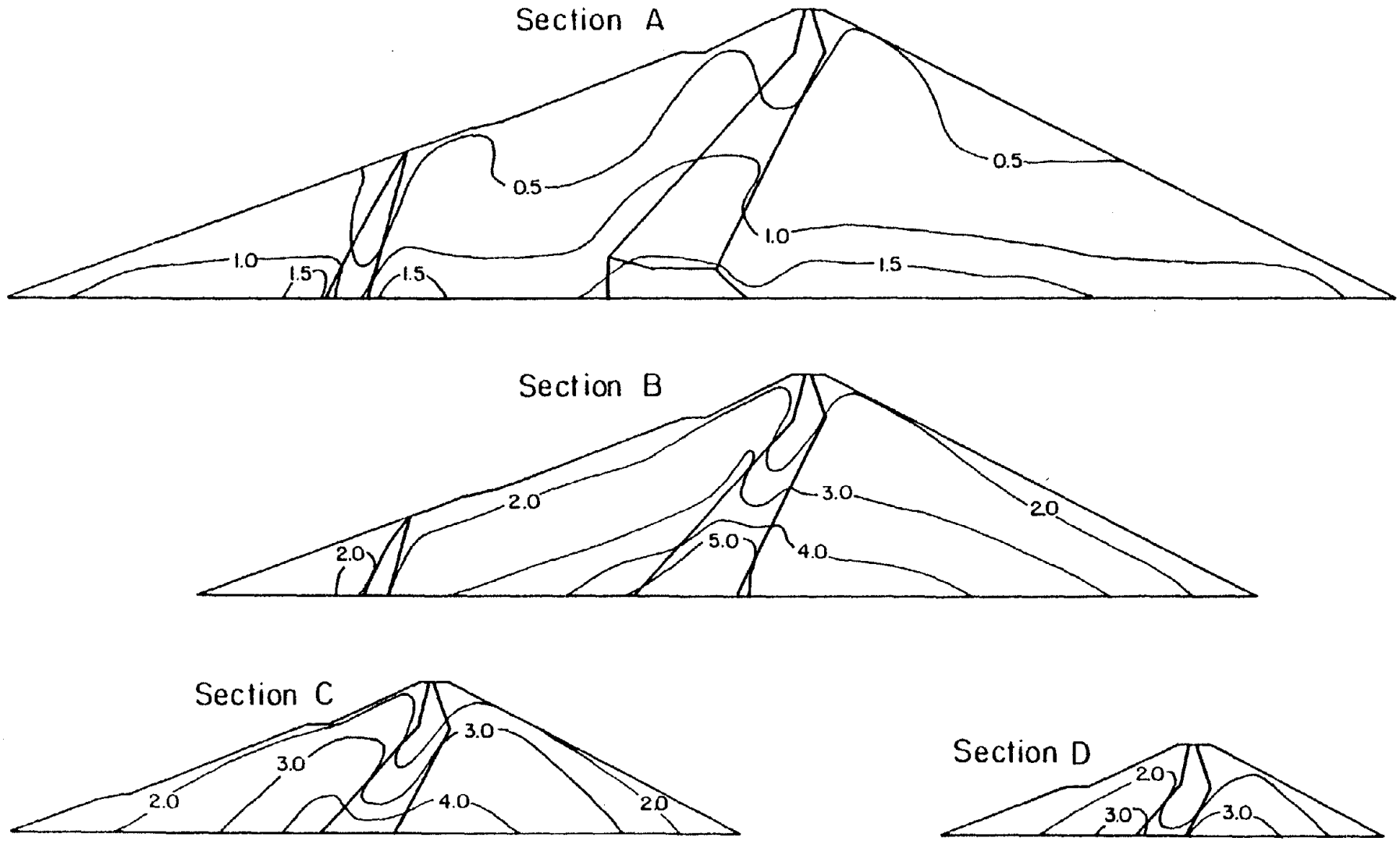

Fig. 4-20 Distribution of Peak Shear Stress τ_{xz} in Tsf Computed from 3-D Analysis of Dam with Valley Wall Slopes of 1:1 for the Reanalysis Earthquake.

this distribution is similar to that of the τ_{xy} stresses with the highest stresses occurring near the center of the section. However, for section B these contours have a different appearance than the contours of equal values of τ_{xy} stresses. Depending on the elevation being examined the highest maximum shear stresses can occur at sections other than section A indicating that the main section of the dam may not be the most critical from a stability point of view.

That the τ_{xy} stresses are not the only dominant component of the state of stresses in the dam with valley wall slopes of 1:1 can also be seen by examining the values of the ratio τ_{xy}/τ_{max}. Contours of equal values of this ratio have been computed and are plotted in Fig. 4-22. It can be seen in this figure that except for a zone comprising 20% of the height of the section, near the base, the above ratio is greater than 95% throughout most of section A. However, for other sections of the dam this ratio is well below 1.0, with an average value on the order of 70%. It can be concluded that for the dam with a crest length to height ratio, L/H, of 2 the τ_{xy} stresses do not approximate the maximum shear stresses and therefore, they might not be an appropriate parameter indicative of the behavior of the dam materials.

4.6 Analysis of Dam with Valley Wall Slopes of 1:1 for the Oroville Earthquake

The results from the analysis of the dam with a crest length to height ratio, L/H, of 2 for the Oroville earthquake are presented in this section. The acceleration amplification function for the midpoint of the crest of the dam is shown in Fig. 4-23. From this figure it may

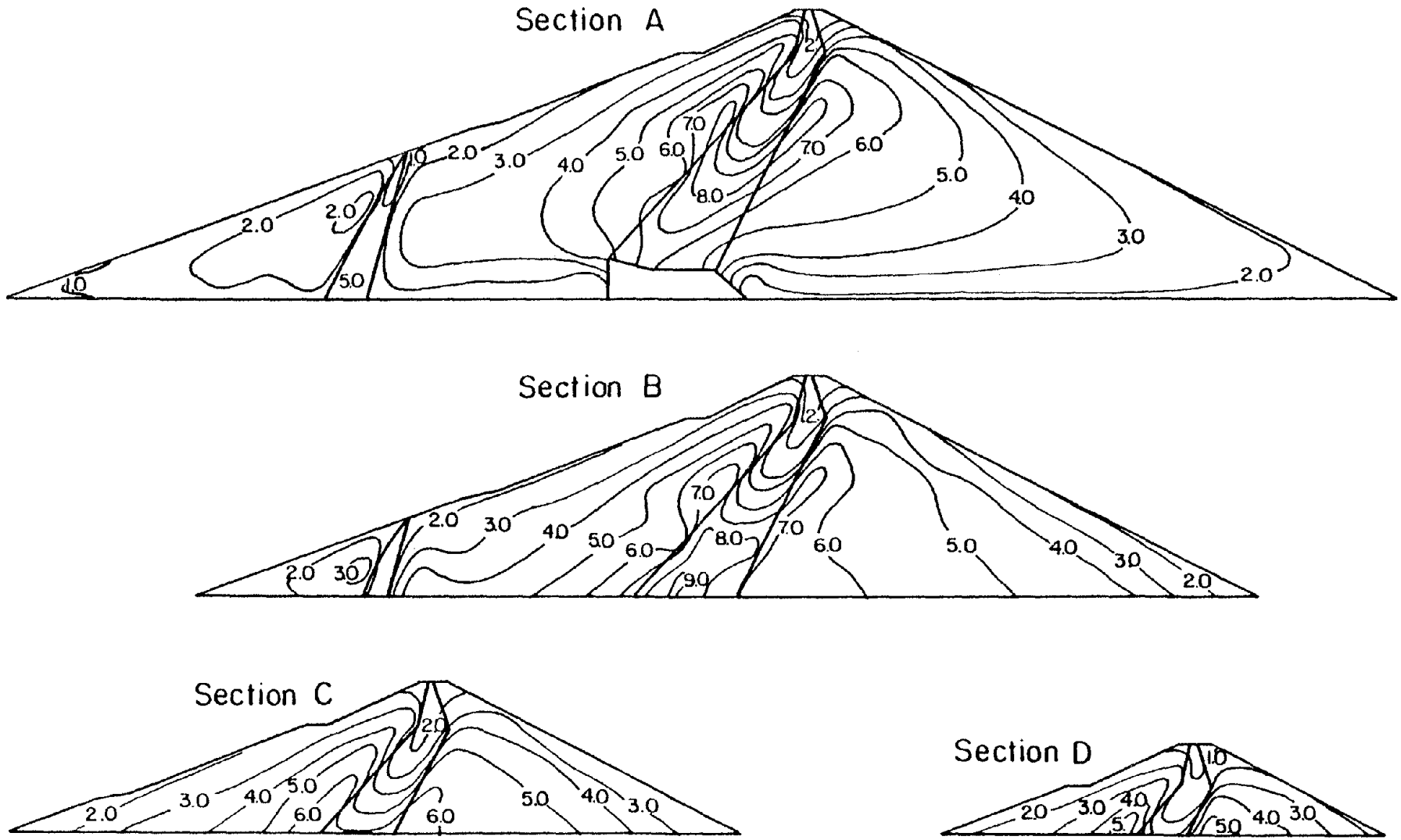

Fig. 4-21 Distribution of Peak Maximum Shear Stress, τ_{max}, in Tsf Computed from 3-D Analysis of Dam with Valley Wall Slopes of 1:1 for the Reanalysis Earthquake.

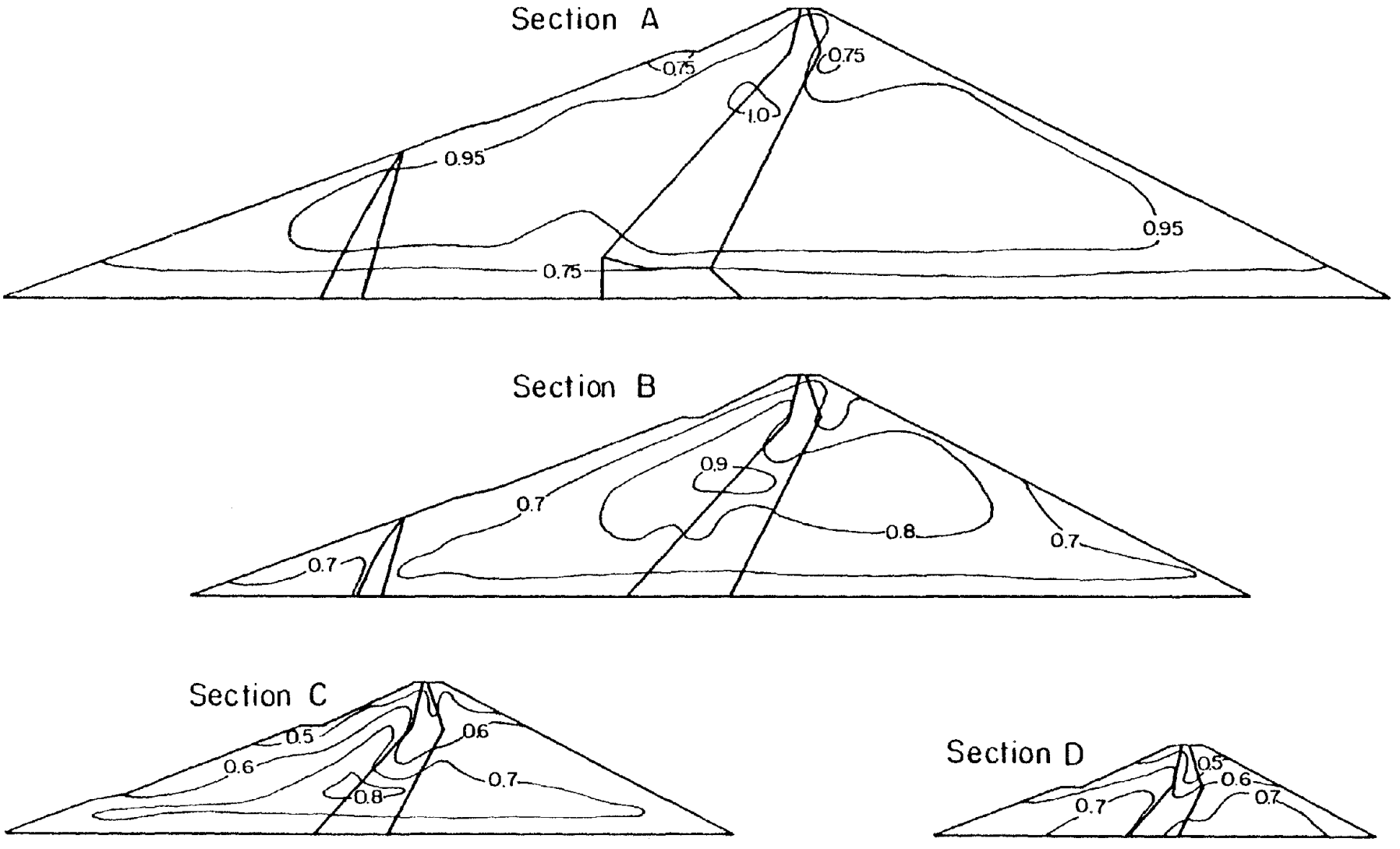

Fig. 4-22 Distribution of the Ratio τ_{xy}/τ_{max} Computed from 3-D Analysis of Dam with Valley Wall Slopes of 1:1 for the Reanalysis Earthquake.

be seen that the computed natural period of vibration of the dam is about 0.68 seconds. This value is 37% lower than the value obtained in the previous section for the Reanalysis earthquake and is 18% lower than the value obtained for the Oroville Dam when analyzed for the Oroville earthquake. The peak amplification has a value of 33.8 and the average level of damping throughout the dam is on the order of 4%. It is interesting to compare the shape of the amplification functions at the crest of the dam for the Reanalysis earthquake and for the Oroville earthquake. It can be seen that the amplification function for the latter presents a much higher number of frequency peaks indicating a significant contribution of the higher modes of vibration to the response at the crest of the dam.

The variation of peak accelerations along the contact between the core and the downstream shell, along the downstream slope and along the crest of the dam is shown if Fig. 4-24. The peak acceleration at the crest is on the order of 0.33 g. It is interesting to note that for the two earthquakes used in the analyses, the profiles of peak acceleration for the dam with steep valley walls result in higher values on the average than those for the Oroville Dam. As shown in Fig. 4-24 the peak accelerations on the downstream slope vary quite erratically and a very high value of 0.38 g is computed at elevation 175 feet. Peak accelerations along the crest also vary erratically near the abutments of the dam.

The contours of peak shear stresses on horizontal planes in the x direction, τ_{yx}, are shown in Fig. 4-25. As in the case of the Reanalysis earthquake the highest stresses in the dam for section A are

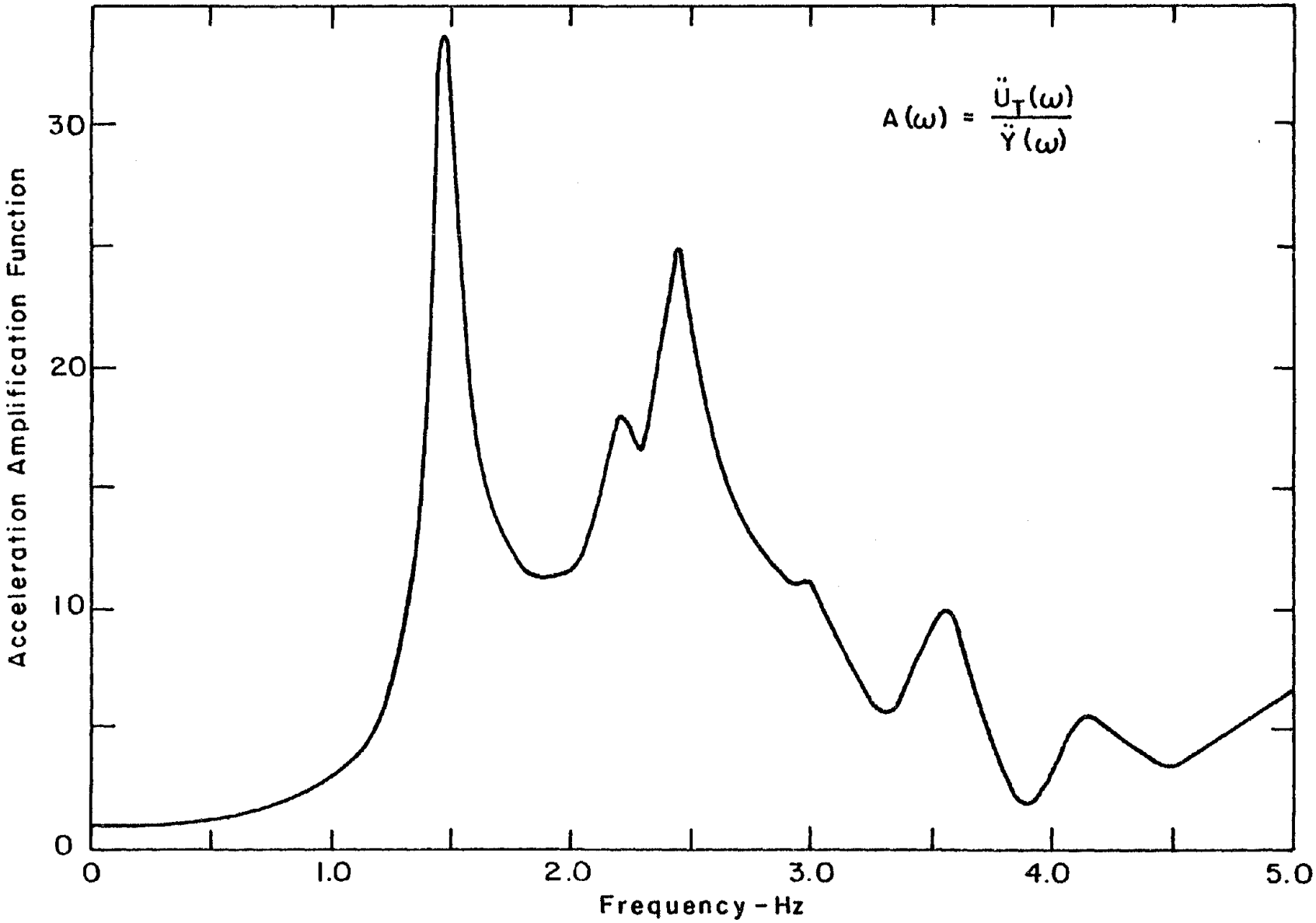

Fig. 4-23 Acceleration Amplification Function for Crest Midpoint of Dam with Valley Wall Slopes of 1:1.

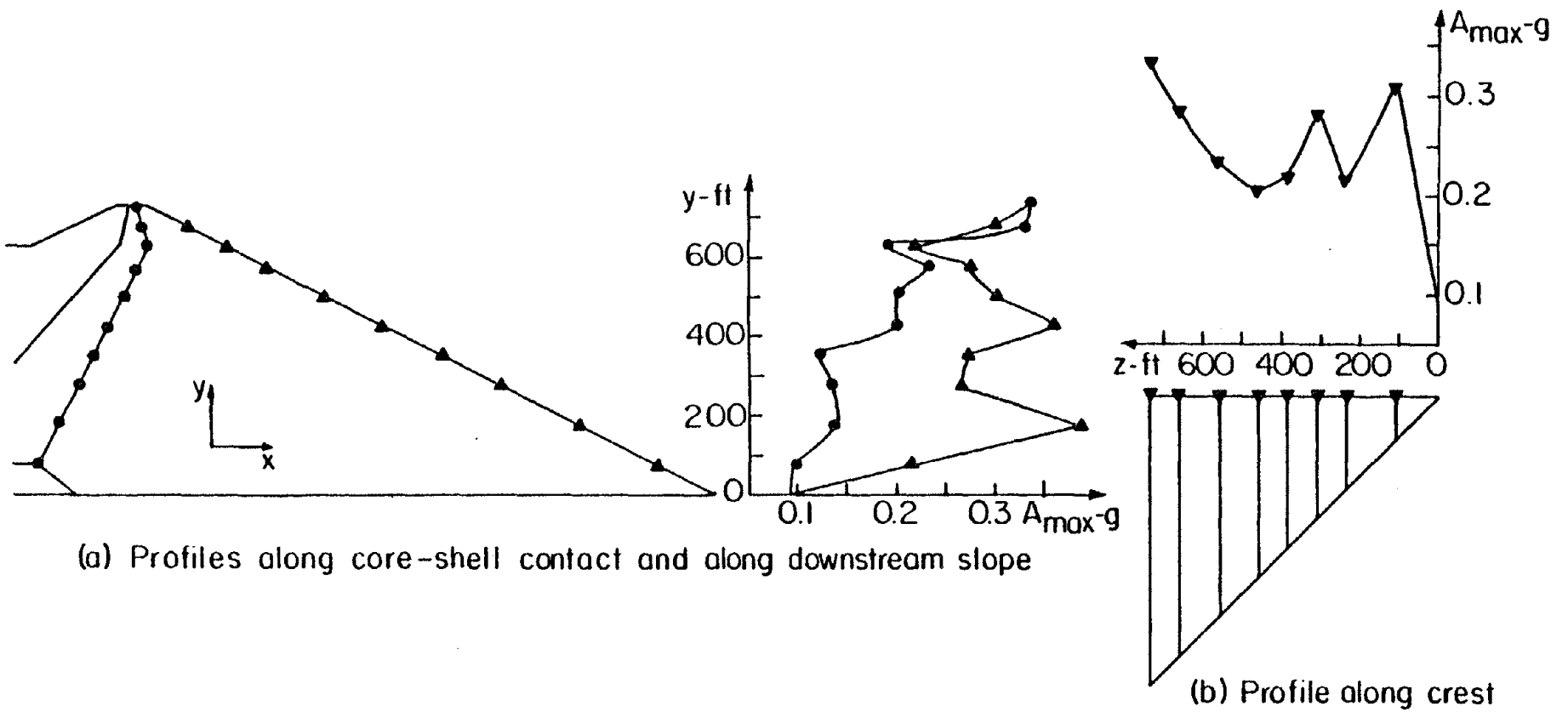

Fig. 4-24 Peak Horizontal Acceleration Computed from 3-D Analysis of Dam with Valley Wall Slopes of 1:1 for the Oroville Earthquake.

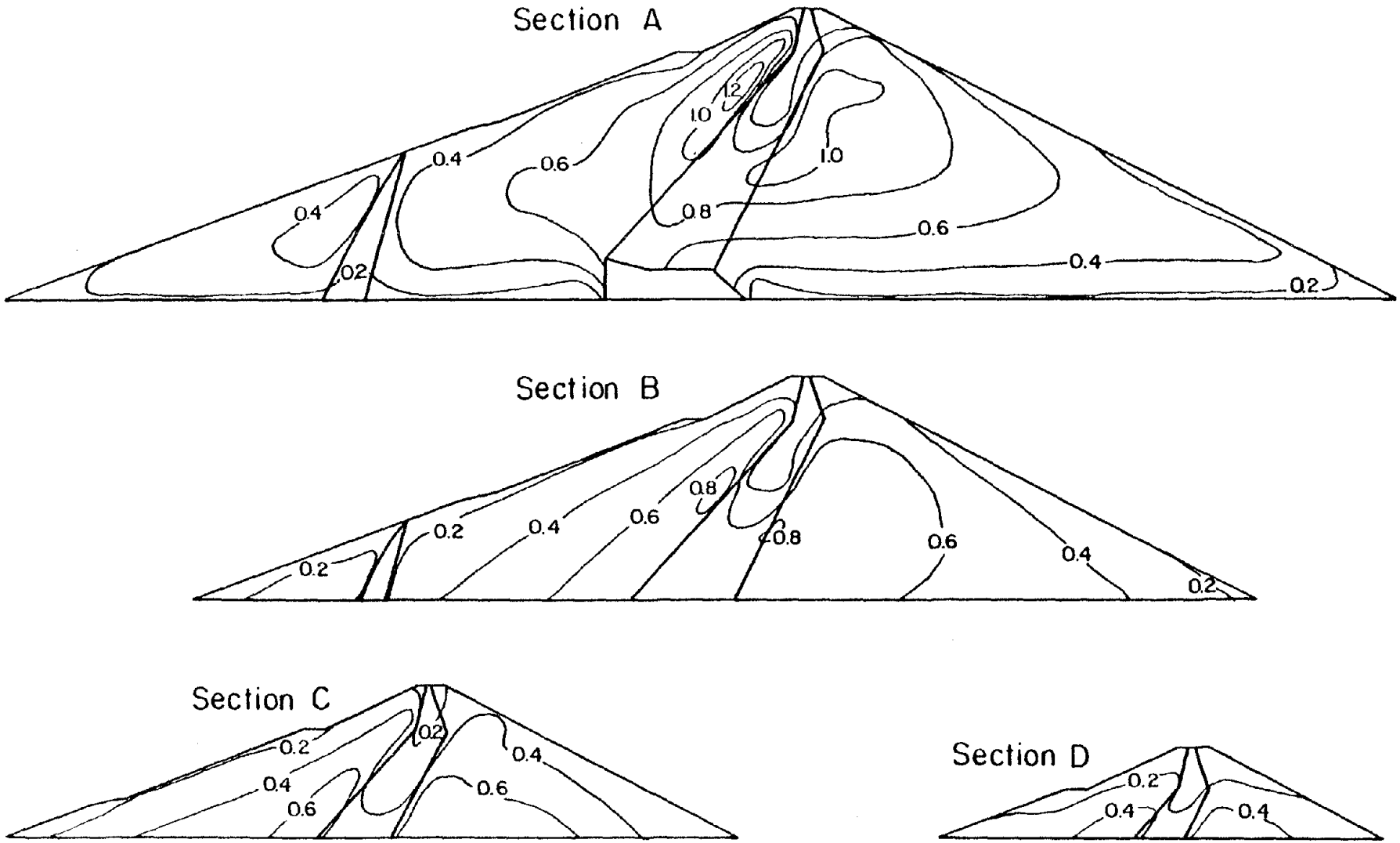

Fig. 4-25 Distribution of Peak Shear Stress τ_{xy} in Tsf Computed from 3-D Analysis of Dam with Valley Wall Slopes of 1:1 for the Oroville Earthquake.

computed in the shells near the core at midheight. There is a decrease in stresses with increasing distance from the maximum section. It is also observed that the stresses are lower than those computed for Oroville Dam for the same earthquake (Fig. 4-15) and that on the average they are about 6 or 7 times lower than those computed for the Reanalysis earthquake (Fig. 4-19). Once again the τ_{zx} stresses were found to be of comparable magnitude to the τ_{xy} stresses. Therefore, it is of interest to examine the distribution of peak maximum shear stresses which is shown in Fig. 4-26. As in the analysis presented in the previous section it can be observed from this figure that the main section of the dam may not be the most critical from a stability point of view.

4.7 Conclusions

Three-dimensional finite element procedures have been used to analyze the dynamic response of two dam models to two different input motions and the results of these analyses have been presented. In order to study the effects of the canyon geometry on the dynamic response, the models were assumed to have the same main section and material properties but were situated in triangular canyons with different wall slopes. The two earthquakes used had different amplitude, duration and frequency characteristics so that the effects of the nature of the input motions on the response could be studied. Although the number of analyses was limited, several conclusions of importance can be made:

(1) High amplitude motions induce high levels of strain, high levels of damping and low modulus values in the dam materials. As a consequence, lower natural frequencies of vibration and a small

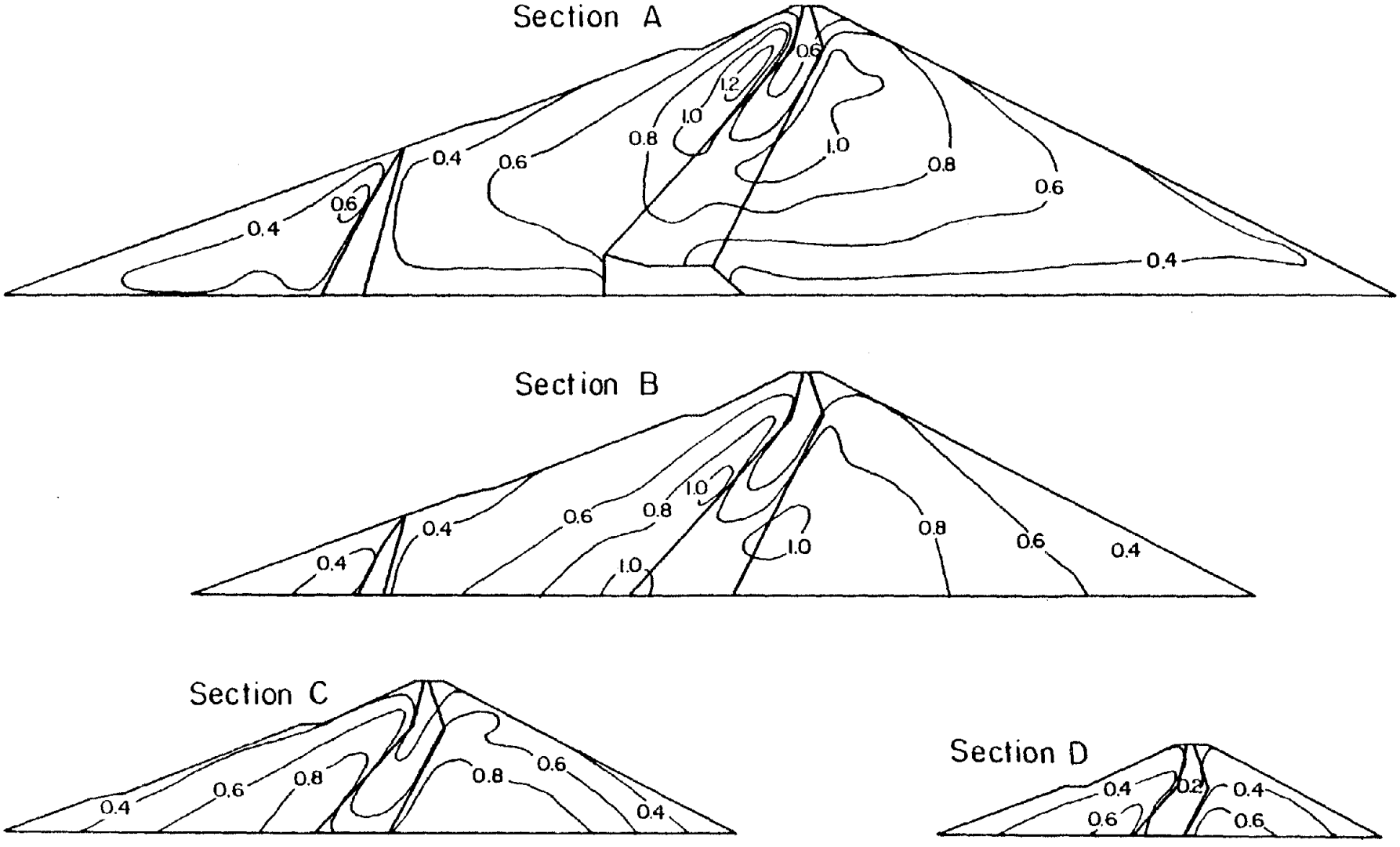

Fig. 4-26 Distribution of Peak Maximum Shear Stress, τ_{max}, in Tsf Computed from 3-D Analysis of Dam with Valley Wall Slopes of 1:1 for the Oroville Earthquake.

contribution of the higher modes of vibration to the response, are observed.

(2) Very high accelerations were observed at the crest of both models when analyzed for the Reanalysis earthquake. These were the result of the amplification of a strong pulse occurring near the beginning of the input motions record; this pulse had a period close to the natural period of vibration of the dams. Under these conditions stability of the crest is uncertain. The higher accelerations obtained for the dam with valley wall slopes of 1:1 do not necessarily imply higher elastic or permanent displacements.

(3) For both dams and for both input motions the computed stress time histories exhibited a very similar pattern; approximately the same number of equivalent cycles was observed at all points examined.

(4) For Oroville Dam it was found that the horizontal shear stresses on the z plane, τ_{zx}, were substantially smaller in magnitude than the shear stresses on the horizontal plane in the x direction, τ_{yx}. As a consequence the ratio τ_{yx}/τ_{max} was very close to 1.0 throughout the dam. The τ_{yx} stresses were highest for the main section and decreased with increasing distance from that section. The stresses were highest near the center of the dam in the bottom third of the maximum section above the core block.

(5) For the dam in the canyon with wall slopes of 1:1 the τ_{zx} stresses were of the same order of magnitude as the τ_{yx} stresses. The ratio τ_{yx}/τ_{max} had an average value of about 0.7 and values as low as 0.5 were computed. Therefore, the τ_{yx} stresses might not be

representative of the state of stresses that determines the behavior of the dam materials. The peak maximum shear stresses were computed for four sections of the dam. At the maximum section, they were found to be highest near the core of the dam, at midheight. However this section may not be the most critical section of the dam.

CHAPTER 5

TWO DIMENSIONAL ANALYSIS OF THREE DIMENSIONAL DAMS

5.1 Introduction

Dynamic response analysis of two dams where three-dimensional behavior is of concern have been performed for two earthquake motions and the results have been presented in the preceding Chapter. The effects of the nature of the input motions and of canyon geometry on the response have been studied, and the latter have been shown to be quite significant for dams in steep walled canyons (L/H=2). These effects can be further studied by comparing the response computed for two-dimensional and three-dimensional models of the dams. Accordingly, plane strain analysis of the maximum section of the same dams have been made and the results compared with those obtained from three-dimensional analyses.

It is common practice in the evaluation of the stability of earth dams in triangular canyons to analyze different sections in addition to the main section of the dam, assuming plane strain conditions. A convenient way to investigate the validity of this procedure is to perform comparisons between the results of plane strain analyses of the quarter section and those obtained from 3-D analyses of the corresponding dam.

Comparisons of the types described in the above paragraphs will also help to establish some of the criteria on which to base the selection of the numerical procedure to use in the analysis of a particular earth dam. Although recent advances in computer technology have

permitted the development of 3-D finite element procedures the computational and engineering efforts required for their use are substantially larger than those needed to perform 2-D analyses and therefore the development of criteria to determine when 3-D analyses are required is desirable.

Few comparisons between two-dimensional and three-dimensional analyses of earth dams have been reported. Hatanaka (1955) and Ambraseys (1960) studied the dynamic response of dams in rectangular canyons and found that for crest length to height ratios, L/H, greater than 4, the fundamental period of a dam computed from a plane strain analysis was within 10% of that computed with a 3-D model. Makdisi (1976) performed comparisons between the results obtained with 2-D and 3-D models of dams in triangular canyons. He used 100 foot high dams with a constant shear wave velocity of 500 fps and a damping ratio of 0.1, and presented comparisons between the computed natural frequencies for different crest length to height ratios, L/H. For a dam with L/H=3 subjected to the motions recorded at Taft during the 1952 Kern County earthquake he also found considerable differences between accelerations and stresses computed with 2-D and 3-D models of the dam. Severn et al. (1979) computed natural frequencies of vibration for the Llyn Brianne Dam using shear moduli from static strength data and 2-D and 3-D models of the dam.

A summary of the comparisons between natural frequencies made in the above mentioned studies is presented in Fig 5-1. This figure shows the ratio between natural frequencies computed from 3-D and 2-D models of dams in triangular and rectangular canyons as a function of the crest length to height ratio. Also shown are the corresponding values for

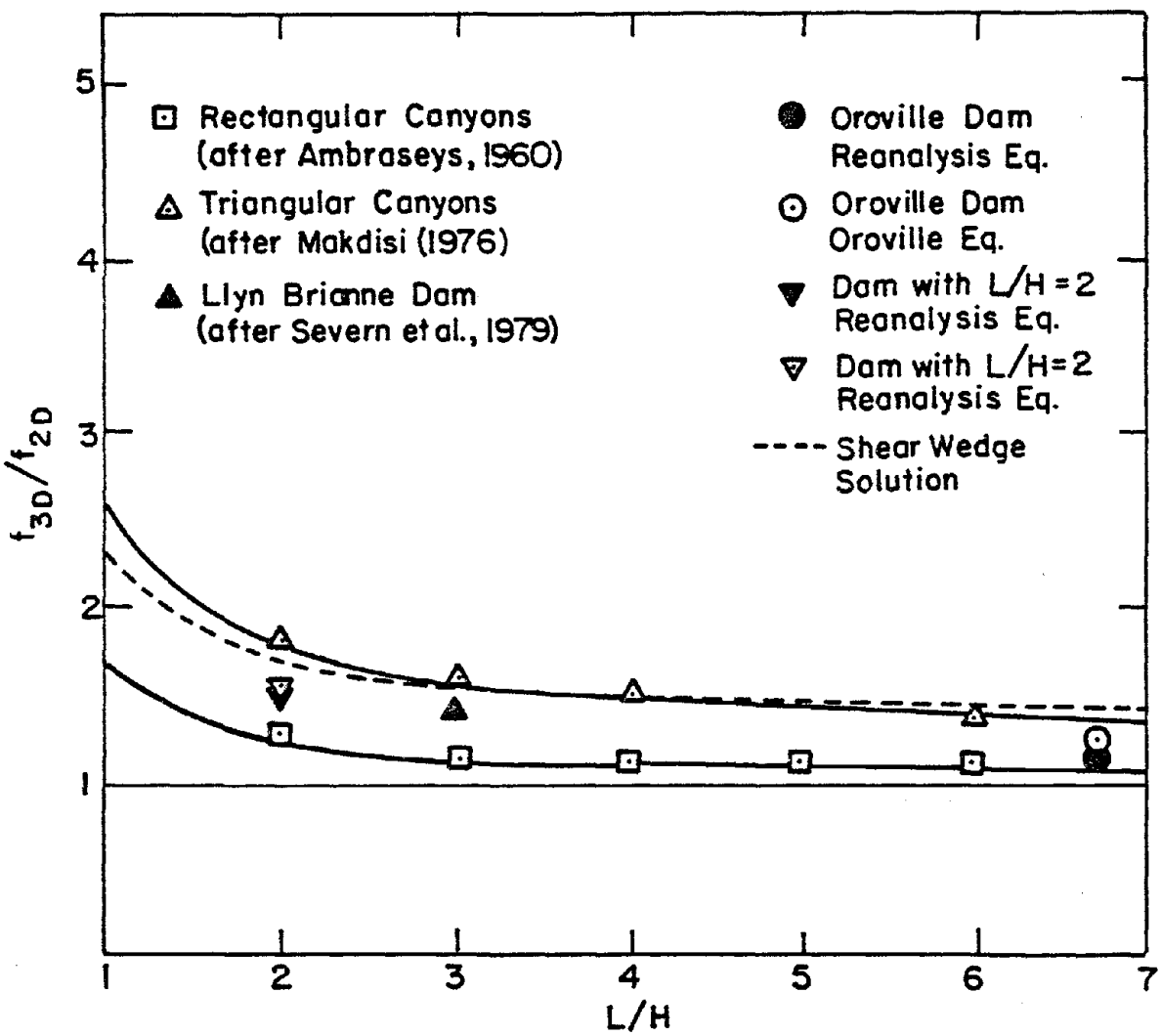

Fig. 5-1 Comparison Between Natural Frequencies Computed from 2-D and 3-D Analyses of Dams in Triangular and Rectangular Canyons.

Oroville Dam and the dam with valley wall slopes of 1:1 computed during this study for both the Oroville and the Reanalysis earthquakes. Additionally, the 3-D shear wedge method of analysis has been used to compute the natural frequencies of vibration of dams in triangular canyons and these results have been combined with those obtained from a 2-D shear beam analysis of the main section to give the dashed line. Derivation of the equation of motion for a dam in a triangular canyon using the shear wedge method and an approximate eigen-value solution of this equation for the first natural frequency of vibration are presented in Appendix A. It may be seen that for dams in triangular canyons with crest length to height ratios, L/H, lower than 2, the ratio between fundamental natural frequencies computed by 3-D and 2-D models of the dams, is greater than 1.6. As the ratio L/H increases, the ratio between natural frequencies decreases so that at a value of L/H of 6, it has a magnitude of about 1.3. For dams in rectangular canyons the ratios between 3-D and 2-D natural frequencies are substantially lower than those for dams in triangular canyons.

The comparisons illustrated in Fig. 5-1 are indicative of only one aspect of the three-dimensional behavior of earth dams. Close agreement in the natural frequencies of vibration of the 2-D and 3-D models of a dam does not imply close agreement in the computed response to earthquake motions. Therefore it seems desirable to study the effects of 3-D behavior on the parameters of dynamic response used in the assessment of deformations and stability of earth dams. The purpose of this chapter is to present the results, in terms of these parameters, of the plane strain analyses of the maximum section and the quarter section of the dams previously analyzed in three dimensions, for the Reanalysis and

Oroville earthquakes, and to compare the results of the 2-D and 3-D computations. The validity of an approximate methods used by DWR (1979) and Banerjee et al.(1979) to take into account the three-dimensional behavior of Oroville Dam during the re-evaluation of its seismic stability will also be investigated.

The next section of this chapter has been subdivided into five subsections. A description of the dam sections analyzed and other details of the analyses are included in the first subsection. The following subsections present the results of the plane strain analyses of the maximum and quarter sections of the dams previously analyzed in three dimensions and a comparison with these results. The results from plane strain analyses of the maximum section of Oroville Dam using a modified stiffness, for the Oroville and Reanalysis earthquakes, and a comparison with the results from 3-D analyses are presented in the following section. Finally, a summary of conclusions is included in the last section.

5.2 Comparisons Between Two-Dimensional and Three-Dimensional Analyses

5.2.1 Sections Analyzed

In the absence of numerical procedures for three-dimensional analysis it is general practice to carry out the dynamic analysis of a dam in a triangular canyon by performing plane strain analyses of several sections of the dam. Only two sections, as shown in Fig 5-2(a), have been selected for the analyses and comparisons presented herein. These sections correspond to the maximum and quarter sections of

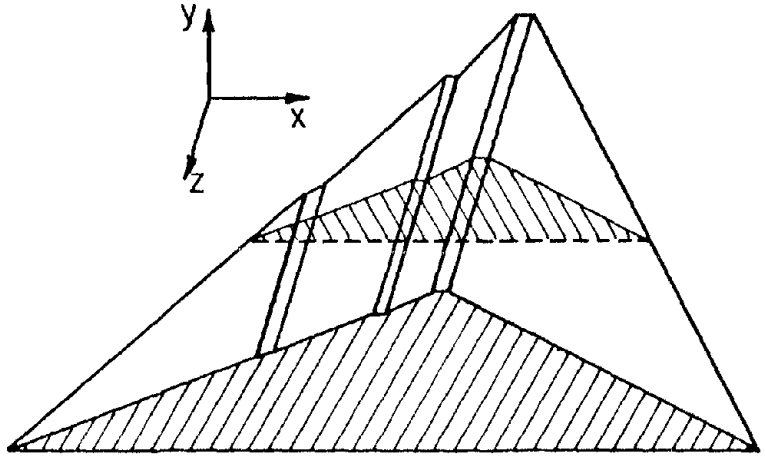

(a) Location of sections

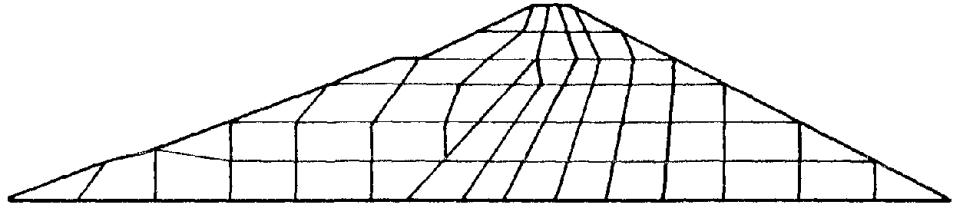

(c) Finite element mesh for quarter section

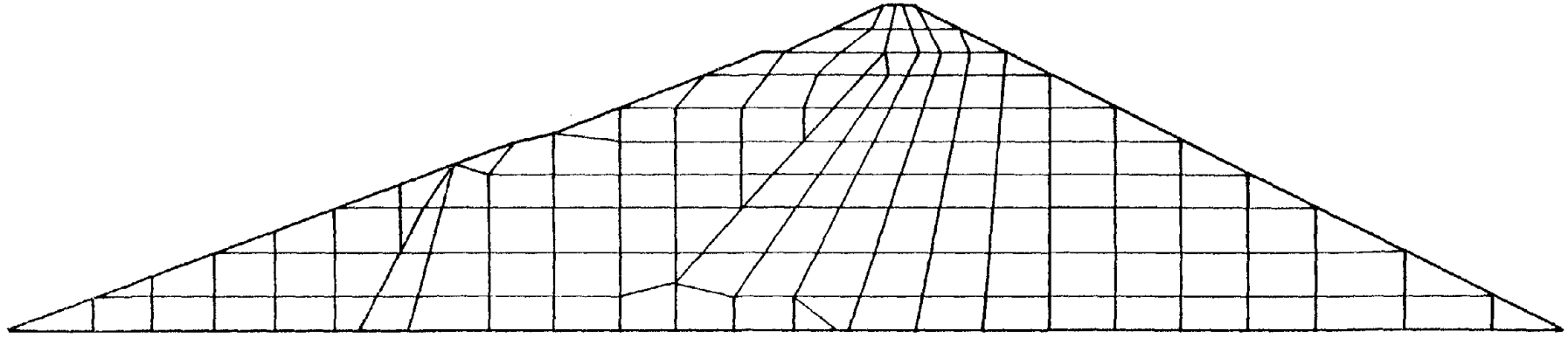

(b) Finite element mesh for maximum section

Fig. 5-2 Finite Element Models for Two Dimensional Analyses.

Oroville Dam and the dam with valley wall slopes of 1:1 which were previously analyzed in three dimensions for the Reanalysis and Oroville earthquakes. These two dams have similar shapes since the geometry for the dam with canyon wall slopes of 1:1 was obtained by scaling down the dimensions of Oroville Dam in the longitudinal direction and therefore, they have identical maximum and quarter sections. These sections do not correspond exactly to sections A and C of Fig 4-10 which were used to illustrate the stress distributions computed from 3-D analyses. However, the differences in location are sufficiently small that the stresses can be compared directly.

The static stress distribution and the material properties for these two sections have been assumed to be the same as those for the corresponding sections in the 3-D models of the dams. The two-dimensional finite element computer program FLUSH (Lysmer et al., 1975) was used in the analysis of both sections with a cut-off frequency of 8 Hz. The finite element meshes for the two dam sections, which are shown in Figs. 5-2(b) and 5-2(c), correspond to the cross sections at the midpoint and quarter point of the longitudinal axes of the 3-D finite element meshes of both dams.

The ground motions used correspond to the records previously shown for the Reanalysis and Oroville earthquakes. They are assumed to be input through a rigid base and to act in the upstream-downstream direction.

5.2.2 Dynamic Response of Maximum Section to the Reanalysis Earthquake

As mentioned in Chapter 4 the dynamic response parameters generally used in the assessment of stability and deformations of an earth dam are the accelerations and stresses induced by the earthquake motions. The results of the 2-D analysis of the maximum section for the Reanalysis earthquake will be presented here in terms of these parameters and a comparison with analogous parameters computed from the 3-D analyses of Oroville Dam and the dam with canyon wall slopes of 1:1 will be made.

Using a 2-D analysis, the natural period of the maximum section for the level of strain induced by the Reanalysis earthquake was computed from the amplification function for the crest point and was found to be 1.58 seconds. It is noted that this value is 12% and 46% higher (see Fig. 5-1) than the values computed for the Oroville Dam and the dam with steep canyon walls respectively. The average levels of modulus degradation and of damping were about the same for these three analyses and therefore the lower periods obtained with the 3-D models are mostly the result of a stiffening effect of canyon geometry. The plane strain amplification function showed only one significant peak and very little response beyond 2.5 Hz.

The acceleration time histories computed at points along the contact between the core and the downstream shell are shown in Fig. 5-3. Amplification of low frequency and filtering of high frequency motions with increasing elevation in the section can be observed. Very high long period accelerations, with a peak value of 1.08 g, were obtained at the crest of the 2-D model. These are the result of the amplification of the strong pulse present at the beginning of the input motions (see Fig.

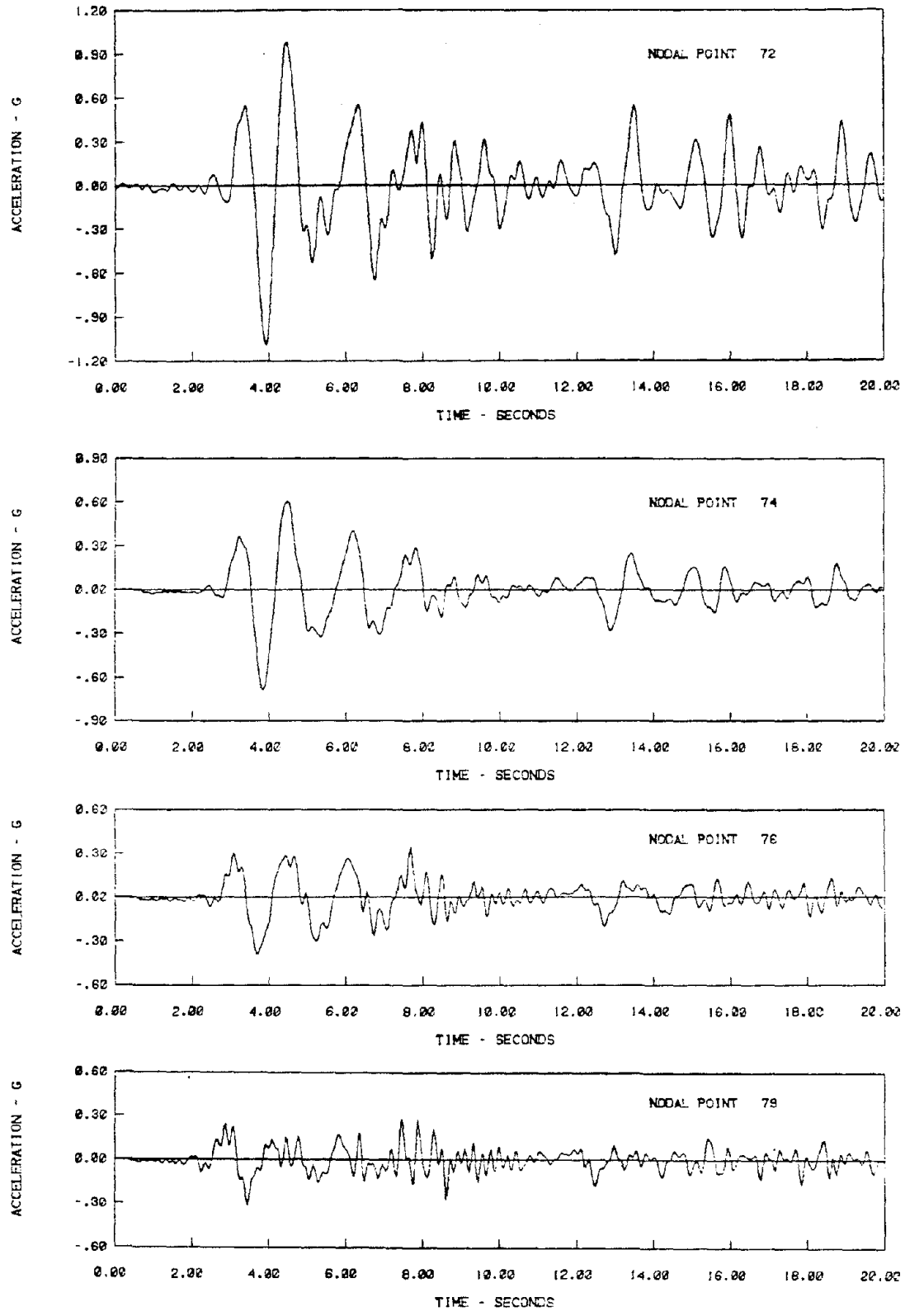

Fig. 5-3 Acceleration Time Histories for Points Along Core-shell Contact Computed from Plane Strain Analysis of Maximum Section.

4-1). In general, the time histories computed from a plane strain analysis of the maximum section for the Reanalysis earthquake are very similar to those computed with a 3-D model of Oroville Dam but differ significantly from those computed in the 3-D analysis of the dam with valley wall slopes of 1:1 (see Figs. 4-5 and 4-17).

A better comparison between acceleration time histories is presented in Fig. 5-4. Fig. 5-4(a) shows a comparison between the acceleration time histories at the crest of the maximum section computed from a plane strain analysis and by a 3-D analysis of Oroville Dam. Except for a small difference in phase caused by the slightly higher period of the 2-D model these time histories are very similar. This similarity in motions along the core-shell contact is due to the predominance of the first mode in the response and the fact that the cross sections and the natural frequencies of vibration for this mode are very close for both the 2-D and 3-D models of the dam (see Fig. 2-11). Fig. 5-4(b) shows an analogous comparison between the crest acceleration time histories for the dam with valley wall slopes of 1:1 computed using the 2-D and 3-D models. In this case a significant discrepancy between time histories is observed. The predominant frequency is higher and the acceleration amplitudes are larger for the 3-D model than for the 2-D model.

The variation of peak accelerations along the contact between the core and the downstream shell and along the downstream slope for the plane strain analysis of the maximum section is shown in Fig. 5-5. As in the case of the three-dimensional analyses for the Reanalysis earthquake of the two dams studied, the stability of the crest seems to be

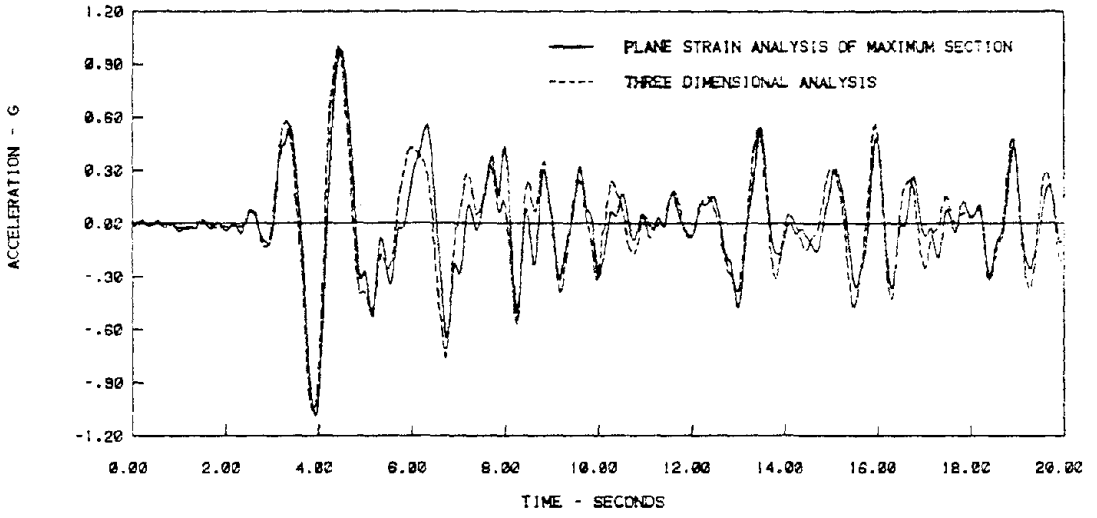

(a) Oroville Dam

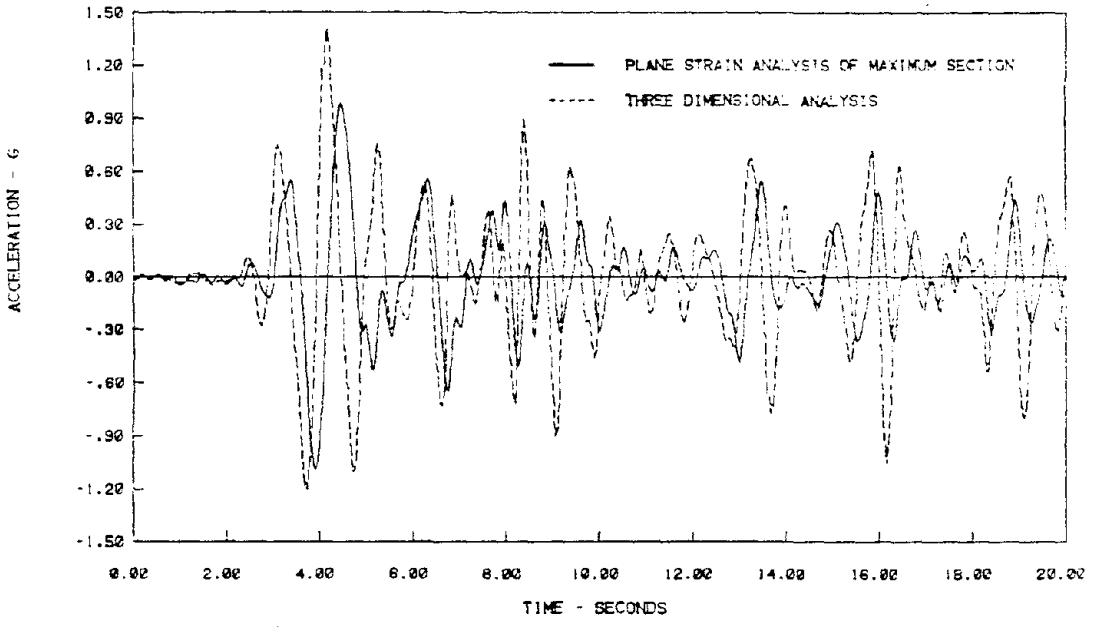

(b) Dam with valley wall slopes of 1:1

Fig. 5-4 Crest Acceleration Time Histories Computed from 2-D and 3-D Analyses - Reanalysis Earthquake.

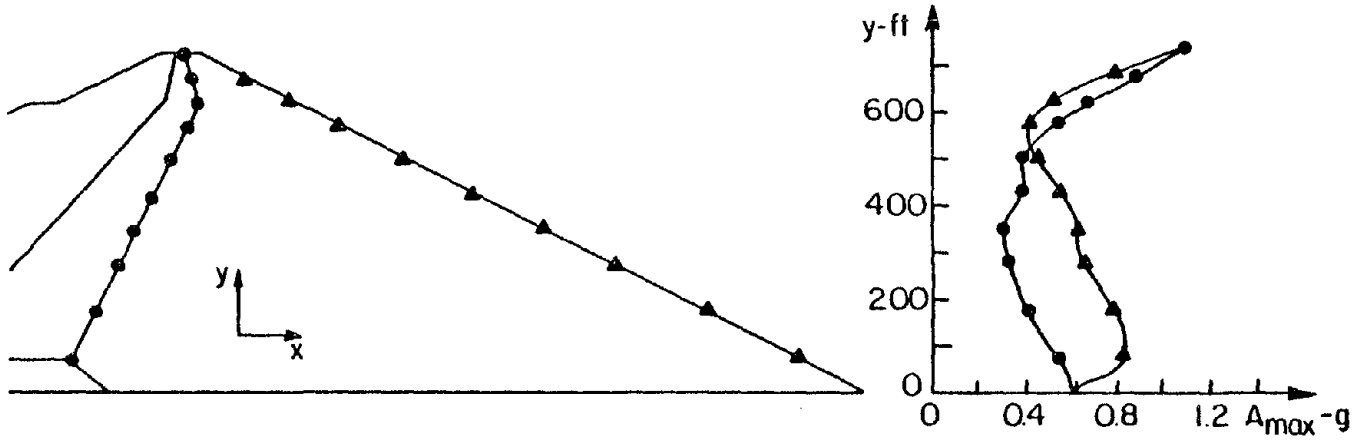

Fig. 5-5 Peak Horizontal Acceleration Computed from 2-D Analysis of Maximum Section for the Reanalysis Earthquake.

uncertain under the high accelerations computed at the crest. A decrease in peak acceleration from 0.6 g at the base to 0.3 g at elevation 350 feet and a rapid increase to 1.08 g at the crest are observed. Very high peak accelerations were also computed along the downstream slope. Up to elevation 500 feet peak accelerations result from the amplification of high frequency motions and above this point they are the result of the amplification of the long period pulse present in the input motions at about 3.5 seconds.

A remarkable similarity between the profiles of peak accelerations for the 2-D and 3-D models of Oroville Dam is noticed when comparing Fig. 5-5 with Fig. 4-7. On the other hand, comparison of Fig. 5-5 with Fig. 4-18 indicates that a plane strain analysis of the maximum section does not give a good prediction of the accelerations computed from a 3-D analysis of a dam with valley wall slopes of 1:1. The poor agreement in results is due to the large difference in predominant period (46%) and differences in mode shapes of vibration.

Under plane strain conditions the state of stress at a point is given by three independent components. In a Cartesian coordinate system these components are σ_{xx}, σ_{yy} and τ_{xy}. The other shear stress components, τ_{xz} and τ_{yz} are nil, and σ_{zz} is dependent on σ_{xx} and σ_{yy} (see Fig. 4-4). In view of the fact that the mean normal stress does not have a significant influence on the deformational behavior of soils under undrained conditions, it is common practice in the evaluation of seismic stability of earth dams to use the shear stress on horizontal planes, τ_{xy}, as the parameter that controls the generation of pore pressures and deformations of dam materials. The variation with time of

this parameter is taken into account by using an average shear stress equal to about 2/3 of the peak shear stress and an equivalent number of cycles. Therefore, it is of interest to study the distribution of peak values of τ_{xy} computed from the plane strain analysis of the maximum section of Oroville Dam and the dam with valley wall slopes of 1:1. Fig. 5-6(a) shows contours of equal values of τ_{xy} stresses computed in this section for the Reanalysis earthquake. Except within a small zone at the base of the section, in the vicinity of the core block, there is a general increase in stresses with depth and towards the center line of the section. The maximum stresses are observed immediately above the core block although at higher elevations, the core exhibits smaller stresses than the nearby zones of the shells.

The ratio between the shear stresses on horizontal planes and the maximum shear stresses, τ_{yx}/τ_{max}, can be considered to be an approximate measure of the degree to which the τ_{yx} stresses are representative of the stress level responsible for the deformational behavior of the dam materials. Fig 5-6(b) shows the distribution of this ratio computed from the plane strain analysis of the maximum section. It can be seen that this ratio is greater than 85% everywhere in the section and that it is greater than 95% over large portions of the section. Accordingly, it can be concluded that for the 2-D model of the dams studied herein, subjected to earthquake motions in the upstream-downstream direction, the τ_{yx} stresses are representative of the stress levels responsible for the deformational behavior of the dam materials.

An evaluation of: a) the applicability of 2-D dynamic analysis procedures to predict the response of three-dimensional dams and b) the

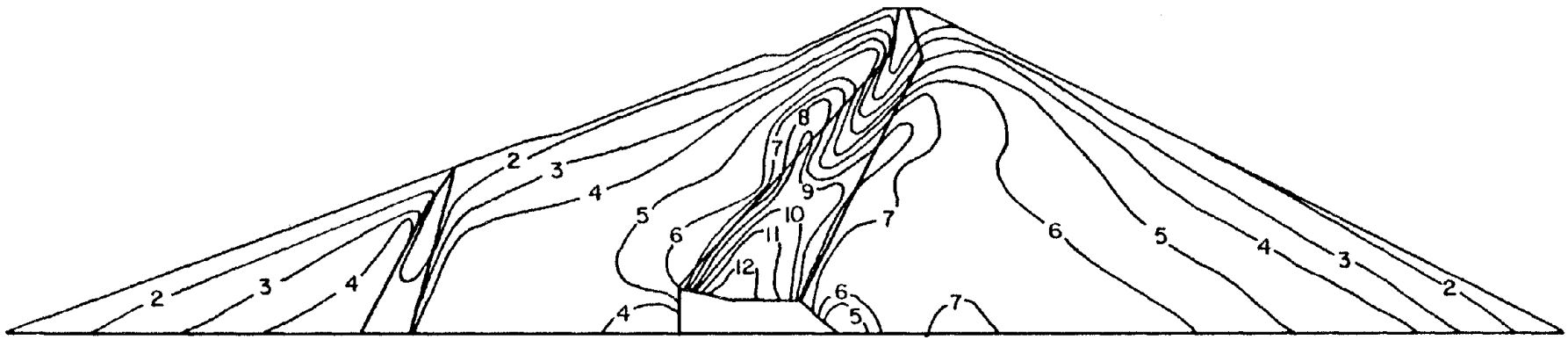

Fig. 5-6a Distribution of Peak Shear Stress τ_{xy} in Tsf Computed from Plane Strain Analysis of Maximum Section for the Reanalysis Earthquake.

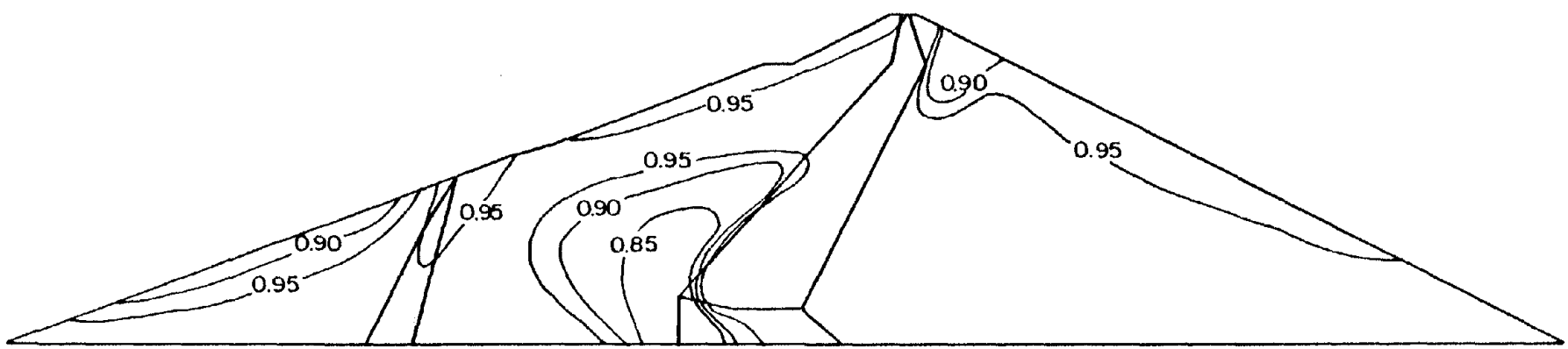

Fig. 5-6b Distribution of the Ratio τ_{xy}/τ_{max} Computed from Plane Strain Analysis of Maximum Section for the Reanalysis Earthquake.

effects of three-dimensional behavior on the dynamic response of earth dams, requires a comparison between the dynamic stresses obtained by the use of 2-D and 3-D dam models. This comparison however, is not straightforward since the nature of the stress state is very different in two and three-dimensions.

It has been shown by several case studies (Seed et al., 1969; Seed et al., 1973; Makdisi et al., 1978) that where two-dimensional conditions prevail, the use of the shear stress on horizontal planes, τ_{yx}, as an indicative parameter of material behavior, results in a satisfactory assessment of the seismic stability of earth dams. However, the same cannot be said for cases where the effects of 3-D behavior on the dynamic response of earth dams are significant. The behavior of soils under complex dynamic stress states is not well known and under these conditions the τ_{yx} stresses may not be representative of the stress levels responsible for material behavior.

In spite of the uncertainties discussed above the comparison between dynamic stresses obtained with the 2-D and 3-D models of the dams studied herein has been made in terms of the τ_{xy} stresses for the following reasons:

1. For the dams previously analyzed in three dimensions the peak values of τ_{yx} were found to be very close to the peak values of τ_{max} at the maximum section and therefore the former are a dominant component of the 3-D stress state at points in that section.

2. A comparison between stresses acting on different planes is less meaningful than one between stresses on the same plane.

3. The τ_{yx} stresses are commonly used in engineering practice as the parameters that indicate material behavior.

4. Practical convenience in performing the corresponding computations.

The ratio between the peak τ_{xy} stresses obtained using 2-D and 3-D models, τ_{xy2D}/τ_{xy3D}, was computed for the maximum section of the two dams previously analyzed for the Reanalysis earthquake. Fig. 5-7(a) shows the distribution of this ratio for the maximum section of Oroville Dam. It can be seen that for this section the plane strain analysis gives higher stresses than the three-dimensional analysis of the dam. However, the stresses obtained from the 2-D analysis are within 5% of the 3-D stresses in the upper 3/4 of the section. Small differences of about 15% in the upstream shell and of about 20% in the downstream shell can be observed near the base of the section showing some constraining effects of the canyon vertex. On the basis of these results it can be concluded that for strong motions a plane strain analysis of the maximum section gives slightly higher stresses than a 3-D analysis at the base of a dam with similar characteristics to Oroville Dam.

The distribution of the ratio τ_{xy2D}/τ_{xy3D} for the dam with valley wall slopes of 1:1 is shown in Fig. 5-7(b). It is observed again that except for a small zone near the crest where this ratio falls below 1.0 the plane strain analysis of the main section gives higher stresses than the 3-D analysis of the dam. The differences in stresses increase towards the base of the section and they are larger than 10% for the

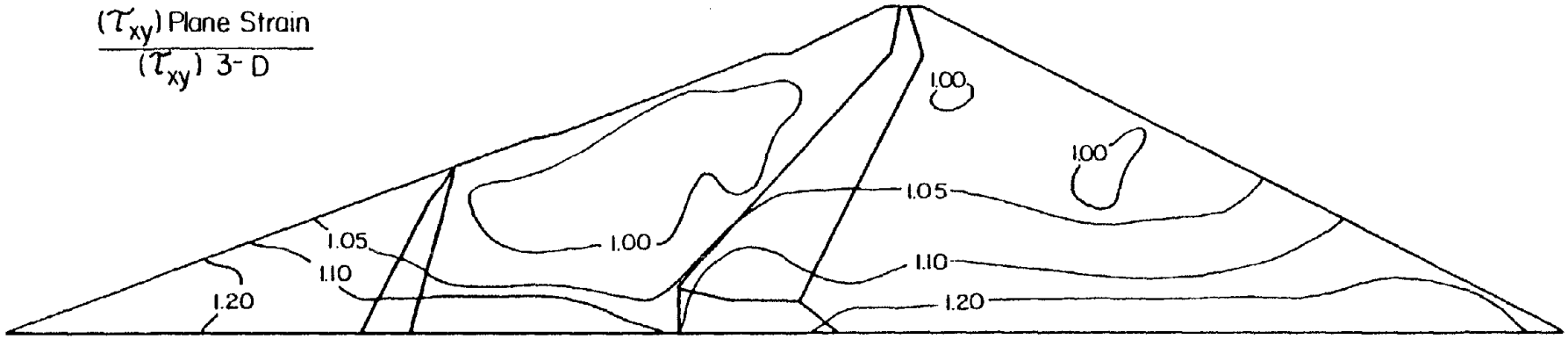

Fig. 5-7a Distribution of the Ratio τ_{xy2D}/τ_{xy3D} Computed for the Maximum Section of Oroville Dam - Reanalysis Earthquake.

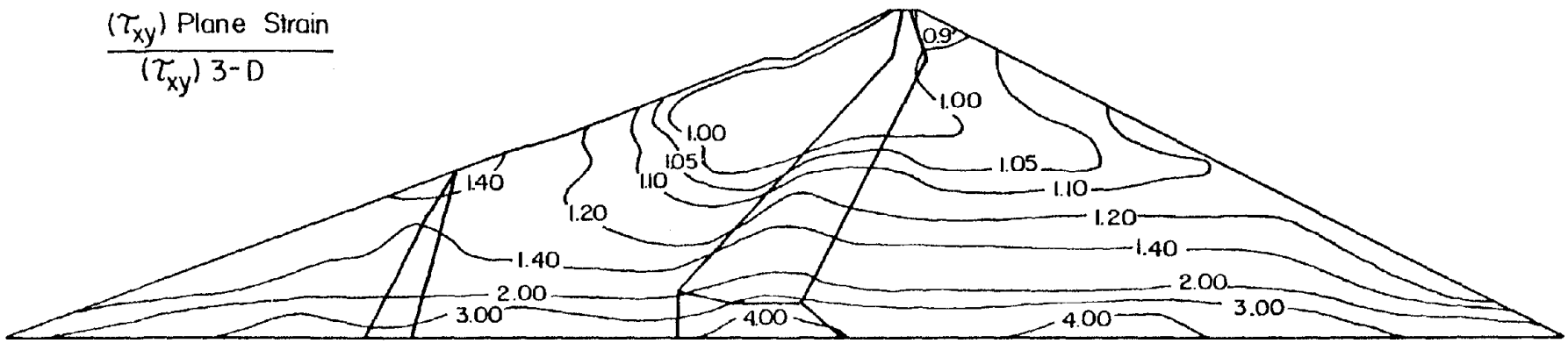

Fig. 5-7b Distribution of Ratio τ_{xy2D}/τ_{xy3D} Computed for the Maximum Section of Dam with Valley Wall Slopes of 1:1 - Reanalysis Earthquake.

bottom half of the section and larger than 40% for the bottom third. Near the base the stresses can differ by a factor of 4. These differences reflect the constraining effects of the narrow triangular shape of the canyon.

In view of the fact that for the dam with valley wall slopes of 1:1 the τ_{xy} stresses may not be an indicative parameter of material behavior, a comparison of results from the 2-D and 3-D models of the dam, in terms of maximum shear stresses, has also been performed. The ratio between maximum shear stresses from the plane strain analysis and 3-D analysis of the dam, $\tau_{max2D}/\tau_{max3D}$, has been computed. The distribution of this ratio throughout the maximum section is shown in Fig. 5-7(c) which can be seen to have a similar appearance to Fig. 5-7(b). Although the values of the $\tau_{max2D}/\tau_{max3D}$ ratio are somewhat lower than those of the ratio τ_{xy2D}/τ_{xy3D}, they are still well above 1.0 throughout most of the section. On the basis of these results it can be concluded that a plane strain analysis of the maximum section gives significantly higher stresses than a 3-D analysis in the bottom third of a dam in a triangular canyon with valley wall slopes of 1:1.

5.2.3 Dynamic Response of Maximum Section to the Oroville Earthquake

The results from the plane strain analysis of the maximum section of Oroville Dam and of the dam with valley wall slopes of 1:1 for the Oroville earthquake are presented in this section. Additionally, comparisons with the results from three-dimensional analysis of these dams for the same earthquake are included. These results will serve to illustrate the effects of the nature of the input accelerations since

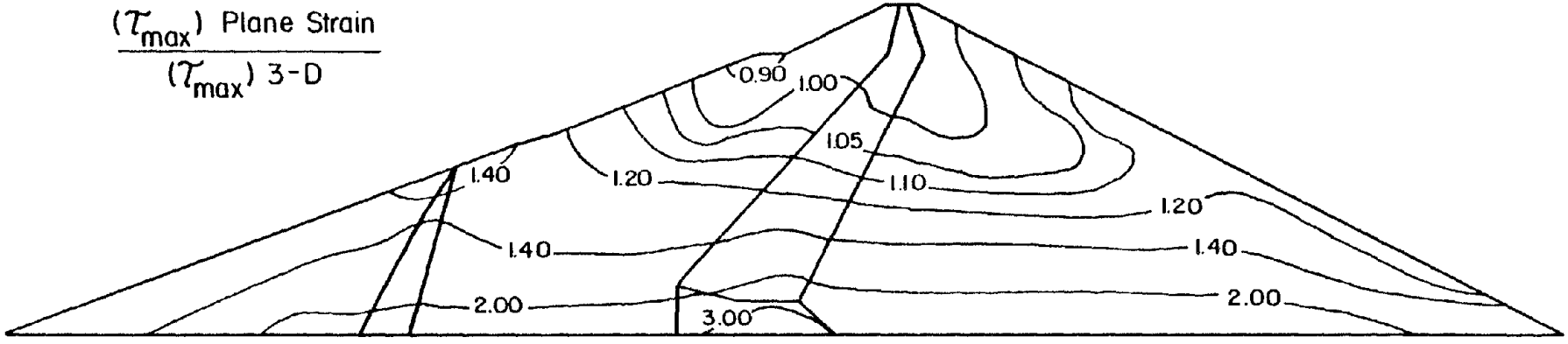

Fig. 5-7c Distribution of the Ratio $\tau_{max\,2D}/\tau_{max\,3D}$ Computed for the Maximum Section of Dam with Valley Wall Slopes of 1:1 - Reanalysis Earthquake.

the Oroville earthquake motions have low amplitudes and a high frequency content and will therefore induce small embankment response and significant contributions to the response from the higher modes of vibration.

The natural period of the maximum section for the level of strain induced by the Oroville earthquake was computed to be 1.02 seconds. This value is 23% higher than that computed for the 3-D model of Oroville Dam and 50% higher than the value computed for the 3-D model of the dam with valley wall slopes of 1:1 (see Fig. 5-1). Since the level of strain induced in the 2-D and 3-D models is about the same, the above differences are mostly the result of the stiffening effect of canyon geometry. It may be noted that these differences are of the same order of magnitude as those computed for the Reanalysis earthquake indicating that the effects of the nature of input motions are small.

Acceleration time histories were computed at several points in the section. Fig 5-8(a) shows a comparison between acceleration time histories at the crest for the 2-D and 3-D models of Oroville Dam. The continuous trace corresponds to the time history computed from the plane strain analysis of the maximum section and the dashed line corresponds to the time history computed from the three-dimensional analysis of the dam. It is interesting to note that the time history for the 3-D model displays the predominant period of the dam while the time history for the 2-D model does not. The latter shows a higher predominant frequency than the former even though the natural frequency of vibration for the 2-D model of the dam is lower than the corresponding value for the 3-D model. This fact indicates the predominance of higher modes of vibration in the response of the 2-D model.

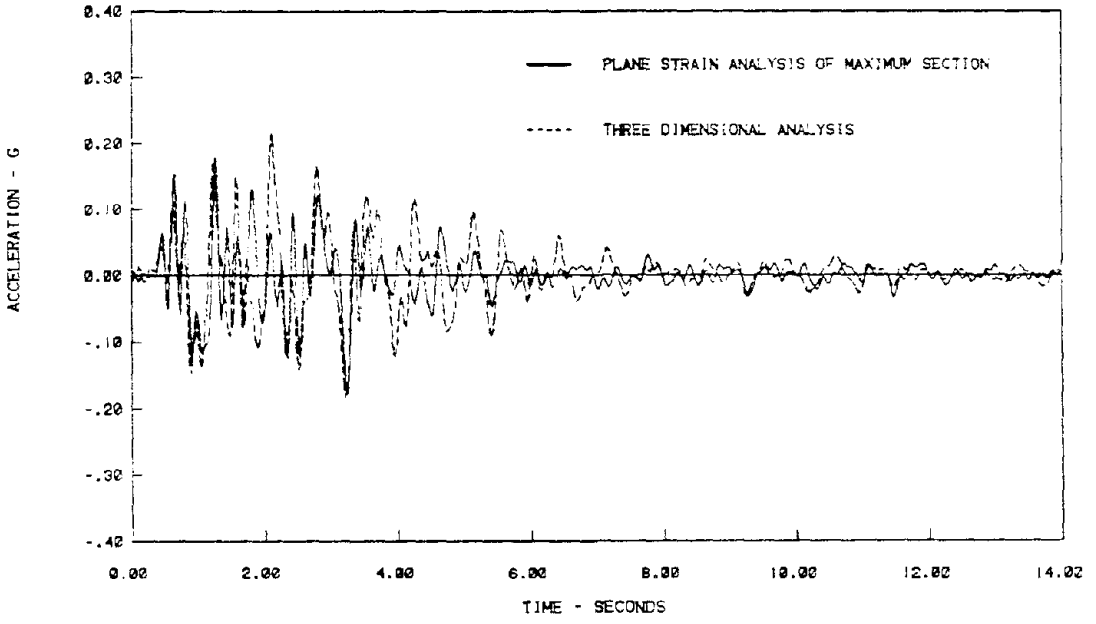

(a) Oroville Dam

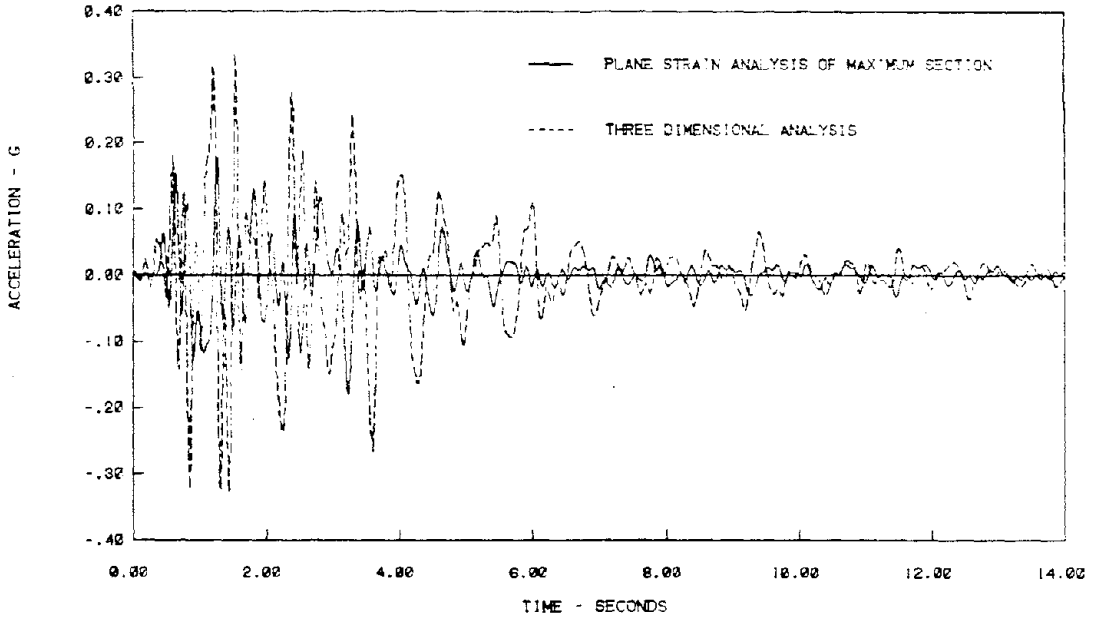

(b) Dam with valley wall slopes of 1:1

Fig. 5-8 Crest Acceleration Time Histories Computed from 2-D and 3-D Analyses - Oroville Earthquake.

Fig. 5-8(b) shows an analogous comparison between the computed acceleration time histories at the crest of the dam with valley wall slopes of 1:1. The differences in this case are larger than those observed for the Oroville Dam. On the basis of the preceding results it can be concluded that for the Oroville earthquake motions a plane strain analysis of the maximum section does not give a reasonable prediction of the acceleration time history computed at the crest of the two dams analyzed in three dimensions.

Fig. 5-9 shows the profile of peak horizontal accelerations along the contact between the core and the downstream shell and along the downstream slope of the maximum section. It can be seen that along the core-shell contact the peak acceleration decreases from 0.09 g to 0.06 g at an elevation of 350 feet and increases to 0.18 g at the crest. The variation of peak accelerations along the surface of the downstream slope is more erratic. There is some similarity between these acceleration profiles and the corresponding profiles in Fig. 4-14. However, comparison of Fig. 5-9 with Fig. 4-24 indicates that the peak accelerations computed from a plane strain analysis of the maximum section are not in good agreement with the values computed from a 3-D analysis of the dam with valley wall slopes of 1:1.

The distribution of peak values of τ_{xy} computed from a plane strain analysis of the maximum section for the Oroville earthquake is shown in Fig. 5-10. As in the case of the Reanalysis earthquake a considerable reduction in stresses due to the presence of the core block is noticed at the base of the section. Comparison of these stresses with the corresponding τ_{xy} stresses obtained from the 3-D analyses of the two

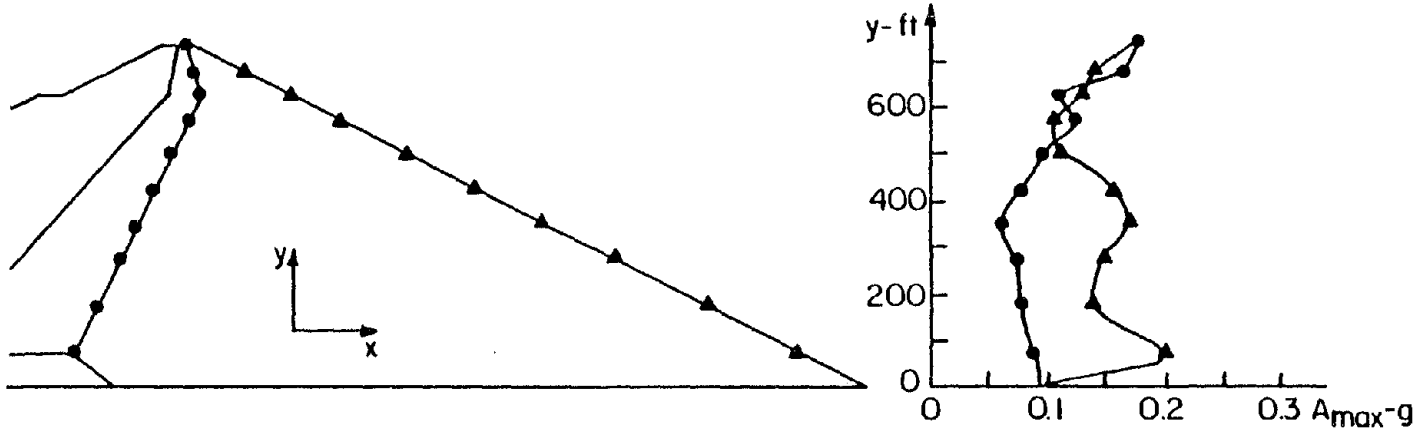

Fig. 5-9 Peak Horizontal Acceleration Computed from 2-D Analysis of Maximum Section for the Oroville Earthquake.

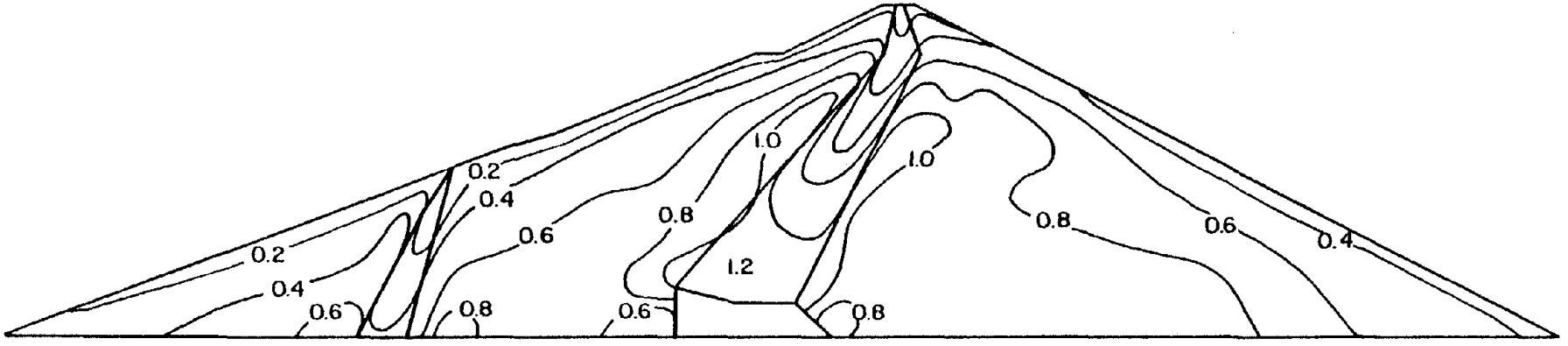

Fig. 5-10 Distribution of Peak Shear Stress τ_{xy} in Tsf Computed from Plane Strain Analysis of Maximum Section for the Oroville Earthquake.

dams studied is shown by computing the ratio τ_{xy2D}/τ_{xy3D}. Contours of equal values of this ratio are shown in Figs. 5-11(a) and 5-11(b) for the Oroville Dam and the dam with valley wall slopes of 1:1 respectively.

The distribution of the ratio τ_{xy2D}/τ_{xy3D} shown in Fig. 5-11(a) is quite erratic. However, the stresses computed from the plane strain analysis of the maximum section are within 20% of the stresses computed from a three-dimensional analysis of Oroville Dam.

For the dam with valley wall slopes of 1:1 the ratio τ_{xy2D}/τ_{xy3D} increases from a value of 0.5 near the crest to a value of about 1.0 at midheight and to a value of 4.0 near the base. As for the Reanalysis earthquake, the contours of this ratio are close to horizontal. This distribution of the ratio between 2-D and 3-D stresses reflects the constraining effects on the dam of the narrow triangular shape of the canyon.

On the basis of the above results, it can be concluded that for low amplitude motions a 2-D analysis of the maximum section of a dam with the characteristics of Oroville Dam yields shear stresses within 20% of those computed from a 3-D analysis. However, for a dam with steeper canyon walls large differences will exist between the stresses computed from 2-D analysis of the main section and 3-D analysis of the dam.

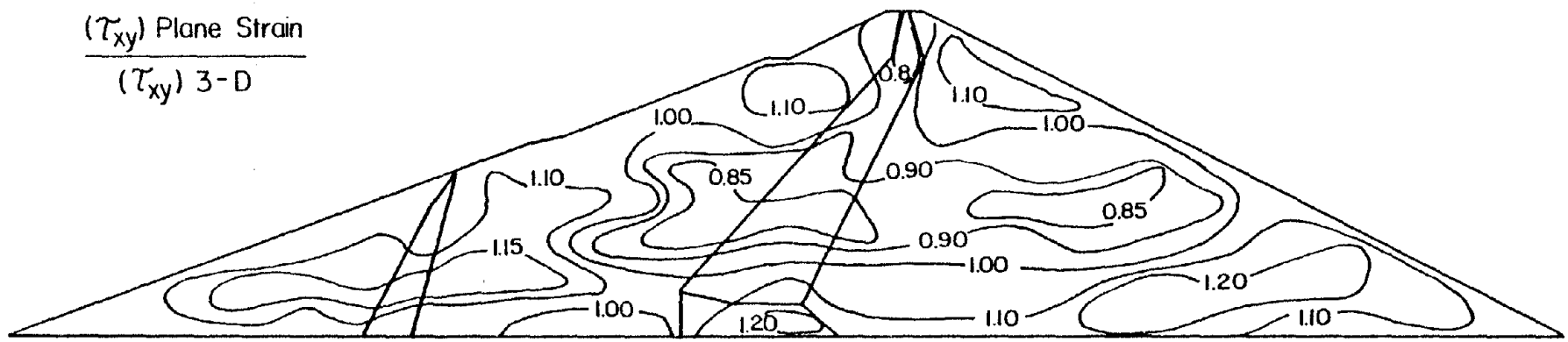

Fig. 5-11a Distribution of the Ratio τ_{xy2D}/τ_{xy3D} Computed for the Maximum Section of Oroville Dam - Oroville Earthquake.

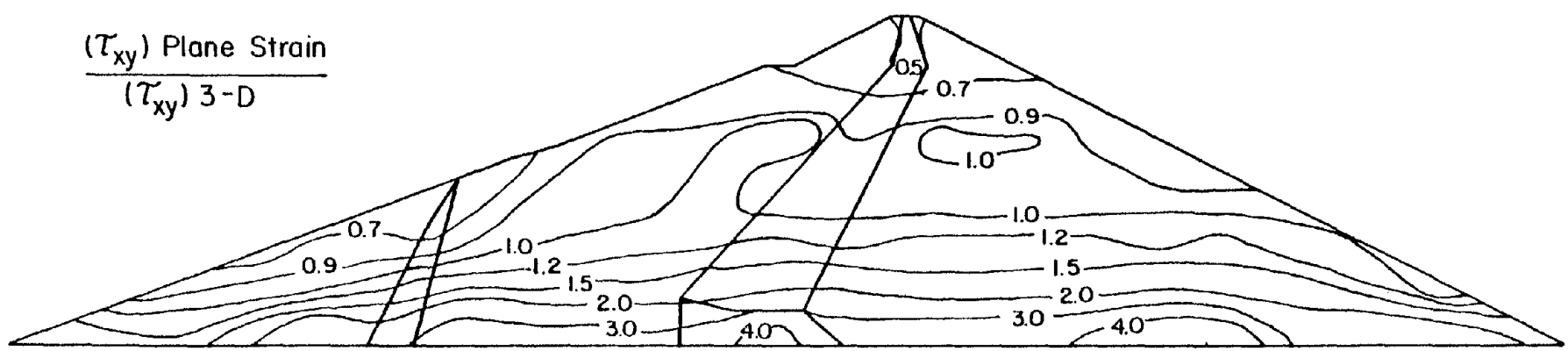

Fig. 5-11b Distribution of the Ratio τ_{xy2D}/τ_{xy3D} Computed for the Maximum Section of Dam with Valley Wall Slopes of 1:1 - Oroville Earthquake.

5.2.4 Dynamic Response of Quarter Section to the Reanalysis Earthquake

It is common practice in the dynamic analysis of earth dams in triangular canyons to study, in addition to the main section, the response of other sections using plane strain analysis procedures. In order to investigate the validity of this method and to further study the effects of three-dimensional behavior, plane strain analyses of the quarter section of the Oroville Dam and of the dam with valley wall slopes of 1:1 have been performed, and the results have been compared with the results from 3-D analyses of these dams. Results for the Reanalysis earthquake are presented in this subsection and those for the Oroville earthquake are presented in the next subsection.

The acceleration time history at the crest of the quarter section has been compared in Fig. 5-12(a) with that obtained from a 3-D analysis of Oroville Dam. It can be observed that there is considerable similarity between the two time histories. The analogous comparison for the dam with valley wall slopes of 1:1 is less favorable as shown in Fig. 5-12(b).

The top part of Fig. 5-13 shows the variation of peak acceleration along the contact core-shell and along the downstream slope computed from the plane strain analysis of the quarter section. The continuous trace shows a decrease in peak acceleration from 0.6 g at the base to 0.45 g at a point 75 ft above the base and an increase to 0.85 g at the crest. These profiles resemble those computed from the plane strain analysis of the maximum section (see Fig. 5-5) the shape of which is due to the amplification and filtering phenomena previously described. The bottom part of the figure shows the corresponding profiles computed from

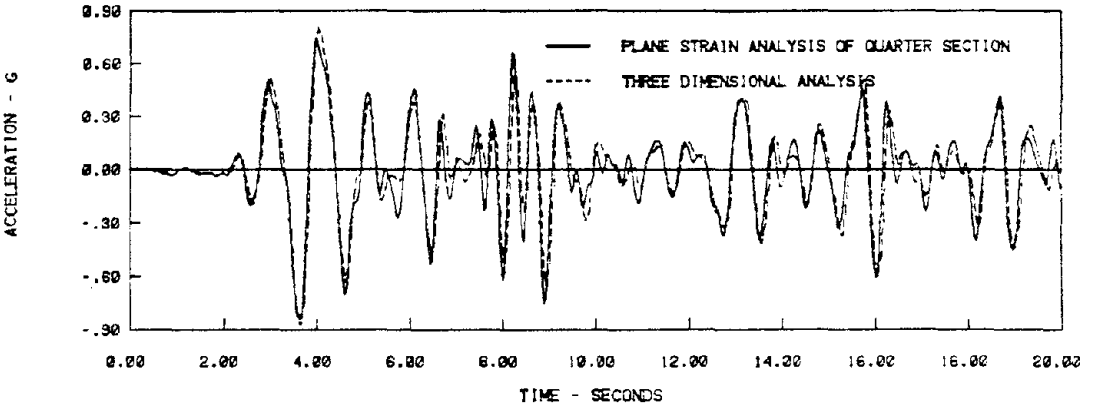

(a) Oroville Dam

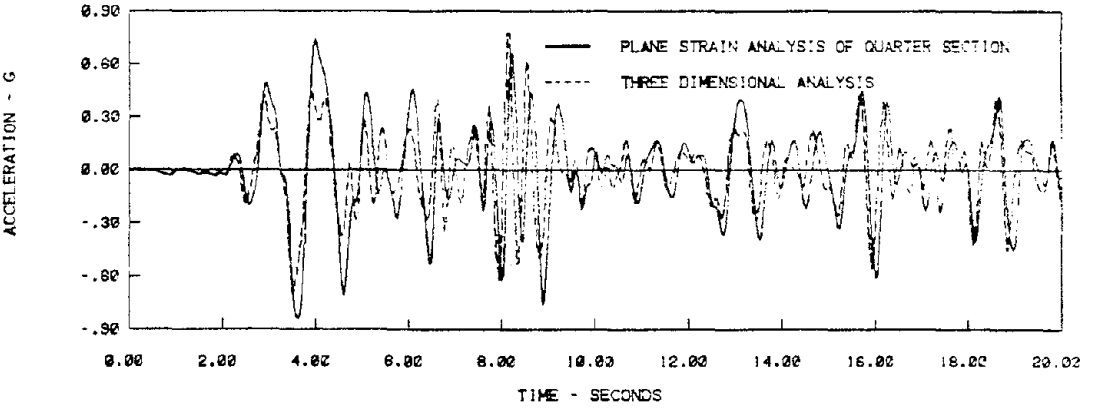

(b) Dam with valley wall slopes of 1:1

Fig. 5-12 Crest Acceleration Time Histories Computed from 2-D and 3-D Analyses - Reanalysis Earthquake.

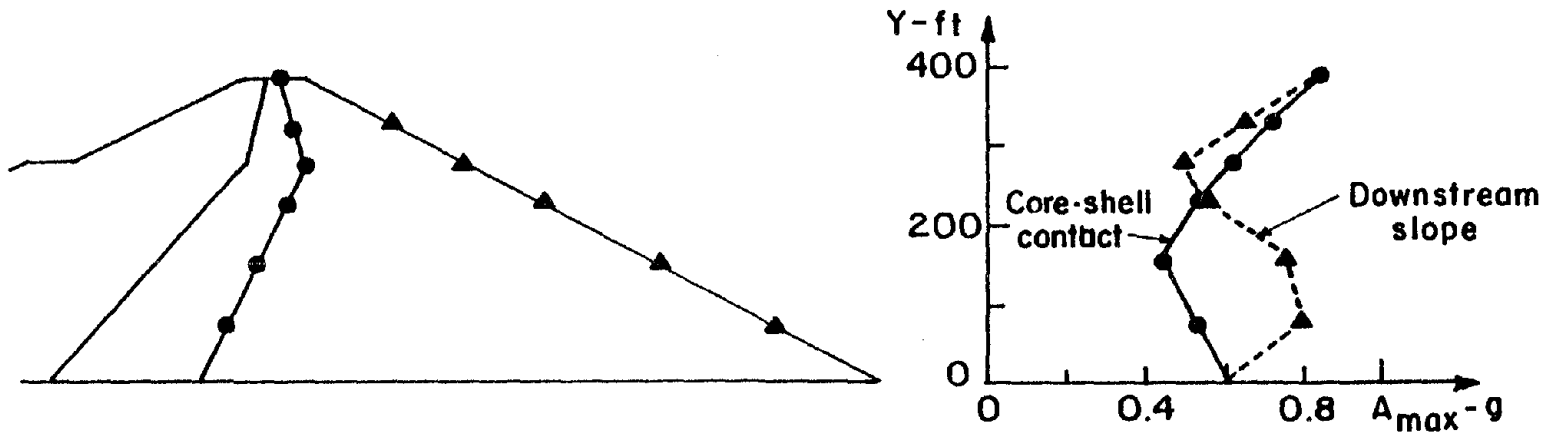

(a) Plane strain analysis of quarter section

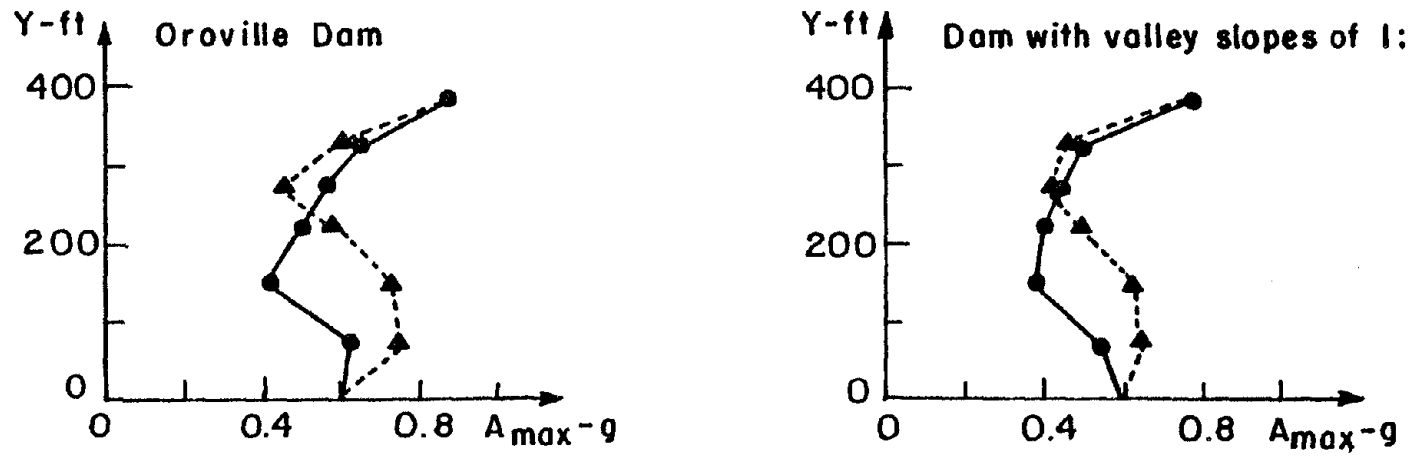

(b) Three dimensional analysis

Fig. 5-13 Peak Horizontal Accelerations Computed at Quarter Section for the Reanalysis Earthquake.

the three-dimensional analyses of the two dams treated in this study. A comparison between acceleration profiles for the Oroville Dam shows good agreement in pattern and amplitudes of acceleration. However, the levels of acceleration obtained from the 3-D analysis of the dam with valley wall slopes of 1:1 are lower than those computed from a plane strain analysis of the quarter section.

The distribution of peak values of the τ_{xy} stresses within the quarter section is shown in Fig. 5-14. As before, an increase in stress with depth and proximity to the center of the section is noticed. The lower shear moduli for the core materials cause the shear stresses in the core to be lower than those in the shell. Higher stresses in the downstream shell than in the upstream shell are obtained for the same reason.

In order to compare the stresses computed from the plane strain analysis of the quarter section with those computed from a 3-D analysis of the dams, the ratio τ_{xy2D}/τ_{xy3D} has been computed. Fig. 5-15(a) shows the distribution of this ratio for the quarter section of Oroville Dam. It can be seen that the stresses computed from a plane strain analysis of the section are on the average 20% higher than those computed with a 3-D model of the dam. Near the rigid boundary they are only higher by about 10%. The contours of equal values of the same ratio for the quarter section of the dam with valley wall slopes of 1:1 are shown in Fig. 5-15(b). It can be seen that for this dam the τ_{xy} stresses obtained from a 2-D analysis of the quarter section are substantially higher than those computed with a 3-D model of the dam. Except for a small zone near the base of the dam the differences are

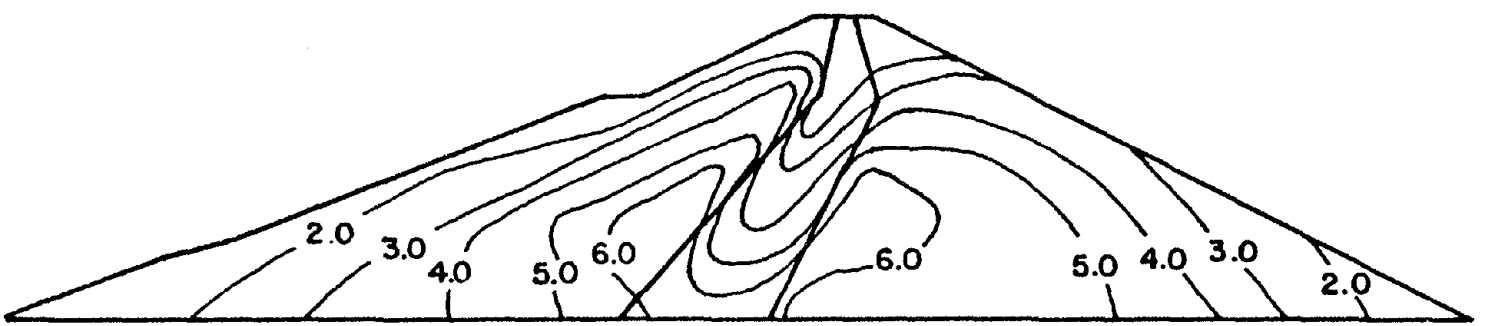

Fig. 5-14 Distribution of Peak Shear Stress τ_{xy} in Tsf Computed from Plane Strain Analysis of Quarter Section for the Reanalysis Earthquake.

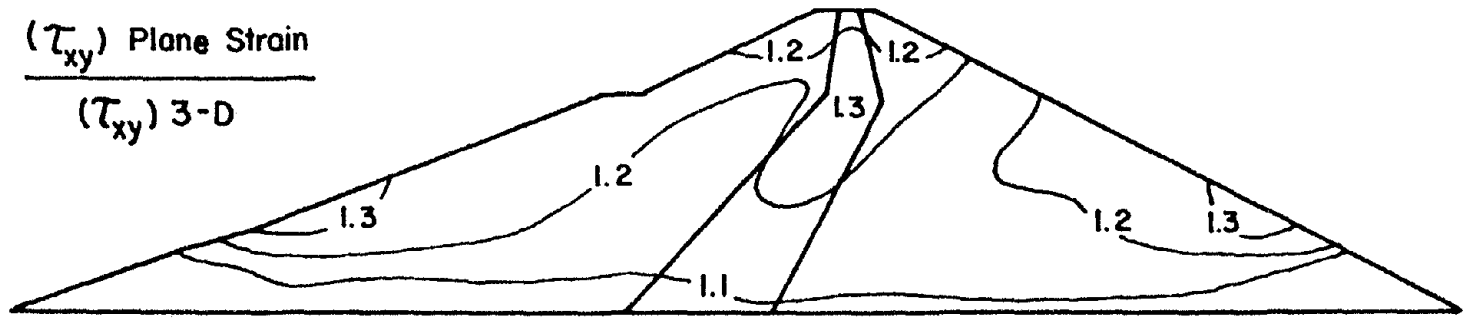

Fig. 5-15a Distribution of the Ratio τ_{xy2D}/τ_{xy3D} Computed for the Quarter Section of Oroville Dam - Reanalysis Earthquake.

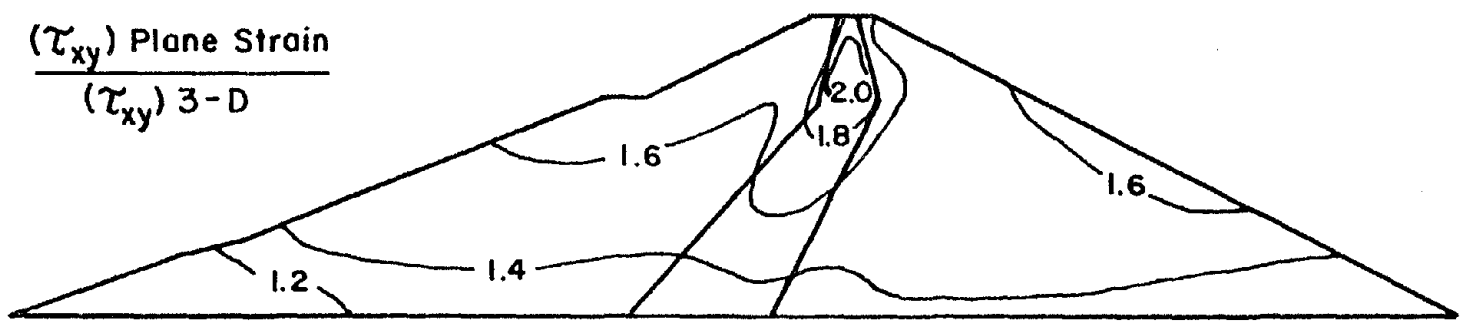

Fig. 5-15b Distribution of the ratio τ_{xy2D}/τ_{xy3D} Computed for the Quarter Section of Dam with Valley Slopes of 1:1 - Reanalysis Earthquake.

larger than 40% and they get to be as high as 100% near the crest of the section.

It was shown in Chapter 4 by the results from the 3-D analysis of the dam with valley wall slopes of 1:1 that the τ_{xy} stresses are not a dominant component of the stress tensor and that significant horizontal shear stresses exist on the vertical plane at the quarter section of the dam. In particular, the ratio τ_{xy}/τ_{max} which has been adopted as a measure of the degree to which the τ_{xy} stresses determine material behavior, is well below 1.0 for this section. In spite of this fact, other comparisons different than the one given by the ratio τ_{xy2D}/τ_{xy3D} have not been performed since it is not well known what their meaning would be.

On the basis of the results presented and in light of the above discussion, it can be concluded that for strong motions, a two-dimensional analysis of the quarter section yields stresses within 20% of those computed from a 3-D analysis of dams with similar characteristics to Oroville Dam. However, for dams with steeper valley wall slopes a plane strain analysis of the quarter section yields a response that differs significantly from that computed from a three-dimensional analysis.

5.2.5 Dynamic Response of Quarter Section to the Oroville Earthquake

The results from the plane strain analysis of the quarter section for the Oroville earthquake and a comparison with the results computed for the same section from 3-D analyses of the Oroville Dam and of the dam with valley wall slopes of 1:1 are presented in this subsection.

The acceleration time history at the crest computed with the 2-D analysis of the quarter section showed poor agreement with the time histories computed from a 3-D analysis of the dams. The top part of Fig. 5-16 shows the profile of peak horizontal accelerations along the core-shell contact and along the downstream slope of the section. The computed peak horizontal acceleration at the crest is 0.24 g. The bottom of the figure shows analogous profiles computed from the 3-D analysis of the two dams studied. The acceleration profiles for Oroville Dam shown in Fig. 5-16 show very irregular patterns. Overall it can be observed that for the Oroville earthquake a plane strain analysis of the quarter section does not give a good estimate of the peak accelerations computed with 3-D models of Oroville Dam and the dam with valley wall slopes of 1:1.

The distribution of peak values of the τ_{xy} stresses computed from a plane strain analysis of the quarter section is shown in Fig. 5-17. The magnitude of these stresses is on the average 6 or 7 times lower than the magnitude of the stresses computed for the Reanalysis earthquake. The contours of equal values of the ratio τ_{xy2D}/τ_{xy3D} are shown in Figs. 5-18(a) and 5-18(b) for the quarter section of Oroville Dam and the dam with valley wall slopes of 1:1 respectively. As in the case of the Reanalysis earthquake a 2-D analysis of the quarter section of Oroville Dam gives τ_{xy} stresses which are on the average 20% higher than those computed from a 3-D analysis of the dam. Very small differences are observed near the base of the section. For the dam with valley wall slopes of 1:1 the differences between stresses are on the order of 30%. It is interesting to note that much larger differences were observed in similar comparisons for the Reanalysis earthquake. The distribution of

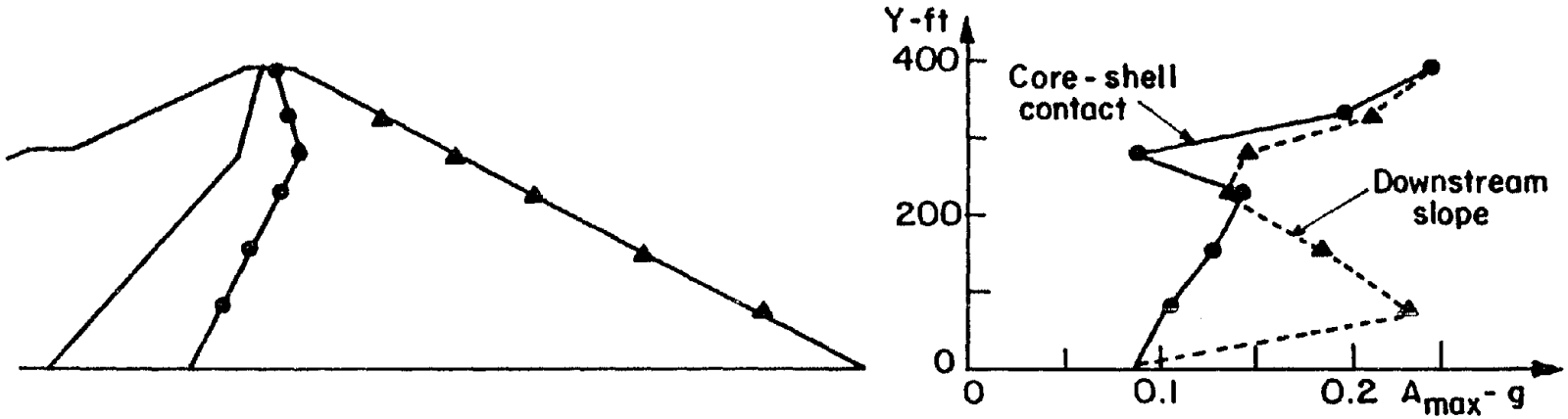

(a) Plane strain analysis of quarter section

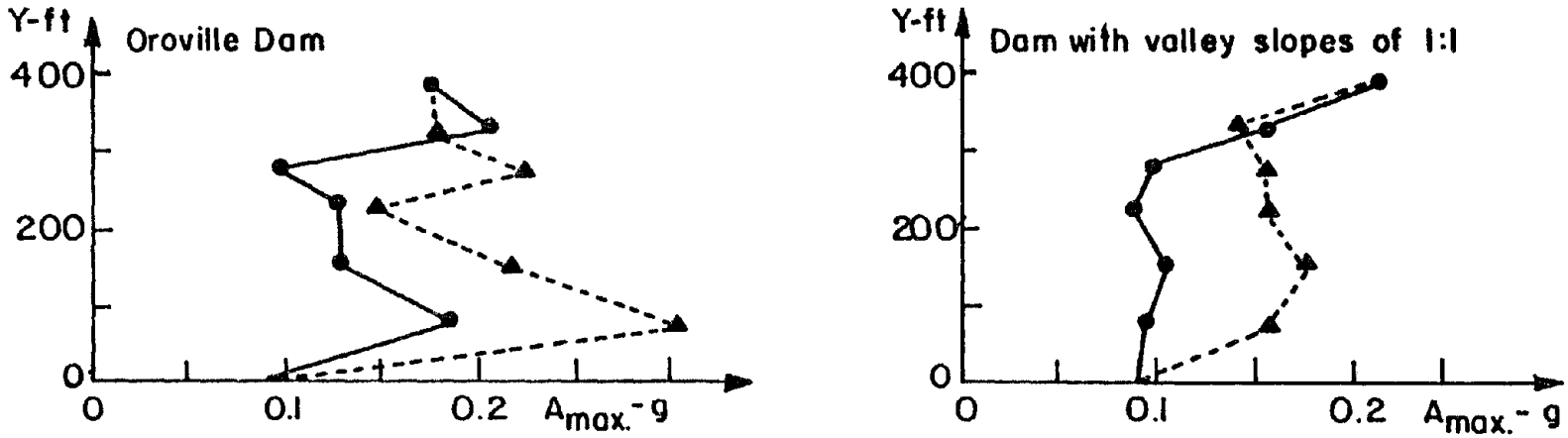

(b) Three dimensional analysis

Fig. 5-16 Peak Horizontal Accelerations Computed at Quarter Section for the Oroville Earthquake.

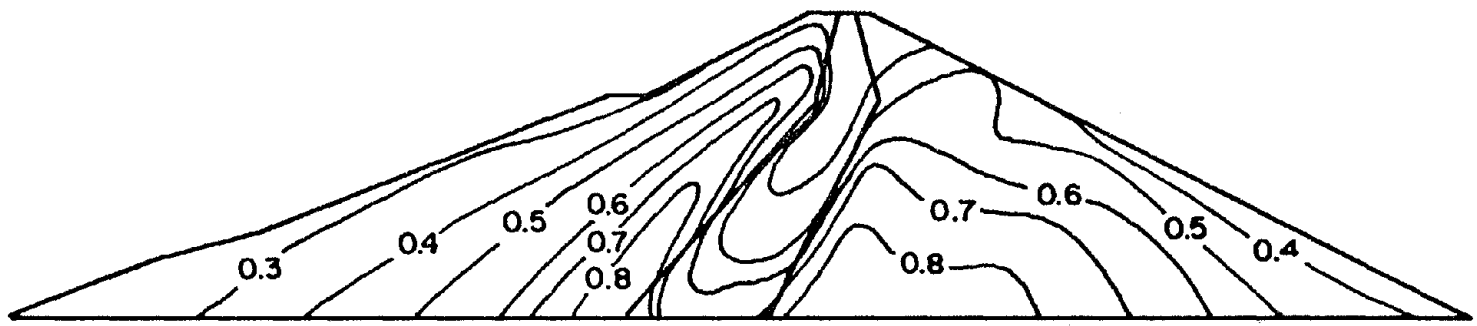

Fig. 5-17 Distribution of Peak Shear Stress τ_{xy} in Tsf Computed from Plane Strain Analysis of Quarter Section for the Oroville Earthquake.

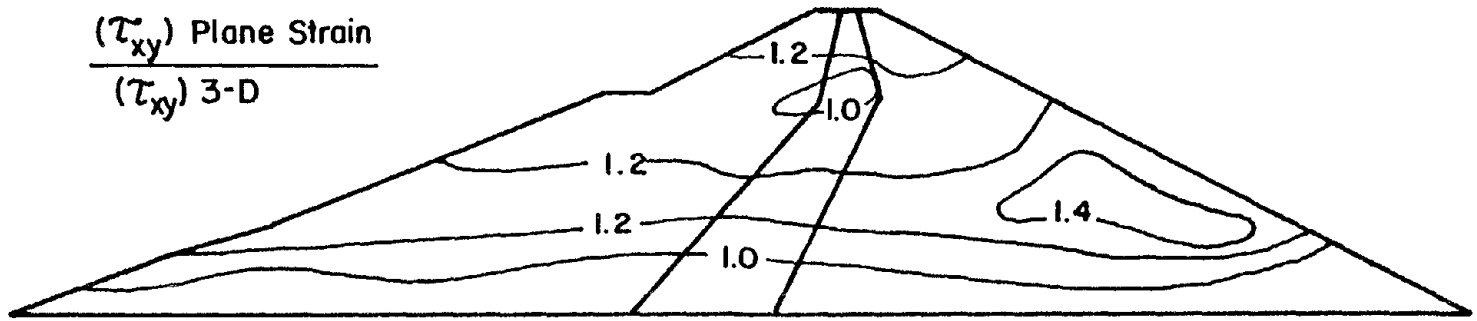

Fig. 5-18a Distribution of the Ratio τ_{xy2D}/τ_{xy3D} Computed for the Quarter Section of Oroville Dam - Oroville Earthquake.

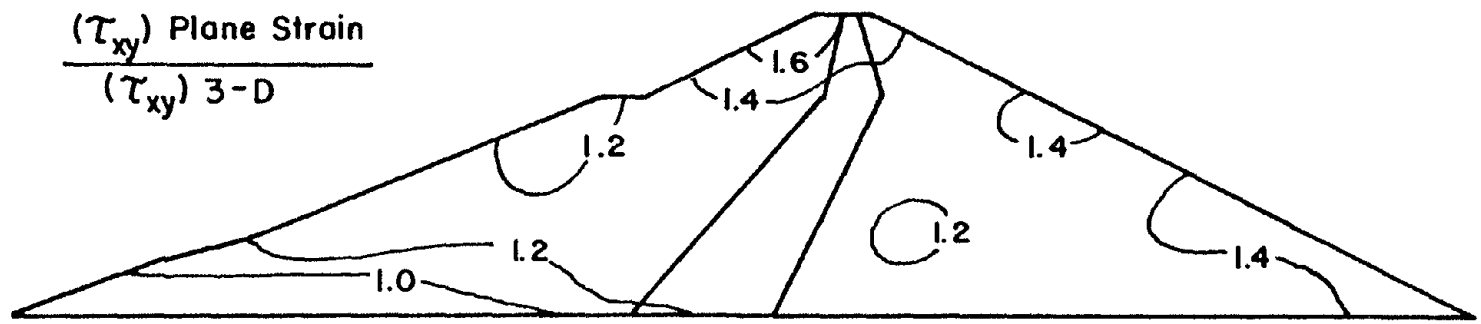

Fig. 5-18b Distribution of the Ratio τ_{xy2D}/τ_{xy3D} Computed for the Quarter Section of Dam with Valley Slopes of 1:1 - Oroville Earthquake.

τ_{xy2D}/τ_{xy3D}, shown in Fig. 5-18(b), does not show any regular pattern and there is a small zone in which this ratio gets to be on the order of 1.6.

On the basis of the preceding results it can be concluded that a plane strain analysis of the quarter section of a dam with similar characteristics to Oroville Dam yields horizontal shear stresses which are up to 20% higher than the stresses computed from a 3-D analysis of the dam. For dams in canyons with steeper walls the differences in stresses will be larger and will depend on the geometry of the canyon. Accelerations are more sensitive than stresses to the higher modes of vibration of the dams studied and therefore a plane strain analysis of the quarter section does not yield values which are in good agreement with those computed from three-dimensional analyses of the dams.

5.3 Evaluation of Two-Dimensional Analyses Using Modified Soil Stiffness Characteristics

5.3.1 General Considerations

The three-dimensional dynamic response of earth dams has been studied in previous sections of this Chapter and in Chapter 4. The most important effect of 3-D behavior has been shown to be a stiffening of the dam due to the restraint imposed by the canyon geometry. Other important effects are the reduction in shear stresses near the bottom of the canyon, the overall change in stress distribution, and the existence of significant horizontal shear stresses on vertical planes.

As shown in Chapter 2 there exists some similarity between the first natural three-dimensional mode shape of vibration of a dam in a triangular canyon and the first natural 2-D mode shape of the maximum section of the dam. Assuming that the response of the dam to ground motions depends mainly on the first natural mode of vibration it is reasonable to think that the response of the dam can be simulated approximately by a 2-D model of the dam that has the same predominant period of vibration as the 3-D model of the dam.

The above assumption is the basis of the approximate procedure used to account for the 3-D behavior of Oroville Dam during the re-evaluation of its stability for a 6.5 magnitude earthquake (DWR, 1979; Banerjee et al., 1979). A plane strain analysis of the maximum section of the dam with a K_2max value of 350 for the shell materials, was one of the methods used to compute the dynamic response of the dam to the Reanalysis earthquake. Although as shown in Chapter 3 the in-situ K_2max value for the shell materials is approximately 170, the above value gave the correct natural period of the dam with a 2-D analysis of the maximum section for the Oroville earthquake (see Fig. 3-7) and therefore it was considered reasonable to assume, in accordance with the above discussion, that it would give the correct dynamic response of the dam for the design earthquake. It was assumed that the correct accelerations and strains would be obtained but that due to the fact that the moduli in the finite element model were twice as high as the in-situ moduli for the dam, the stresses would be over-predicted by a factor of two. For this reason half of the computed stresses were used in the assessment of the deformations and stability of the dam.

The above procedure would be a means of simplifying the dynamic analysis of three-dimensional earth dams and therefore it seems desirable to investigate its validity. For this reason 2-D analyses of the main section of Oroville Dam, using a K_2max value of 350 for the shell materials, have been performed for the Oroville and Reanalysis earthquakes and the results have been compared with the results obtained from three-dimensional analyses of the dam for the same earthquakes.

5.3.2 Plane Strain Analysis of the Maximum Section with K_2max=350 for the Oroville Earthquake.

The results from the plane strain analysis of the maximum section of Oroville Dam for the Oroville earthquake, using a K_2max value of 350 for the shell materials, are presented in this subsection. Additionally these results are compared with those obtained from a three-dimensional analysis of the dam.

The natural period of the maximum section with K_2max=350 computed from a plane strain analysis for the Oroville earthquake is 0.73 seconds. This value is 9% lower than the expected value of 0.8 seconds. However, the difference is sufficiently small to have no significant effects on the dynamic response. It is of interest to examine the time history of horizontal acceleration computed at the crest of the maximum section. It can be seen from Fig. 5-19 that this time history displays approximately the natural period of vibration of the section (0.73 seconds). The lower part of Fig. 5-19 shows the acceleration time history at the crest computed from a three-dimensional analysis of the dam for the same earthquake. An easier comparison between the computed

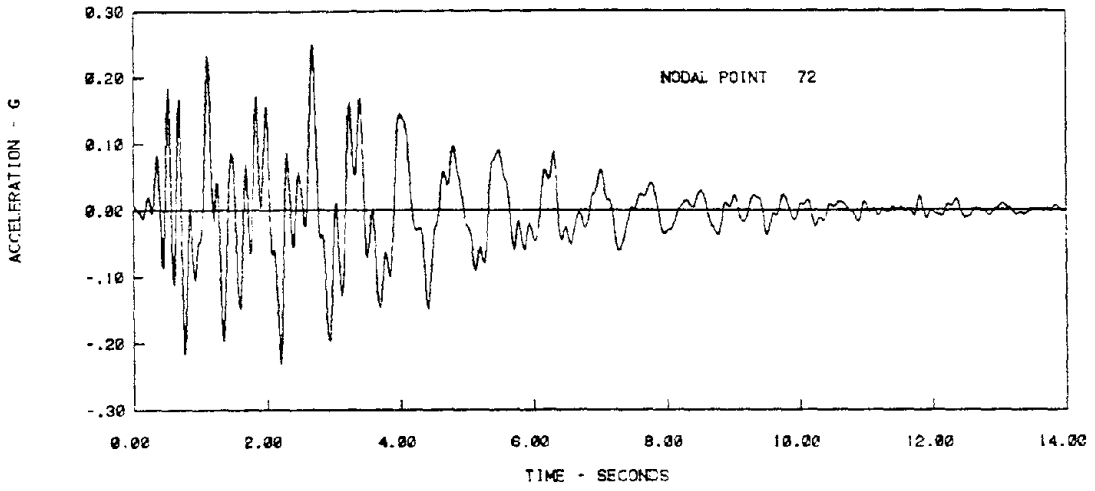

(a) Plane strain analysis of maximum section with $K_2max=350$

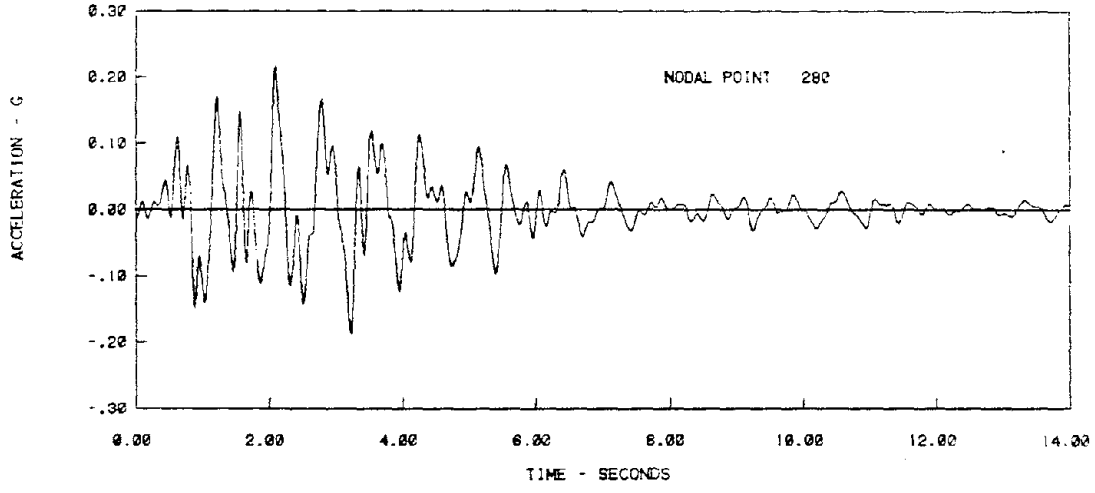

(b) Three-dimensional analysis

Fig. 5-19 Crest Acceleration Time Histories Computed from Analyses of Oroville Dam for the Oroville Earthquake.

response at the crest of the two models can be made in terms of the acceleration response spectra for the above time histories. These acceleration spectra are shown in Fig. 5-20 from which it can be seen that a significant difference exists at a period value of 0.15 seconds. However, at other frequencies, the spectra are quite similar.

Fig. 5-21 shows the variation of peak horizontal accelerations along the contact between the core and the downstream shell and along the downstream slope of the section. The peak acceleration at the crest is about 0.25 g. It is of interest to compare these profiles of peak acceleration with those computed from a 3-D analysis of the dam (see Fig. 4-14). Little agreement, especially on the downstream slope, is observed between the results of the two analyses.

The distribution of peak values of the τ_{xy} stresses computed for the section is shown in Fig. 5-22(a). A general increase in stress level with depth and with proximity to the core is observed. However, at the base of the section, there is a decrease in stress in the vicinity of the core block due to the presence of this rigid member. The contours of stress bend sharply at the contacts between the core and the shells due to the much lower shear moduli of the core materials (G/S_u=2200). Fig. 5-22(b) shows the contours of equal values of the ratio τ_{xy2D}/τ_{xy3D}. If the assumptions on which the previously proposed method of accounting for 3-D behavior were completely valid, with the exception of the core, this ratio should have a value of about 2.0 throughout the section. It can be seen that values close to 2.0 are obtained in the upstream shell except near the base of the section. However, in the downstream shell this ratio is significantly lower than

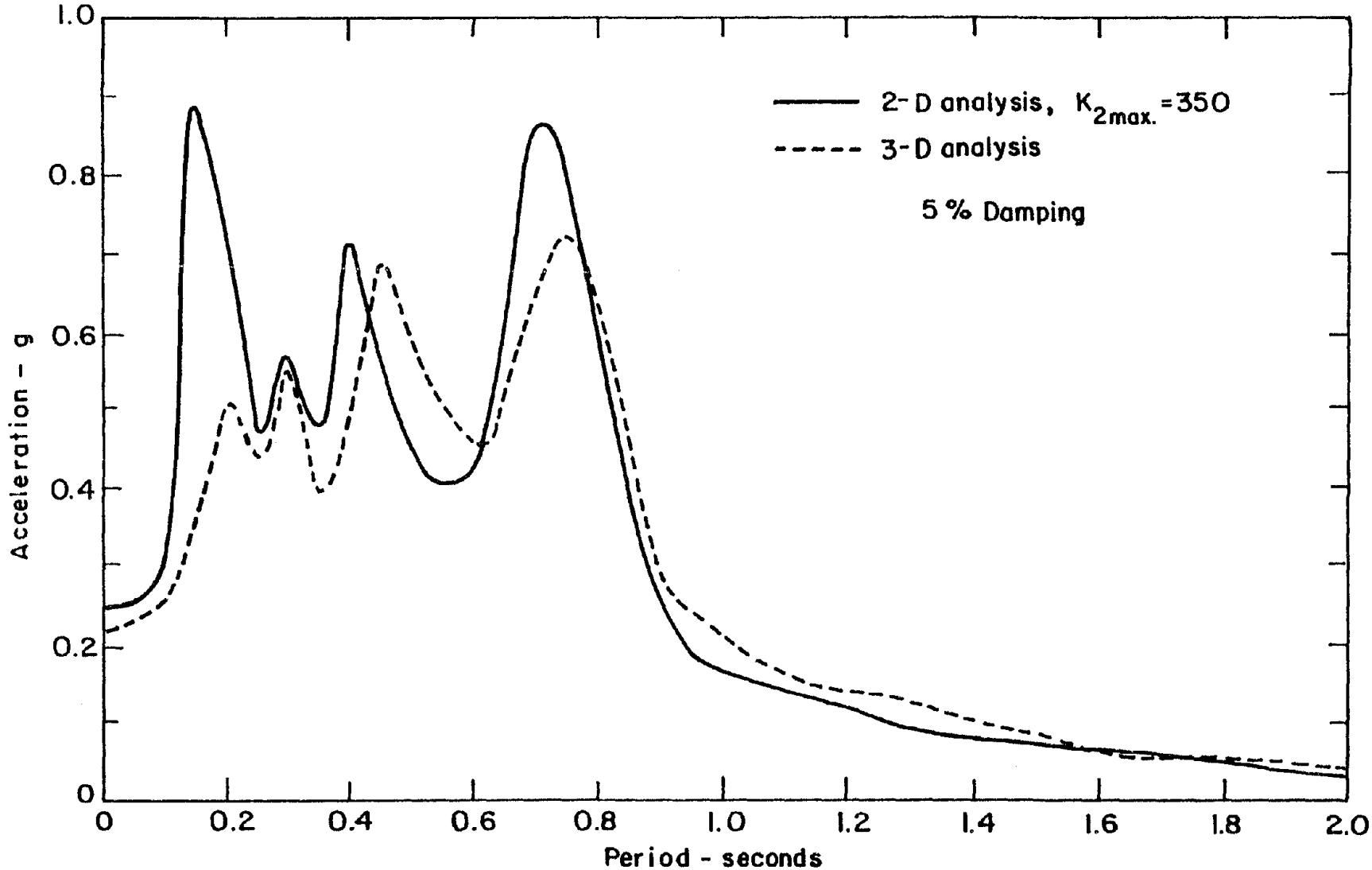

Fig. 5-20 Acceleration Response Spectra for Motions Computed at Crest of Oroville Dam.

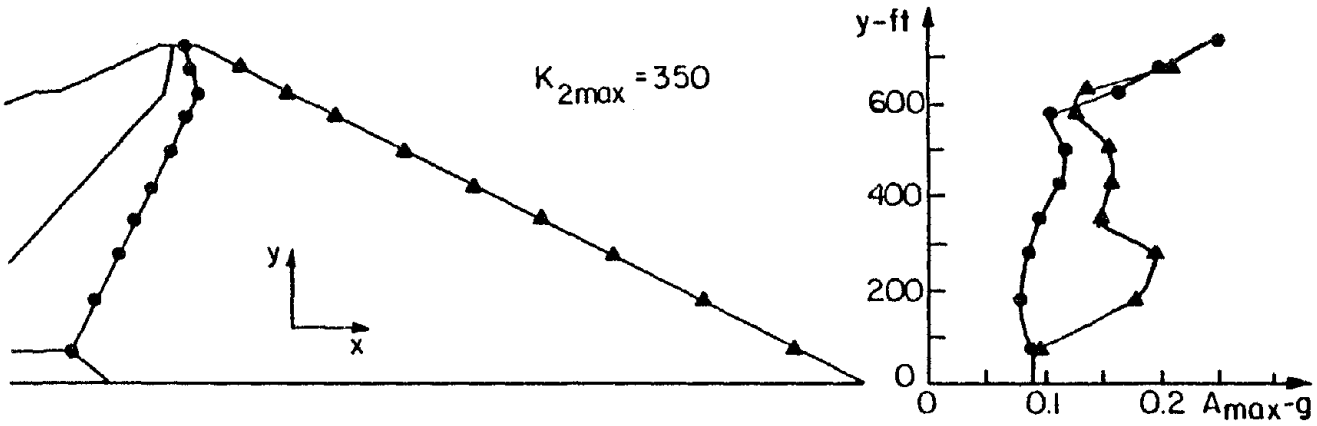

Fig. 5-21 Peak Horizontal Accelerations Computed from 2-D Analysis of Maximum Section for the Oroville Earthquake (K_{2max}=350).

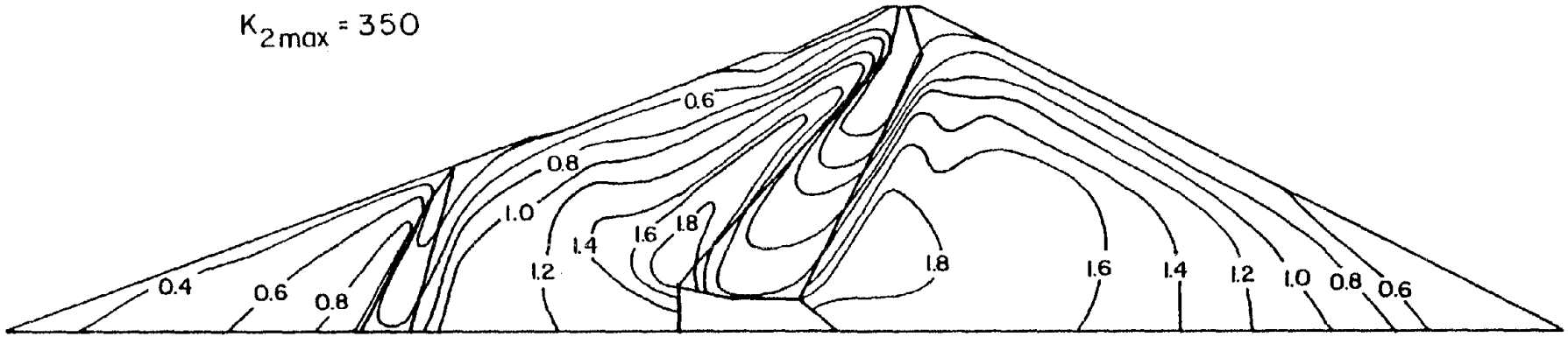

Fig. 5-22a Distribution of Peak Shear Stress τ_{xy} in Tsf Computed from 2-D Analysis of Maximum Section for the Oroville Earthquake.

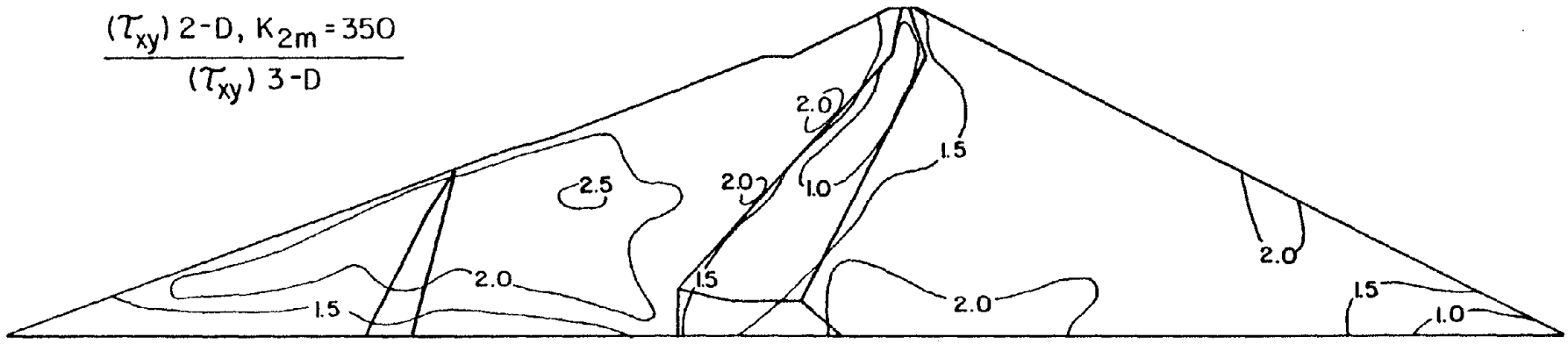

Fig. 5-22b Distribution of the Ratio τ_{xy2D}/τ_{xy3D} Computed for the Maximum Section of Oroville Dam - Oroville Earthquake.

2.0. The low values obtained in the core (about 1.0) are due to the fact that the shear moduli for the core materials are approximately the same in the two analyses compared (G/S_u=2200).

From the above results it can be concluded that the assumptions on which the method is based are not quite correct and therefore the stresses in the main section can only be predicted within 25%. It follows that the fact that a plane strain analysis of the maximum section with $k_2$max=350 gives the correct natural period of vibration for Oroville Dam does not imply that other response parameters are correctly predicted.

5.3.3 Plane Strain Analysis of the Maximum Section with K_2max=350 for the Reanalysis Earthquake.

As mentioned before an attempt to account for the 3-D behavior of Oroville Dam was made by Banerjee et al.(1979) and by the Department of Water Resources during the analysis of the dam for the design earthquake motions. It was assumed that if a plane strain analysis using a value of K_2max=350 for the shell materials gave the correct natural period of the embankment for the Oroville earthquake the same analysis should give the correct dynamic response for the Reanalysis earthquake. The results from a plane strain analysis of the dam using a K_2max value of 350 for this last earthquake are presented in this section.

Following this approach, the computed period of this 2-D model of the dam for the level of strain induced by the Reanalysis earthquake is 1.05 seconds. This value is 25% lower than the value computed with a 3-D model of the dam for the same earthquake. The above difference is

somewhat larger than that computed in the analogous case for the Oroville earthquake. This observation indicates that there is a moderate non-linear effect caused by the difference in level of shaking between the two earthquakes.

The acceleration time history computed at the crest of the section is shown in the upper part of Fig. 5-23. The bottom part of this figure shows the time history computed using a 3-D model of the dam. Even though the time histories present some common features the overall agreement is not very good. Better results were obtained from a 2-D analysis of the dam using the in-situ material properties as shown in Fig. 5-4(a). Some high frequency (5 Hz) low amplitude oscillations are present in the time history computed from the 2-D analysis with K_2max=350 which are the result of defective interpolation on the amplification function for the crest.

The variation of peak horizontal accelerations along the contact between the core and the downstream shell and along the downstream slope of the section are shown in Fig. 5-24. At the core-shell contact the peak acceleration decreases from 0.6 g to 0.4 g at elevation of 200 feet and increases gradually to 1.05 g at the crest. A comparison of this figure with Fig. 4-7 shows that this 2-D model gives accelerations about 40% higher than the 3-D model through considerable portions of the core-shell contact and of the downstream slope of the dam.

The distribution of τ_{xy} stresses computed from the plane strain analysis of the maximum section with K_2max=350 is shown in Fig. 5-25(a). A comparison of these stresses with those computed with a 3-D model of the Oroville Dam has been performed by computing the ratio

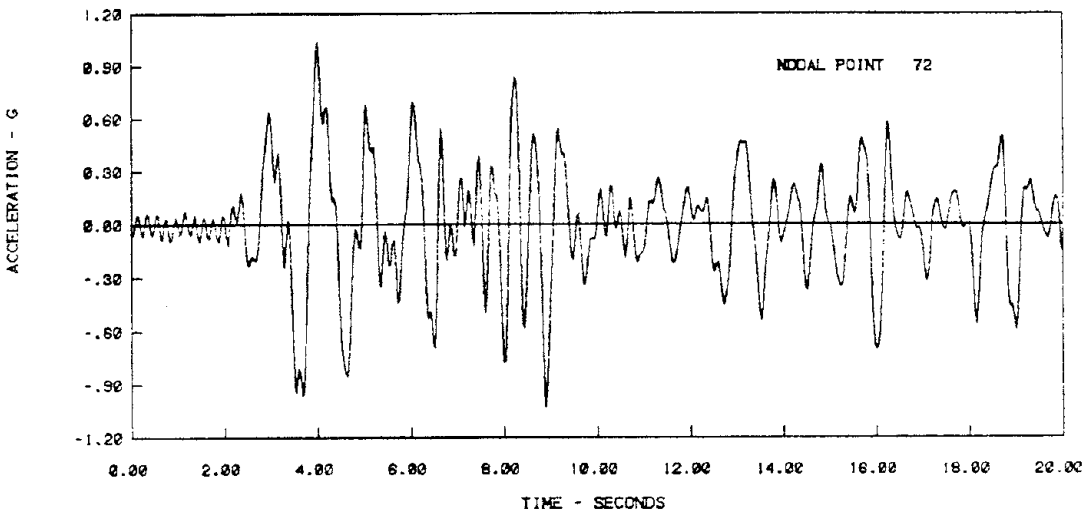

(a) Plane strain analysis of maximum section with K_2max=350

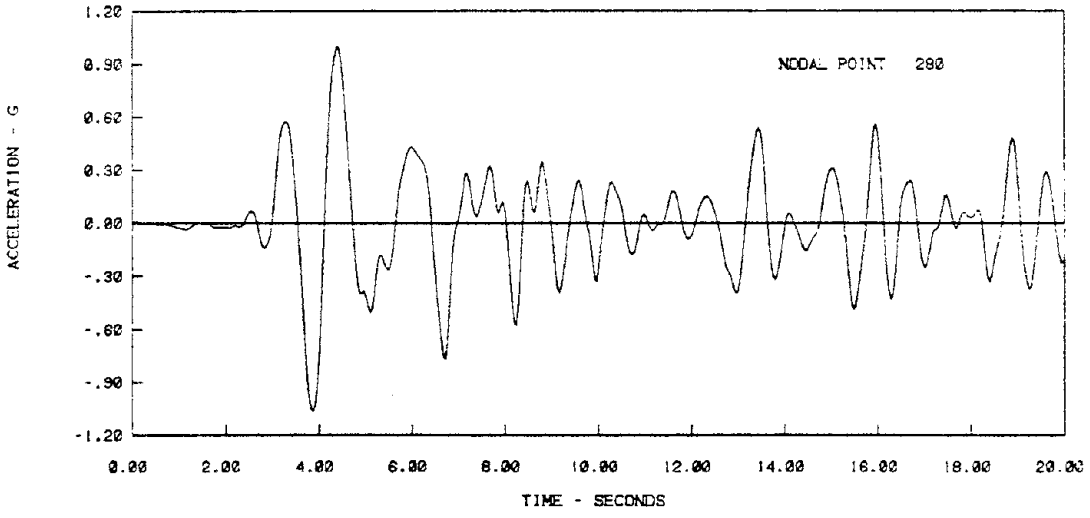

(b) Three-dimensional analysis

Fig. 5-23 Crest Acceleration Time Histories Computed from Analyses of Oroville Dam for the Reanalysis Earthquake.

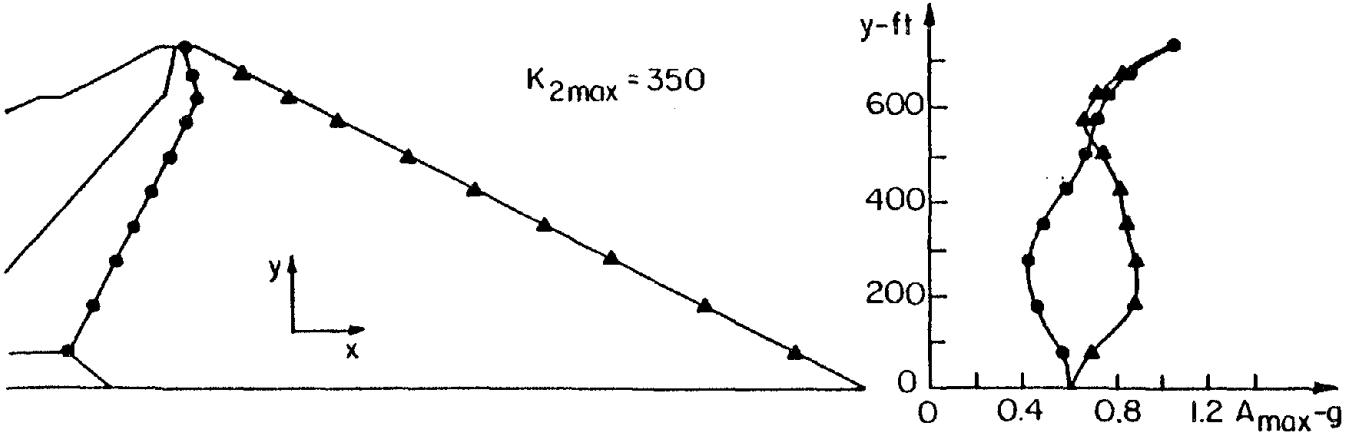

Fig. 5-24 Peak Horizontal Accelerations Computed from 2-D Analysis of Maximum Section for the Reanalysis Earthquake (K_{2max}=350).

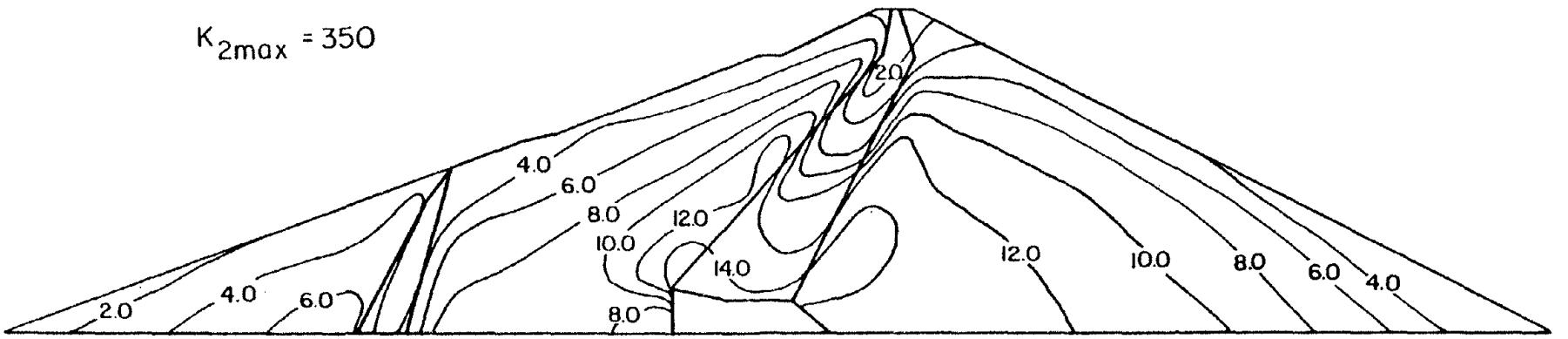

Fig. 5-25a Distribution of Peak Shear Stress τ_{xy} in Tsf Computed from 2-D Analysis of Maximum Section for the Reanalysis Earthquake.

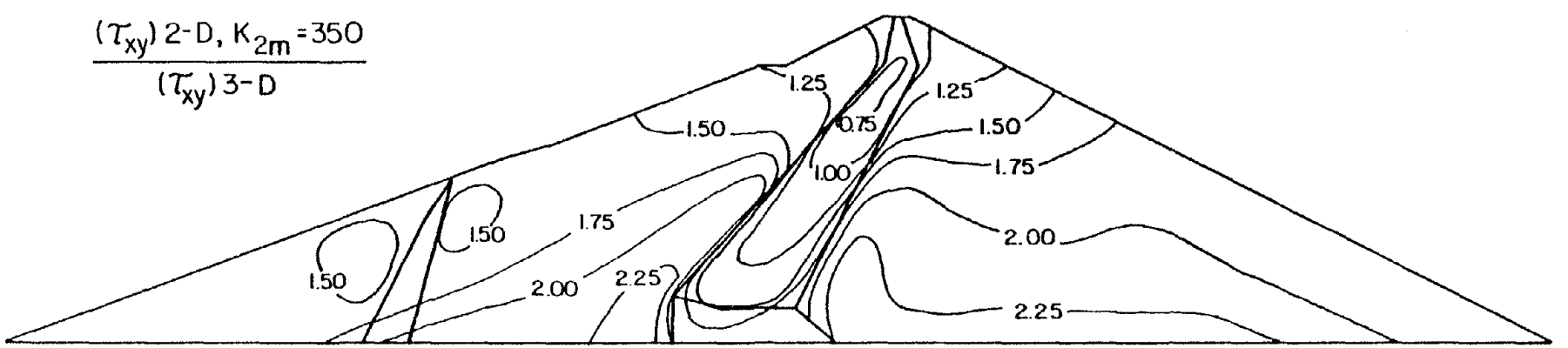

Fig. 5-25b Distribution of the Ratio τ_{xy2D}/τ_{xy3D} Computed for the Maximum Section of Oroville Dam - Reanalysis Earthquake.

τ_{xy2D}/τ_{xy3D}. Fig. 5-25(b) shows the contours of equal values of this ratio for the main section of the dam. It can be seen that except for small zones adjacent to the core and near the base of the section, values of this ratio are lower than 2.0 throughout the maximum section. They decrease from a value of 2.25 in a zone near the base and adjacent to the core block to a value of 1.25 in the upper fourth of the section. In large portions of the upstream shell an average value of 1.5 prevails. Values of about 1.0 are obtained in the core due to the fact that the same G/S_u ratio was used in both the 2-D and 3-D analyses of the dam.

In view of the above results it can be concluded that the assumptions on which the proposed approximate method to take 3-D behavior into account is based, are not entirely valid. The nature of the 3-D mode shapes of vibration of the dam is completely different than that of the mode shapes for the 2-D model of the dam. In particular, the 2-D model cannot simulate the constraining effects of the vertex of the canyon. Additionally, a significant contribution of the higher modes of vibration and some non-linear effects seem to exist.

5.4. Conclusions

An attempt to show the effects of three-dimensional behavior on the dynamic response of earth dams, to establish criteria for the use of two-dimensional or three-dimensional analysis to compute the dynamic response of earth dams, and to evaluate the capability of two-dimensional analysis procedures to predict the three-dimensional response of earth dams has been made.

It was found that a plane strain analysis of the maximum section of Oroville Dam gave values for the shear stresses that were within 20% of those computed from a three-dimensional analysis of the dam. Slight effects of canyon geometry were observed, particularly near the vertex of the canyon. Accelerations were found to be more sensitive to the boundary conditions and therefore less accurately computed from a two-dimensional analysis than stresses. Similar conclusions were made in regard to the plane strain analysis of the quarter section of the dam.

For dams in steeper canyons than that of Oroville Dam the results seem to indicate that plane strain analyses of the maximum section and the quarter section of the dam cannot simulate correctly the behavior of the embankment.

In all cases the effects of the nature of the input motions were found to be considerably smaller than the effects of canyon geometry.

Finally, it was found that a plane strain analysis with modified shear moduli did not approximate the dynamic response of a three-dimensional earth dam any better than a conventional two-dimensional analysis.

CHAPTER 6

MESH SIZE REQUIREMENTS FOR THREE DIMENSIONAL ANALYSIS

6.1 Introduction

The use of the finite element method for the dynamic response analysis of an earth dam requires the discretization of the structure by subdivision into a particular number of elements of finite size. This representation of a continuous system with a finite number of degrees of freedom introduces some approximation in the computed response. The accuracy of the solution depends on the number and the type of degrees of freedom selected to represent the structure, and in general it increases as the degree of discretization becomes finer. However, the computational and engineering efforts required to carry out the analysis also increase as the number of degrees of freedom used to represent the structure increases. Therefore, the selection of the finite element model to be used in the dynamic response analysis of an embankment requires a trade-off between the degree of accuracy obtained in the solution and the cost of the analysis. Accordingly it is desirable to investigate the degree of discretization required to achieve an acceptable level of accuracy.

Elaborate mathematical analyses have been carried out to determine the order of convergence and error bounds applicable to the finite element analysis of a variety of problems (Johnson and McLay, 1968; Strang and Fix, 1973). The order of convergence of the finite element method depends on the type of function used for interpolation of the solution. For plane static elasticity problems, where linear interpolation is used

on the displacement field, the order of convergence is proportional to the square of the element size (Zienkiewicz, 1977). However, in the case of the dynamic analysis of earth dams, mathematical determination of the accuracy of a solution would be extremely difficult.

Two criteria are usually used to determine an appropriate mesh size for the 2-D dynamic finite element analysis of soil structures. The first criterion requires that the element size be sufficiently small that a good approximation of the predominant mode shapes of vibration of the system can be obtained. The second criterion requires that the element size should not be larger than a certain fraction (generally 1/5) of the shortest wavelengths to be transmitted through the finite element mesh (Lysmer, 1974). In the case of the 3-D analysis of earth dams the same criteria should be applicable to the determination of a suitable element size in the direction of the dam axis. However, few 3-D analyses of earth dams have been carried out and little is known about the predominant mode shapes of vibration of three-dimensional earth dams or the cut-off frequencies to be used in their analysis.

The purpose of this chapter is to present the results of 3-D analyses of the Oroville Dam and the dam with valley wall slopes of 1:1 for the Oroville Dam Reanalysis earthquake using a finite element mesh with fewer elements in the direction of the dam axis than the mesh used for the analyses described in Chapter 4. Comparison of the results presented in this chapter with those presented in Chapter 4 will enable conclusions to be drawn concerning: a) the accuracy of the results obtained with the two finite element meshes and b) the appropriate number of elements to use in the direction of the dam axis in order to

obtain a good representation of the predominant modes of vibration of the structure.

6.2 Finite Element Model

The most straightfoward method of determining the accuracy of the results obtained from the dynamic response analysis of an earth dam using a particular finite element model is to compare these results with those obtained from a similar analysis using a finite element model with a different degree of discretization. This comparison will also serve to define the criterion for selecting the degree of discretization of a model in order to obtain a particular level of accuracy in the computed response of a structure. In the case of earth dams it will help to illustrate the level of refinement needed in a finite element model in order to correctly represent the vibration characteristics of an embankment.

The above mentioned approach was used to evaluate the accuracy of the results, presented in Chapter 4, obtained from the three-dimensional analyses of Oroville Dam and the dam with valley wall slopes of 1:1. The finite element model used in these computations was shown in Fig. 3-12 and from now on it will be referred to as the refined model. By evaluating the accuracy of the results obtained with this model it was possible to determine whether the finite element discretization used in the direction of the longitudinal axis was appropriate for the correct representation of the natural transverse modes of vibration of the embankments.

The three-dimensional dynamic analysis of the Oroville Dam and the dam with valley wall slopes of 1:1 for the Reanalysis earthquake was repeated using the finite element model shown in Fig. 6-1 which from now on will be referred to as the coarse model. Since the geometries of these two dams differ only on the slopes of the canyon walls, their corresponding models differ only in the element size in the cross-valley direction.

Except for the number of elements in the direction of the longitudinal axis of the dam the coarse model shown in Fig. 6-1 is the same as the refined model shown in Fig. 3-12. Thus, only the degree of discretization in the cross-valley direction has been changed and therefore, only the effects of varying the element size in this direction on the accuracy of the results can be studied. However, the degree of discretization in the other two directions (x and y), that is the mesh size in the plane of the transverse sections of the dams, has been chosen so that an appropriate representation of the cross sections of the predominant modes of vibration of the structures is obtained. Therefore, the degree of discretization in these directions is adequate for obtaining a degree of accuracy satisfactory for engineering purposes.

The material properties, static stress distribution and other characteristics of the analyses presented herein are the same as those for the analyses presented in Chapter 4.

Comparison between the results obtained with the two finite element models of the Oroville Dam and the dam with valley wall slopes of 1:1 will be done in terms of horizontal accelerations and shear stresses on horizontal planes in the upstream-downstream direction. The comparison

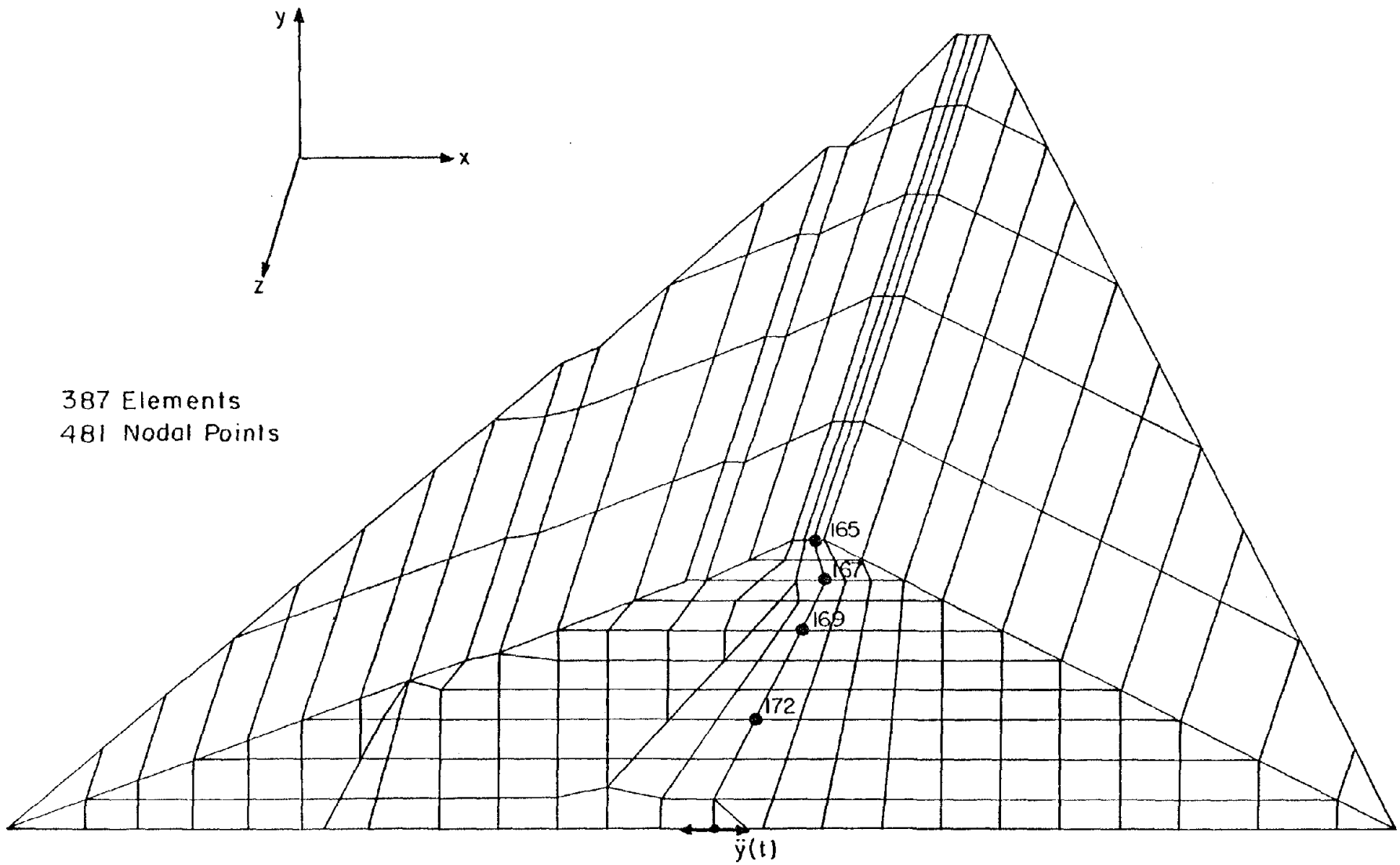

Fig. 6-1 Coarse Finite Element Model for Three Dimensional Analysis.

between accelerations at analogous points in the two models is straightforward. On the other hand, since the stresses are computed at the centroid points of the elements they are not available at the same points for the two models. Fortunately, as can be seen from a comparison between Figs. 6-1 and 3-12, the points at which shear stresses will be computed lie on planes of the models that are sufficiently close to each other, to permit a direct comparison between stress values to be made.

6.3 Analysis of Oroville Dam for the Reanalysis Earthquake

The results from the analysis of Oroville Dam for the Reanalysis earthquake using the coarse model shown in Fig. 6-1, are presented in this section and are compared with those obtained from a similar analysis using the refined model shown in Fig. 3-12.

The computed acceleration amplification function at the crest midpoint of the dam is shown with a continuous trace in Fig. 6-2. It can be seen that for the level of strain induced by the Reanalysis earthquake a predominant frequency of 0.71 Hz is obtained with the coarse model of the dam. This frequency corresponds to a natural period of vibration of 1.41 seconds. Also shown in the same figure with a dashed line is the amplification function at the same point computed with the refined model of the dam. Agreement between the two curves is very good. Both models of the dam give the exact same fundamental natural period of the dam. Since the level of strain induced by the input motions in the two analyses is approximately the same, this agreement indicates that the two models give a good representation of the first mode of vibration of the dam and that the accuracy of the computed

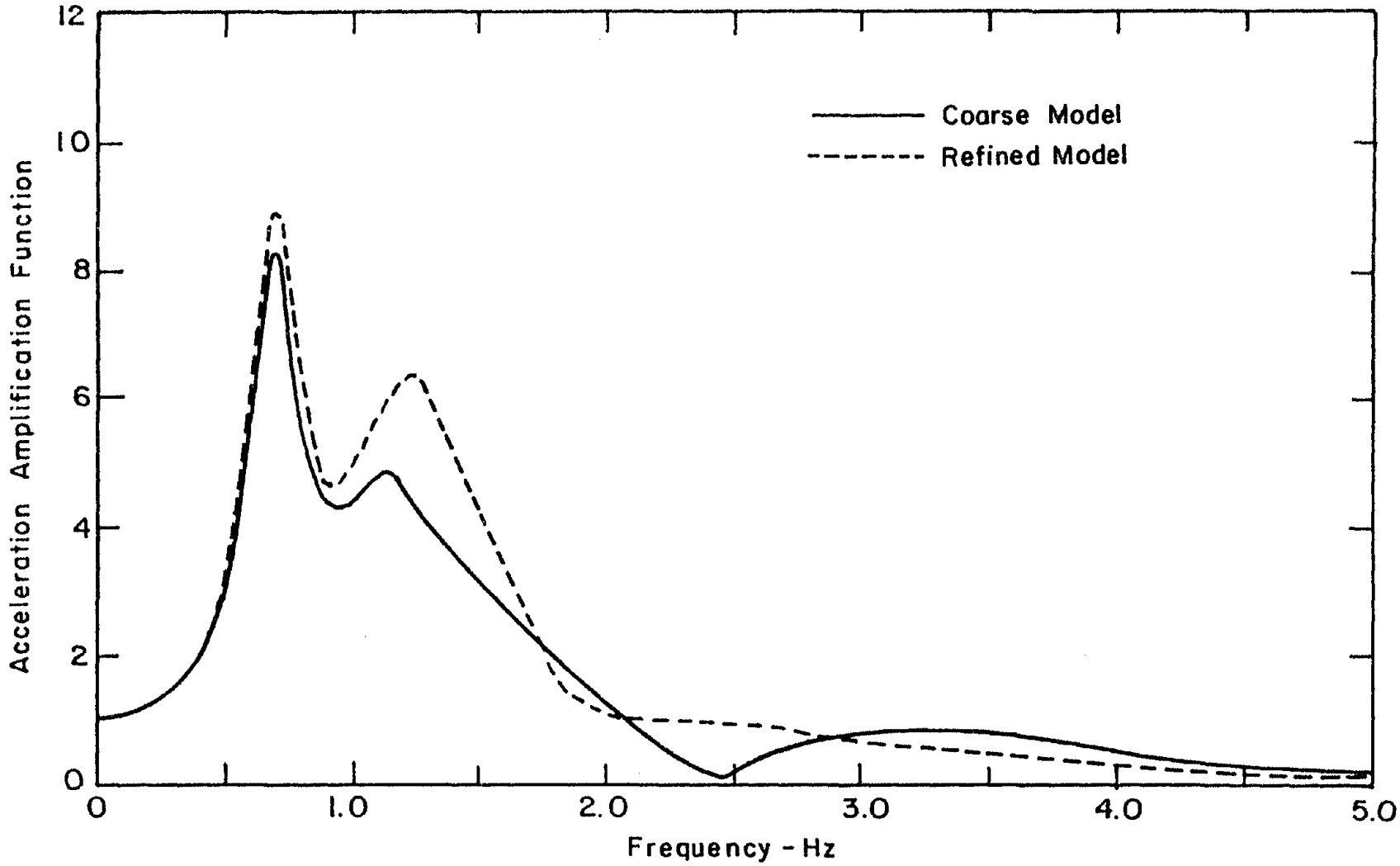

Fig. 6-2 Acceleration Amplification Function for Crest Midpoint of Oroville Dam.

period is excellent. A lower degree of agreement is observed at the higher frequencies indicating a lower capability of the coarse model to fit the higher mode shapes of vibration of the dam. However, the discrepancies are moderate and will not have a large influence on the results since the contribution of these modes to the response of the dam is small. That this is so, can be verified from a comparison between other response parameters like accelerations and stresses.

Fig. 6-3 shows the time histories of horizontal acceleration computed at the nodal points shown in Fig. 6-1 which correspond to the same nodal points of the refined model of the dam for which time histories were computed in Chapter 4 (see Fig. 4-4). The progressive amplification of low frequency motions and filtering of high frequency motions with increasing elevation, previously observed in Fig. 4-5, is again observed in this case. A better comparison between acceleration time histories at the crest midpoint of the two models is shown in Fig. 6-4. The good agreement between these two time histories is noteworthy and corroborates the fact previously stated about the relative contribution of the different mode shapes of vibration of the dam. The coarse model of the dam yields a peak acceleration at the crest 9.5% lower than that computed with the refined model of the dam.

The variations of peak horizontal accelerations along the contact between the core and the downstream shell, along the downstream slope and along the crest of the dam, computed using the coarse model shown in Fig. 6-1 are shown in Fig. 6-5. Good agreement is observed between these profiles of peak accelerations and the profiles shown in Fig. 4-7 except for those corresponding to the crest. Along the crest of the dam

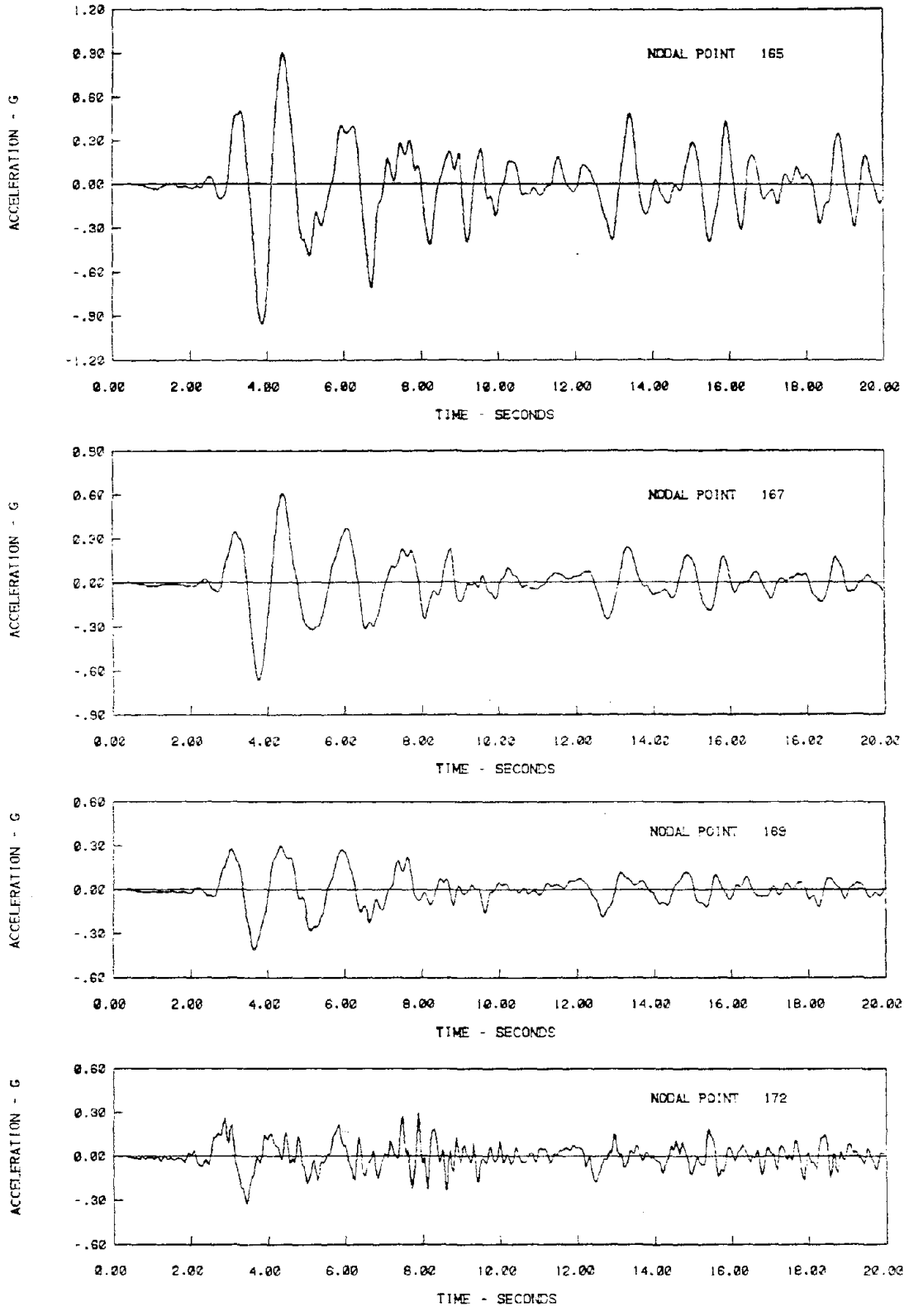

Fig. 6-3 Acceleration Time Histories for Points Along Core-shell Contact of Oroville Dam (Coarse Model).

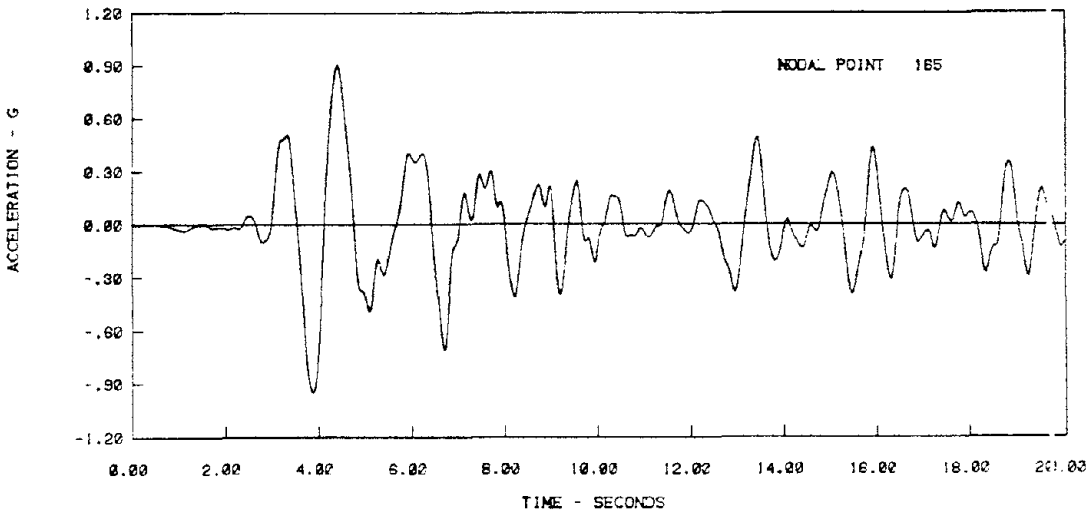

(a) Coarse model

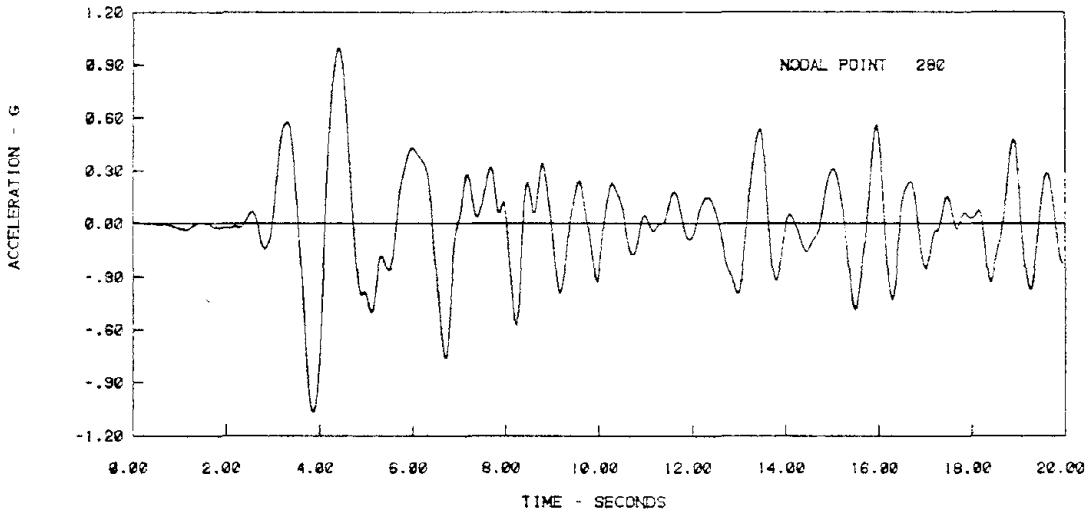

(b) Refined model

Fig. 6-4 Crest Acceleration Time Histories Computed from 3-D Analyses of Oroville Dam for the Reanalysis Earthquake.

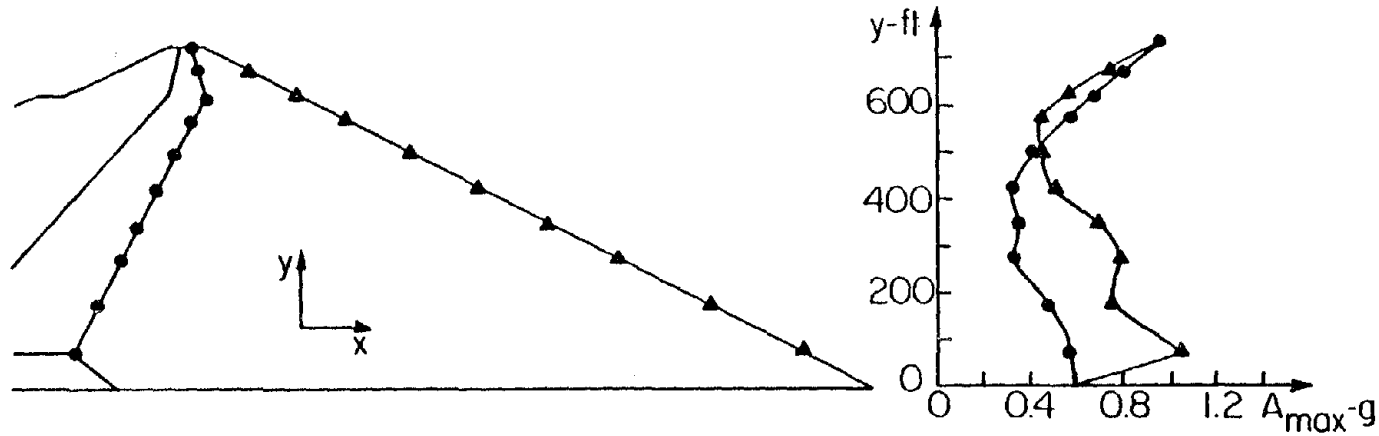

(a) Profiles along core-shell contact and along downstream slope

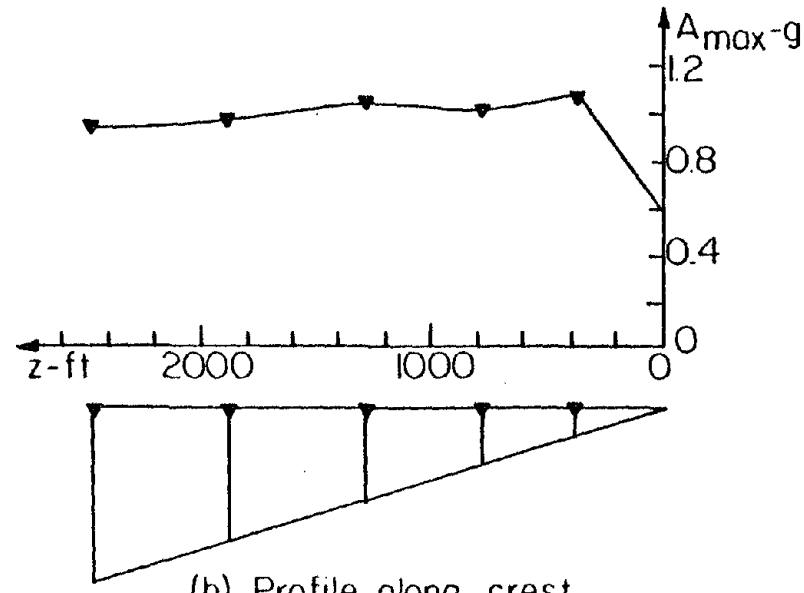

(b) Profile along crest

Fig. 6-5 Peak Horizontal Accelerations Computed From 3-D Analysis of Oroville Dam for the Reanalysis Earthquake (Coarse Model).

the coarse model does not give a distribution of peak accelerations that matches the sharp variations observed in the peak accelerations computed with the refined model of the dam. However, on the average the degree of agreement is good. Along the core-shell contact and along the downstream slope of the dam, the coarse model of the dam predicts peak accelerations within 10% of those computed with the fine mesh of the dam.

The distribution of peak shear stresses on horizontal planes computed with the coarse model of the dam is shown in Fig. 6-6. This distribution of peak τ_{xy} stresses is generally similar to that computed with the refined model of the dam (see Fig. 4-11). In order to facilitate the comparison between the stresses computed from these two analyses, the ratio between the peak horizontal shear stresses obtained with the coarse mesh and the peak horizontal shear stresses obtained with the fine mesh, τ_{xyCM}/τ_{xyFM}, has been computed for four sections of the dam. Contours of equal values of this ratio are shown in Fig. 6-7 from which it can be seen that the τ_{xy} stresses computed with the coarse model are within 10% of those computed with the refined model of the dam.

On the basis of the preceding results it can be concluded that for the strong shaking induced by the Reanalysis earthquake, the model of Oroville Dam shown in Fig. 6-1 yields parameters of response that are within 10% of those computed with the model shown in Fig. 3-12. Thus, the former model is able to appropriately represent the modes of vibration of the dam predominant during strong shaking and can be satisfactorily used to computed the response of the dam in these cases.

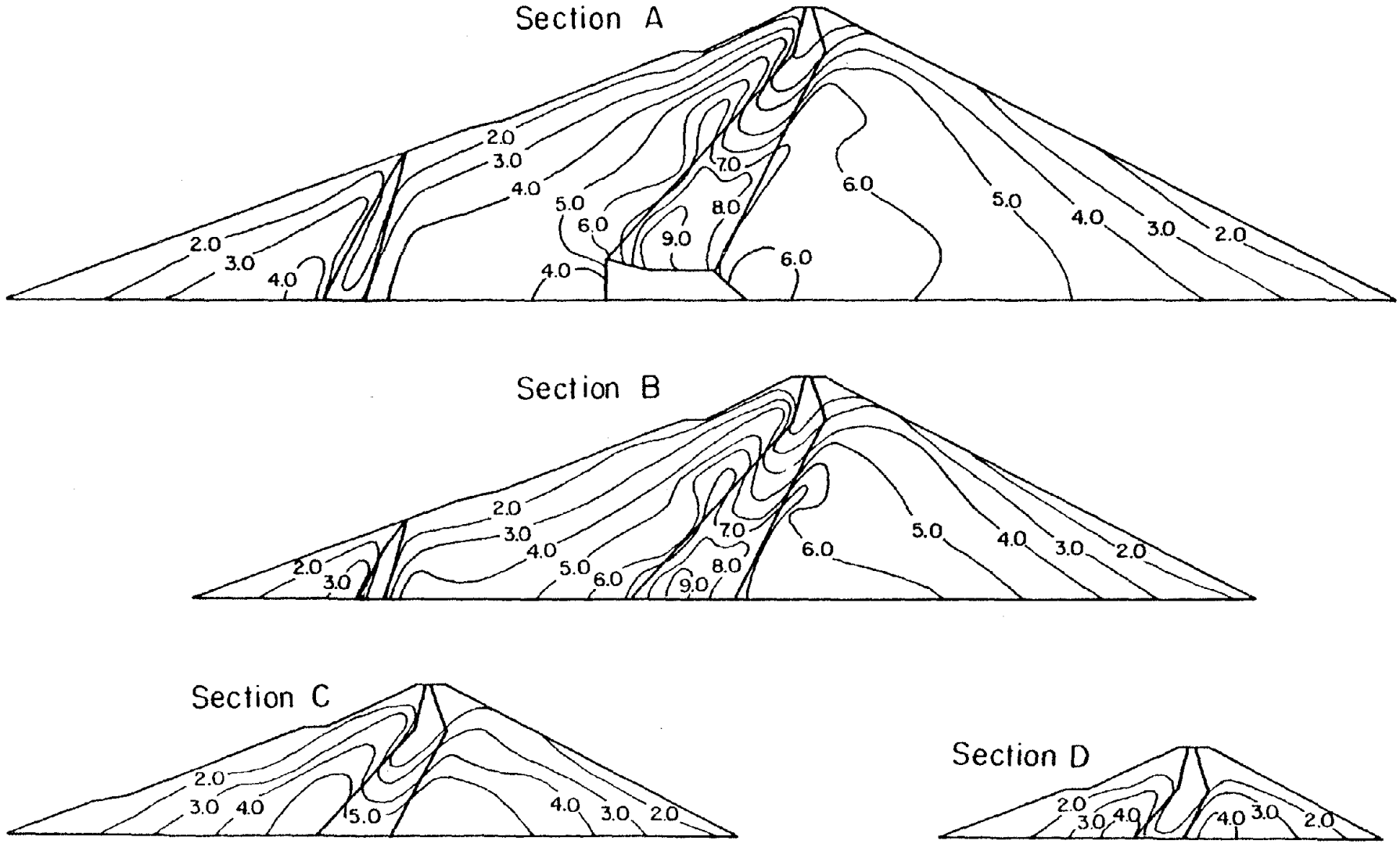

Fig. 6-6 Distribution of Peak Shear Stress τ_{xy} in Tsf Computed from 3-D Analysis (Coarse Model) of Oroville Dam for the Reanalysis Earthquake.

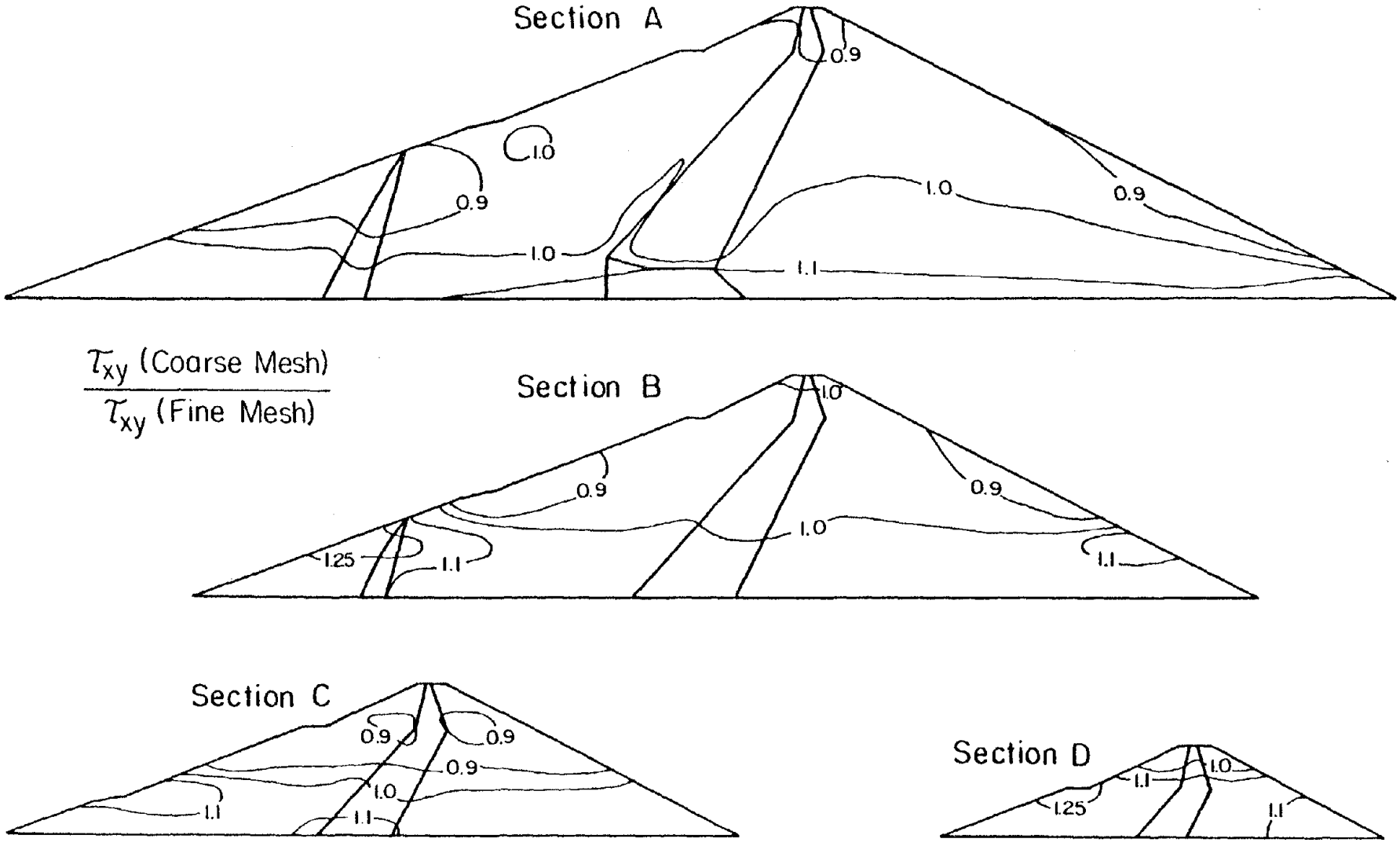

Fig. 6-7 Distribution of the Ratio τ_{xyCM}/τ_{xyFM} Computed for Oroville Dam - Reanalysis Earthquake.

Additionally it can be concluded that the accuracy of the results obtained with the refined model of the dam is very good.

6.4 Analysis of Dam With Valley Wall Slopes of 1:1 for the Reanalysis Earthquake

The results from the dynamic analysis of the dam with valley wall slopes of 1:1 for the Reanalysis earthquake using the coarse model shown in Fig. 6-1, and a comparison of these results with the results obtained using the refined model of the dam will be presented in this section.

The acceleration amplification function at the crest midpoint of the dam computed from the analysis with the coarse mesh of the dam is shown with a solid line in Fig. 6.8. Also shown in this figure with a dashed line is the amplification function for the same point computed with the fine mesh of the dam. It is apparent that the degree of agreement between the two curves is quite good. The fundamental natural frequency computed with the coarse model of the dam is about 0.90 Hz which corresponds to natural a period of vibration of 1.10 seconds. This value is slightly higher (2%) than the value computed with the refined model of the dam (1.08 seconds). The degree of agreement between the peak amplitudes of the amplification functions is also very good (2.5% difference). As in the case of Oroville Dam a moderate discrepancy between the two curves is observed at higher frequencies. However, the effects of those differences on the computed parameters of response are very small as will be shown by the subsequent comparisons between accelerations and stresses.

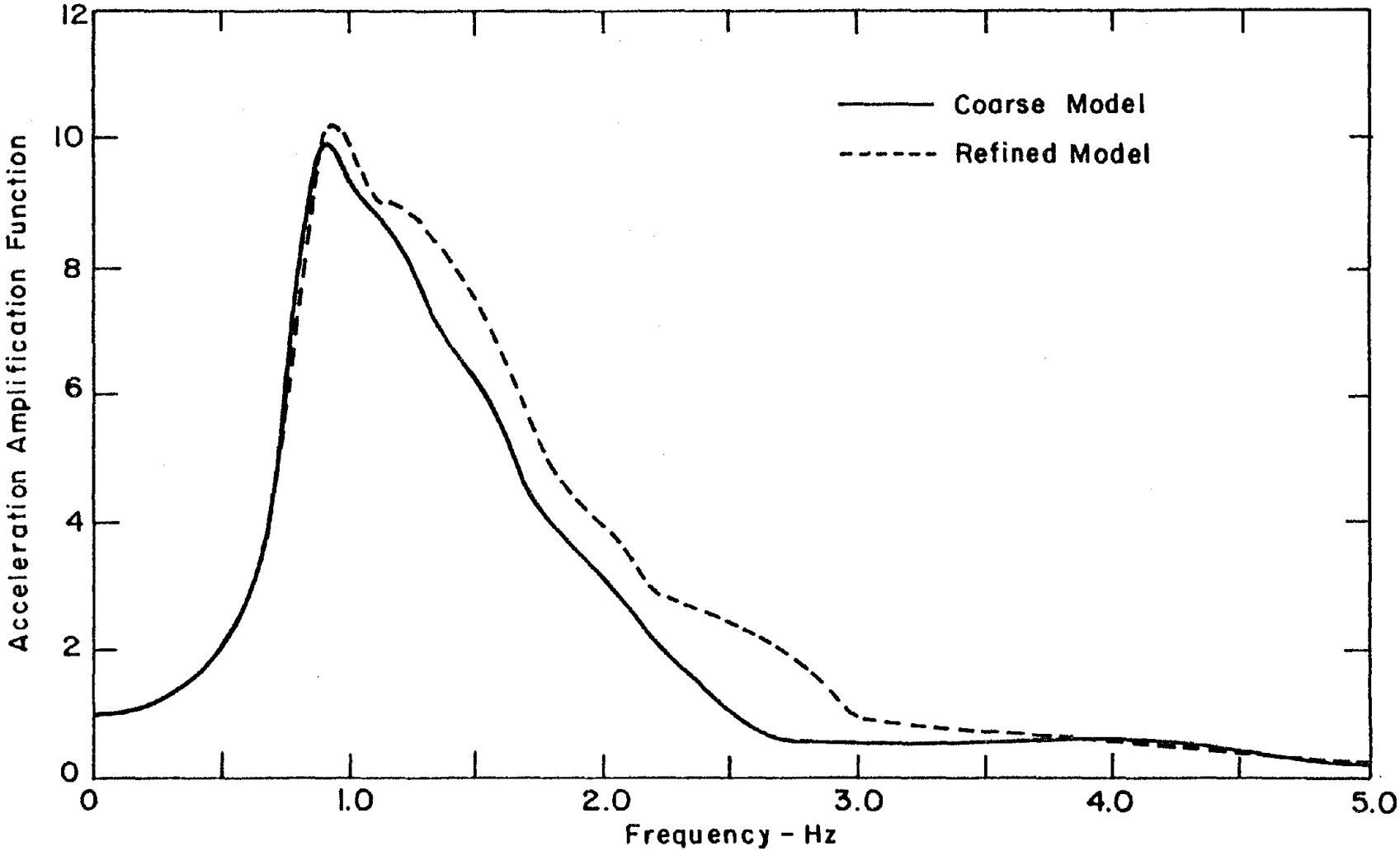

Fig. 6-8 Acceleration Amplification Function for Crest Midpoint of Dam with Valley Slopes of 1:1.

Acceleration time histories were computed for the nodal points along the contact between the core and the downstream shell shown in Fig. 6-1. These time histories are shown in Fig. 6-9. Very high accelerations at the crest of the dam are observed. A comparison with Fig. 4-17 indicates very good agreement between time histories of acceleration computed with the two models of the dam. A specific example of this comparison is shown in Fig. 6-10. The top part of this figure shows the crest acceleration time history computed with the coarse model of the dam and the bottom part shows the time history computed with the refined model of the dam. The agreement between the two curves in noteworthy.

The variation of peak horizontal acceleration, computed with the coarse model, along the contact between the core and the downstream shell, along the downstream slope and along the crest of the dam, is shown in Fig. 6-11. The peak acceleration computed with the coarse model at the crest of the dam was 1.36 g, a value which is 2% lower than that computed with the refined model of the dam. In fact, comparison of the profiles shown in Fig. 6-11 with those shown in Fig. 4-18 indicates that the peak accelerations computed with the coarse model at several points of the dam are in very good agreement with those computed with the refined model of the dam. Thus, it can be concluded that a finite element model with the degree of discretization corresponding to the model of Fig. 6-1 can be used to compute the acceleration response of three-dimensional dams with a sufficient degree of accuracy for practical purposes.

The distribution of peak horizontal shear stresses, τ_{xy}, at 4

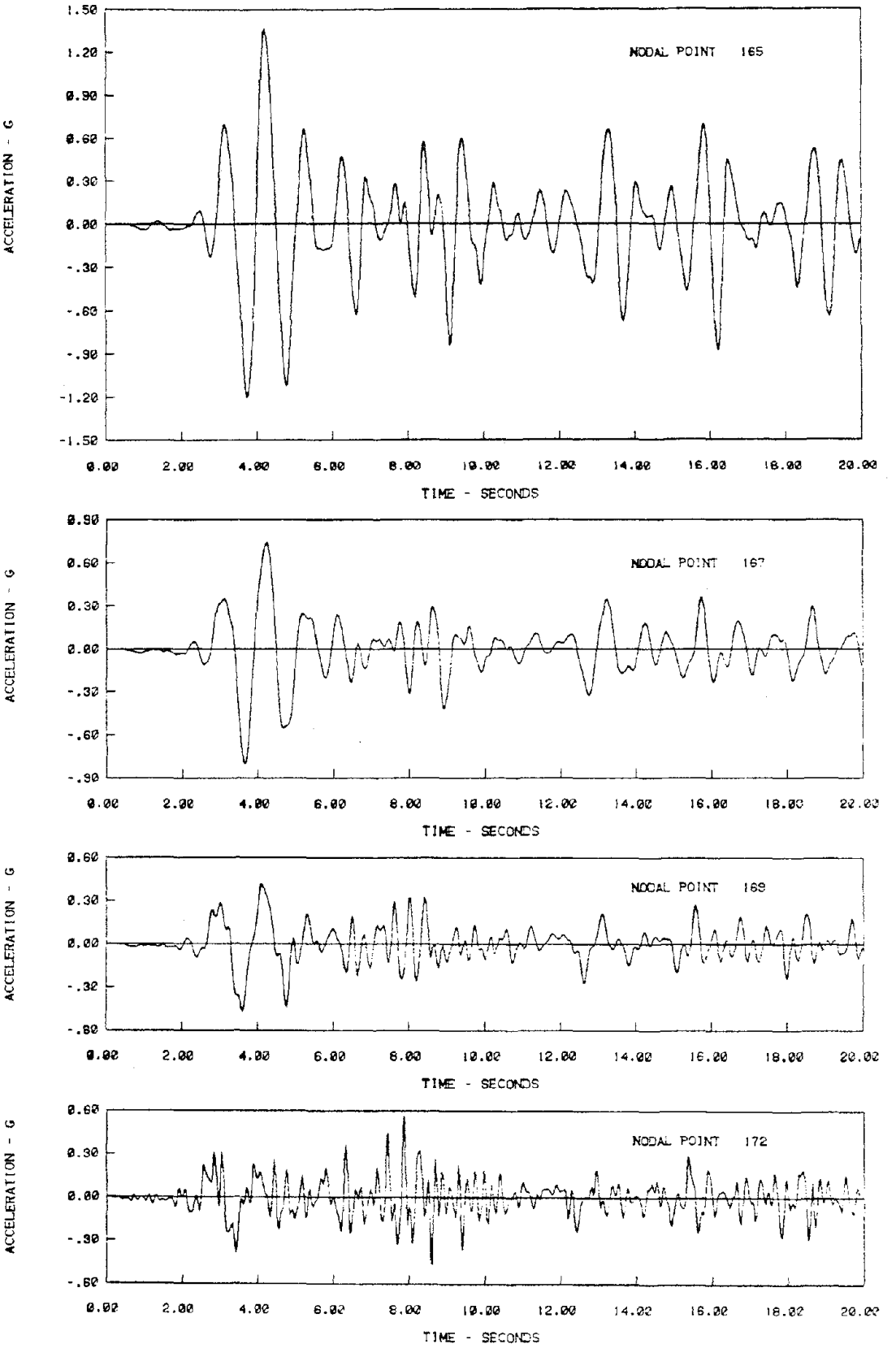

Fig. 6-9 Acceleration Time Histories for Points Along Core-shell Contact of Dam with Valley Wall Slopes of 1:1 (Coarse Model).

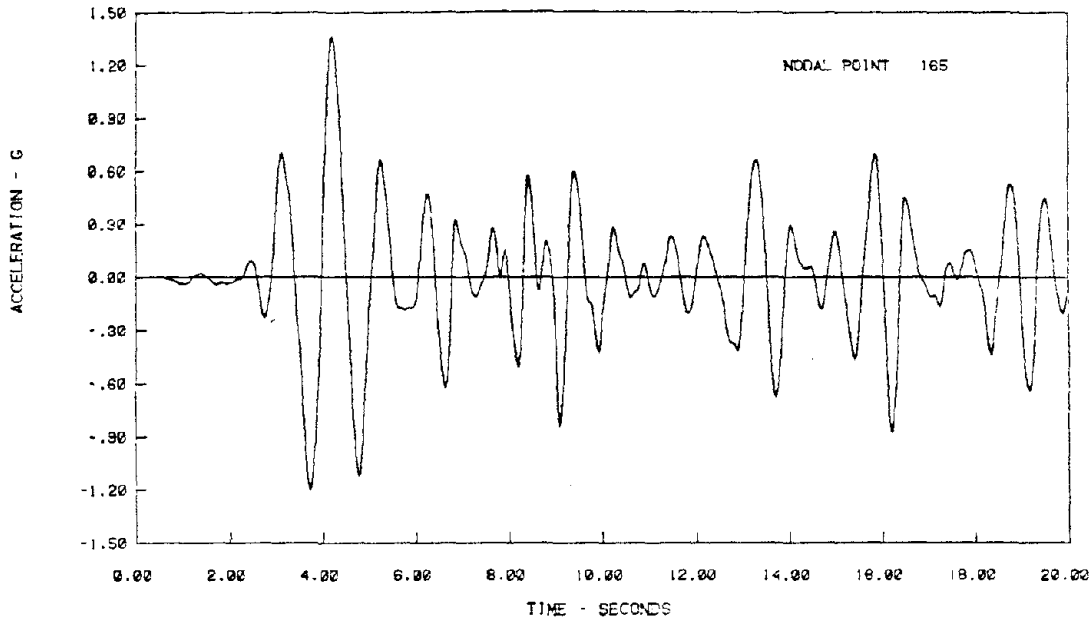

(a) Coarse model

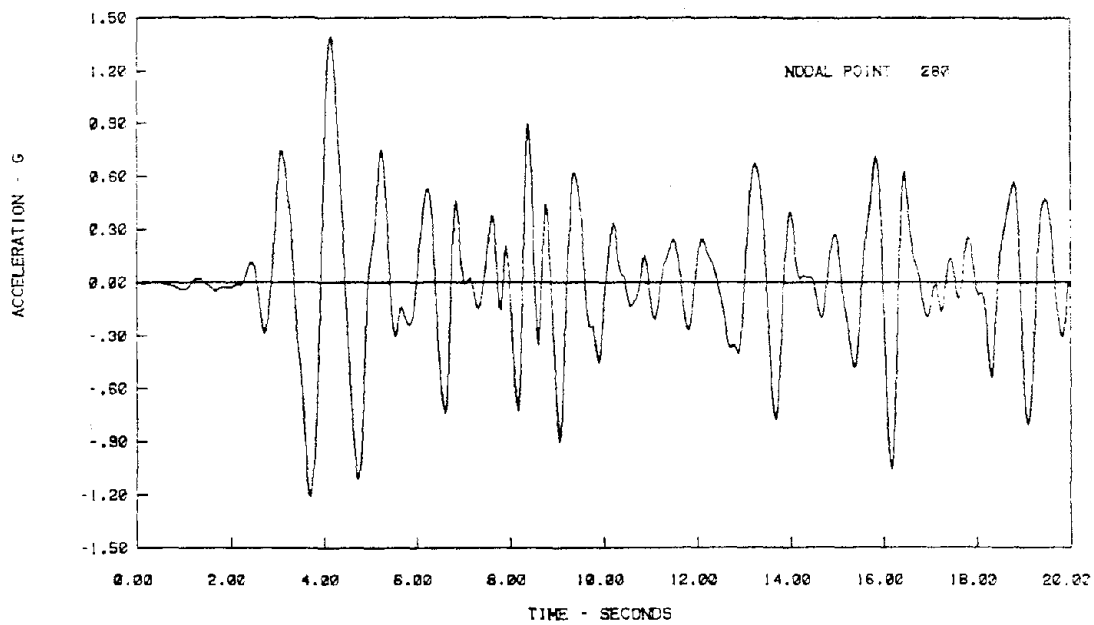

(b) Refined model

Fig. 6-10 Crest Acceleration Time Histories computed from 3-D Analyses of Dam with Valley Wall Slopes of 1:1 for the Reanalysis Earthquake.

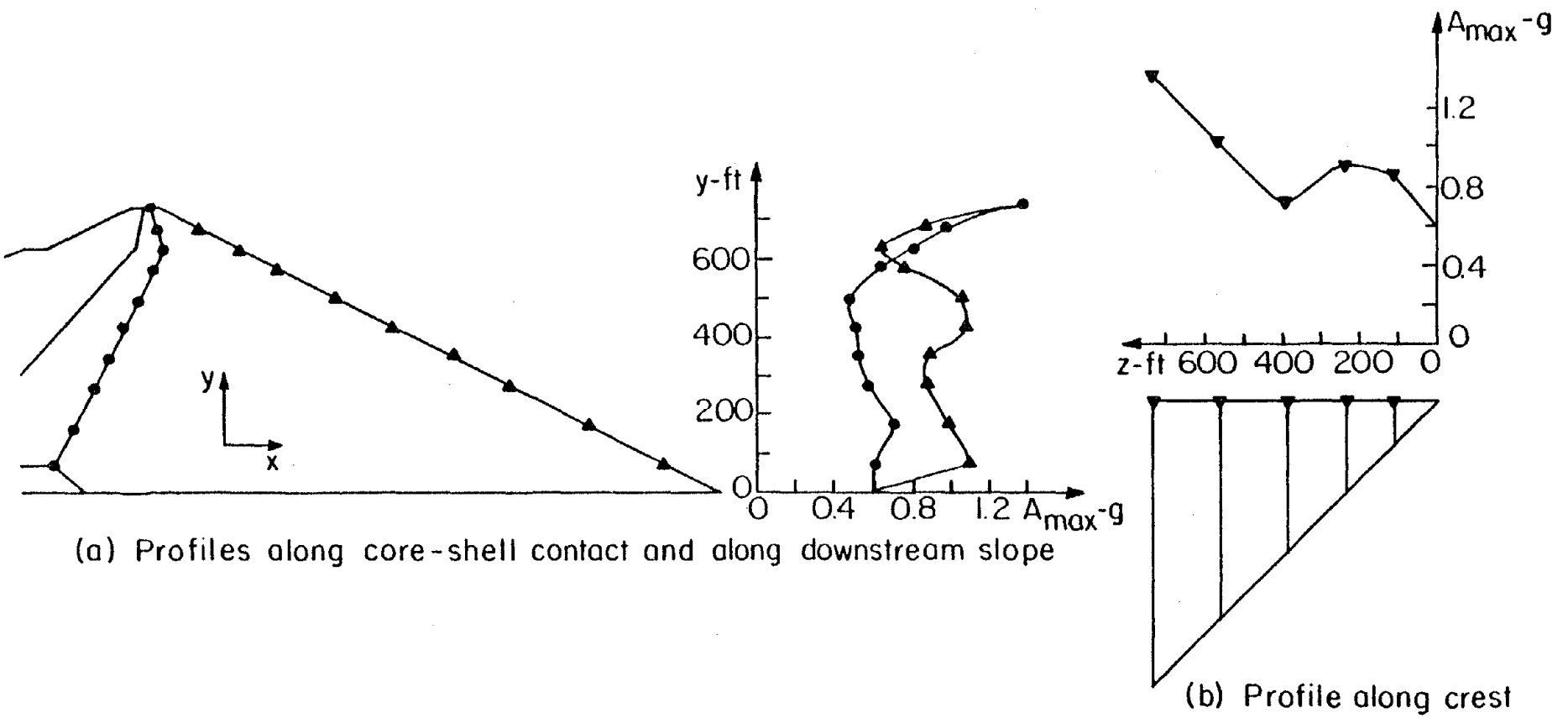

Fig. 6-11 Peak Horizontal Accelerations computed from 3-D Analysis of Dam with Valley Wall Slopes of 1:1 for the Reanalysis Earthquake (Coarse Model).

sections of the dam computed using the coarse model of Fig. 6-1 is shown in Fig. 6-12. The contours shown in this figure reflect the strong influence of the canyon geometry on the dynamic behavior of the dam and are similar to those shown in Fig. 4-19. The ratio between the horizontal shear stresses computed with the coarse mesh and those computed with the fine mesh of the dam, τ_{xyCM}/τ_{xyFM}, has been computed for points on the four sections previously shown. Contours of equal values of this ratio are shown in Fig. 6-13 from which it can be seen that this ratio varies, throughout most of the dam, between values of 0.9 and 1.1. That is, the stresses computed with the coarse model shown in Fig. 6-1 are within 10% of the stresses computed with the refined model of the dam shown in Fig. 3-12.

On the basis of the results previously shown in this section, it can be concluded that the accuracy of the response parameters obtained from the dynamic analysis of the dam with valley wall slopes of 1:1 for the Reanalysis earthquake using the refined model of the dam is excellent. Additionally, it can be concluded that the finite element model shown in Fig. 6-1 can be used to compute the dynamic response of dams in steep canyons subjected to strong shaking with a degree of accuracy satisfactory for engineering purposes.

6.5 Conclusions

A qualitative evaluation of the degree of accuracy of the response computed from the three-dimensional analyses of the Oroville Dam and the dam with valley wall slopes of 1:1 has been presented. Additionally, an attempt to empirically determine the degree of discretization necessary

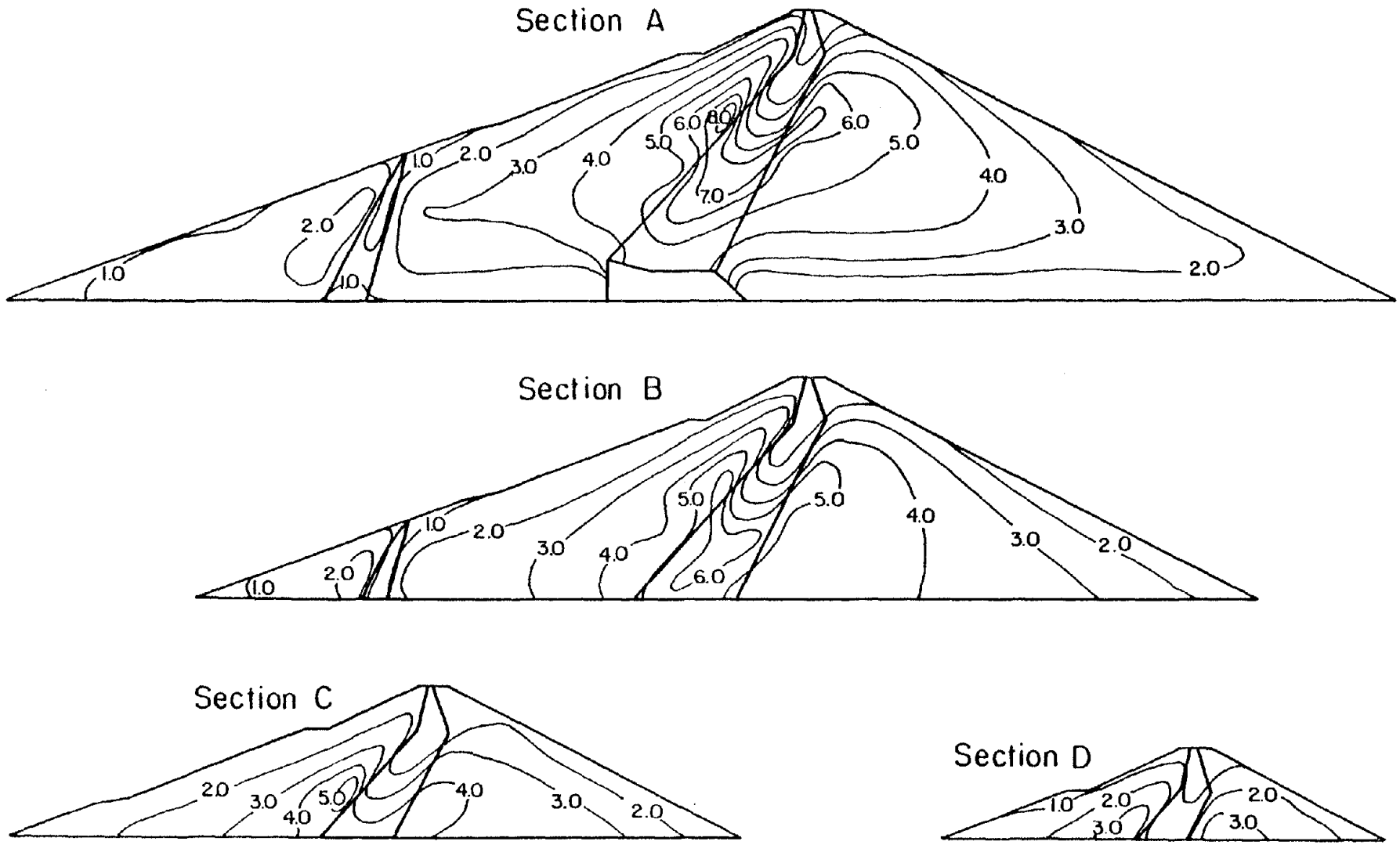

Fig. 6-12 Distribution of Peak Shear Stress τ_{xy} in Tsf computed from 3-D Analysis (Coarse Model) of Dam with Valley Wall Slopes of 1:1 for the Reanalysis Earthquake.

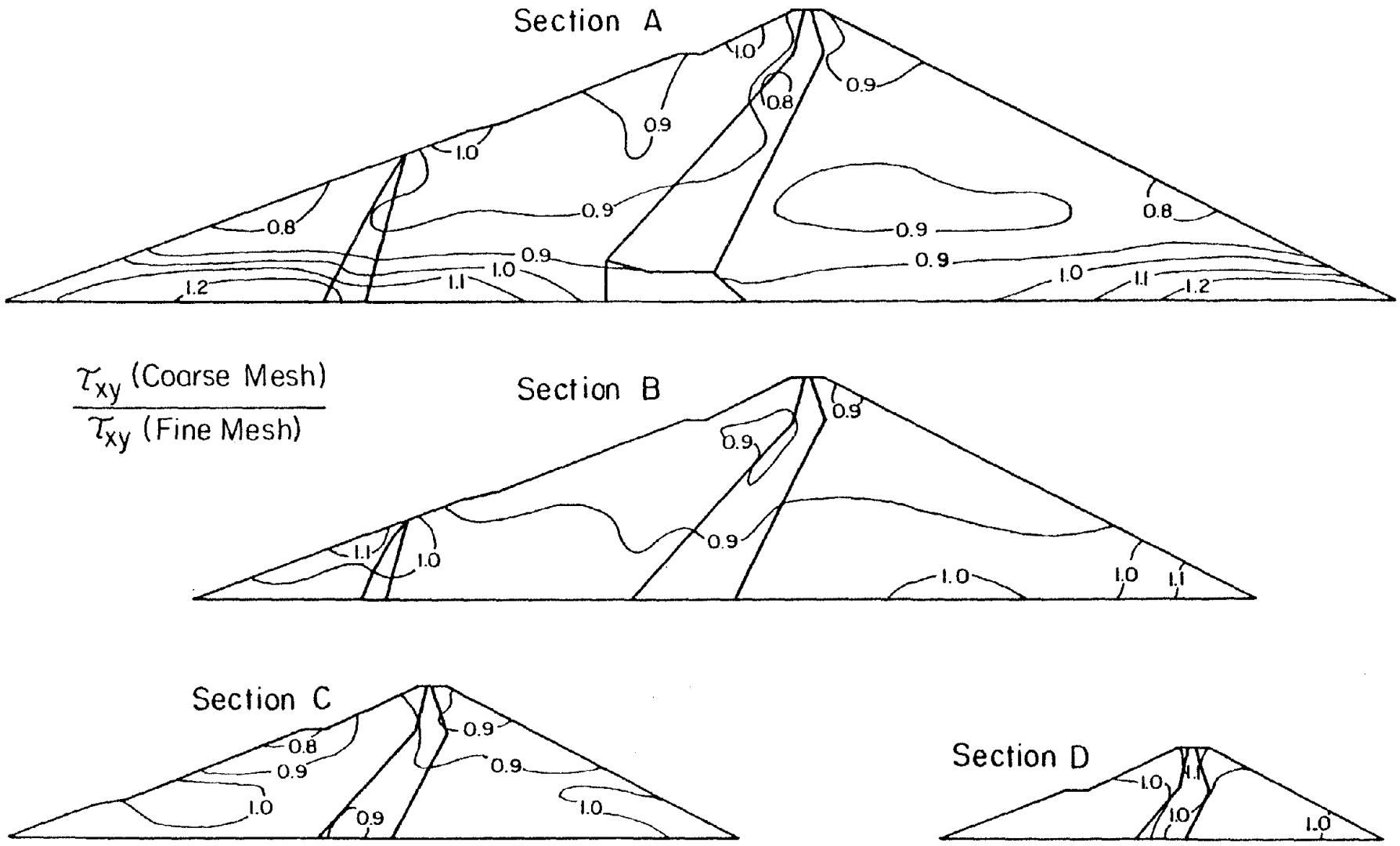

Fig. 6-13 Distribution of the Ratio τ_{xyCM}/τ_{xyFM} Computed for Dam with Valley Wall Slopes of 1:1 - Reanalysis Earthquake.

in a 3-D finite element model to obtain the dynamic response of earth dams with a satisfactory degree of accuracy for engineering purposes has been made. Specifically, the degree of discretization in the cross-valley direction has been studied.

The three-dimensional dynamic analyses of the Oroville dam and the dam with valley wall slopes of 1:1 for the Reanalysis earthquake were repeated using a finite element mesh with fewer elements in the cross-valley direction than the mesh used for the analyses presented in Chapter 4. Comparisons between the results of these four analyses were also included.

On the basis of the results presented and the comparisons made, it can be concluded that a model with the degree of discretization of that used in the analyses is appropriate for the computation of the dynamic response of 3-D dams subjected to strong shaking. It appears therefore that a finite element model with about 10 elements in the cross-valley direction of a dam and an appropriate degree of discretization in the other two directions, is able to represent correctly the modes of vibration predominant during strong shaking of dams in triangular canyons with different geometries and therefore, will yield results with an accuracy satisfactory from an engineering point of view.

In view of the fact that at lower levels of shaking the higher modes of vibration of a dam may play an important role in the response, the above conclusions may not be applicable to dynamic analyses of dams for low amplitude input motions. In the case of the dams previously analyzed in Chapter 4 it was shown that the effects on the response of the nature of the input motions and the influence of the higher modes of

vibration were small. Therefore, in these cases it would appear that the conclusion previously stated in the above paragraph would be applicable.

The small reduction in the degree of accuracy would seem to be acceptable for engineering studies in view of the fact that the cost of the analyses with the coarse finite element model of Fig. 6-1 was only about 16% of that of the analyses with the finer finite element model of Fig. 3-12.

CHAPTER 7

CONCLUSIONS

The most powerful tool presently available for performing a dynamic response analysis of an earth dam is probably the finite element method. Due mainly to limitations of computer storage capacity and to computational costs, only two-dimensional finite element analysis procedures have been used until now for seismic stability analyses of earth dams. Recent developments in computer technology however, have provided the necessary storage and speed requirements to make the three-dimensional analysis of embankment dams feasible.

In the preceding chapters, numerical techniques for the three-dimensional dynamic response analysis of earth and rockfill dams have been developed and an attempt to study the dynamic behavior of embankment dams in three dimensions has been made. Existing two-dimensional finite element programs have been modified and further developed to produce a finite element program suitable for the three-dimensional dynamic response analysis of earth dams. This program has been used to back-calculate the dynamic material properties of Oroville Dam from the recorded response of the dam to the August 1, 1975 Oroville earthquake. An attempt to study the dynamic response characteristics of earth dams which exhibit considerable three-dimensional behavior and to evaluate the applicability of two-dimensional analyses to the computation of the dynamic response of such structures, has been made. Additionally, the effects that the degree of discretization in the cross-valley direction has on the computed three-dimensional dynamic response of earth dams, have been studied.

The two-dimensional finite element techniques presented by Lysmer et al., (1974, 1975) which use the concepts of a complex shear modulus, and equivalent linear dynamic material properties and which solve the equations of motion in the frequency domain, were partially extended to three dimensions by Kagawa (1977). During the course of the work presented herein these changes were further improved so that each nodal point in the system would have three degrees of freedom. Additional modifications were made in the element stiffness matrix generating routines, in the equation solver, and a sophisticated interpolation scheme was implemented.

Comparisons between the results of analyses with three degrees of freedom per node and the results of analyses with two degrees of freedom per node (z direction constrained) were made. A 100 feet high linear elastic dam with a shear wave velocity of 500 fps and with varying crest length to height ratio was used in the analyses. A close spacing between natural frequencies of vibration was observed. Differences between the computed natural frequencies from the two types of analyses were on the order of 10% and differences between computed maximum displacements and stresses were as large as 50%. Additionally, the natural mode shapes of vibration for the dam with a crest length to height ratio, L/H, of 3 were computed. It was observed that: a) the abutment ends of the dam do not seem to show appreciable displacements in the lower modes of vibration, b) the displacements in the z direction can be as large as those in the x direction in the lower parts of the dam and c) the variation of displacements in the z direction could be well fitted with 5 or 6 elements. The above results and observations led to the conclusion that the z displacements can not be neglected and have to be

taken into account in the three-dimensional analysis of an earth dam unless a high degree of accuracy is not required.

The three-dimensional finite element techniques developed were used to compute the dynamic response of Oroville Dam to the August 1, 1975 Oroville earthquake. In view of the fact that the dynamic properties for the dam materials were not available these computations served to back-calculate such properties. On the basis of previous experimental studies it was concluded that it was necessary to determine only the value of K_2max for the shell gravels in order to completely define the dynamic behavior of the dam materials. Therefore, three-dimensional dynamic finite element analyses were performed for three different values of K_2max, using appropriate input motions for the August 1, 1975 Oroville earthquake. The results of these computations were compared with the response at the crest of the dam recorded during the same earthquake. Comparisons were made between acceleration time histories and acceleration response spectra of the computed and recorded motions at the crest of the dam. Additionally, the computed natural period of the dam was compared to the value displayed by the recorded free vibrations at the crest. On the basis of these comparisons it was concluded that a K_2max value of 170 is representative of the in-situ dynamic characteristics of the Oroville gravels and therefore, can be used in the dynamic response analysis of the dam to earthquake motions.

In order to study the dynamic response of dams for which three-dimensional behavior is of concern, dynamic analyses in three dimensions of two dams were performed for two earthquake motions. The two dams selected were the Oroville Dam, which has a crest length to height

ratio, L/H, of 7, and a fictitious dam with the same section as Oroville Dam and with a crest length to height ratio, L/H, of 2. The two earthquakes for which these dams were analyzed were the Oroville Dam design earthquake or Reanalysis earthquake and the August 1, 1975 Oroville earthquake.

In the analysis of the two dams to the Reanalysis earthquake, very high accelerations at the crest of the embankments were observed. In all cases, the computed stress time histories exhibited patterns from which it could be concluded that, for practical purposes, a unique number of equivalent cycles could be taken as representative of the time variation of stresses throughout the dam.

Canyon geometry was found to be an important factor affecting the distribution of peak shear stresses within a dam. In the case of Oroville Dam, which is representative of dams with a crest length to height ratio, L/H, of about 7, shear stresses on the horizontal plane in the upstream-downstream direction, τ_{xy}, were found to be the dominant component of the stress tensor. Thus, they were very close in magnitude to the maximum shear stress at each point. Also, they were highest at the maximum section and a moderate reduction in their absolute values was observed near the vertex of the canyon. This effect was found to be very pronounced in the case of a dam with a crest length to height ratio, L/H, of 2. Additionally, shear stresses on the vertical plane in the upstream-downstream direction, of comparable magnitude to the τ_{xy} stresses, were computed. As a consequence, the ratio between peak τ_{xy} stresses and peak maximum shear stresses had values much lower than 1.0 at most points beyond a short distance from the maximum section of the

dam. Peak maximum shear stresses were highest near the quarter section. On the basis of these results it could be concluded that the maximum section of the dam might not be the most critical from a stability point of view and that the τ_{xy} stresses are not necessarily the parameter most indicative of the deformational behavior of the dam materials.

After comparing the results of analyses for the two earthquakes used it was concluded that the nature of the input motions has significant effects on the relative importance of the higher modes of vibration of the dam.

Plane strain analyses of the maximum section and the quarter section of Oroville Dam were performed for the Oroville and Reanalysis earthquakes and the results of these analyses were compared with the dynamic response computed with a three-dimensional model of the dam. Since they are also applicable to the maximum section and quarter section of the dam with valley wall slopes of 1:1, the results of the two-dimensional analyses were also compared with those obtained with a 3-D model of this dam. These comparisons served to evaluate the applicability of two-dimensional analysis to the computation of the dynamic response of three-dimensional structures.

The plane strain analyses of the maximum section and quarter section of Oroville Dam for the Reanalysis earthquake yielded peak accelerations and acceleration time histories which were in excellent agreement with those obtained from the three-dimensional analysis of the dam. The peak shear stresses on horizontal planes, τ_{xy}, computed from the 2-D analyses were within 20% of the peak τ_{xy} stresses computed with the 3-D model. A lower degree of agreement was obtained in the

parameters of response corresponding to the Oroville earthquake due to a greater contribution of the higher modes of vibration.

On the other hand, comparisons of the three-dimensional dynamic response of the dam with valley wall slopes of 1:1 with the results from the two-dimensional analyses showed that these analyses cannot simulate correctly the dynamic behavior of embankments in narrow canyons. No agreement was observed in the computed peak accelerations and acceleration time histories, and the 2-D τ_{xy} stresses were larger than the 3-D τxy stresses by factors as high as 4.0.

On the basis of the above results it can be concluded that the dynamic response of earth dams in triangular canyons with crest length to height ratios, L/H, greater than 7, subjected to strong motions, can be approximated within engineering accuracy with plane strain analyses of some sections of the dams. However, it can also be concluded that two-dimensional analyses are not appropriate for computing the dynamic response of dams in steeper canyons and therefore, these dams need to be analyzed in three-dimensions with the exercise of adequate judgement in the interpretation of the results.

An alternative approach which consists in performing 2-D analysis of the maximum section of a dam using material properties such that the fundamental period of vibration of the three-dimensional model is obtained, was also studied. However, the results obtained by means of this procedure showed a lower degree of agreement with the three-dimensional results than that obtained with the results from conventional two-dimensional analyses. For example, for the Reanalysis earthquake, the computed peak shear stresses, τ_{xy}, were 20% lower on the

average than the peak τ_{xy} stresses obtained from a three-dimensional analysis. On the other hand, the τ_{xy} stresses computed with a plane strain analysis using the "true" material properties, were 5% higher on the average than the 3-D stresses.

In order to study the effects that the degree of discretization in the cross-valley direction has on the computed three-dimensional response of earth dams, the dynamic analyses of Oroville Dam and of the dam with valley wall slopes of 1:1 were repeated using a 3-D model with a smaller number of elements in the direction of the longitudinal axes of the dams. The results of these analyses were compared with those obtained initially with a finer degree of discretization. Very good agreement was observed between the amplification functions and the acceleration time histories at the crest of the dams, computed with the two finite element models. Additionally, the peak accelerations and peak shear stresses computed with the coarse finite element model of the dams were within 10% of those computed with the refined model of the dams. On the basis of these results, it was concluded that a finite element model with about 10 elements in the cross-valley direction of a dam, is appropriate for the computation of its three-dimensional dynamic response with an accuracy satisfactory from an engineering point of view. It was also concluded that the accuracy of the results obtained from the analyses performed with both models of the dams is very good.

The results obtained as well as some of the difficulties encountered during the course of the investigation have served not only to develop an improved understanding of the three-dimensional dynamic response of earth dams but also to point out a few of the needs for

future research. Most of these concern some of the assumptions initially made to develop the methods of analysis. It is evident that there is a need for a more realistic picture of the ground motions affecting a dam during an earthquake than the one implicit in the analytical model used in this work. In this regard it is particularly important to determine the effects on the computed three-dimensional response of a dam of assuming that the walls of the canyon behave as a rigid unit. That is, the effects of the differential motions in the valley walls and of the interaction between the dam and its abutments on the seismic response of the dam. Just as important, and perhaps more, is the need for developing practical constitutive relationships that can adequately simulate the three-dimensional dynamic behavior of soils. It is necessary to determine how to relate soil deformations to a complex stress state that varies with time. The high accelerations obtained in some of the analyses previously described suggest the need to evaluate the stability of the crest of dams under these conditions; that is, dams subjected to strong ground motions that will induce high crest accelerations.

In spite of some of the shortcomings of the method of analysis mentioned above, it is considered that the present study has thrown considerable light on the dynamic response of earth dams in three dimensions. In fact, the great majority of the conclusions derived from this investigation are not likely to be affected significantly by the assumptions used in the method of analysis. Therefore, it seems worthwhile to summarize the main conclusions of this work as follows:

1. Numerical techniques based on state-of-the-art procedures, are now available for the three-dimensional dynamic response analysis of earth dams.

2. If the displacements in the direction of the longitudinal axis of a dam subjected to upstream-downstream earthquake motions are neglected, errors in the computed peak stresses in the dam can be as large as 20% and those in the computed peak horizontal displacements can be as large as 50% of the correct values.

3. The recorded response of the Oroville Dam to the August 1, 1975 Oroville earthquake has been simulated reasonably well using a three-dimensional dynamic analysis of the dam.

4. A K_2max value of 170 seems to be representative of the in-situ dynamic characteristics of the Oroville gravels.

5. For dams in triangular canyons with a crest length to height ratio, L/H, of about 7, the τ_{xy} stresses are a dominant component of the stress state at each point and the three-dimensional effects of canyon geometry on the dynamic response of the dam are small.

6. For dams with a ratio L/H of about 2, the τ_{xz} stresses are of the same order of magnitude as the τ_{xy} stresses and the effects of canyon geometry on the response of the dam are very pronounced.

7. The dynamic response of earth dams in triangular canyons with crest length to height ratios, L/H, grater than 7 can be computed within engineering accuracy with plane strain analyses of different sections of the dams.

8. Two-dimensional analyses cannot simulate correctly the dynamic response of dams in steep triangular canyons ($L/H < 6$) and therefore, a three-dimensional analysis and the exercise of adequate judgement are needed to assess the seismic response of these dams.

9. A plane strain analysis using modified soil stiffness characteristics does not approximate the dynamic response of a three-dimensional earth dam any better than a conventional two-dimensional analysis.

10. A finite element model with about 10 elements in the cross-valley direction is adequate for the computation of the three-dimensional dynamic response of an earth dam with a degree of accuracy satisfactory for engineering purposes.

REFERENCES

Abdel-Ghaffar, A.M. and Scott, R.F. (1978) "An Investigation of the Dynamic Characteristics of an Earth Dam," Report No. EERL 78-02, Earthquake Engineering Research Laboratory, California Institute of Technology, Pasadena, August.

Abdel-Ghaffar, A.M. and Scott, R.F. (1979) "Experimental Investigation of the Dynamic Response Characteristics of an Earth Dam," Proceedings of the 2nd U.S. National Conference on Earthquake Engineering, Stanford University, California, 1979.

Ambraseys, N.N. (1960) "On the Seismic Behavior of Earth Dams," Proceedings of the Second World Conference on Earthquake Engineering, Japan, 1960, Vol. I, pp. 331-354.

Ambraseys, N.N. (1960) "On the Shear Response of a Two Dimensional Wedge Subjected to an Arbitrary Disturbance," Bulletin of the Seismological Society of America, Vol. 50, January, 1960, pp. 45-56.

Ambraseys, N.N. and Sarma, S.K. (1967) "The Response of Earth Dams to Strong Earthquakes," Geotechnique 17:181-213, September.

Banerjee, N.G., Seed, H.B. and Clarence, C.K. (1979) "Cyclic Behavior of Dense Coarse-Grained Materials in Relation to the Seismic Stability of Dams," Report No. EERC 79-13, Earthquake Engineering Research Center, University of California, Berkeley, June.

Bathe, K.J., Wilson, E.L. and Peterson, F.E. (1973) "SAPIV: A Structural Analysis Program for Static and Dynamic Response of Linear Systems," Report No. EERC 73-11, Earthquake Engineering Research Center, University of California, Berkeley, June.

Becker, E., Chan, C.K. and Seed, H.B. (1972) "Strength and Deformation Characteristics of Rockfill Materials in Plane Strain and Triaxial Compression Tests," Report No. TE 72-3, Department of Civil Engineering, University of California, Berkeley.

Bouchon, M. (1973) "Effect of Topography on Surface Motion," Bulletin of the Seismological Society of America, Vol. 63, No. 3, April 1973, pp. 615-632.

Chopra, A.K. (1966) "Earthquake Effects on Dams," Thesis submitted in partial satisfaction of the requirements for the degree of Doctor of Philosophy, University of California, Berkeley.

Clough, R.W. and Chopra, A.K. (1966) "Earthquake Stress Analysis in Earth Dams," Journal of the Engineering Mechanics Division, ASCE, Vol. 2, No. EM 2, Proc. Paper 4793, April.

Cooley, J.W. and Tukey, J.W. (1965) "An Algorithm for the Machine Calculation of Complex Fourier Series," Mathematics of Computation, Vol. 19, No. 90, pp. 297-301.

DWR Report (1969) "Report on Unconsolidated-Undrained Triaxial Shear Tests for the Core of Oroville Dam," Department of Water Resources, State of California, The Resources Agency.

DWR Report (1979) "The August 1, 1975 Oroville Earthquake Investigations," Bulletin 203-78, Department of Water Resources, State of California, The Resources Agency, February.

Goodman, R.E. and Seed, H.B. (1966) "Earthquake Induced Displacements in Sand Embankments," Journal of the Soil Mechanics and Foundations Division, ASCE, Vol. 92, SM 2, March, pp. 125-146.

Griffin, P. and Houston, W.N. (1980) "Interaction Effects of Simultaneous Torsional and Compressional Cyclic Loading of Sand," Report No. EERC 79-34, Earthquake Engineering Research Center, University of California, Berkeley, December.

Hardin, B.O. and Drnevich, V.P. (1970) "Shear Modulus and Damping in Soils: 1. Measurement and Parameter Effects, 2. Design Equations and Curves," Technical Reports UKY 27-70-CE 2 and 3, College of Engineering, University of Kentucky, Lexington, Kentucky, July.

Hatanaka, M. (1955) "Fundamental Considerations on the Earthquake Resistant Properties of the Earth Dam," Bulletin No. 11, Disaster Prevention Research Institute, Kyoto University, Kyoto, Japan.

Idriss, I.M., Lysmer, J., Hwang, R.N. and Seed, H.B. (1973) "QUAD4: A Computer Program for Evaluating the Seismic Response of Soil Structures by Variable Damping Finite Element Procedures," Report No. EERC 73-16, Earthquake Engineering Research Center, University of California, Berkeley, July.

Idriss, I.M. and Seed, H.B. (1967) "Response of Earth Banks During Earthquakes," Journal of the Soil Mechanics and Foundations Division, ASCE, Vol. 93, No. SM 3, May, pp. 61-82.

Idriss, I.M. and Seed, H.B. (1967) "Response of Horizontal Soil Layers During Earthquakes," Internal Report, Department of Civil Engineering, University of California, Berkeley, August.

Johnson, M.W. and McLay, R.W. (1968) "Convergence of the Finite Element Method in the Theory of Elasticity," Journal of Applied Mechanics, Transactions of the American Society of Mechanical Engineers.

Kagawa, T. (1977) "Shaking Table Tests and Analysis of Soil-Structure Systems," Thesis submitted in partial satisfaction of the requirements for the degree of Doctor of Philosophy, University of California, Berkeley.

Kulhawy, F.H. and Duncan, J.M. (1970) "Nonlinear Finite Element Analyses of Stresses and Movements in Oroville Dam," Report No. TE 70-2, Department of Civil Engineering, University of California, Berkeley.

Kulhawy, F.H., Duncan, J.M. and Seed, H.B. (1969) "Finite Element Analysis of Stresses and Movements in Embankments During Construction," Geotechnical Engineering Research Report, Department of Civil Engineering, University of California, Berkeley.

Lefebvre, G. Duncan, J.M. and Wilson, E.L. (1973) "Three-Dimensional Finite Element Analyses of Dams," Journal of the Soil Mechanics and Foundations Division, ASCE, Vol. 99, No. SM 7, July, pp. 495-507.

Lysmer, J., Udaka, T., Seed, H.B. and Hwang, R.N. (1974) "LUSH: A Computer Program For Complex Response Analysis of Soil-Structure Systems," Report No. EERC 74-4, Earthquake Engineering Research Center, University of California, Berkeley, April.

Lysmer, J., Udaka, T., Tsai, C.F. and Seed, H.B. (1975) "FLUSH: A Computer Program for Approximate 3-D Analysis of Soil-Structure Interaction Problems," Report No. EERC 75-30, Earthquake Engineering Research Center, University of California, Berkeley, November.

Makdisi, F.I. (1976) "Performance and Analysis of Earth Dams During Strong Earthquakes," Thesis submitted in partial satisfaction of the requirements for the degree of Doctor of Philosophy, University of California, Berkeley.

Makdisi, F.I. and Seed, H.B. (1977) "A Simplified Procedure For Estimating Earthquake-Induced Deformations in Dams and Embankments," Report No. EERC 77-19, Earthquake Engineering Research Center, University of California, Berkeley, August.

Makdisi, F.I., Seed, H.B. and Idriss, I.M. (1978) "Analysis of Chabot Dam During the 1906 Earthquake," Proceedings of the ASCE Geotechnical Engineering Division, Specialty Conference on Earthquake Engineering and Soil Dynamics, Pasadena, California, June.

Marachi, N.D., Chan, C.K., Seed, H.B. and Duncan, J.M. (1969) "Strength and Deformation Characteristics of Rockfill Materials," Report No. TE 69-5, Department of Civil Engineering, University of California, Berkeley.

Mikhlin, S.C. (1964) "Variational Methods in Mathematical Physics," Macmillan, 1964.

Mononobe, N., Takata, A., and Matamura, M. (1936) "Seismic Stability of the Earth Dam," Transactions, Vol. 4, Second Congress on Large Dams, Washington, D.C.

Newmark, N.M. (1965) "Effects of Earthquakes on Dams and Embankments," Geotechnique, Vol. 15, No. 2, June, pp. 139-173.

Nobari, E.S. and Duncan, J.M. (1972) "Effect of Reservoir Filling on Stresses and Movements in Earth and Rockfill Dams," Report No. TE 72-1, Department of Civil Engineering, University of California, Berkeley.

Ozawa, Y. and Duncan, J.M. (1973) "ISBILD: A Computer Program for Analysis of Static Stresses and Movements in Embankments," Report No. TE 73-4, Department of Civil Engineering, University of California, Berkeley.

Seed, H.B. (1963) "Model Studies of the Stability of Oroville Dam during Earthquakes," Research Report No. TE 63-1, Department of Civil Engineering, University of California, Berkeley, February.

Seed, H.B. (1966) "A Method for Earthquake Resistant Design of Earth Dams," Journal of the Soil Mechanics and Foundations Division, ASCE, Vol. 92, SM 1, January, pp. 13-41.

Seed, H.B. and Idriss, I.M. (1970) "Soil Moduli and Damping Factors for Dynamic Response Analysis," Report No. EERC 70-10, Earthquake Engineering Research Center, University of California, Berkeley, December.

Seed, H.B., Idriss, I.M., Makdisi, F. and Banerjee, N. (1975) "Representation of Irregular Stress Time Histories by Equivalent Uniform Stress Series in Liquefaction Analyses," Report No. EERC 75-29, Earthquake Engineering Research Center, University of California, Berkeley, October.

Seed, H.B., Lee, K.L. and Idriss, I.M. (1969) "An Analysis of the Sheffield Dam Failure," Journal of the Soil Mechanics and Foundation Engineering Division, ASCE, Vol. 94, No. SM 6, November.

Seed, H.B., Lee, K.L., Idriss, I.M. and Makdisi, F. (1973) "Analysis of the Slides in the San Fernando Dams During the Earthquake of February 9, 1971," Report no. EERC 73-2, Earthquake Engineering Research Center, University of California, Berkeley.

Seed, H.B., Makdisi, R.I. and DeAlba, P. (1977) "The Performance of Earth Dams During Earthquakes," Report No. EERC 77-20, Earthquake Engineering Research Center, University of California, Berkeley, August.

Seed, H.B. and Martin, G.R. (1966) "The Seismic Coefficient in Earth Dam Design," Journal of the Soil Mechanics and Foundations Division, ASCE, Vol. 92, No. SM 3, May.

Serff, N., Seed, H.B., Makdisi, F.I. and Chang, C.Y. (1976) "Earthquake Induced Deformations of Earth Dams," Report No. EERC 76-4, Earthquake Engineering Research Center, University of California, Berkeley, September.

Severn, R. T., Jeary, A.P. and Ellis, B.R. (1980) "Forced Vibration Tests and Theoretical Studies on Dams," Submitted for publication in the Proceedings of ICE, March, 1980.

Severn, R.T., Jeary, A.P., Ellis, B.R. and Dungar, R. (1979) "Prototype Dynamic Studies on a Rockfill Dam and on a Buttress Dam," Proceedings of the Thirteenth International Congress on Large Dams, Q. 51, R. 16, New Delhi, 1979.

Strang, G. and Fix, G.J. (1973) "An Analysis of the Finite Element Method," Ed. Prentice-Hall.

Stroppini, E.W. (1976) "The Oroville Earthquake and Oroville Dam," Evaluation of Dam Safety, ASCE, pp. 301-328.

Tajirian, F. (1981) "Impedance Matrices and Interpolation Techniques for 3-D Interaction Analysis by the Flexible Volume Method," Thesis submitted in partial satisfaction of the requirements for the degree of Doctor of Philosophy, University of California, Berkeley.

Trifunac, M.D. (1973) "Scattering of Plane SH Waves by a Semi-Cylindrical Canyon," International Journal of Earthquake Engineering and Structural Dynamics, Vol. 1, No. 3, January 1973, pp. 267-281.

Turner, M.J., Clough, R.W., Martin, H.C. and Topp, L.J. (1956) "Stiffness and Deflection Analysis of Complex Structures," Journal of Aeronautical Science, Vol. 23, pp. 805-823.

Wilson, E.L. (1971) "SOLID SAP: A Static Analysis Program for Three-Dimensional Solid Structures," Report No. UCSESM 71-19, University of California, Berkeley.

Wilson, E.L., Bathe, K.J., Peterson, J.E. and Dovey, H.H. (1972) "Computer Program for Static and Dynamic Analysis of Linear Structural Systems," Report No. EERC 72-10, Earthquake Engineering Research Center, University of California, Berkeley.

Wilson, E.L. and Clough, R.W. (1962) "Dynamic Response by Step-by-Step Matrix Analysis," Symposium on the Use of Computers in Civil Engineering, Lisbon, October.

Wong, R.T. (1971) "Deformation Characteristics of Gravels and Gravelly Soils Under Cyclic Loading Conditions," Thesis submitted in partial satisfaction of the requirements for the degree of Doctor of Philosophy, University of California, Berkeley.

Zienkiewicz, O.C. (1977) "The Finite Element Method," Ed. McGraw Hill, London.

APPENDIX A

SHEAR WEDGE ANALYSIS OF DAMS IN TRIANGULAR CANYONS

A-1 Equation of Motion

Formulation of the equation of motion for a symmetrical earth dam in a triangular canyon by means of a shear wedge analysis will be presented in this appendix. Also included is an approximate eigenvalue solution of this equation for the fundamental natural frequency of vibration of the dam.

The assumptions inherent to a shear wedge analysis of a symmetrical earth dam are the following:

1. The canyon walls are perfectly rigid.
2. The direction of the ground motion is horizontal and parallel to the canyon walls and there are no displacements in other directions.
3. The dam is homogeneous and the dam materials are linearly elastic.
4. Interaction between water in the reservoir and the dam is negligible.
5. Shear stresses are uniformly distributed along lines parallel to the canyon walls.

6. Only shear deformations are considered.

On the basis of these assumptions a symmetrical earth dam in a triangular canyon can be represented by the model shown in Fig. A-1. As shown in this figure, under undamped conditions, four shear forces and one inertia force act on each one-dimensional transverse slice of the dam. Dynamic equilibrium of each slice requires that:

$$F_i + F_{sy+dy} + F_{sz} - F_{sy} - F_{sz+dz} = 0 \qquad (A-1)$$

where:

F_i = inertia force on the slice.

F_{sy} = shear force on the y plane.

F_{sz} = shear force on the z plane.

If:

U = the displacement in the x direction relative to the rigid boundary.

U_t = the total displacement in the x direction.

U_g = the rigid boundary displacement in the x direction.

Then we have:

$$U_t = U_g + U$$

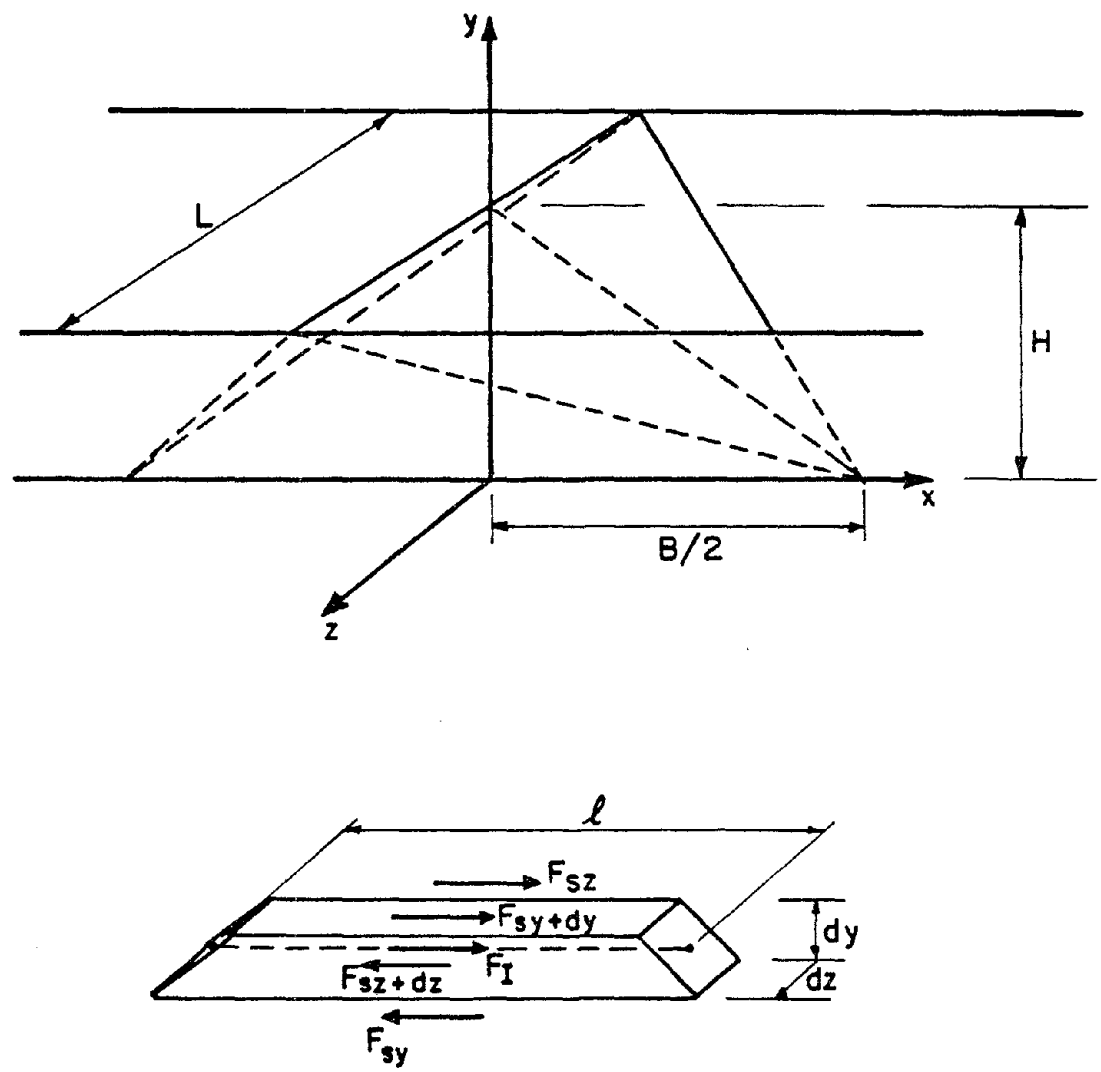

Fig. A-1 Analytical Model of Dam in Triangular Canyon for Shear Wedge Analysis.

$$\ddot{U}_t = \ddot{U}_g + \ddot{U} \tag{A-2}$$

and:

$$F_i = -\rho(1 + \frac{1}{2}\frac{\partial l}{\partial y}dy)dydz\ \ddot{U}_t$$

$$F_{sy} = lG\frac{\partial U}{\partial y}dz$$

$$F_{sy+dy} = G(\frac{\partial U}{\partial y} + \frac{\partial^2 U}{\partial y^2}dy)\ (l + \frac{\partial l}{\partial y}dy)dz \tag{A-3}$$

$$F_{sz} = -G\frac{\partial U}{\partial z}(l + \frac{1}{2}\frac{\partial l}{\partial y}dy)dy$$

$$F_{sz+dz} = -G(\frac{\partial U}{\partial z} + \frac{\partial^2 U}{\partial z^2}dz)\ (l + \frac{1}{2}\frac{\partial l}{\partial y}dy)dy$$

where:

ρ = density of the material.

G = shear modulus of the material.

l = length of the slice.

Substituting equations (A-3) into equation (A-1) and simplifying the following equation is obtained:

$$G \frac{\partial^2 U}{\partial y^2} + G \frac{\partial^2 U}{\partial z^2} + \frac{G}{l} \frac{\partial l}{\partial y} \frac{\partial U}{\partial y} - \rho \ddot{U}_t = 0 \qquad \text{(A-4)}$$

From geometrical considerations it follows that:

$$\frac{1}{l} \frac{\partial l}{\partial y} = \frac{1}{y-H} \qquad \text{(A-5)}$$

Substituting equation (A-5) into equation (A-4) and simplifying the equation of motion of the dam under undamped conditions is obtained:

$$V_s^2 \frac{\partial^2 U}{\partial y^2} + V_s^2 \frac{\partial^2 U}{\partial z^2} + \frac{V_s^2}{y-H} \frac{\partial U}{\partial y} - \ddot{U}_t = 0 \qquad \text{(A-6)}$$

where:

$V_s = \sqrt{G/\rho}$ = shear wave velocity of the material.

H = height of the dam (Fig. A-1).

For free vibration we have:

$$U_g = 0 \quad \text{and} \quad U_t = U$$

Therefore:

$$V_s^2 \frac{\partial^2 U}{\partial y^2} + V_s^2 \frac{\partial^2 U}{\partial z^2} + \frac{V_s^2}{y-H} \frac{\partial U}{\partial y} - \frac{\partial^2 U}{\partial t^2} = 0 \qquad \text{(A-7)}$$

This is the differential equation of motion for undamped free vibration of a dam. The following boundary conditions are applicable for the case of a symmetrical dam in a triangular canyon:

1. $\frac{\partial U}{\partial y} = 0$ at $y=H$

2. $\frac{\partial U}{\partial z} = 0$ at $z=0$

3. $U = 0$ at $y = \frac{2H}{L}z$

where L = length of dam crest.

A-2 Solution for First Natural Frequency

The solution to equation (A-7) is of the form:

$$U = R \cdot T \tag{A-9}$$

where:

R = a function of y and z only.

T = a function of t only

Therefore:

$$\frac{\partial U}{\partial y} = \frac{\partial R}{\partial y} T$$

$$\frac{\partial^2 U}{\partial y^2} = \frac{\partial^2 R}{\partial y^2} T \tag{A-10}$$

$$\frac{\partial^2 U}{\partial z^2} = \frac{\partial^2 R}{\partial z^2} T$$

$$\frac{\partial^2 U}{\partial t^2} = \frac{\partial^2 T}{\partial t^2} R$$

Substituting equations (A-10) into equation (A-7) and simplifying the following is obtained:

$$\frac{V_s^2}{R} \left(\frac{\partial^2 R}{\partial y^2} + \frac{\partial^2 R}{\partial z^2} + \frac{1}{y-H} \frac{\partial R}{\partial y}\right) = \frac{1}{T} \frac{\partial^2 T}{\partial t^2} \qquad \text{(A-11)}$$

It follows that the two sides of equation (A-11) are equal to a constant. That is:

$$\frac{1}{T} \frac{\partial^2 T}{\partial t^2} = -\omega^2 \qquad \text{(A-12)}$$

or:

$$\frac{\partial^2 T}{\partial t^2} + \omega^2 T = 0 \qquad \text{(A-13)}$$

Therefore:

$$T = A_1 \cos\omega t + A_2 \sin\omega t \qquad \text{(A-14)}$$

where: ω = angular frequency.

Substituting equation (A-12) into equation (A-11) the following is also obtained:

$$\frac{\partial^2 R}{\partial y^2} + \frac{\partial^2 R}{\partial z^2} + \frac{1}{y-H}\frac{\partial R}{\partial y} + \frac{\omega^2}{V_s^2} R = 0 \qquad \text{(A-15)}$$

Since the boundary conditions given by equations (A-8) have to be satisfied at all times, the following boundary conditions can be imposed on the function R:

1. $\frac{\partial R}{\partial y} = 0$ at $y=H$

2. $\frac{\partial R}{\partial z} = 0$ at $z=0$ (A-16)

3. $R = 0$ at $y = \frac{2H}{L}z$

Solution in closed form of equation (A-15), such that the boundary conditions given by equations (A-16) are satisfied, is difficult and will not be attempted here. However, an approximate eigenvalue solution of equation (A-15) can easily be used to obtain a rather accurate value for the first natural frequency of vibration of the system.

According to the Bubnov-Galerkin method (Mikhlin, 1964), if a function R which satisfies the boundary conditions given by equations (A-16) can be found, the following integral:

$$\int_y F(R)\cdot R \, dy = 0 \qquad \text{(A-17)}$$

where:

$F(R)$ = the differential equation.

$\mathcal{Y}$ = solution domain.

yields an algebraic equation from which the frequency of the system can be determined. In the particular case examined here, equation (A-17) takes the form:

$$\int_0^H \int_0^{y/c} \left(\frac{\partial^2 R}{\partial y^2} + \frac{\partial^2 R}{\partial z^2} + \frac{1}{y-H}\frac{\partial R}{\partial y} + \frac{\omega^2}{V_s^2} R\right) R \, dz dy = 0 \qquad \text{(A-18)}$$

where c has been defined as:

$$c = \frac{2H}{L} \qquad \text{(A-19)}$$

It can easily be shown that the function:

$$R = (y+cz)(y-cz)(y-2H-cz)(y-2H+cz) \qquad \text{(A-20)}$$

satisfies the boundary conditions given by equations (A-16).

After substituting equation (A-20) into equation (A-18) and performing the integration the following algebraic equation is obtained:

$$\frac{32}{225}\frac{\omega^2}{c}\frac{H^2}{V_s^2} - \frac{8}{5c} - \frac{32}{45}c = 0 \qquad \text{(A-21)}$$

Solving equation (A-21) for ω we obtain:

$$\omega = \frac{V_s}{H} \sqrt{\frac{45}{4} + 5c^2} \qquad \text{(A-22)}$$

This expression gives the first natural frequency of a symmetrical dam in a triangular canyon as a function of the shear wave velocity of the dam material V_s, the height of the dam H, and the ratio 2H/L, where L is the length of the crest of the dam. However, it only yields acceptable values of the natural frequency for crest length to height ratios, L/H, lower than about 6. For ratios higher than this value the computed natural frequencies are too high since the assumption for the function R is not a good approximation of the first mode shape of vibration of dams in canyons with gentle side slopes.

It is interesting to compare this expression with that corresponding to the two-dimensional case. The first natural frequency of vibration of an infinitely long dam, obtained from a shear beam analysis, is given by:

$$\omega_{2D} = 2.404\ V_s/H \qquad \text{(A-23)}$$

where V_s and H are the shear wave velocity of the material and the height of the dam, respectively.

The ratio between the first natural frequency computed with a 3-D model and that computed with a 2-D model of a dam in a triangular canyon is given by:

$$\frac{\omega_{3D}}{\omega_{2D}} = \frac{1}{2.404}\sqrt{\frac{45}{4} + 5c^2} \qquad \text{(A-24)}$$

The variation of the above ratio as a function of the crest length to height ratio L/H is shown in table A-1 and in Fig. 5-1.

TABLE A-1

RATIO BETWEEN FUNDAMENTAL FREQUENCIES COMPUTED WITH 2-D AND 3-D MODELS OF DAMS IN TRIANGULAR CANYONS

L/H	c	ω_{3D}/ω_{3D}
1	2	2.33
2	1	1.68
3	0.667	1.53
4	0.5	1.47
5	0.4	1.44
6	0.333	1.43
7	0.286	1.42

EARTHQUAKE ENGINEERING RESEARCH CENTER REPORTS

NOTE: Numbers in parenthesis are Accession Numbers assigned by the National Technical Information Service; these are followed by a price code. Copies of the reports may be ordered from the National Technical Information Service, 5285 Port Royal Road, Springfield, Virginia, 22161. Accession Numbers should be quoted on orders for reports (PB --- ---) and remittance must accompany each order. Reports without this information were not available at time of printing. Upon request, EERC will mail inquirers this information when it becomes available.

EERC 67-1 "Feasibility Study Large-Scale Earthquake Simulator Facility," by J. Penzien, J.G. Bouwkamp, R.W. Clough and D. Rea - 1967 (PB 187 905)A07

EERC 68-1 Unassigned

EERC 68-2 "Inelastic Behavior of Beam-to-Column Subassemblages Under Repeated Loading," by V.V. Bertero - 1968 (PB 184 888)A05

EERC 68-3 "A Graphical Method for Solving the Wave Reflection-Refraction Problem," by H.D. McNiven and Y. Mengi - 1968 (PB 187 943)A03

EERC 68-4 "Dynamic Properties of McKinley School Buildings," by D. Rea, J.G. Bouwkamp and R.W. Clough - 1968 (PB 187 902)A07

EERC 68-5 "Characteristics of Rock Motions During Earthquakes," by H.B. Seed, I.M. Idriss and F.W. Kiefer - 1968 (PB 188 338)A03

EERC 69-1 "Earthquake Engineering Research at Berkeley," - 1969 (PB 187 906)All

EERC 69-2 "Nonlinear Seismic Response of Earth Structures," by M. Dibaj and J. Penzien - 1969 (PB 187 904)A08

EERC 69-3 "Probabilistic Study of the Behavior of Structures During Earthquakes," by R. Ruiz and J. Penzien - 1969 (PB 187 886)A06

EERC 69-4 "Numerical Solution of Boundary Value Problems in Structural Mechanics by Reduction to an Initial Value Formulation," by N. Distefano and J. Schujman - 1969 (PB 187 942)A02

EERC 69-5 "Dynamic Programming and the Solution of the Biharmonic Equation," by N. Distefano - 1969 (PB 187 941)A03

EERC 69-6 "Stochastic Analysis of Offshore Tower Structures," by A.K. Malhotra and J. Penzien - 1969 (PB 187 903)A09

EERC 69-7 "Rock Motion Accelerograms for High Magnitude Earthquakes," by H.B. Seed and I.M. Idriss - 1969 (PB 187 940)A02

EERC 69-8 "Structural Dynamics Testing Facilities at the University of California, Berkeley," by R.M. Stephen, J.G. Bouwkamp, R.W. Clough and J. Penzien - 1969 (PB 189 111)A04

EERC 69-9 "Seismic Response of Soil Deposits Underlain by Sloping Rock Boundaries," by H. Dezfulian and H.B. Seed 1969 (PB 189 114)A03

EERC 69-10 "Dynamic Stress Analysis of Axisymmetric Structures Under Arbitrary Loading," by S. Ghosh and E.L. Wilson 1969 (PB 189 026)A10

EERC 69-11 "Seismic Behavior of Multistory Frames Designed by Different Philosophies," by J.C. Anderson and V. V. Bertero - 1969 (PB 190 662)A10

EERC 69-12 "Stiffness Degradation of Reinforcing Concrete Members Subjected to Cyclic Flexural Moments," by V.V. Bertero, B. Bresler and H. Ming Liao - 1969 (PB 202 942)A07

EERC 69-13 "Response of Non-Uniform Soil Deposits to Travelling Seismic Waves," by H. Dezfulian and H.B. Seed - 1969 (PB 191 023)A03

EERC 69-14 "Damping Capacity of a Model Steel Structure," by D. Rea, R.W. Clough and J.G. Bouwkamp - 1969 (PB 190 663)A06

EERC 69-15 "Influence of Local Soil Conditions on Building Damage Potential during Earthquakes," by H.B. Seed and I.M. Idriss - 1969 (PB 191 036)A03

EERC 69-16 "The Behavior of Sands Under Seismic Loading Conditions," by M.L. Silver and H.B. Seed - 1969 (AD 714 982)A07

EERC 70-1 "Earthquake Response of Gravity Dams," by A.K. Chopra - 1970 (AD 709 640)A03

EERC 70-2 "Relationships between Soil Conditions and Building Damage in the Caracas Earthquake of July 29, 1967," by H.B. Seed, I.M. Idriss and H. Dezfulian - 1970 (PB 195 762)A05

EERC 70-3 "Cyclic Loading of Full Size Steel Connections," by E.P. Popov and R.M. Stephen - 1970 (PB 213 545)A04

EERC 70-4 "Seismic Analysis of the Charaima Building, Caraballeda, Venezuela," by Subcommittee of the SEAONC Research Committee: V.V. Bertero, P.F. Fratessa, S.A. Mahin, J.H. Sexton, A.C. Scordelis, E.L. Wilson, L.A. Wyllie, H.B. Seed and J. Penzien, Chairman - 1970 (PB 201 455)A06

EERC 70-5 "A Computer Program for Earthquake Analysis of Dams," by A.K. Chopra and P. Chakrabarti - 1970 (AD 723 994)A05

EERC 70-6 "The Propagation of Love Waves Across Non-Horizontally Layered Structures," by J. Lysmer and L.A. Drake 1970 (PB 197 896)A03

EERC 70-7 "Influence of Base Rock Characteristics on Ground Response," by J. Lysmer, H.B. Seed and P.B. Schnabel 1970 (PB 197 897)A03

EERC 70-8 "Applicability of Laboratory Test Procedures for Measuring Soil Liquefaction Characteristics under Cyclic Loading," by H.B. Seed and W.H. Peacock - 1970 (PB 198 016)A03

EERC 70-9 "A Simplified Procedure for Evaluating Soil Liquefaction Potential," by H.B. Seed and I.M. Idriss - 1970 (PB 198 009)A03

EERC 70-10 "Soil Moduli and Damping Factors for Dynamic Response Analysis," by H.B. Seed and I.M. Idriss - 1970 (PB 197 869)A03

EERC 71-1 "Koyna Earthquake of December 11, 1967 and the Performance of Koyna Dam," by A.K. Chopra and P. Chakrabarti 1971 (AD 731 496)A06

EERC 71-2 "Preliminary In-Situ Measurements of Anelastic Absorption in Soils Using a Prototype Earthquake Simulator," by R.D. Borcherdt and P.W. Rodgers - 1971 (PB 201 454)A03

EERC 71-3 "Static and Dynamic Analysis of Inelastic Frame Structures," by F.L. Porter and G.H. Powell - 1971 (PB 210 135)A06

EERC 71-4 "Research Needs in Limit Design of Reinforced Concrete Structures," by V.V. Bertero - 1971 (PB 202 943)A04

EERC 71-5 "Dynamic Behavior of a High-Rise Diagonally Braced Steel Building," by D. Rea, A.A. Shah and J.G. Bouwkamp 1971 (PB 203 584)A06

EERC 71-6 "Dynamic Stress Analysis of Porous Elastic Solids Saturated with Compressible Fluids," by J. Ghaboussi and E. L. Wilson - 1971 (PB 211 396)A06

EERC 71-7 "Inelastic Behavior of Steel Beam-to-Column Subassemblages," by H. Krawinkler, V.V. Bertero and E.P. Popov 1971 (PB 211 335)A14

EERC 71-8 "Modification of Seismograph Records for Effects of Local Soil Conditions," by P. Schnabel, H.B. Seed and J. Lysmer - 1971 (PB 214 450)A03

EERC 72-1 "Static and Earthquake Analysis of Three Dimensional Frame and Shear Wall Buildings," by E.L. Wilson and H.H. Dovey - 1972 (PB 212 904)A05

EERC 72-2 "Accelerations in Rock for Earthquakes in the Western United States," by P.B. Schnabel and H.B. Seed - 1972 (PB 213 100)A03

EERC 72-3 "Elastic-Plastic Earthquake Response of Soil-Building Systems," by T. Minami - 1972 (PB 214 868)A08

EERC 72-4 "Stochastic Inelastic Response of Offshore Towers to Strong Motion Earthquakes," by M.K. Kaul - 1972 (PB 215 713)A05

EERC 72-5 "Cyclic Behavior of Three Reinforced Concrete Flexural Members with High Shear," by E.P. Popov, V.V. Bertero and H. Krawinkler - 1972 (PB 214 555)A05

EERC 72-6 "Earthquake Response of Gravity Dams Including Reservoir Interaction Effects," by P. Chakrabarti and A.K. Chopra - 1972 (AD 762 330)A08

EERC 72-7 "Dynamic Properties of Pine Flat Dam," by D. Rea, C.Y. Liaw and A.K. Chopra - 1972 (AD 763 928)A05

EERC 72-8 "Three Dimensional Analysis of Building Systems," by E.L. Wilson and H.H. Dovey - 1972 (PB 222 438)A06

EERC 72-9 "Rate of Loading Effects on Uncracked and Repaired Reinforced Concrete Members," by S. Mahin, V.V. Bertero, D. Rea and M. Atalay - 1972 (PB 224 520)A08

EERC 72-10 "Computer Program for Static and Dynamic Analysis of Linear Structural Systems," by E.L. Wilson, K.-J. Bathe, J.E. Peterson and H.H.Dovey - 1972 (PB 220 437)A04

EERC 72-11 "Literature Survey - Seismic Effects on Highway Bridges," by T. Iwasaki, J. Penzien and R.W. Clough - 1972 (PB 215 613)A19

EERC 72-12 "SHAKE-A Computer Program for Earthquake Response Analysis of Horizontally Layered Sites," by P.B. Schnabel and J. Lysmer - 1972 (PB 220 207)A06

EERC 73-1 "Optimal Seismic Design of Multistory Frames," by V.V. Bertero and H. Kamil - 1973

EERC 73-2 "Analysis of the Slides in the San Fernando Dams During the Earthquake of February 9, 1971," by H.B. Seed, K.L. Lee, I.M. Idriss and F. Makdisi - 1973 (PB 223 402)A14

EERC 73-3 "Computer Aided Ultimate Load Design of Unbraced Multistory Steel Frames," by M.B. El-Hafez and G.H. Powell 1973 (PB 248 315)A09

EERC 73-4 "Experimental Investigation into the Seismic Behavior of Critical Regions of Reinforced Concrete Components as Influenced by Moment and Shear," by M. Celebi and J. Penzien - 1973 (PB 215 884)A09

EERC 73-5 "Hysteretic Behavior of Epoxy-Repaired Reinforced Concrete Beams," by M. Celebi and J. Penzien - 1973 (PB 239 568)A03

EERC 73-6 "General Purpose Computer Program for Inelastic Dynamic Response of Plane Structures," by A. Kanaan and G.H. Powell - 1973 (PB 221 260)A08

EERC 73-7 "A Computer Program for Earthquake Analysis of Gravity Dams Including Reservoir Interaction," by P. Chakrabarti and A.K. Chopra - 1973 (AD 766 271)A04

EERC 73-8 "Behavior of Reinforced Concrete Deep Beam-Column Subassemblages Under Cyclic Loads," by O. Küstü and J.G. Bouwkamp - 1973 (PB 246 117)A12

EERC 73-9 "Earthquake Analysis of Structure-Foundation Systems," by A.K. Vaish and A.K. Chopra - 1973 (AD 766 272)A07

EERC 73-10 "Deconvolution of Seismic Response for Linear Systems," by R.B. Reimer - 1973 (PB 227 179)A08

EERC 73-11 "SAP IV: A Structural Analysis Program for Static and Dynamic Response of Linear Systems," by K.-J. Bathe, E.L. Wilson and F.E. Peterson - 1973 (PB 221 967)A09

EERC 73-12 "Analytical Investigations of the Seismic Response of Long, Multiple Span Highway Bridges," by W.S. Tseng and J. Penzien - 1973 (PB 227 816)A10

EERC 73-13 "Earthquake Analysis of Multi-Story Buildings Including Foundation Interaction," by A.K. Chopra and J.A. Gutierrez - 1973 (PB 222 970)A03

EERC 73-14 "ADAP: A Computer Program for Static and Dynamic Analysis of Arch Dams," by R.W. Clough, J.M. Raphael and S. Mojtahedi - 1973 (PB 223 763)A09

EERC 73-15 "Cyclic Plastic Analysis of Structural Steel Joints," by R.B. Pinkney and R.W. Clough - 1973 (PB 226 843)A08

EERC 73-16 "QUAD-4: A Computer Program for Evaluating the Seismic Response of Soil Structures by Variable Damping Finite Element Procedures," by I.M. Idriss, J. Lysmer, R. Hwang and H.B. Seed - 1973 (PB 229 424)A05

EERC 73-17 "Dynamic Behavior of a Multi-Story Pyramid Shaped Building," by R.M. Stephen, J.P. Hollings and J.G. Bouwkamp - 1973 (PB 240 718)A06

EERC 73-18 "Effect of Different Types of Reinforcing on Seismic Behavior of Short Concrete Columns," by V.V. Bertero, J. Hollings, O. Küstü, R.M. Stephen and J.G. Bouwkamp - 1973

EERC 73-19 "Olive View Medical Center Materials Studies, Phase I," by B. Bresler and V.V. Bertero - 1973 (PB 235 986)A06

EERC 73-20 "Linear and Nonlinear Seismic Analysis Computer Programs for Long Multiple-Span Highway Bridges," by W.S. Tseng and J. Penzien - 1973

EERC 73-21 "Constitutive Models for Cyclic Plastic Deformation of Engineering Materials," by J.M. Kelly and P.P. Gillis 1973 (PB 226 024)A03

EERC 73-22 "DRAIN - 2D User's Guide," by G.H. Powell - 1973 (PB 227 016)A05

EERC 73-23 "Earthquake Engineering at Berkeley - 1973," (PB 226 033)A11

EERC 73-24 Unassigned

EERC 73-25 "Earthquake Response of Axisymmetric Tower Structures Surrounded by Water," by C.Y. Liaw and A.K. Chopra 1973 (AD 773 052)A09

EERC 73-26 "Investigation of the Failures of the Olive View Stairtowers During the San Fernando Earthquake and Their Implications on Seismic Design," by V.V. Bertero and R.G. Collins - 1973 (PB 235 106)A13

EERC 73-27 "Further Studies on Seismic Behavior of Steel Beam-Column Subassemblages," by V.V. Bertero, H. Krawinkler and E.P. Popov - 1973 (PB 234 172)A06

EERC 74-1 "Seismic Risk Analysis," by C.S. Oliveira - 1974 (PB 235 920)A06

EERC 74-2 "Settlement and Liquefaction of Sands Under Multi-Directional Shaking," by R. Pyke, C.K. Chan and H.B. Seed 1974

EERC 74-3 "Optimum Design of Earthquake Resistant Shear Buildings," by D. Ray, K.S. Pister and A.K. Chopra - 1974 (PB 231 172)A06

EERC 74-4 "LUSH - A Computer Program for Complex Response Analysis of Soil-Structure Systems," by J. Lysmer, T. Udaka, H.B. Seed and R. Hwang - 1974 (PB 236 796)A05

EERC 74-5 "Sensitivity Analysis for Hysteretic Dynamic Systems: Applications to Earthquake Engineering," by D. Ray 1974 (PB 233 213)A06

EERC 74-6 "Soil Structure Interaction Analyses for Evaluating Seismic Response," by H.B. Seed, J. Lysmer and R. Hwang 1974 (PB 236 519)A04

EERC 74-7 Unassigned

EERC 74-8 "Shaking Table Tests of a Steel Frame - A Progress Report," by R.W. Clough and D. Tang - 1974 (PB 240 869)A03

EERC 74-9 "Hysteretic Behavior of Reinforced Concrete Flexural Members with Special Web Reinforcement," by V.V. Bertero, E.P. Popov and T.Y. Wang - 1974 (PB 236 797)A07

EERC 74-10 "Applications of Reliability-Based, Global Cost Optimization to Design of Earthquake Resistant Structures," by E. Vitiello and K.S. Pister - 1974 (PB 237 231)A06

EERC 74-11 "Liquefaction of Gravelly Soils Under Cyclic Loading Conditions," by R.T. Wong, H.B. Seed and C.K. Chan 1974 (PB 242 042)A03

EERC 74-12 "Site-Dependent Spectra for Earthquake-Resistant Design," by H.B. Seed, C. Ugas and J. Lysmer - 1974 (PB 240 953)A03

EERC 74-13 "Earthquake Simulator Study of a Reinforced Concrete Frame," by P. Hidalgo and R.W. Clough - 1974 (PB 241 944)A13

EERC 74-14 "Nonlinear Earthquake Response of Concrete Gravity Dams," by N. Pal - 1974 (AD/A 006 583)A06

EERC 74-15 "Modeling and Identification in Nonlinear Structural Dynamics - I. One Degree of Freedom Models," by N. Distefano and A. Rath - 1974 (PB 241 548)A06

EERC 75-1 "Determination of Seismic Design Criteria for the Dumbarton Bridge Replacement Structure, Vol. I: Description, Theory and Analytical Modeling of Bridge and Parameters," by F. Baron and S.-H. Pang - 1975 (PB 259 407)A15

EERC 75-2 "Determination of Seismic Design Criteria for the Dumbarton Bridge Replacement Structure, Vol. II: Numerical Studies and Establishment of Seismic Design Criteria," by F. Baron and S.-H. Pang - 1975 (PB 259 408)A11 (For set of EERC 75-1 and 75-2 (PB 259 406))

EERC 75-3 "Seismic Risk Analysis for a Site and a Metropolitan Area," by C.S. Oliveira - 1975 (PB 248 134)A09

EERC 75-4 "Analytical Investigations of Seismic Response of Short, Single or Multiple-Span Highway Bridges," by M.-C. Chen and J. Penzien - 1975 (PB 241 454)A09

EERC 75-5 "An Evaluation of Some Methods for Predicting Seismic Behavior of Reinforced Concrete Buildings," by S.A. Mahin and V.V. Bertero - 1975 (PB 246 306)A16

EERC 75-6 "Earthquake Simulator Study of a Steel Frame Structure, Vol. I: Experimental Results," by R.W. Clough and D.T. Tang - 1975 (PB 243 981)A13

EERC 75-7 "Dynamic Properties of San Bernardino Intake Tower," by D. Rea, C.-Y. Liaw and A.K. Chopra - 1975 (AD/A008 406) A05

EERC 75-8 "Seismic Studies of the Articulation for the Dumbarton Bridge Replacement Structure, Vol. I: Description, Theory and Analytical Modeling of Bridge Components," by F. Baron and R.E. Hamati - 1975 (PB 251 539)A07

EERC 75-9 "Seismic Studies of the Articulation for the Dumbarton Bridge Replacement Structure, Vol. 2: Numerical Studies of Steel and Concrete Girder Alternates," by F. Baron and R.E. Hamati - 1975 (PB 251 540)A10

EERC 75-10 "Static and Dynamic Analysis of Nonlinear Structures," by D.P. Mondkar and G.H. Powell - 1975 (PB 242 434)A08

EERC 75-11 "Hysteretic Behavior of Steel Columns," by E.P. Popov, V.V. Bertero and S. Chandramouli - 1975 (PB 252 365)A11

EERC 75-12 "Earthquake Engineering Research Center Library Printed Catalog," - 1975 (PB 243 711)A26

EERC 75-13 "Three Dimensional Analysis of Building Systems (Extended Version)," by E.L. Wilson, J.P. Hollings and H.H. Dovey - 1975 (PB 243 989)A07

EERC 75-14 "Determination of Soil Liquefaction Characteristics by Large-Scale Laboratory Tests," by P. De Alba, C.K. Chan and H.B. Seed - 1975 (NUREG 0027)A08

EERC 75-15 "A Literature Survey - Compressive, Tensile, Bond and Shear Strength of Masonry," by R.L. Mayes and R.W. Clough - 1975 (PB 246 292)A10

EERC 75-16 "Hysteretic Behavior of Ductile Moment Resisting Reinforced Concrete Frame Components," by V.V. Bertero and E.P. Popov - 1975 (PB 246 388)A05

EERC 75-17 "Relationships Between Maximum Acceleration, Maximum Velocity, Distance from Source, Local Site Conditions for Moderately Strong Earthquakes," by H.B. Seed, R. Murarka, J. Lysmer and I.M. Idriss - 1975 (PB 248 172)A03

EERC 75-18 "The Effects of Method of Sample Preparation on the Cyclic Stress-Strain Behavior of Sands," by J. Mulilis, C.K. Chan and H.B. Seed - 1975 (Summarized in EERC 75-28)

EERC 75-19 "The Seismic Behavior of Critical Regions of Reinforced Concrete Components as Influenced by Moment, Shear and Axial Force," by M.B. Atalay and J. Penzien - 1975 (PB 258 842)A11

EERC 75-20 "Dynamic Properties of an Eleven Story Masonry Building," by R.M. Stephen, J.P. Hollings, J.G. Bouwkamp and D. Jurukovski - 1975 (PB 246 945)A04

EERC 75-21 "State-of-the-Art in Seismic Strength of Masonry - An Evaluation and Review," by R.L. Mayes and R.W. Clough 1975 (PB 249 040)A07

EERC 75-22 "Frequency Dependent Stiffness Matrices for Viscoelastic Half-Plane Foundations," by A.K. Chopra, P. Chakrabarti and G. Dasgupta - 1975 (PB 248 121)A07

EERC 75-23 "Hysteretic Behavior of Reinforced Concrete Framed Walls," by T.Y. Wong, V.V. Bertero and E.P. Popov - 1975

EERC 75-24 "Testing Facility for Subassemblages of Frame-Wall Structural Systems," by V.V. Bertero, E.P. Popov and T. Endo - 1975

EERC 75-25 "Influence of Seismic History on the Liquefaction Characteristics of Sands," by H.B. Seed, K. Mori and C.K. Chan - 1975 (Summarized in EERC 75-28)

EERC 75-26 "The Generation and Dissipation of Pore Water Pressures during Soil Liquefaction," by H.B. Seed, P.P. Martin and J. Lysmer - 1975 (PB 252 648)A03

EERC 75-27 "Identification of Research Needs for Improving Aseismic Design of Building Structures," by V.V. Bertero 1975 (PB 248 136)A05

EERC 75-28 "Evaluation of Soil Liquefaction Potential during Earthquakes," by H.B. Seed, I. Arango and C.K. Chan - 1975 (NUREG 0026)A13

EERC 75-29 "Representation of Irregular Stress Time Histories by Equivalent Uniform Stress Series in Liquefaction Analyses," by H.B. Seed, I.M. Idriss, F. Makdisi and N. Banerjee - 1975 (PB 252 635)A03

EERC 75-30 "FLUSH - A Computer Program for Approximate 3-D Analysis of Soil-Structure Interaction Problems," by J. Lysmer, T. Udaka, C.-F. Tsai and H.B. Seed - 1975 (PB 259 332)A07

EERC 75-31 "ALUSH - A Computer Program for Seismic Response Analysis of Axisymmetric Soil-Structure Systems," by E. Berger, J. Lysmer and H.B. Seed - 1975

EERC 75-32 "TRIP and TRAVEL - Computer Programs for Soil-Structure Interaction Analysis with Horizontally Travelling Waves," by T. Udaka, J. Lysmer and H.B. Seed - 1975

EERC 75-33 "Predicting the Performance of Structures in Regions of High Seismicity," by J. Penzien - 1975 (PB 248 130)A03

EERC 75-34 "Efficient Finite Element Analysis of Seismic Structure - Soil - Direction," by J. Lysmer, H.B. Seed, T. Udaka, R.N. Hwang and C.-F. Tsai - 1975 (PB 253 570)A03

EERC 75-35 "The Dynamic Behavior of a First Story Girder of a Three-Story Steel Frame Subjected to Earthquake Loading," by R.W. Clough and L.-Y. Li - 1975 (PB 248 841)A05

EERC 75-36 "Earthquake Simulator Study of a Steel Frame Structure, Volume II - Analytical Results," by D.T. Tang - 1975 (PB 252 926)A10

EERC 75-37 "ANSR-I General Purpose Computer Program for Analysis of Non-Linear Structural Response," by D.P. Mondkar and G.H. Powell - 1975 (PB 252 386)A08

EERC 75-38 "Nonlinear Response Spectra for Probabilistic Seismic Design and Damage Assessment of Reinforced Concrete Structures," by M. Murakami and J. Penzien - 1975 (PB 259 530)A05

EERC 75-39 "Study of a Method of Feasible Directions for Optimal Elastic Design of Frame Structures Subjected to Earthquake Loading," by N.D. Walker and K.S. Pister - 1975 (PB 257 781)A06

EERC 75-40 "An Alternative Representation of the Elastic-Viscoelastic Analogy," by G. Dasgupta and J.L. Sackman - 1975 (PB 252 173)A03

EERC 75-41 "Effect of Multi-Directional Shaking on Liquefaction of Sands," by H.B. Seed, R. Pyke and G.R. Martin - 1975 (PB 258 781)A03

EERC 76-1 "Strength and Ductility Evaluation of Existing Low-Rise Reinforced Concrete Buildings - Screening Method," by T. Okada and B. Bresler - 1976 (PB 257 906)A11

EERC 76-2 "Experimental and Analytical Studies on the Hysteretic Behavior of Reinforced Concrete Rectangular and T-Beams," by S.-Y.M. Ma, E.P. Popov and V.V. Bertero - 1976 (PB 260 843)A12

EERC 76-3 "Dynamic Behavior of a Multistory Triangular-Shaped Building," by J. Petrovski, R.M. Stephen, E. Gartenbaum and J.G. Bouwkamp - 1976 (PB 273 279)A07

EERC 76-4 "Earthquake Induced Deformations of Earth Dams," by N. Serff, H.B. Seed, F.I. Makdisi & C.-Y. Chang - 1976 (PB 292 065)A08

EERC 76-5 "Analysis and Design of Tube-Type Tall Building Structures," by H. de Clercq and G.H. Powell - 1976 (PB 252 ... A10

EERC 76-6 "Time and Frequency Domain Analysis of Three-Dimensional Ground Motions, San Fernando Earthquake," by T. ... and J. Penzien (PB 260 556)A11

EERC 76-7 "Expected Performance of Uniform Building Code Design Masonry Structures," by R.L. Mayes, Y. Omote, S.W. ... and R.W. Clough - 1976 (PB 270 098)A05

EERC 76-8 "Cyclic Shear Tests of Masonry Piers, Volume 1 - Test Results," by R.L. Mayes, Y. Omote, R.W. Clough - 1976 (PB 264 424)A06

EERC 76-9 "A Substructure Method for Earthquake Analysis of Structure - Soil Interaction," by J.A. Gutierrez and A.K. Chopra - 1976 (PB 257 783)A08

EERC 76-10 "Stabilization of Potentially Liquefiable Sand Deposits using Gravel Drain Systems," by H.B. Seed and J.R. Booker - 1976 (PB 258 820)A04

EERC 76-11 "Influence of Design and Analysis Assumptions on Computed Inelastic Response of Moderately Tall Frames," by G.H. Powell and D.G. Row - 1976 (PB 271 409)A06

EERC 76-12 "Sensitivity Analysis for Hysteretic Dynamic Systems: Theory and Applications," by D. Ray, K.S. Pister and E. Polak - 1976 (PB 262 859)A04

EERC 76-13 "Coupled Lateral Torsional Response of Buildings to Ground Shaking," by C.L. Kan and A.K. Chopra - 1976 (PB 257 907)A09

EERC 76-14 "Seismic Analyses of the Banco de America," by V.V. Bertero, S.A. Mahin and J.A. Hollings - 1976

EERC 76-15 "Reinforced Concrete Frame 2: Seismic Testing and Analytical Correlation," by R.W. Clough and J. Gidwani - 1976 (PB 261 323)A08

EERC 76-16 "Cyclic Shear Tests of Masonry Piers, Volume 2 - Analysis of Test Results," by R.L. Mayes, Y. Omote and R.W. Clough - 1976

EERC 76-17 "Structural Steel Bracing Systems: Behavior Under Cyclic Loading," by E.P. Popov, K. Takanashi and C.W. Roeder - 1976 (PB 260 715)A05

EERC 76-18 "Experimental Model Studies on Seismic Response of High Curved Overcrossings," by D. Williams and W.G. Godden - 1976 (PB 269 548)A08

EERC 76-19 "Effects of Non-Uniform Seismic Disturbances on the Dumbarton Bridge Replacement Structure," by F. Baron and R.E. Hamati - 1976 (PB 282 981)A16

EERC 76-20 "Investigation of the Inelastic Characteristics of a Single Story Steel Structure Using System Identification and Shaking Table Experiments," by V.C. Matzen and H.D. McNiven - 1976 (PB 258 453)A07

EERC 76-21 "Capacity of Columns with Splice Imperfections," by E.P. Popov, R.M. Stephen and R. Philbrick - 1976 (PB 260 378)A04

EERC 76-22 "Response of the Olive View Hospital Main Building during the San Fernando Earthquake," by S. A. Mahin, V.V. Bertero, A.K. Chopra and R. Collins - 1976 (PB 271 425)A14

EERC 76-23 "A Study on the Major Factors Influencing the Strength of Masonry Prisms," by N.M. Mostaghel, R.L. Mayes, R. W. Clough and S.W. Chen - 1976 (Not published)

EERC 76-24 "GADFLEA - A Computer Program for the Analysis of Pore Pressure Generation and Dissipation during Cyclic or Earthquake Loading," by J.R. Booker, M.S. Rahman and H.B. Seed - 1976 (PB 263 947)A04

EERC 76-25 "Seismic Safety Evaluation of a R/C School Building," by B. Bresler and J. Axley - 1976

EERC 76-26 "Correlative Investigations on Theoretical and Experimental Dynamic Behavior of a Model Bridge Structure," by K. Kawashima and J. Penzien - 1976 (PB 263 388)A11

EERC 76-27 "Earthquake Response of Coupled Shear Wall Buildings," by T. Srichatrapimuk - 1976 (PB 265 157)A07

EERC 76-28 "Tensile Capacity of Partial Penetration Welds," by E.P. Popov and R.M. Stephen - 1976 (PB 262 899)A03

EERC 76-29 "Analysis and Design of Numerical Integration Methods in Structural Dynamics," by H.M. Hilber - 1976 (PB 264 410)A06

EERC 76-30 "Contribution of a Floor System to the Dynamic Characteristics of Reinforced Concrete Buildings," by L.E. Malik and V.V. Bertero - 1976 (PB 272 247)A13

EERC 76-31 "The Effects of Seismic Disturbances on the Golden Gate Bridge," by F. Baron, M. Arikan and R.E. Hamati - 1976 (PB 272 279)A09

EERC 76-32 "Infilled Frames in Earthquake Resistant Construction," by R.E. Klingner and V.V. Bertero - 1976 (PB 265 892)A13

UCB/EERC-77/01 "PLUSH - A Computer Program for Probabilistic Finite Element Analysis of Seismic Soil-Structure Interaction," by M.P. Romo Organista, J. Lysmer and H.B. Seed - 1977

UCB/EERC-77/02 "Soil-Structure Interaction Effects at the Humboldt Bay Power Plant in the Ferndale Earthquake of June 7, 1975," by J.E. Valera, H.B. Seed, C.F. Tsai and J. Lysmer - 1977 (PB 265 795)A04

UCB/EERC-77/03 "Influence of Sample Disturbance on Sand Response to Cyclic Loading," by K. Mori, H.B. Seed and C.K. Chan - 1977 (PB 267 352)A04

UCB/EERC-77/04 "Seismological Studies of Strong Motion Records," by J. Shoja-Taheri - 1977 (PB 269 655)A10

UCB/EERC-77/05 "Testing Facility for Coupled-Shear Walls," by L. Li-Hyung, V.V. Bertero and E.P. Popov - 1977

UCB/EERC-77/06 "Developing Methodologies for Evaluating the Earthquake Safety of Existing Buildings," by No. 1 - B. Bresler; No. 2 - B. Bresler, T. Okada and D. Zisling; No. 3 - T. Okada and B. Bresler; No. 4 - V.V. Bertero and B. Bresler - 1977 (PB 267 354)A08

UCB/EERC-77/07 "A Literature Survey - Transverse Strength of Masonry Walls," by Y. Omote, R.L. Mayes, S.W. Chen and R.W. Clough - 1977 (PB 277 933)A07

UCB/EERC-77/08 "DRAIN-TABS: A Computer Program for Inelastic Earthquake Response of Three Dimensional Buildings," by R. Guendelman-Israel and G.H. Powell - 1977 (PB 270 693)A07

UCB/EERC-77/09 "SUBWALL: A Special Purpose Finite Element Computer Program for Practical Elastic Analysis and Design of Structural Walls with Substructure Option," by D.Q. Le, H. Peterson and E.P. Popov - 1977 (PB 270 567)A05

UCB/EERC-77/10 "Experimental Evaluation of Seismic Design Methods for Broad Cylindrical Tanks," by D.P. Clough (PB 272 280)A13

UCB/EERC-77/11 "Earthquake Engineering Research at Berkeley - 1976," - 1977 (PB 273 507)A09

UCB/EERC-77/12 "Automated Design of Earthquake Resistant Multistory Steel Building Frames," by N.D. Walker, Jr. - 1977 (PB 276 526)A09

UCB/EERC-77/13 "Concrete Confined by Rectangular Hoops Subjected to Axial Loads," by J. Vallenas, V.V. Bertero and E.P. Popov - 1977 (PB 275 165)A06

UCB/EERC-77/14 "Seismic Strain Induced in the Ground During Earthquakes," by Y. Sugimura - 1977 (PB 284 201)A04

UCB/EERC-77/15 "Bond Deterioration under Generalized Loading," by V.V. Bertero, E.P. Popov and S. Viwathanatepa - 1977

UCB/EERC-77/16 "Computer Aided Optimum Design of Ductile Reinforced Concrete Moment Resisting Frames," by S.W. Zagajeski and V.V. Bertero - 1977 (PB 280 137)A07

UCB/EERC-77/17 "Earthquake Simulation Testing of a Stepping Frame with Energy-Absorbing Devices," by J.M. Kelly and D.F. Tsztoo - 1977 (PB 273 506)A04

UCB/EERC-77/18 "Inelastic Behavior of Eccentrically Braced Steel Frames under Cyclic Loadings," by C.W. Roeder and E.P. Popov - 1977 (PB 275 526)A15

UCB/EERC-77/19 "A Simplified Procedure for Estimating Earthquake-Induced Deformations in Dams and Embankments," by F.I. Makdisi and H.B. Seed - 1977 (PB 276 820)A04

UCB/EERC-77/20 "The Performance of Earth Dams during Earthquakes," by H.B. Seed, F.I. Makdisi and P. de Alba - 1977 (PB 276 821)A04

UCB/EERC-77/21 "Dynamic Plastic Analysis Using Stress Resultant Finite Element Formulation," by P. Lukkunapvasit and J.M. Kelly - 1977 (PB 275 453)A04

UCB/EERC-77/22 "Preliminary Experimental Study of Seismic Uplift of a Steel Frame," by R.W. Clough and A.A. Huckelbridge 1977 (PB 278 769)A08

UCB/EERC-77/23 "Earthquake Simulator Tests of a Nine-Story Steel Frame with Columns Allowed to Uplift," by A.A. Huckelbridge - 1977 (PB 277 944)A09

UCB/EERC-77/24 "Nonlinear Soil-Structure Interaction of Skew Highway Bridges," by M.-C. Chen and J. Penzien - 1977 (PB 276 176)A07

UCB/EERC-77/25 "Seismic Analysis of an Offshore Structure Supported on Pile Foundations," by D.D.-N. Liou and J. Penzien 1977 (PB 283 180)A06

UCB/EERC-77/26 "Dynamic Stiffness Matrices for Homogeneous Viscoelastic Half-Planes," by G. Dasgupta and A.K. Chopra - 1977 (PB 279 654)A06

UCB/EERC-77/27 "A Practical Soft Story Earthquake Isolation System," by J.M. Kelly, J.M. Eidinger and C.J. Derham - 1977 (PB 276 814)A07

UCB/EERC-77/28 "Seismic Safety of Existing Buildings and Incentives for Hazard Mitigation in San Francisco: An Exploratory Study," by A.J. Meltsner - 1977 (PB 281 970)A05

UCB/EERC-77/29 "Dynamic Analysis of Electrohydraulic Shaking Tables," by D. Rea, S. Abedi-Hayati and Y. Takahashi 1977 (PB 282 569)A04

UCB/EERC-77/30 "An Approach for Improving Seismic - Resistant Behavior of Reinforced Concrete Interior Joints," by B. Galunic, V.V. Bertero and E.P. Popov - 1977 (PB 290 870)A06

UCB/EERC-78/01 "The Development of Energy-Absorbing Devices for Aseismic Base Isolation Systems," by J.M. Kelly and D.F. Tsztoo - 1978 (PB 284 978)A04

UCB/EERC-78/02 "Effect of Tensile Prestrain on the Cyclic Response of Structural Steel Connections, by J.G. Bouwkamp and A. Mukhopadhyay - 1978

UCB/EERC-78/03 "Experimental Results of an Earthquake Isolation System using Natural Rubber Bearings," by J.M. Eidinger and J.M. Kelly - 1978 (PB 281 686)A04

UCB/EERC-78/04 "Seismic Behavior of Tall Liquid Storage Tanks," by A. Niwa - 1978 (PB 284 017)A14

UCB/EERC-78/05 "Hysteretic Behavior of Reinforced Concrete Columns Subjected to High Axial and Cyclic Shear Forces," by S.W. Zagajeski, V.V. Bertero and J.G. Bouwkamp - 1978 (PB 283 858)A13

UCB/EERC-78/06 "Inelastic Beam-Column Elements for the ANSR-I Program," by A. Riahi, D.G. Row and G.H. Powell - 1978

UCB/EERC-78/07 "Studies of Structural Response to Earthquake Ground Motion," by O.A. Lopez and A.K. Chopra - 1978 (PB 282 790)A05

UCB/EERC-78/08 "A Laboratory Study of the Fluid-Structure Interaction of Submerged Tanks and Caissons in Earthquakes," by R.C. Byrd - 1978 (PB 284 957)A08

UCB/EERC-78/09 "Model for Evaluating Damageability of Structures," by I. Sakamoto and B. Bresler - 1978

UCB/EERC-78/10 "Seismic Performance of Nonstructural and Secondary Structural Elements," by I. Sakamoto - 1978

UCB/EERC-78/11 "Mathematical Modelling of Hysteresis Loops for Reinforced Concrete Columns," by S. Nakata, T. Sproul and J. Penzien - 1978

UCB/EERC-78/12 "Damageability in Existing Buildings," by T. Blejwas and B. Bresler - 1978

UCB/EERC-78/13 "Dynamic Behavior of a Pedestal Base Multistory Building," by R.M. Stephen, E.L. Wilson, J.G. Bouwkamp and M. Button - 1978 (PB 286 650)A08

UCB/EERC-78/14 "Seismic Response of Bridges - Case Studies," by R.A. Imbsen, V. Nutt and J. Penzien - 1978 (PB 286 503)A10

UCB/EERC-78/15 "A Substructure Technique for Nonlinear Static and Dynamic Analysis," by D.G. Row and G.H. Powell - 1978 (PB 288 077)A10

UCB/EERC-78/16 "Seismic Risk Studies for San Francisco and for the Greater San Francisco Bay Area," by C.S. Oliveira - 1978

UCB/EERC-78/17 "Strength of Timber Roof Connections Subjected to Cyclic Loads," by P. Gülkan, R.L. Mayes and R.W. Clough - 1978

UCB/EERC-78/18 "Response of K-Braced Steel Frame Models to Lateral Loads," by J.G. Bouwkamp, R.M. Stephen and E.P. Popov - 1978

UCB/EERC-78/19 "Rational Design Methods for Light Equipment in Structures Subjected to Ground Motion," by J.L. Sackman and J.M. Kelly - 1978 (PB 292 357)A04

UCB/EERC-78/20 "Testing of a Wind Restraint for Aseismic Base Isolation," by J.M. Kelly and D.E. Chitty - 1978 (PB 292 833)A03

UCB/EERC-78/21 "APOLLO - A Computer Program for the Analysis of Pore Pressure Generation and Dissipation in Horizontal Sand Layers During Cyclic or Earthquake Loading," by P.P. Martin and H.B. Seed - 1978 (PB 292 835)A04

UCB/EERC-78/22 "Optimal Design of an Earthquake Isolation System," by M.A. Bhatti, K.S. Pister and E. Polak - 1978 (PB 294 735)A06

UCB/EERC-78/23 "MASH - A Computer Program for the Non-Linear Analysis of Vertically Propagating Shear Waves in Horizontally Layered Deposits," by P.P. Martin and H.B. Seed - 1978 (PB 293 101)A05

UCB/EERC-78/24 "Investigation of the Elastic Characteristics of a Three Story Steel Frame Using System Identification, by I. Kaya and H.D. McNiven - 1978

UCB/EERC-78/25 "Investigation of the Nonlinear Characteristics of a Three-Story Steel Frame Using System Identification," by I. Kaya and H.D. McNiven - 1978

UCB/EERC-78/26 "Studies of Strong Ground Motion in Taiwan," by Y.M. Hsiung, B.A. Bolt and J. Penzien - 1978

UCB/EERC-78/27 "Cyclic Loading Tests of Masonry Single Piers: Volume 1 - Height to Width Ratio of 2," by P.A. Hidalgo, R.L. Mayes, H.D. McNiven and R.W. Clough - 1978

UCB/EERC-78/28 "Cyclic Loading Tests of Masonry Single Piers: Volume 2 - Height to Width Ratio of 1," by S.-W.J. Chen, P.A. Hidalgo, R.L. Mayes, R.W. Clough and H.D. McNiven - 1978

UCB/EERC-78/29 "Analytical Procedures in Soil Dynamics," by J. Lysmer - 1978

UCB/EERC-79/01 "Hysteretic Behavior of Lightweight Reinforced Concrete Beam-Column Subassemblages," by B. Forzani, E.P. Popov and V.V. Bertero - April 1979(PB 298 267)A06

UCB/EERC-79/02 "The Development of a Mathematical Model to Predict the Flexural Response of Reinforced Concrete Beams to Cyclic Loads, Using System Identification," by J. Stanton & H. McNiven - Jan. 1979(PB 295 875)A10

UCB/EERC-79/03 "Linear and Nonlinear Earthquake Response of Simple Torsionally Coupled Systems," by C.L. Kan and A.K. Chopra - Feb. 1979(PB 298 262)A06

UCB/EERC-79/04 "A Mathematical Model of Masonry for Predicting its Linear Seismic Response Characteristics," by Y. Mengi and H.D. McNiven - Feb. 1979(PB 298 266)A06

UCB/EERC-79/05 "Mechanical Behavior of Lightweight Concrete Confined by Different Types of Lateral Reinforcement," by M.A. Manrique, V.V. Bertero and E.P. Popov - May 1979(PB 301 114)A06

UCB/EERC-79/06 "Static Tilt Tests of a Tall Cylindrical Liquid Storage Tank," by R.W. Clough and A. Niwa - Feb. 1979 (PB 301 167)A06

UCB/EERC-79/07 "The Design of Steel Energy Absorbing Restrainers and Their Incorporation into Nuclear Power Plants for Enhanced Safety: Volume 1 - Summary Report," by P.N. Spencer, V.F. Zackay, and E.R. Parker - Feb. 1979(UCB/EERC-79/07)A09

UCB/EERC-79/08 "The Design of Steel Energy Absorbing Restrainers and Their Incorporation into Nuclear Power Plants for Enhanced Safety: Volume 2 - The Development of Analyses for Reactor System Piping,""Simple Systems" by M.C. Lee, J. Penzien, A.K. Chopra and K, Suzuki "Complex Systems" by G.H. Powell, E.L. Wilson, R.W. Clough and D.G. Row - Feb. 1979(UCB/EERC-79/08)A10

UCB/EERC-79/09 "The Design of Steel Energy Absorbing Restrainers and Their Incorporation into Nuclear Power Plants for Enhanced Safety: Volume 3 - Evaluation of Commercial Steels," by W.S. Owen, R.M.N. Pelloux, R.O. Ritchie, M. Faral, T. Ohhashi, J. Toplosky, S.J. Hartman, V.F. Zackay and E.R. Parker - Feb. 1979(UCB/EERC-79/09)A04

UCB/EERC-79/10 "The Design of Steel Energy Absorbing Restrainers and Their Incorporation into Nuclear Power Plants for Enhanced Safety: Volume 4 - A Review of Energy-Absorbing Devices," by J.M. Kelly and M.S. Skinner - Feb. 1979(UCB/EERC-79/10)A04

UCB/EERC-79/11 "Conservatism In Summation Rules for Closely Spaced Modes," by J.M. Kelly and J.L. Sackman - May 1979(PB 301 328)A03

UCB/EERC-79/12 "Cyclic Loading Tests of Masonry Single Piers; Volume 3 - Height to Width Ratio of 0.5," by P.A. Hidalgo, R.L. Mayes, H.D. McNiven and R.W. Clough - May 1979(PB 301 321)A08

UCB/EERC-79/13 "Cyclic Behavior of Dense Course-Grained Materials in Relation to the Seismic Stability of Dams," by N.G. Banerjee, H.B. Seed and C.K. Chan - June 1979(PB 301 373)A13

UCB/EERC-79/14 "Seismic Behavior of Reinforced Concrete Interior Beam-Column Subassemblages," by S. Viwathanatepa, E.P. Popov and V.V. Bertero - June 1979(PB 301 326)A10

UCB/EERC-79/15 "Optimal Design of Localized Nonlinear Systems with Dual Performance Criteria Under Earthquake Excitations," by M.A. Bhatti - July 1979(PB 80 167 109)A06

UCB/EERC-79/16 "OPTDYN - A General Purpose Optimization Program for Problems with or without Dynamic Constraints," by M.A. Bhatti, E. Polak and K.S. Pister - July 1979(PB 80 167 091)A05

UCB/EERC-79/17 "ANSR-II, Analysis of Nonlinear Structural Response, Users Manual," by D.P. Mondkar and G.H. Powell - July 1979(PB 80 113 301)A05

UCB/EERC-79/18 "Soil Structure Interaction in Different Seismic Environments," A. Gomez-Masso, J. Lysmer, J.-C. Chen and H.B. Seed - August 1979(PB 80 101 520)A04

UCB/EERC-79/19 "ARMA Models for Earthquake Ground Motions," by M.K. Chang, J.W. Kwiatkowski, R.F. Nau, R.M. Oliver and K.S. Pister - July 1979(PB 301 166)A05

UCB/EERC-79/20 "Hysteretic Behavior of Reinforced Concrete Structural Walls," by J.M. Vallenas, V.V. Bertero and E.P. Popov - August 1979(PB 80 165 905)A12

UCB/EERC-79/21 "Studies on High-Frequency Vibrations of Buildings - 1: The Column Effect," by J. Lubliner - August 1979 (PB 80 158 553)A03

UCB/EERC-79/22 "Effects of Generalized Loadings on Bond Reinforcing Bars Embedded in Confined Concrete Blocks," by S. Viwathanatepa, E.P. Popov and V.V. Bertero - August 1979

UCB/EERC-79/23 "Shaking Table Study of Single-Story Masonry Houses, Volume 1: Test Structures 1 and 2," by P. Gülkan, R.L. Mayes and R.W. Clough - Sept. 1979

UCB/EERC-79/24 "Shaking Table Study of Single-Story Masonry Houses, Volume 2: Test Structures 3 and 4," by P. Gülkan, R.L. Mayes and R.W. Clough - Sept. 1979

UCB/EERC-79/25 "Shaking Table Study of Single-Story Masonry Houses, Volume 3: Summary, Conclusions and Recommendations," by R.W. Clough, R.L. Mayes and P. Gülkan - Sept. 1979

UCB/EERC-79/26 "Recommendations for a U.S.-Japan Cooperative Research Program Utilizing Large-Scale Testing Facilities," by U.S.-Japan Planning Group - Sept. 1979(PB 301 407)A06

UCB/EERC-79/27 "Earthquake-Induced Liquefaction Near Lake Amatitlan, Guatemala," by H.B. Seed, I. Arango, C.K. Chan, A. Gomez-Masso and R. Grant de Ascoli - Sept. 1979(NUREG-CR1341)A03

UCB/EERC-79/28 "Infill Panels: Their Influence on Seismic Response of Buildings," by J.W. Axley and V.V. Bertero - Sept. 1979(PB 80 163 371)A10

UCB/EERC-79/29 "3D Truss Bar Element (Type 1) for the ANSR-II Program," by D.P. Mondkar and G.H. Powell - Nov. 1979 (PB 80 169 709)A02

UCB/EERC-79/30 "2D Beam-Column Element (Type 5 - Parallel Element Theory) for the ANSR-II Program," by D.G. Row, G.H. Powell and D.P. Mondkar - Dec. 1979(PB 80 167 224)A03

UCB/EERC-79/31 "3D Beam-Column Element (Type 2 - Parallel Element Theory) for the ANSR-II Program," by A. Riahi, G.H. Powell and D.P. Mondkar - Dec. 1979(PB 80 167 216)A03

UCB/EERC-79/32 "On Response of Structures to Stationary Excitation," by A. Der Kiureghian - Dec. 1979(PB 80166 929)A03

UCB/EERC-79/33 "Undisturbed Sampling and Cyclic Load Testing of Sands," by S. Singh, H.B. Seed and C.K. Chan - Dec. 1979(

UCB/EERC-79/34 "Interaction Effects of Simultaneous Torsional and Compressional Cyclic Loading of Sand," by P.M. Griffin and W.N. Houston - Dec. 1979

UCB/EERC-80/01 "Earthquake Response of Concrete Gravity Dams Including Hydrodynamic and Foundation Interaction Effects," by A.K. Chopra, P. Chakrabarti and S. Gupta - Jan. 1980(AD-A087297)A10

UCB/EERC-80/02 "Rocking Response of Rigid Blocks to Earthquakes," by C.S. Yim, A.K. Chopra and J. Penzien - Jan. 1980 (PB80 166 002)A04

UCB/EERC-80/03 "Optimum Inelastic Design of Seismic-Resistant Reinforced Concrete Frame Structures," by S.W. Zagajeski and V.V. Bertero - Jan. 1980(PB80 164 635)A06

UCB/EERC-80/04 "Effects of Amount and Arrangement of Wall-Panel Reinforcement on Hysteretic Behavior of Reinforced Concrete Walls," by R. Iliya and V.V. Bertero - Feb. 1980(PB81 122 525)A09

UCB/EERC-80/05 "Shaking Table Research on Concrete Dam Models," by A. Niwa and R.W. Clough - Sept. 1980(PB81 122 368)A06

UCB/EERC-80/06 "The Design of Steel Energy-Absorbing Restrainers and their Incorporation into Nuclear Power Plants for Enhanced Safety (Vol 1A): Piping with Energy Absorbing Restrainers: Parameter Study on Small Systems," by G.H. Powell, C. Oughourlian and J. Simons - June 1980

UCB/EERC-80/07 "Inelastic Torsional Response of Structures Subjected to Earthquake Ground Motions," by Y. Yamazaki April 1980(PB81 122 327)A08

UCB/EERC-80/08 "Study of X-Braced Steel Frame Structures Under Earthquake Simulation," by Y. Ghanaat - April 1980 (PB81 122 335)A11

UCB/EERC-80/09 "Hybrid Modelling of Soil-Structure Interaction," by S. Gupta, T.W. Lin, J. Penzien and C.S. Yeh May 1980(PB81 122 319)A07

UCB/EERC-80/10 "General Applicability of a Nonlinear Model of a One Story Steel Frame," by B.I. Sveinsson and H.D. McNiven - May 1980(PB81 124 877)A06

UCB/EERC-80/11 "A Green-Function Method for Wave Interaction with a Submerged Body," by W. Kioka - April 1980 (PB81 122 269)A07

UCB/EERC-80/12 "Hydrodynamic Pressure and Added Mass for Axisymmetric Bodies," by F. Nilrat - May 1980(PB81 122 343)A08

UCB/EERC-80/13 "Treatment of Non-Linear Drag Forces Acting on Offshore Platforms," by B.V. Dao and J. Penzien May 1980(PB81 153 413)A07

UCB/EERC-80/14 "2D Plane/Axisymmetric Solid Element (Type 3 - Elastic or Elastic-Perfectly Plastic) for the ANSR-II Program," by D.P. Mondkar and G.H. Powell - July 1980(PB81 122 350)A03

UCB/EERC-80/15 "A Response Spectrum Method for Random Vibrations," by A. Der Kiureghian - June 1980(PB81 122 301)A03

UCB/EERC-80/16 "Cyclic Inelastic Buckling of Tubular Steel Braces," by V.A. Zayas, E.P. Popov and S.A. Mahin June 1980(PB81 124 885)A10

UCB/EERC-80/17 "Dynamic Response of Simple Arch Dams Including Hydrodynamic Interaction," by C.S. Porter and A.K. Chopra - July 1980(PB81 124 000)A13

UCB/EERC-80/18 "Experimental Testing of a Friction Damped Aseismic Base Isolation System with Fail-Safe Characteristics," by J.M. Kelly, K.E. Beucke and M.S. Skinner - July 1980(PB81 148 595)A04

UCB/EERC-80/19 "The Design of Steel Energy-Absorbing Restrainers and their Incorporation into Nuclear Power Plants for Enhanced Safety (Vol 1B): Stochastic Seismic Analyses of Nuclear Power Plant Structures and Piping Systems Subjected to Multiple Support Excitations," by M.C. Lee and J. Penzien - June 1980

UCB/EERC-80/20 "The Design of Steel Energy-Absorbing Restrainers and their Incorporation into Nuclear Power Plants for Enhanced Safety (Vol 1C): Numerical Method for Dynamic Substructure Analysis," by J.M. Dickens and E.L. Wilson - June 1980

UCB/EERC-80/21 "The Design of Steel Energy-Absorbing Restrainers and their Incorporation into Nuclear Power Plants for Enhanced Safety (Vol 2): Development and Testing of Restraints for Nuclear Piping Systems," by J.M. Kelly and M.S. Skinner - June 1980

UCB/EERC-80/22 "3D Solid Element (Type 4-Elastic or Elastic-Perfectly-Plastic) for the ANSR-II Program," by D.P. Mondkar and G.H. Powell - July 1980(PB81 123 242)A03

UCB/EERC-80/23 "Gap-Friction Element (Type 5) for the ANSR-II Program," by D.P. Mondkar and G.H. Powell - July 1980 (PB81 122 285)A03

UCB/EERC-80/24 "U-Bar Restraint Element (Type 11) for the ANSR-II Program," by C. Oughourlian and G.H. Powell July 1980(PB81 122 293)A03

UCB/EERC-80/25 "Testing of a Natural Rubber Base Isolation System by an Explosively Simulated Earthquake," by J.M. Kelly - August 1980

UCB/EERC-80/26 "Input Identification from Structural Vibrational Response," by Y. Hu - August 1980(PB81 152 308)A05

UCB/EERC-80/27 "Cyclic Inelastic Behavior of Steel Offshore Structures," by V.A. Zayas, S.A. Mahin and E.P. Popov August 1980

UCB/EERC-80/28 "Shaking Table Testing of a Reinforced Concrete Frame with Biaxial Response," by M.G. Oliva October 1980(PB81 154 304)A10

UCB/EERC-80/29 "Dynamic Properties of a Twelve-Story Prefabricated Panel Building," by J.G. Bouwkamp, J.P. Kollegger and R.M. Stephen - October 1980

UCB/EERC-80/30 "Dynamic Properties of an Eight-Story Prefabricated Panel Building," by J.G. Bouwkamp, J.P. Kollegger and R.M. Stephen - October 1980

UCB/EERC-80/31 "Predictive Dynamic Response of Panel Type Structures Under Earthquakes," by J.P. Kollegger and J.G. Bouwkamp - October 1980(PB81 152 316)A04

UCB/EERC-80/32 "The Design of Steel Energy-Absorbing Restrainers and their Incorporation into Nuclear Power Plants for Enhanced Safety (Vol 3): Testing of Commercial Steels in Low-Cycle Torsional Fatigue," by P. Spencer, E.R. Parker, E. Jongewaard and M. Drory

UCB/EERC-80/33 "The Design of Steel Energy-Absorbing Restrainers and their Incorporation into Nuclear Power Plants for Enhanced Safety (Vol 4): Shaking Table Tests of Piping Systems with Energy-Absorbing Restrainers," by S.F. Stiemer and W.G. Godden - Sept. 1980

UCB/EERC-80/34 "The Design of Steel Energy-Absorbing Restrainers and their Incorporation into Nuclear Power Plants for Enhanced Safety (Vol 5): Summary Report," by P. Spencer

UCB/EERC-80/35 "Experimental Testing of an Energy-Absorbing Base Isolation System," by J.M. Kelly, M.S. Skinner and K.E. Beucke - October 1980(PB81 154 072)A04

UCB/EERC-80/36 "Simulating and Analyzing Artificial Non-Stationary Earthquake Ground Motions," by R.F. Nau, R.M. Oliver and K.S. Pister - October 1980(PB81 153 397)A04

UCB/EERC-80/37 "Earthquake Engineering at Berkeley - 1980," - Sept. 1980

UCB/EERC-80/38 "Inelastic Seismic Analysis of Large Panel Buildings," by V. Schricker and G.H. Powell - Sept. 1980 (PB81 154 338)A13

UCB/EERC-80/39 "Dynamic Response of Embankment, Concrete-Gravity and Arch Dams Including Hydrodynamic Interaction," by J.F. Hall and A.K. Chopra - October 1980(PB81 152 324)A11

UCB/EERC-80/40 "Inelastic Buckling of Steel Struts Under Cyclic Load Reversal," by R.G. Black, W.A. Wenger and E.P. Popov - October 1980(PB81 154 312)A08

UCB/EERC-80/41 "Influence of Site Characteristics on Building Damage During the October 3, 1974 Lima Earthquake," by P. Repetto, I. Arango and H.B. Seed - Sept. 1980(PB81 161 739)A05

UCB/EERC-80/42 "Evaluation of a Shaking Table Test Program on Response Behavior of a Two Story Reinforced Concrete Frame," by J.M. Blondet, R.W. Clough and S.A. Mahin

UCB/EERC-80/43 "Modelling of Soil-Structure Interaction by Finite and Infinite Elements," by F. Medina

UCB/EERC-81/01 "Control of Seismic Response of Piping Systems and Other Structures by Base Isolation," edited by J. M. Kelly - January 1981 (PB81 200 735)A05

UCB/EERC-81/02 "OPTNSR - An Interactive Software System for Optimal Design of Statically and Dynamically Loaded Structures with Nonlinear Response," by M. A. Bhatti, V. Ciampi and K. S. Pister - January 1981 (PB81 218 851)A09

UCB/EERC-81/03 "Analysis of Local Variations in Free Field Seismic Ground Motion," by J.-C. Chen, J. Lysmer and H. B. Seed - January 1981 (AD-A099508)A13

UCB/EERC-81/04 "Inelastic Structural Modeling of Braced Offshore Platforms for Seismic Loading," by V. A. Zayas, P.-S. B. Shing, S. A. Mahin and E. P. Popov - January 1981

UCB/EERC-81/05 "Dynamic Response of Light Equipment in Structures," by A. Der Kiureghian, J. L. Sackman and B. Nour-Omid - April 1981 (PB81 218 497)A04

UCB/EERC-81/06 "Preliminary Experimental Investigation of a Broad Base Liquid Storage Tank," by J. G. Bouwkamp, J. P. Kollegger and R. M. Stephen - May 1981

UCB/EERC-81/07 "The Seismic Resistant Design of Reinforced Concrete Coupled Structural Walls," by A. E. Aktan and V. V. Bertero - June 1981

UCB/EERC-81/08 "The Undrained Shearing Resistance of Cohesive Soils at Large Deformation," by M. R. Piles and H. B. Seed - August 1981

UCB/EERC-81/09 "Experimental Behavior of a Spatial Piping System with Steel Energy Absorbers Subjected to a Simulated Differential Seismic Input," by S. F. Stiemer, W. G. Godden and J. M. Kelly - July 1981

UCB/EERC-81/10 "Evaluation of Seismic Design Provisions for Masonry in the United States," by B. I. Sveinsson, R. L. Mayes and H. D. McNiven - August 1981

UCB/EERC-81/11 "Two-Dimensional Hybrid Modelling of Soil-Structure Interaction," by T.-J. Tzong, S. Gupta and J. Penzien - August 1981

UCB/EERC-81/12 "Studies on Effects of Infills in Seismic Resistant R/C Construction," by S. Brokker and V. V. Bertero - September 1981

UCB/EERC-81/13 "Linear Models to Predict the Nonlinear Seismic Behavior of a One-Story Steel Frame," by H. Valdimarsson, A. H. Shah and H. D. McNiven - September 1981

UCB/EERC-81/14 "TLUSH: A Computer Program for the Three-Dimensional Dynamic Analysis of Earth Dams," by Takaaki Kagawa, Lelio H. Mejia, H. Bolton Seed and John Lysmer - September 1981.

UCB/EERC-81/15 "Three Dimensional Dynamic Response Analysis of Earth Dams," by Lelio H. Mejia and H. Bolton Seed - September 1981.